The American Mineralogist

Journal of the Mineralogical Society of America

VOL. 44 JANUARY–FEBRUARY 1959 Nos. 1 and 2

Contents

(*Continued on Cover 2*)

Published bi-monthly by the Society

Mineralogical Society of America

ASSOCIATED WITH THE GEOLOGICAL SOCIETY OF AMERICA

The enlarged issues of this journal for 1959 are made possible by a grant from the Penrose Fund of the Geological Society of America.

The American Mineralogist—Journal of the Mineralogical Society of America

The journal, containing articles on mineralogy, crystallography, and allied sciences, is issued every two months. Contributions are invited.

The general conduct of the journal is in the hands of the editor, Lewis S. Ramsdell, Department of Mineralogy, University of Michigan, to whom all manuscripts should be submitted. To assist the editor, the Council of the Society has appointed the following Board of Associate Editors:

Robert M. Garrels, Harvard University, Cambridge 38, Massachusetts.
Joseph Murdoch, University of California at Los Angeles, Los Angeles, California.
D. Jerome Fisher, University of Chicago, Chicago 37, Illinois.
George T. Faust, U. S. Geological Survey, Washington 25, D. C.
George W. Brindley, Pennsylvania State University, University Park, Pennsylvania.
A. Pabst, University of California, Berkeley 4, California.

Authors are requested to submit two copies of each manuscript, typewritten on standard size paper, 8½×11 inches. Photographs submitted for cuts should be glossy prints.

Authors are entitled to 50 free reprints, without covers, of each article published.

Sent to all members and fellows of the Mineralogical Society of America. Membership dues $4.00 annually, fellowship dues $5.00 annually, which includes receipt of the American Mineralogist and GeoTimes, which is published by the American Geological Institute. Subscriptions for libraries, colleges, institutions, companies and similar organizations $6.00 annually.

Entered as second class matter at the post office at Menasha, Wis., under Act of March 3, 1879. Acceptance for mailing at the special rate of postage provided for in section 1103, Act of Oct. 3, 1917, paragraph 4 section 429 P. L. & R. authorized March 13, 1922.

Notice of change of address, orders, and remittances should be sent to Marjorie Hooker, c/o U. S. Geological Survey, Washington 25, D. C.

Printed by the George Banta Company, Inc., Menasha, Wisconsin
Printed in the United States of America

Leitz **first in precision optics**

NEW POLARIZING MICROSCOPE SM-pol

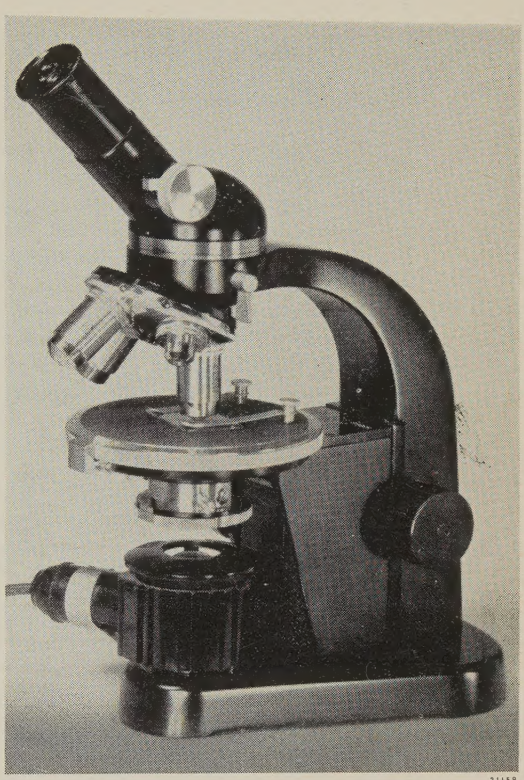

21158

Leitz sets a new standard with this student polarizing and chemical microscope of modern design, with dual, low-position focusing controls and large field of view. A reasonably priced polarizing microscope, the model SM-pol, has rugged, one-piece construction with Bertrand lens and pinhole diaphragm built into the tube. Inclined monocular tube will accommodate wide-field eyepieces and the microscope can be used faced away from the observer, permitting easy accessibility to the stage.

A reputation for integrity and a tradition of service have led thousands of scientific workers to bring their optical problems to Leitz. If you have problems in this field, why not let us help you with them?

See your Leitz dealer and examine these Leitz instruments soon. Write for information.

E. LEITZ, INC., Dept. AM-1
468 Fourth Avenue, New York 16, N. Y.

Please send me the Leitz _____ brochure.

NAME _____

STREET _____

CITY _____ ZONE _____ STATE _____

E. LEITZ, INC., 468 FOURTH AVENUE, NEW YORK 16, N. Y.
Distributors of the world-famous products of
Ernst Leitz G. m. b. H., Wetzlar, Germany—Ernst Leitz Canada Ltd.
LEICA CAMERAS · LENSES · MICROSCOPES · BINOCULARS

Here at last . . .

IS AN
ACCURATE
BALANCE
at a moderate price

ONLY **$35.00**

Capacity 311 Grams
Yet Weighs to 1/100 Grams
(.01) or 5/100 carats

IT IS IDEAL FOR THE

- GEM CUTTER
- COLLECTOR
- GEOLOGIST
- MINERALOGIST
- SCHOOLS

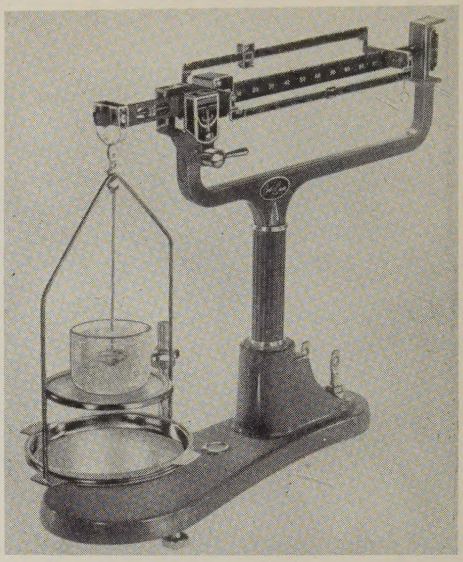

SPECIALLY FITTED FOR THE DETERMINATION OF SPECIFIC GRAVITY BY DIRECT READING

The serious gem cutter, collector or hobbyist has long wished for such a balance, but before now they have always been priced up into the hundreds of dollars. Lapidabrade went to work on the problem, and now we have the solution . . . a well-made simple and accurate scale on which you can do all the needed weighing of precious stones, determine specific gravity, or weigh quantities of gem rough. All this has been achieved at a price now within the reach of all!

STUDY THESE FEATURES

LIGHT WEIGHT DURALUMIN BEAM

This balance has a light-weight, high strength duralumin beam. The inherent load is kept at an absolute minimum, thereby insuring maximum sensitivity. Permanent protection against chemical action is achieved by attractive black anodized finish. To this beam is attached the relief-etched stainless steel beams which are equipped with sliding-type center pointed indicators. The graduated portions are tiered at three levels for easy reading.

SELF-ALIGNING AGATE BEARINGS

This balance gives you the ultimate in bearing construction. The bearing blocks are of high grade polished agate and are especially mounted so as to be free to align themselves with the beam knife edges at all times, resulting in greater sensitivity and longer life.

PRECISION GROUND STEEL KNIVES

The balance knives are made from a select grade of steel which is passed through a special heat-treating process to impart maximum hardness to the surface, while the core remains relatively soft, tough and shock resistant.

STAINLESS STEEL BOWS AND PANS

At all points of actual usage this balance is prepared to stand even the most corrosive of atmospheres. The pan is equipped with two lips so that it can be readily picked up from either side. Pan holder is concave to insure proper positioning of pan.

SPECIALLY FITTED FOR GEM WORK

Note especially that this balance has a swing out pan and hook, with container so that the taking of the components for a specific gravity determination can be done quickly and accurately.

LEVEL AND LEVELING SCREWS

This scale is equipped with a level, and two adjustable screws, so that the balance can be brought to a level position on any working surface in a matter of seconds, insuring the accuracy of weighings.

ORDER NOW or send for FREE literature

LAPIDABRADE PRODUCTS AVAILABLE THROUGH WARDS
NATURAL SCIENCE ESTABLISHMENT, ROCHESTER, N.Y.

Lapidabrade, Inc.

"The Complete Supply House"

400 LEEDOM ST., JENKINTOWN, PA.

ZEISS — *finest name in optics*

BRINKMANN — *largest ZEISS distributor*

ANNOUNCE "GF POL"

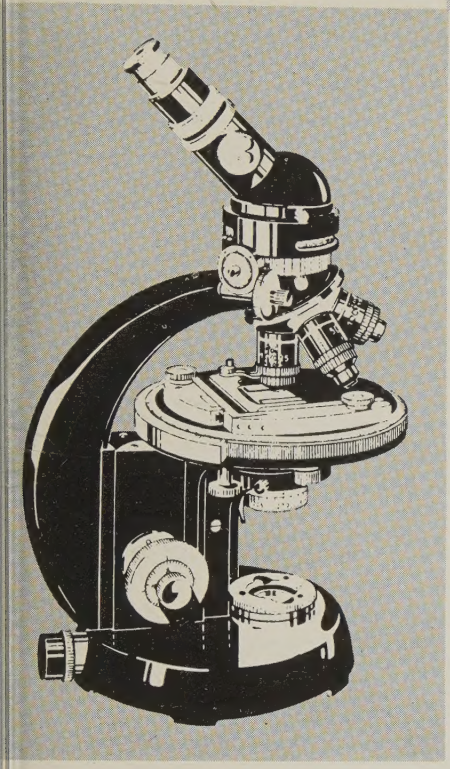

the most advanced

polarizing microscope

***for* MINERALOGY**
PETROGRAPHY
GEOLOGY

FIRST...

with interchangeable INCLINED
Monocular & Binocular Tubes
with ball bearing stage with built-in click stops
with REALLY LOW coaxial coarse and fine adjustment
with Hi-Intensity built-in light AND
instant change over to external sources
with self centering objectives with retracting
mounts for full specimen protection
with QUINTUPLE nosepiece on dovetail-slider
with 360° rotating analyzer
with clip-on synchronous rotating device
with polarizing PHASE condenser and objective
and many other unique features

ZEISS GF, first introduced two years ago
truly revolutionary improvement.

its unique features are now also avail-
on the new ZEISS Camera microscopes
aphot-Pol. and Photomat-Pol.

NO WAITING for delivery!

The ZEISS GF-Pol is here NOW!

Orders will be shipped immediately!

BRINKMANN INSTRUMENTS, INC.
115 CUTTER MILL RD., GREAT NECK, L. I., N. Y.

☐ Please send complete information on Zeiss Polarizing Microscopes.

☐ Please have representative demonstrate.

NAME_____

ADDRESS_____

CITY_____ ZONE_____ STATE_____

BRINKMANN INSTRUMENTS, INC.

BRINKMANN HOUSE, 115 CUTTER MILL RD., GREAT NECK, L. I., N. Y.

also in: PHILADELPHIA, PA. CLEVELAND, O. HOUSTON, TEXAS

BRINKMANN, the largest ZEISS dealer in the United States, for prompt delivery and nationwide service!

THE AMERICAN MINERALOGIST
JOURNAL OF THE MINERALOGICAL SOCIETY OF AMERICA

Vol. 44 JANUARY–FEBRUARY 1959 Nos. 1 and 2

SECOND OCCURRENCE OF FERSMITE

H. D. HESS AND H. J. TRUMPOUR, *Petrographic Laboratory, Bureau of Mines, U. S. Department of the Interior, Albany, Oregon.*

ABSTRACT

Fersmite, (Ca, Ce, Na)(Cb, Ti, Fe, Al)$_2$ (O, OH, F)$_6$, occurs as small anhedral inclusions and intergrowths with a tantalum-free columbite occurring in Ravalli County, Montana. Chemical and crystallographic data, along with the physical and optical properties, agree in general with those given in the original description of fersmite from the Ural Mountains of Russia. *X*-ray diffraction data, not given in the original description, and more specific optical data have been determined.

INTRODUCTION

Fersmite is a rare calcium columbate of the AB_2O_6 group, (Ca, Ce, Na) (Cb, Ti, Fe, Al)$_2$ (O, OH, F)$_6$, first described from the pegmatites of the Vishnevye Mountains, Central Urals, Russia, by Bohnstedt-Kupletskaya and Burova (1946).

The new locality for fersmite, representing the first recorded occurrence in North America and apparently only the second reported occurrence in the world, is the Dark Star claim in sections 3 and 4, T4S, R22W, Bitterroot Base Line, Ravalli County, Montana. The prospect is in the ruggedly dissected east slope of the Bitterroot Mountains approximately five miles south of Alta, Montana, and is easily accessible by highway and Forest Service access roads. The region is composed chiefly of schists and gneisses believed to have been originally Belt-series argillaceous and calcareous sediments of Precambrian age that were metamorphosed during the introduction of the Idaho batholith (Ross 1950). Intermittent amphibolite, quartzite, and thin-bedded marble also are present. Rhyolite and pegmatite dikes crosscut and intrude the metamorphic complex in a number of areas.

The fersmite described herein occurs as small anhedral inclusions and intergrowths with a tantalum-free columbite associated with monazite, ancylite, barite, quartz, and apatite in a fine-grained buff-colored marble. The bed ranges in thickness from approximately 1 to 6 feet, and reportedly can be traced for approximately 700 feet along the surface. Accord-

ing to Sahinen (1957), the strike of the marble is N. $67\frac{1}{2}°$ W, and the dip is 77° NE at the surface but straightens to vertical near the bottom of a 12-foot cut.

As shown in Fig. 1, the columbite, along with intergrown fersmite, occurs as well-defined blebs and irregular masses ranging up to 2 inches across. The microcrystalline structure of these black masses, and particularly the close relationship of the fersmite to columbite, is illus-

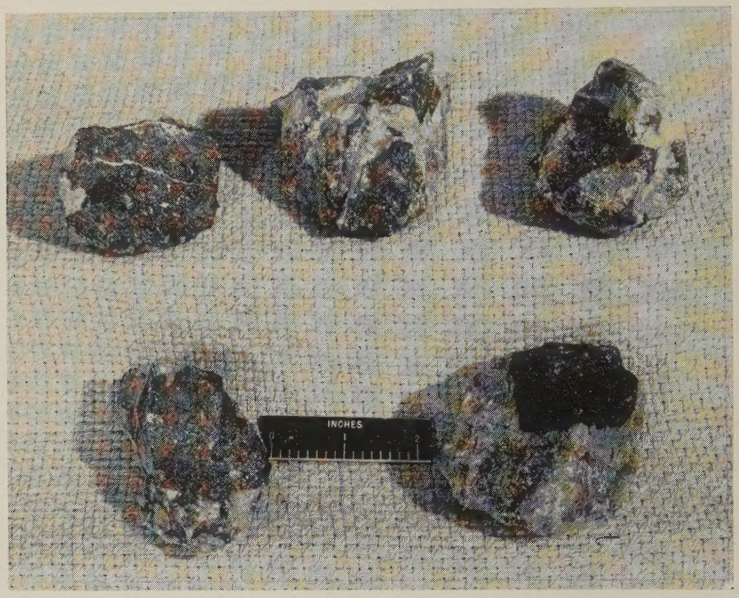

FIG. 1. Photograph of selected specimens illustrating the occurrence of the black columbite masses which contain the fersmite.

trated in Fig. 2. Monazite is observed only as small sparsely disseminated anhedral inclusions in the columbite masses, and can be recognized with the unaided eye in contrast to the black host mineral. Conversely, the the ancylite is not directly associated with the columbite, but rather occurs as a fine-grained pinkish material associated with the carbonate host rock.

The presence of these columbium and rare-earth minerals—ordinarily regarded as being of granitic or pegmatitic origin, but here occurring in a metamorphosed limestone of probably sedimentary origin—represents a unique occurrence. It also is of interest to note that high-purity columbite concentrates analyzed by optical and x-ray spectrographic methods at the Albany, Oregon, laboratory of the Federal Bureau of Mines were found to contain no tantalum. The tantalum-free nature of columbite from the Dark Star claim originally was reported by Sahinen (1957)

on the basis of analyses made by the Montana Bureau of Mines and the U. S. Geological Survey. However, the black homogeneous-appearing columbium-bearing masses were described by Sahinen as being "stubby prismatic crystals of columbite as much as two inches across," and no mention was made of the intimately intergrown fersmite.

FIG. 2. Plane light, ×45. Photomicrograph of columbite masses showing the relationship of anhedral fersmite (gray, high relief) to subhedral columbite (black) and interstitial calcite (white).

The Montana fersmite first was noticed in January 1954 during a routine mineralogical examination of a prospector's sample submitted by Louis Erickson, Corvallis, Montana, to the U. S. Bureau of Mines Petrographic Laboratory at Albany. At that time, R. E. Lubker, the laboratory geologist examining the sample, called the authors' attention to a small quantity of a dark brown, translucent mineral which he observed in the nonmagnetic fraction of crushed material passed through the Frantz isodynamic magnetic separator at 1.5 amperes.

When the mineral could not be classified by *x*-ray diffraction analysis, a more thorough study and literature search was made to determine the possibility of a new mineral species. It was through this detailed study, and subsequent tests made on a suite of selected samples supplied by

Louis Erickson, that the unidentified mineral was found to have the properties of fersmite as described by Bohnstedt-Kupletskaya and Burova (1946). Unfortunately, the original description of fersmite lacked x-ray diffraction data, and attempts to obtain identified samples for comparison purposes were unsuccessful. However, the chemical, physical and optical properties and limited crystallographic data listed correspond so closely with the material from Ravalli County that the relationship seems unquestionable.

Crystallography

The Montana fersmite occurs as small anhedral inclusions and intergrowths with columbite. This, plus its extreme brittleness, made it impossible to obtain individual crystals suitable for detailed study with the optical goniometer. However, through considerable search and effort, several imperfect crystals and crystal fragments were isolated permitting limited single-crystal study.

Study of these fersmite grains indicates that the mineral is orthorhombic in crystallization and belongs to the bipyramidal class. The few distinct crystals observed measure from 0.5 to 1 millimeter across, while the predominant anhedral forms are somewhat larger. The habit is prismatic, with the unit prism (110) predominating, and less commonly tabular parallel to (100). Macrodome and macropinacoid modifications also are observed on some of the crystalline grains. The prism faces are striated, and several crystal fragments showed parting parallel to (100).

The axial ratio, as derived from x-ray study, is $a:b:c=0.381:1:0.346$ which compares with the "approximate ratio" $a:b:c=0.377:1:0.356$ reported by Bohnstedt-Kupletskaya and Burova (1946) on the Russian fersmite.

Unit Cell and Space Group

The unit cell dimensions of the Montana fersmite were obtained with MoKα radiation using a cylindrical camera. Following the same technique, the cell dimensions of the associated columbite also were determined to illustrate the rather close similarity of these two intimately associated minerals.

The space group of fersmite was found to be the same as for columbite and tantalite, D_{2h}^{14}—$Pbcn$. The cell dimensions obtained for the fersmite and associated columbite are as follows, with the order of listing in conformance with the International Tables for X-ray Crystallography:

Fersmite	Columbite
$a_o=$ 5.764 Å	$a_o=$ 5.730 Å
$b_o=$15.09 Å	$b_o=$14.238 Å
$c_o=$ 5.232 Å	$c_o=$ 5.082 Å

X-ray Powder Diffraction Data

The original description of fersmite reported by Bohnstedt-Kupletskaya and Burova did not include powder diffraction data, and therefore a comparison could not be made. The powder diffraction data obtained for the Montana fersmite, using a Norelco Geiger Counter Spectrometer and CuKα radiation, are listed in Table 1.

Table 1. X-Ray Powder Spacing Data for Fersmite from Ravalli County, Montana

CuKα radiation

d (meas.)	d (calc.)	I/I_0	hkl	d (meas.)	d (calc.)	I/I_0	hkl
7.449	7.54	6	020	1.626	1.62	6	350
5.345	5.38	9	110	1.580	1.58	4	043
3.762	3.77	21	111 040	1.537	1.54	2	312 262 191
3.427	3.44	9	121				
3.049	3.07	100	131	1.527	1.53	15	082
2.864	2.88	8	200	1.512	1.52	3	322
2.684	2.69	4	220	1.502	1.51	1	0.10.0 281
2.606	2.62	7	002				
2.514	2.52	8	060	1.489	1.49	2	213
2.493	2.47	14	022	1.482	1.48	2	332
2.385	2.38	1	102	1.476	1.46	5	361 223
2.367	2.38	1	151				
2.279	2.27	1	061	1.427	1.43	1	370
2.247	2.26	5	231	1.387	1.38	4	411
2.145	2.15	4	132	1.380	1.38	2	352
2.117	2.11	1	161	1.363	1.37	1	421
2.087	2.10	5	241	1.334	1.33	1	1.11.0
2.004	2.01	3	142	1.229	1.30	1	441
1.967	1.94	10	251	1.256	1.26	6	402 451
1.929	1.93	3	202				
1.916	1.91	1	310	1.248	1.25	1	333
1.899	1.89	1	080	1.245	1.25	1	183
1.882	1.88	9	171 222	1.222	1.22	3	343
				1.211	1.21	11	144
1.862	1.87	1	152	1.192	1.19	1	204
1.804	1.81	9	232	1.183	1.18	13	154
1.789	1.80	7	330	1.158	1.16	1	064
1.786	1.79	8	311	1.145	1.15	1	480
1.771	1.77	8	081	1.133	1.14	1	392
1.691	1.70	6	023 331 181	1.126	1.13	<1	462
				1.121	1.12	3	511
				1.107	1.11	1	521
1.629	1.63	4	252 341				

Physical Properties

The specific gravity of the Ravalli County fersmite was determined by two methods: (1) with a Berman density balance, in which fragments were first weighed in air and then in toluene; and (2) with a pycnometer, using xylene as the displacement liquid. These procedures were necessitated by the small size of the fragments because grinding through 48-mesh or finer was required to insure liberation from any contaminating columbite. The results of the two methods show close agreement, with specific gravity values of 4.79 and 4.80 obtained by using the Berman balance and the pycnometer, respectively. Even though the values were redetermined several times with complete agreement, there is a noted variation with the 4.69 value reported by Bohnstedt-Kupletskaya and Burova (1946) for the Ural Mountains fersmite.

A further comparison of the physical properties of fersmite from the two localities is listed in Table 2.

Table 2. A Comparison of the Physical Properties of Fersmite

	Ravalli County Montana	Vischnevye Mts. Central Urals
Specific gravity	4.79	4.69
Color	Dark brown to black	Black
Streak	Grayish-brown	Grayish brown
Luster	Resinous	Subvitreous to resinous
Hardness	4–4½	4½
Cleavage	None	None
Fracture	Subconchoidal	Uneven to subconchoidal
Tenacity	Brittle	Brittle

Optical Properties

The fersmite from Ravalli County is translucent and dark honey yellow in thin section and fragment mounts, and exhibits moderate pleochroism. Information on the optical properties of the Russian fersmite is incomplete, and only the roughest comparison can be made. However, the optical properties listed in the initial description of fersmite, together with the optical constants of the Ravalli County material as measured by the writers, are given in Table 3.

The minimum and maximum indices of refraction were measured in lithium light using the procedures outlined by Merwin and Larsen (1912) in which mixtures of selenium and amorphous sulfur are used for immersion media. The 2V was established by use of a universal stage.

TABLE 3. A COMPARISON OF OPTICAL DATA FOR FERSMITE

	Ravalli County, Montana	Vischnevye Mts. Central Urals
Indices of refraction	α=2.07 (Li) β=2.08 (Calc.) γ=2.19 (Li)	About 2
Pleochroism	x and y=pale greenish yellow to colorless z =dark greenish yellow to olive yellow	Not listed
2V	20°–25°	Large
Sign	+	Probably +
Birefringence	0.12	Medium

TABLE 4. A COMPARISON OF CHEMICAL ANALYSES OF FERSMITE

Ravalli County, Montana		Vishnevye Mts. Central Urals	
		Pegmatite 1 (complete anal.)	Pegmatite 2 (partial anal.)
CaO	15.02	14.49	15.53
Cb_2O_5	74.44	70.12	71.51
Ta_2O_5	n.d.	Trace	
REO	6.36[a]	4.79[b]	3.98
TiO_2	2.01	3.21	2.94
SiO_2	0.32	0.72	
MnO	0.11	0.48	
Fe_2O_3	0.34	1.71	1.25
ThO_2	0.10		
Al_2O_3	0.10	1.28	
MgO	n.d.	0.98	0.97
Na_2O	n.d.[c]	0.46	
F	n.d.[d]	1.87	
U_3O_8	0.08		
H_2O	0.18	0.72	
Total	99.04	100.83	96.18

n.d.—not detected.

[a] Shown to be essentially La_2O_3 by x-ray spectrographic analysis with only minor CeO_2.

[b] Reported as 80% Ce group, 10% Y group, and 10% ThO_2.

[c] Confirmed by flame photometry.

[d] Confirmed by molecular spectroscopy.

Chemical Composition

A chemical analysis of the Ravalli County fersmite conforms closely to the AB_2O_6 formula, (Ca, Ce, Na) (Cb, Ti, Fe, Al)$_2$ (O, OH, F)$_6$, originally reported by Bohnstedt-Kupletskaya and Burova (1946). However, as shown in Table 4, sodium and fluorine are absent in the Ravalli County fersmite, and lanthanum rather than cerium represents the major rare-earth constitutent.

Acknowledgments

The x-ray data included in this report required special effort by P. A. Romans and M. P. Krug of the Albany Bureau of Mines laboratory. The authors also thank Louis Erickson, owner of the Dark Star claim, for supplying the test samples and providing helpful information concerning the deposit. Thanks are extended to Dr. Michael Fleischer of the U. S. Geological Survey who, during a visit by the senior author in March 1956, reviewed the basic data and offered advice concerning proper classification of the mineral.

References

Bohnstedt-Kupletskaya, E. M. and Burova, T. A. (1946), Fersmite, a new calcium niobate from the pegmatites of the Vishnevye Mts., the Central Urals: *Compt. rend. (Doklady) Acad. Sci. U.R.S.S.*, **52,** 69–71.

——— (1947), New mineral names, fersmite: *Am. Mineral.*, **32,** 373.

Sahinen, U. M. (1957), Mines and mineral deposits, Missoula and Ravalli Counties, Montana: *Mont. Bur. Mines and Geol. Bull.* No. 8, 53–54.

Ross, C. P. (1950), The eastern front of the Bitterroot Range, Montana: *U. S. Geol. Surv. Bull. 947-E.*

Merwin, H. E. and Larsen, E. S. (1912), Mixtures of amorphous sulfur and selenium as immersion media for the determination of high refractive indices with the microscope: *Am. Jour. Sci.*, 4th ser., **34,** 42–47.

Manuscript received April 29, 1958

THE AMERICAN MINERALOGIST, VOL. 44, JANUARY-FEBRUARY, 1959

MANGANOMOSSITE RESTUDIED

C. OSBORNE HUTTON, *Stanford University, California.*

ABSTRACT

Manganomossite from Yinnietharra, Western Australia, is metamict columbite with $UO_2 = 0.96$ per cent. The untreated mineral with density = 6.17 and R.I. = 2.27, gives weak, diffuse powder and single crystal patterns with relatively few lines or spots, but after being heated in vacuo at 800° C. or at 1,200° C. for periods of $\frac{3}{4}$ hour, the density of the mineral showed an increase to 6.32 in each case, and powders prepared therefrom yielded identical but strong patterns with numerous lines, although some diffuseness remains in the high 2θ region. This x-ray pattern may be indexed for an orthorhombic unit cell with the following dimensions: $a_o = 5.09$ Å, $b_o = 14.31$ Å, $c_o = 5.725$ Å, but it is not possible to index the films on the basis of tetragonal symmetry. Autoradiographs show that zonary distribution of radioactivity may or may not be present, but the mineral appears to be free from radioactive centers or inclusions.

A complete analysis of the mineral after elimination of water leads to the formula: $(Mn, Fe, U, Th)_{3.97}(Nb, Ta, Ti)_{7.99}O_{24}$.

INTRODUCTION

In his annual report, Bowley (1923, p. 120) states that a mineral found by a Mr. R. C. Black at Yinnietharra, Western Australia, exhibits physical and chemical properties that suggest that it is either orthorhombic "manganocolumbite," or more probably "the corresponding tetragonal species which has not yet received a name." However, the name "manganomossite" was indeed suggested in this report but with some hesitation. At a slightly later date, it was reported by Spencer (1925, p. 460) under the title of manganomossite in his "Tenth List of New Mineral Names." From that time until publication of the first volume of the seventh edition of Dana's System of Mineralogy the original nomenclature was retained and accepted, but Palache, Berman, and Frondel (1946, p. 776) and later Hutchinson (1955, p. 445) clearly draw attention to the doubtful status of the mineral in question. Finally in "Minerals of Western Australia" (Simpson, 1952, p. 184), the mineral is listed once more as manganomossite, but with the comment that it is more probably the tetragonal rather than the orthorhombic species.

During a recent study of tapiolite, the problem arose as to the extent to which tantalum may be replaced by niobium in this mineral group and the mineral described by Bowley appeared worthy of further study. Through the courtesy of Mr. J. C. Hood, Director of the Western Australia Government Chemical Laboratories, a type specimen of manganomossite from Yinnietharra was secured. Upon completion of the work recorded here with the material just mentioned, a second specimen labelled "manganomossite, W. Australia" was found in an old collection. Whether this latter material is from Yinnietharra is quite uncertain, but

it should be noted that the density and x-ray diffraction patterns are identical with those determined for the precisely located specimen. In only one respect, however, may some distinction be made, and this concerns the different autoradiographs obtained from the two specimens.

Physical Properties

When crushed, manganomossite breaks into fragments bounded by strikingly brilliant conchoidal fracture surfaces; this is characteristic of many minerals that have been transformed into the metamict state, such as polycrase-euxenite, eschynite-priorite and many others. On the other hand, the general appearance of the fragments of manganomossite is rather distinct from that found for undoubted tapiolite-mossite from several localities, e.g. mossite from Råde, Norway, and tapiolite from Tazenakht, Morocco. In oblique illumination, the black or dark brown fragments exhibit an adamantine luster with occasional deep red internal reflections, and the very thin edges of conchoidally fractured particles are translucent and deep brown in color. In thin section or in particles less than 0.02 mm. in thickness, the Yinnietharra mineral, which appears to be quite homogeneous, is translucent with a clear brown color reminiscent of that observed for picotite. Most particles are isotropic but a range of birefringence is apparent in others, and although no exact measurements have been made, a value of 0.015 is certainly not exceeded, and it is usually very much less than this. The refractive index, determined by mounting finely crushed material in sulphur-selenium melts, is 2.27.

The density of carefully hand-picked fragments was determined with a microbalance, and for untreated pure material, a value of 6.17 gm/cm^3 $\pm$0.01 at 21° C. was obtained. The same fragments were then sealed in vacuo in silica capillaries and heated in turn to 800° C. and 1,200° C. for $\frac{3}{4}$ hour, and following these two heat-treatments, the density of the particles was found to be 6.32 gm/cm^3 $\pm$0.02 at 20° C. in each case. These data are to be compared to the figure of 6.21 reported by Bowley (1923), presumably for untreated material. Now all of these values seem to be too low for a member of the tapiolite-mossite series, but are comparable to those expected for a member of the orthorhombic columbite-tantalite group of minerals. Heating at 1,200° C. for periods of time ranging up to 14 hours did not produce any significant change in density from that found for the shorter period of time. This situation is in contrast to the circumstances reported by Arnott (1950, pp. 397–8) for euxenite.

Autoradiographs were prepared with polished sections of the two specimens of manganomossite. The Yinnietharra material exhibits a weak but perfectly uniform distribution of radioactivity, and there are

no indications of inclusions or highly radioactive centers. On the other hand, the radiograph (Fig. 1) yielded by material from an unspecified Western Australia locality clearly shows regular distribution of radioactive matter. A distinct range of uranium and thorium content is evident in the different zones, but there is no progressive increase or decrease in radioactivity from center to periphery. A somewhat similar circumstance has been reported by Heinrich and Giardini (1956, p. 1705) for columbite from an unspecified locality in Canada.

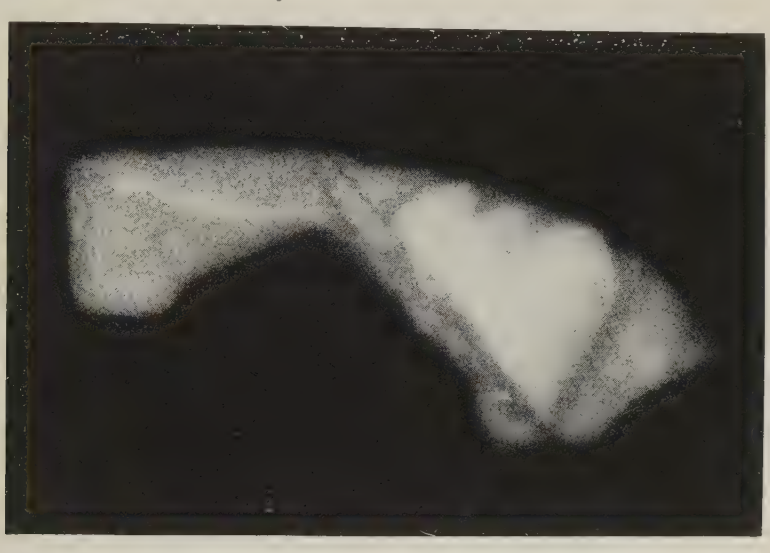

FIG. 1. Autoradiograph of manganomossite (=columbite), from an unspecified locality in Western Australia. Exposure time: 192 hours. Magnification: ×5.5.

X-RAY DATA

The powder pattern yielded by untreated manganomossite exhibits relatively few lines, and those that are found at angles greater than about 65° 2θ are so faint and diffuse that accurate measurement is out of the question. This pattern suggests that the mineral is in a metamict condition, and a single fragment, instead of a powder, was employed as diffraction material to check this suggestion. In the film thus obtained, reflections at low 2θ angles are distinct but not precise spots; at angles greater than 65° 2θ, the reflections are so streaked out that imperfect lines or arcs result.

When the mineral is heated in vacuo at 800° C. or at 1,200° C. for $\frac{3}{4}$ hour, single fragments of the material so prepared are now found to yield similar but much more precise reflections than before, although streak-

ing out of spots into arcs is still quite evident above 90° 2θ. In the powder pattern, the lines are much more precisely defined than in films yielded by unheated manganomossite, except at high 2θ angles, where bands up to 2.0 mm. in width are found. Heat-treatment of this mineral at lower temperatures and for a wide range of periods of time failed to produce material that yielded films with greater sharpness in the back-reflection region.

X-ray diffraction powder patterns for unheated and heated manganomossite are given in Table 1 together with a powder pattern of tantalite from Quixeramobin, Ceará, Brazil. It will be noted that the lines yielded by the unheated material correspond in a general way only with the stronger lines found in the pattern for heat-treated manganomossite. It is evident, however, that the former has slightly larger cell dimensions than the heat-treated mineral; this is in conformity with the data obtained by density determinations. The similarity of the *d*-spacings for manganomossite and tantalite is clear, although a number of fainter lines yielded by the former are not matched in the tantalite pattern.

The powder pattern of the recrystallized mineral may be indexed on the basis of orthorhombic, but not tetragonal, symmetry, and it has been possible to determine the approximate unit cell dimensions. Calculated and measured *d*-spacings conform reasonably well up to about 62° 2θ, but beyond that point, diffuseness of lines has rendered measurements less precise than is desirable, thus preventing refinement of dimensions. Furthermore, without the benefit of single crystal photographs, the large number of choices renders indexing of the larger 2θ values less meaningful. It will be noted that it has not been possible to index four lines, *viz.* 4.62, 3.30, 3.10, and 1.801, and since freedom from impurities seems assured by the care taken to prepare the samples studied, one is led to the belief that heat-treatment may have produced a minute quantity of a second, but as yet unidentified, phase. The unit cell dimensions determined from the powder patterns are as follows: $a_0 = 5.09$ Å, $b_0 = 14.31$ Å, $c_0 = 5.725$ Å; thus $a_0 : b_0 : c_0 = 0.355 : 1 : 0.393$, or $a : b : c = 0.393 : 1 : 0.355$ if the orientation of Schrauf (Palache, Berman, and Frondel, 1946, p. 780) is adopted. These values are comparable to those recorded previously for members of the columbite-tantalite series (Sturdivant, 1930, p. 89), and therefore, there seems little doubt that manganomossite of Yinnietharra, Western Australia is a member of this group of minerals.

Chemical Composition

A sample of nearly five grams was prepared for chemical analysis by electromagnetic fractionation of material that had been crushed and graded to give a particle-size range of 44–62 microns. The material sub-

TABLE 1. *X*-RAY DIFFRACTION DATA FOR TANTALITE AND COLUMBITE (=MANGANOMOSSITE)

Radiation: CuKα=1.5418 Å
Camera diameter: 114.59 mm.

A	B		C			
d Å	*d* meas.	I	*d* meas.	*d* calc.	I	*h k l*
7.11	—		7.07	7.15	2	020
—	—		5.30	5.31	1	011
—	—		4.62	—	<1	—
—	—		—	3.67	6	111
3.66	3.66	3	3.66	3.66		031
—	—		—	3.58	1	040
3.57	—		3.57	—	2	—
—	3.325	<1	3.30	—	<1	—
—	—		3.10	2.97	10	131
2.97	2.98	5	2.97	2.863	3	002
2.86	—		2.852	2.544	2	200
2.54	2.585	1	2.54	2.494	4	102
2.49	2.505	1	2.49	2.397	3	220
—	—		—	2.386		060
2.38	2.38	<1	2.388	2.244	<1	230
—	—		—	2.211	2	221
—	2.221	<1	2.238	2.2095		132
—	—		—	2.091	3	231
2.21	—		2.208	2.046	1	142
—	—		—	1.901	3	202
2.09	2.109	<1	2.081	1.833	4	062
2.04	—		2.045	—	<1	—
1.907	—		1.900	1.772	5	033
1.833	1.824	<1	1.835	1.767		232
1.799	—		1.801	1.7405	3	260
—	—		—	1.734		123
1.774	1.773	<1	1.7715	1.725	6	162
—	—		—	1.673	<1	133
—	—		1.7405	—	<1 B	
—	—		1.734	—	<1	
1.740	1.751	1	1.7405			
—	—		—			
1.724	1.721	2	1.725			
—	—		1.6745			
—	—		1.6125			
—	—		1.578			

A: Tantalite; Quixeramobim, Ceará, Brazil (Tavora, 1955, table 1, p. 18). Nine *d*-spacings listed by Tavora are omitted from Table I.

B: Manganomossite, Yinnietharra, Western Australia. Specimen is unheated.

C: As for B, but specimen has been heated in vacuo for $\frac{3}{4}$ hour at 1,200° C.

(*Continued on the next page*)

TABLE 1—(*Continued*)

A	B		C			
d Å	*d* meas.	I	*d* meas.	*d* calc.	I	*h k l*
1.541	1.551	1	1.5395	—	5	
1.488	—		1.4855	—	2	
—	—		1.471	—	4	
1.461	1.461	2 B	1.4545	—	5	
—	—		1.431	—	<1	
—	—		1.398	—	<1	
1.379	1.384	<1	1.380	—	3	
—	—		1.350	—	<1 B	
1.312	1.338	<1	1.314	—	2	
—	—		1.285	—	<1	
1.275	—		1.272	—	1	
1.247 B	—		1.245	—	2	
1.222 B	—		1.224	—	3	
1.193 B	—		1.195	—	5	
—	—		1.163	—	1	
1.137	—		1.139	—	2	
1.123	—		1.1235	—	1	
—	—		1.1165	—	1	
1.102	—		1.103	—	4	
1.089	—		1.091	—	1 B	
1.076 B	—		1.080	—	2 B	
—	—		1.059	—	<1 B	
—	—		1.0445	—	1 B	
1.035 B	—		1.0335	—	4 B	
1.022 B	—		1.022	—	2 B	
—	—		1.0125	—	1 B	
0.995 B	—		0.995	—	4 B	
0.982 B	—		0.980	—	3 B	
—	—		0.958	—	2 B	
0.932 B	—		0.932	—	3 B	
0.923 B	—		0.925	—	3 B	
—	—		0.916	—	3 B	
0.901 B	—		0.904*	—	1 B	

* About sixteen more lines are present in the film but they are too broad and diffuse to justify any attempt at measurement.

sequently analyzed was rejected at 0.29 amps. and attracted at 0.31 amps. when the Frantz separator was set with a longitudinal slope of 15° and a tilt of 10°.

The analysis of manganomossite carried out by the author is reported here (Table 2) with some reservations owing to the difficulties that were encountered in the work. The methods employed involved, in the main,

pyrosulphate fusion of the finely powdered mineral, and after separation of iron etc., fractionation of niobium and tantalum by the tannin procedure (Schoeller, 1937). Although iron is reported as Fe^{2+}, this element was determined as total iron in the ferric state, and titanium has been determined colorimetrically in a separate portion. Water given off above 105° C. was determined by the standard Penfield method.

The new analysis shows slight differences from that made at an earlier

Table 2. Analyses of Manganomossite, Yinnietharra, Western Australia

	A	*B*	*C*	*D*	Total No. of Metal Atoms
MnO	12.02	9.42	9.66	2.18	3.97
FeO	4.64	7.61	7.77	1.74	
UO_2	—	0.96	0.96	.05	
ThO_2	—	0.059	0.06	—	
Nb_2O_5	34.64	40.69	41.53	5.03	7.99
Ta_2O_5	44.53	38.86	39.66	2.89	
TiO_2	3.92	0.40	0.41	.07	
H_2O+	0.26	2.16			
H_2O-	—	0.31			
	100.1	100.47	100.00		

Formula: $(Mn, Fe, U, Th)_{3.97}(Nb, Ta, Ti)_{7.99}O_{24}$

A: Manganomossite, Yinnietharra, Western Australia. Anal. D. G. Murray (Bowley, 1923, p. 120). The analyst found SnO_2 to be absent.

B: Manganomossite, Yinnietharra, Western Australia. Anal. C. Osborne Hutton. U and Th were determined by Mr. Harry Levine, and that analyst's figure for U has been recalculated by the author as UO_2.

C: Analysis B, after elimination of water, has been recalculated to give a summation of 100, Mr. Levine's figures for U and Th excepted.

D: Metal atoms, calculated from analysis C, on the basis of 24 atoms of oxygen to the unit cell.

date by Murray (Bowley, 1923), notably in the higher ratios of Nb:Ta and Fe:Mn in the former. Through the courtesy of Dr. Esper S. Larsen 3rd, very careful determinations of both uranium and thorium were made by Mr. Harry Levine on a split of the magnetically fractionated material that was used for the full chemical analysis. Mr. Levine reported the following results: $ThO_2 = 0.059$ per cent, ± 0.001, and $U = 0.86$ per cent, ± 0.02; these figures are averages of four and eight determinations respectively.

The analysis in Table 2, column C, has been recalculated on the basis

of 24 oxygens to give the numbers of metal ions in the unit cell (column D), and owing to similar ionic sizes, U^{4+} and Th^{4+} have been grouped with Mn^{2+} and Fe^{2+}, whereas Ti^{4+} has been placed with Ta^{5+} and Nb^{5+}. When this is done, the ratio of A:B ions does not depart significantly from the ratio of 4:8 required by the formula for members of the columbite-tantalite series. The presence of a small amount of titanium and uranium in the mineral described here might lead one to suspect the presence of inclusions of samarskite, or other multiple oxides of Nb, Ta, and Ti, similar to the circumstances described by Karunakaran and Neelakantan (1948) or Grigoriev (1945) for columbite-samarskite intergrowths from Nellore, India, and the Ilmen Mountains, Russia, respectively. However, the *x*-ray diffraction data, autoradiographs, and optical study would seem to discredit this idea, and, therefore, it is believed that titanium, uranium, and thorium are all present as ions in the structure of the Western Australia columbite. In this connection, it should be noted that the mineral described by Ellsworth (1926, pp. 332–334) as toddite contains a high percentage of uranium (U = 9.65 per cent) and a minor amount of titanium (TiO_2 = 0.85 per cent). Hey (1955, p. 225) and Palache, Berman and Frondel (1946, p. 786) suggest that this mineral is a mixture of columbite and perhaps, euxenite, but it is the present writer's view that the low titanium content relative to uranium suggests that some mineral other then euxenite may be a more probable contaminant; samarskite would seem to be a much more likely possibility.

From the relationship, density = $5.20 + (0.03 \times \%\ Ta_2O_5)$ established for the columbite-tantalite series, the mineral analyzed by the present writer should have a density of about 6.38, compared to the values 6.39 calculated from unit cell dimensions and composition, and 6.32 determined experimentally for the heat-treated material. Furthermore, according to the diagram of Hermann and Gastellier (1946, p. 81) a member of the columbite-tantalite series with 38.83 per cent Ta_2O_5 would be expected to have a density of 6.18–6.31, whereas the data of Mathieu (*vide* Herman and Gastellier, 1946, p. 81) suggest a figure of 6.24. The density for manganomossite recorded by Bowley is 6.21, presumably for unheated material, and since Murray's analysis lists an insignificant amount of water, it is assumed that heat-treatment would not alter this figure to any marked degree. Accordingly, a member of the columbite-tantalite series with this density would be expected to have approximately 33.66 per cent Ta_2O_5 compared to the figure of 44.54 per cent reported by Bowley. Alternatively, if we assume that the percentage of Ta_2O_5 in Murray's analysis is correct, or nearly so, the corresponding density would be close to 6.53. These anomalies cannot be clearly re-

solved, but the data set out here suggest that the mineral analyzed by Murray may have contained a great deal more water than the amount reported by him, that is, of course, assuming that his figures for tantalum and niobium are correct or approximately so.

Nomenclature

Physical and chemical data presented here would clearly seem to indicate that manganomossite from Yinnietharra, Western Australia is a member of the columbite-tantalite series, and that it does not belong to the tetragonal tapiolite-mossite group of minerals. Furthermore, the mineral is metamict. In an earlier note on this mineral, and on the basis of a preliminary determination of niobium by fluorescence analysis, the writer (Hutton, 1957) defined this mineral as tantalite. This is incorrect, since the chemical analysis reported here shows that niobium is in excess of tantalum (molecular ratio), and since the ratio Fe:Mn=1.74:2.18, neither of these elements is sufficiently dominant to require specific mention in the mineral name. Accordingly, the mineral previously called manganomossite should be removed from that category, and referred to, instead, as metamict columbite.

Acknowledgments

I wish to extend my thanks to Mr. J. C. Hood, Director of the Western Australia Government Chemical Laboratories for his kindness in making available for this study a specimen of type material from Yinnietharra, and to Dr. Esper S. Larsen 3rd, and Mr. Harry Levine, both of the U. S. Geological Survey, Washington, D.C. for their helpfulness in connection with uranium and thorium determinations. I wish to record my indebtedness to the Shell Fund for Fundamental Research for a grant to purchase accessory equipment to facilitate some of the *x*-ray work carried out in this study.

References

Arnott, R. J. (1950), *X*-ray diffraction data on some radioactive oxide minerals: *Am. Mineral.*, **35,** 386–400.

Bowley, H. (1923), *Ann. Rep. Dept. Mines, W. Australia (for 1922), Div. 7, Sec. 2, Mineralogy. Mineral Technology, and Geochemistry*, 117–120.

Ellsworth, H. V. (1926), Toddite—A new uranium mineral from Sudbury District, Ontario: *Am. Mineral.*, **11,** 332–334.

Grigoriev, D. P. (1945), Regular intergrowth of samarskite and columbite from the Ilmen Mts., *Mem. Soc. Russe Min.*, **74,** 57–60.

Heinrich, E. Wm. and Giardini, A. A. (1956), Radioactive columbite-tantalite: *Geol. Soc. Amer. Bull.*, **67,** 1704–1705.

Herman, P., and Gastellier, S. (1946), Détermination rapide de teneurs en Ta_2O_5 et Cb_2O_5. Des columbites: *Bull. du Service Geologique Congo Belge et Ruanda Urundi*, no. **2,** pt. 1, 73–83.

Hey, M. H. (1955), An index of mineral species and varieties arranged chemically: British Museum, London.

Hutchinson, R. W. (1955), Preliminary report on investigations of minerals of columbium and tantalum and of certain associated minerals: *Am. Mineral.*, **40,** 432–452.

Hutton, C. Osborne (1957), Metamict tantalite from Western Australia: *Nature,* **180,** 248.

Karunakaran, C., and Neelakantam, K. (1948), Samarskite from Nellore District. Part 1. Uranium and earth acid contents: *Proc. Indian Acad. Sci., Sect. A*, **25,** 404–407.

Palache, C., Berman, H., and Frondel, C. (1946), Dana's System of Mineralogy, 7th ed., Vol. I, John Wiley and Sons, Inc., New York.

Schoeller, W. R. (1937), The Analytical Chemistry of Tantalum and Niobium, Chapman and Hall, Ltd., London.

Simpson, E. S. (1952), *Minerals of Western Australia*, vol. **3,** Govt. Printer, Perth, W. Australia.

Spencer, L. J. (1925), Tenth list of new minerals names; with an index of authors: *Mineral. Mag.*, **20,** 44–477.

Sturdivant, J. R. (1930), The crystal structure of columbite: *Zeits. Krist.*, **75,** 88–108.

Tavora, E. (1955), *X*-ray diffraction powder data for some minerals from Brazilian localities: *Anais da Acad. Brazil. de Ciênias*, **27,** 7–27.

Manuscript received April 23, 1958

THE AMERICAN MINERALOGIST, VOL. 44, JANUARY–FEBRUARY, 1959

MATRIX CORRECTIONS IN THE *X*-RAY SPECTROGRAPHIC TRACE ELEMENT ANALYSIS OF ROCKS AND MINERALS

JOHN HOWER, *Montana State University, Missoula, Montana.*

ABSTRACT

Three matrix effects must be accounted for in *x*-ray spectrographic analysis. They are: (1) attenuation of the incoming beam, (2) mutual excitation of the elements, and (3) absorption of the outgoing fluorescent radiation. Only effects (1) and (3) are appreciable for most trace elements in the *x*-ray spectrographic analysis of common rocks and minerals. The effects are determined by the mass absorption coefficient of the rock or mineral. Curves are plotted of the mass absorption coefficient versus wave length for elements that are commonly major constituents in rocks and minerals. These plots show that the relative absorptions of the elements are virtually constant at all wave lengths. Curves are presented of the absorption of various rocks relative to an aluminum oxide standard. The relative absorptions are virtually constant between absorption edges. A complete matrix correction can be made for nickel and heavier elements by determining the absorption of a rock relative to aluminum oxide at one wave length. The relative absorption can be determined by two methods: (1) by calculation if the major constituent analysis is known; the necessary data are presented, (2) by use of an internal standard if it is not. Partial matrix corrections can be made for the lighter elements Co, Mn, Cr, V, and Sc. Both methods are illustrated.

INTRODUCTION

As in other instrumental methods of chemical analysis, the primary problem in *x*-ray spectrography is to adjust intensity measurements on an unknown sample to the basis of a standard. The intensity measurements in *x*-ray spectrography are counting rates of the characteristic radiation of the analysis elements. The purpose of this paper is to outline methods of matrix correction in the quantitative *x*-ray spectrographic trace element analysis of rocks and minerals. The specific method outlined assumes that the rock or mineral contains as major constituents only the following elements: C, O, Na, Mg, Al, Si, K, Ca, Ti, and Fe. The presence of other elements as major constituents will alter the specific method suggested, but not the principles on which it is based.

Emission spectroscopists have developed the internal standard method to correct for the effects of a changing matrix on the intensities of the optical emission lines of the elements. The selection of an internal standard in emission spectroscopy is dictated by the average gross composition of the samples, the chemical compounds present, the relative volatility of the elements, and the excitation potentials of the analysis elements. In trace element analysis of rocks and minerals by *x*-ray spectrography, the matrix correction for most elements is wholly one of correcting the gross *x*-ray absorption coefficient of the analysis sample to the basis of a standard. The gross absorption coefficient of the sample is dependent only on bulk chemical composition. Matrix corrections for major con-

stituent analysis are more complex and have been worked out for simple systems only (Beattie and Brissey, 1954, Burnham et al., 1957). Partial matrix corrections have been used by the addition of an internal standard (e.g. Norton, 1957, Stevenson, 1954).

The following effects have to be taken into account in making a matrix correction in any spectrographic analysis (Sherman, 1955): (1) The attenuation of the incoming exciting beam, (2) mutal excitation of the elements, and (3) absorption of the outgoing fluorescent characteristic radiation of the analysis elements. Methods of correcting for these effects in the trace element analysis of rocks and minerals will be discussed in the main body of this paper.

Use of Absorption Coefficients for Matrix Correction

The equation for the absorption of x-rays takes the form:

$$I_x = I_o e^{-\mu x}$$

where

I_o is the intensity of the primary beam
I_x is the intensity of the beam after passing a distance x through a given material
μ is the linear absorption coefficient of the material

The linear absorption coefficient is dependent on the wavelength of the beam and the density of the material. A more useful form of the absorption coefficient is μ/ρ, where ρ is the density of the material. This is called the mass absorption coefficient and is independent of the physical state of the sample.

A simple example of how mass absorption coefficients can be used in x-ray spectrography is as follows. A sample of iron and a sample of aluminum contain equal amounts of nickel in the part-per-million range. The difference between the measured intensity of the NiKα radiation from the two samples can be determined simply on the basis of the mass absorption coefficients of the matrices. The mass absorption coefficient of iron at 1.659 Å (NiKα radiation) is 410; that of aluminum is 60.7. That is, iron absorbs NiKα radiation 410/60.7 (6.75) times as efficiently as aluminum. As will be shown later, the incoming radiation that excites NiKα radiation is absorbed the same relative amount. Nickel is not excited by either Fe or Al characteristic radiation. The NiKα radiation from the aluminum sample would thus be 6.75 times as intense as that from the iron. Note that only relative absorption is important. If the samples have the same effective volume, the *absolute* amount of nickel in the iron sample is greater by the ratio of the density of iron to the density of aluminum. However, this increase is exactly compensated for by the increase in *absolute* absorption of the iron sample, providing both

samples have the same surface area and their thickness is in excess of significant penetration. In the analysis of unknown samples the process would be worked in reverse; i.e., equal intensities from both samples would mean 6.75 times as much nickel in the iron sample than in the aluminum.

For compounds, the mass absorption coefficients of the constituent elements are additive. A generalized equation for calculating the mass absorption coefficient of a compound (Cullity, 1956) is:

$$\mu/\rho \text{ compound} = w_1(\mu/\rho)_1 + w_2(\mu/\rho)_2 + \cdots w_n(\mu/\rho)_n$$

where, w_1, w_2, $\cdots$, w_n are the weight fractions of each element in the compound and $(\mu/\rho)_1$, $(\mu/\rho)_2$, $\cdots$ $(\mu/\rho)_n$ are the mass absorption coefficients of each element at a given wavelength. As an example, μ/ρ for Al_2O_3 can be calculated for NiKα radiation. Aluminum oxide is 52.9% Al and 47.1% O; μ/ρ of Al at NiKα is 60.7 and μ/ρ of O is 14.0. Therefore, the mass absorption coefficient of Al_2O_3 at NiKα is

$$\mu/\rho(Al_2O_3) = 0.529 \times 60.7 + 0.471 \times 14.0$$
$$= 38.7$$

Efficient Range of the *X*-Ray Spectrograph for Trace Element Analysis

The lightest element that can be detected with present commercially available *x*-ray spectrographic equipment is Mg (atomic number 12). The sensitivity of *x*-ray spectrographs drops off with decreasing atomic number from somewhere around Z=28 (Ni). For the analysis of trace elements in rocks the sensitivity is generally sufficient only for those elements higher than Ca (Z=20). Therefore, the discussion of trace element analysis will be restricted to elements from Z=21 and higher. When desirable, however, the principles can be applied to the other elements.

Calculation of the Mass Absorption Coefficient of a Rock

It is possible, by using data present in the literature (Handbook of Chem. and Phys., 1949, pp. 2031–2036) to calculate the mass absorption coefficient of any rock in the range of wavelengths used for *x*-ray spectrographic trace element analysis (approximately 0.4 to 3.0 Å). Figures 1*a* and 1*b* are plots of the available data of the mass absorption coefficient (μ/ρ) versus wave length (λ) for the elements that are commonly major constituents (>1 per cent) in rocks and minerals. The elements included are Fe, Ca, Mg, Na, Al, O and C. Iron is plotted separately because of its absorption discontinuity (the K absorption edge) in the wave-length

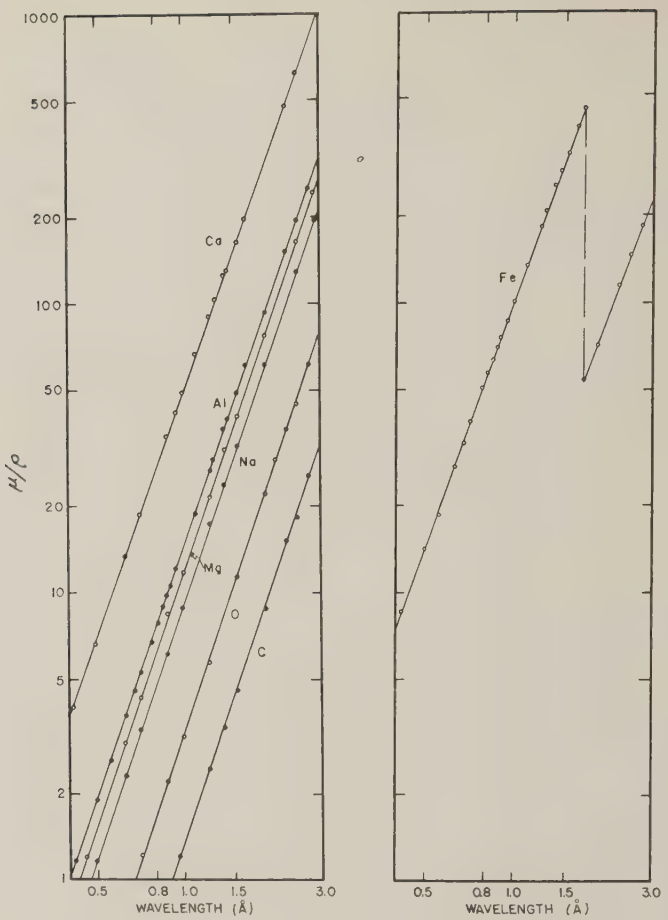

FIG. 1. Plots of the available data of mass absorption coefficient (μ/ρ) versus wave length (λ) for elements that are commonly major constituents in rocks and minerals.

range of interest. The slopes of these curves are tabulated in Table 1. Note that there is only a small change in slope (increasing with decreasing atomic number) between the lightest and heaviest element. This means that the relative absorptions of the elements are virtually independent of wave length.

No mass absorption coefficient data are available for the elements Si, K, and Ti, but it is possible to obtain the data empirically. If several points of the μ/ρ versus λ curve for an element can be found, the full curve can be drawn by using an average slope obtained from two bracketing elements. The points to define the position of the curve can be ob-

TABLE 1. SLOPES OF THE MASS ABSORPTION COEFFICIENT VERSUS WAVE-LENGTH CURVES

Element	Slope of μ/ρ vs. λ curve
Fe	2.81
Ca	2.81
Al	2.84
Mg	2.89
Na	2.89
O	2.93
C	2.94

tained from a relationship between the absorption coefficient at a given wave length and the wave length of the K absorption edge. A plot of this kind is shown in Fig. 2; the mass absorption coefficients at 1.000 Å are plotted against the K absorption edges for the elements bracketing K, Si, and Ti. Since the K absorption edges of K, Si, and Ti are known, their mass absorption coefficients at 1.000 Å can be obtained empirically from the curve. By finding several points in this manner and using slope averages of bracketing elements, accurate curves can be plotted for K, Si, and Ti.

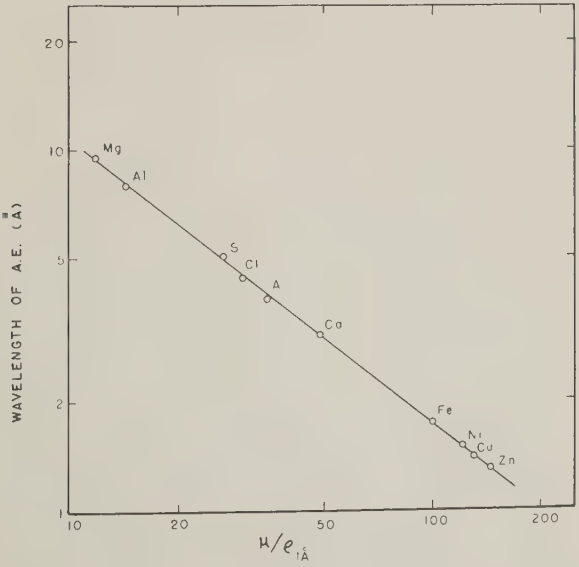

FIG. 2. Relation between the mass absorption coefficient at a given wave length and the wave length of the K absorption edge.

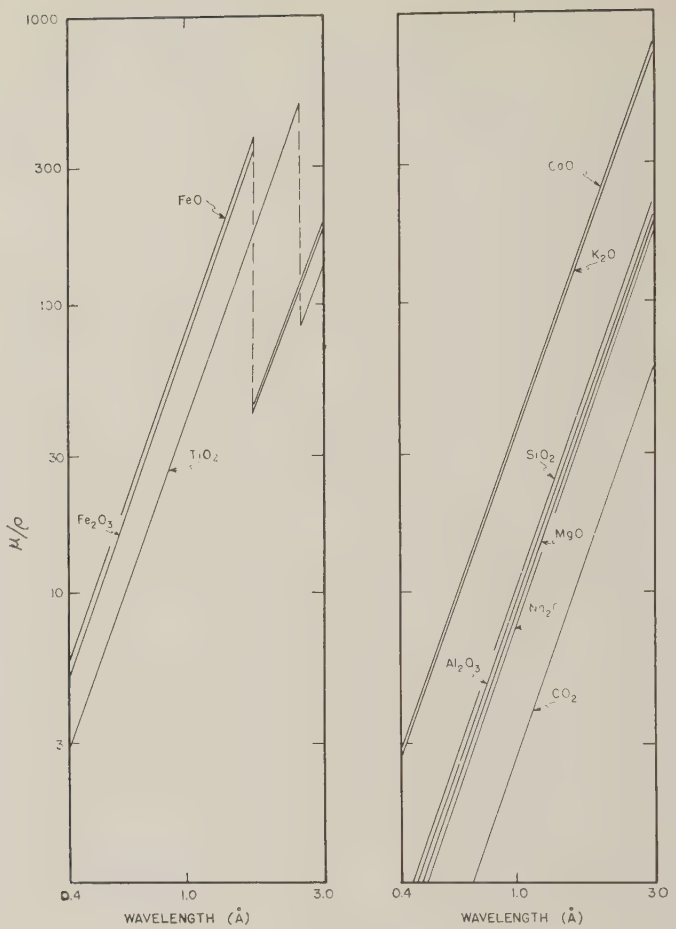

FIG. 3. Plots of the mass absorption coefficients of the oxides of all elements that are commonly major constituents in rocks and minerals.

Since chemical analyses are reported as oxides of the elements, it is more convenient to work with the mass absorption coefficients of the oxides. Mass absorption coefficient versus wave-length curves for the oxides of all the common major elements are plotted in Fig. 3. Points for the curves were calculated by use of equation (2). Now, by further use of equation (2) it is possible to calculate the mass absorption coefficient of a rock or mineral at any wave length. The solid curve in Fig. 4 is a plot of μ/ρ versus λ for the standard diabase W-1. The chemical analysis was taken from Goldich and Oslund (1956). The curve shows discontinuities at 1.744 Å (K absorption edge of Fe) and at 2.497 Å (K absorption edge of

Ti). For use in trace element analysis it is more informative to plot the absorption of W-1 relative to the absorption of some standard matrix. Aluminum oxide has been chosen as a standard matrix because of its practical convenience in the preparation of trace element standards. The dashed curve in Fig. 4 is a plot of the ratio $\mu/\rho_{W-1}/\mu/\rho_{Al_2O_3}$ versus λ. The discontinuities are still present at the absorption edges, but between absorption edges the relative absorptions of the diabase and Al_2O_3 remain virtually constant. For example, there is a change of only 3 per cent between the relative absorptions at 0.4 Å and 1.744 Å.

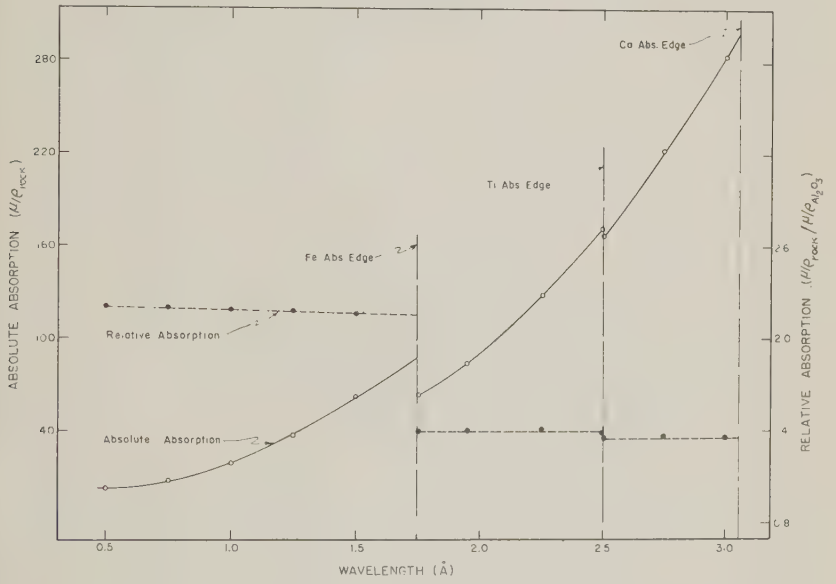

FIG. 4. Plots of the mass absorption coefficient of the standard diabase W-1 (solid curve) and the absorption of the diabase relative to Al_2O_3 versus wave length.

The same relation holds for all varieties of silicate rocks. Figure 5 shows relative absorption curves calculated for a diabase (W-1), a granite (G-1), a shale, and a dunite.

MATRIX CORRECTIONS

For convenience the x-ray spectrum is broken up into three regions: region (1), wave lengths shorter than the K absorption edge of iron, region (2), wave lengths between the K absorption edges of iron and titanium, and region (3), wave lengths between the K absorption edges of titanium and calcium. For the characteristic K radiation, region (1) includes all elements from nickel on up in atomic number; region (2)

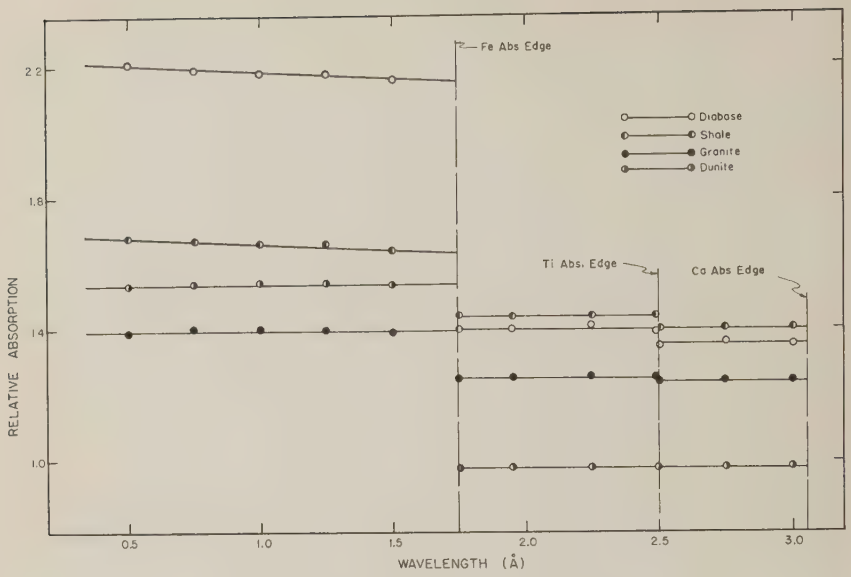

FIG. 5. Plots of the relative absorption versus wave length for a granite[1], a diabase[2], a shale[3], and a dunite[4].

1. The standard granite G-1 from Goldich and Oslund (1956).
2. The standard diabase W-1 from Goldich and Oslund (1956).
3. Analysis from Murray (1954), shale sample M52204.
4. Analysis from Clarke (1924), pg. 468, sample F.

includes cobalt, manganese, chromium, and vanadium; region (3) only scandium. Therefore, region (1) is quantitatively the most important.

The complete and partial corrections of matrix effects can now be discussed.

Attenuation of the Incoming Beam

The characteristic radiation of an element is generated by incoming *x*-rays of wave length shorter than the absorption edge (K or L) of the element. The excitation efficiency is greatest near the absorption edge. The curves in Fig. 5 show that the exciting radiation is absorbed (attenuated) a constant relative amount in a given rock for all elements with absorption edges in region (1). Therefore, the absorption of the analysis sample relative to a standard need be determined at only one point in order to make a quantitative correction for all elements in this region. The situation for elements with absorption edges at longer wave lengths is more complicated. For elements in region (2) a portion of the exciting radiation is absorbed strongly by iron, as it is for elements in region (1), and the rest only weakly absorbed. Unless the relative contributions

from each region to the excitation of the elements in regions (2) and (3) can be determined precisely, a quantitative correction cannot be made. No attempt will be made here to determine precisely this effect in these regions. Therefore, analysis of Co, Mn, Cr, V, and Sc must be considered only semi-quantitative. An approximate correction is suggested below.

Mutual Excitation of the Elements

This effect is negligible for the bulk of the trace elements—all those in region (1). Mutual excitation at the trace element level is not appreciable. Therefore, no correction is necessary when analyzing for Ni and heavier elements by using their K characteristic radiation. The effect should be appreciable for Mn, Cr, V, and Sc since they absorb iron characteristic radiation strongly. If the other matrix effects could be determined quantitatively, this effect could be determined empirically for these lighter elements. An approximate correction is suggested below.

Absorption of the Outgoing Fluorescent Characteristic Radiation

The curves in Fig. 5 show that the absorption of the analysis sample relative to the standard need be known at only one point in each region to make a quantitative correction. Trace elements do not contribute appreciably to the absorption. For example (Fig. 5), TiO_2 as a major constituent at 1.1 per cent in W-1 introduces an absorption difference of only four per cent.

Suggested Analytical Method

Standards for silicate rocks and minerals can be prepared by mixing any desired analysis elements and the internal standards suggested below with aluminum oxide. The specific method of matrix correction is best treated by regions:

Region (1)

This region contains the bulk of the trace elements. A quantitative matrix correction can be made simply by determining the absorption of the analysis sample relative to aluminum oxide at some point in the region. The relative absorption can be determined by calculation if the major constituent analysis is known or by use of an internal standard if it is not. For the calculation method working curves would be drawn on the basis of absolute intensities. The necessary mass absorption coefficient data are presented in Table 2. Any element in region (1) can serve as an internal standard for samples with unknown major constituent analysis. Arsenic (Table 3) is suggested because of its geological rarity.

Table 2. Mass Absorption Coefficients of the Oxides of the Major Elements at 1.000, 1.930, and 2.505 Å

Oxide	1.000 Å (Region 1)	1.930 Å (Region 2)	2.505 Å (Region 3)
SiO_2	10.1	65.8	135
Al_2O_3	9.13	59.8	129
Na_2O	7.56	51.1	106
MgO	8.36	55.1	115
CaO	36.7	228	462
K_2O	34.9	225	450
Fe_2O_3	70.8	56.3	116
FeO	78.5	60.3	124
TiO_2	38.7	248	85.0
CO_2	2.65	18.2	37.2
H_2O	3.13	21.7	44.5

Regions (2) and (3)

Only a semi-quantitative matrix correction can be made for Co, Mn, Cr, V, and Sc. The absorption of the fluorescent radiation can be adjusted quantitatively either by calculation or by use of one of the elements as an internal standard. However, the mutual excitation and the relative absorption of the incoming beam cannot be determined quantitatively. An approximate matrix correction for both of these effects can be made by using one of the elements as internal standard. The correction is only approximate because each element is affected somewhat differently by the matrix. Scandium is suggested as the internal standard when titanium is low, cobalt when titanium is high. A less accurate, but simpler, correction can be made when the major constituent analysis is known by making only an absorption correction by calculation. The necessary data are presented in Table 2.

Carbonate rocks can be analyzed in the same manner, but the standards should be prepared in a calcium carbonate matrix. Calcium is the dominant absorber in carbonate rocks and the slope of the μ/ρ versus λ curve is enough different from aluminum oxide to bring about a ten per

Table 3. Suggested Internal Standards

	Region (1) 1.744 Å	Regions (2) and (3) 1.744–3.070 Å
Low Ti	Arsenic	Scandium
High Ti	Arsenic	Cobalt

cent change from 0.4 to 3.0 Å. A single internal standard would suffice for most carbonate rocks. The data in Table 2 permit calculation if the major constituent analysis is known.

Semi-Quantitative Applications

The gross mass absorption coefficient of rocks is not greatly variable. The absorption usually varies between one and two times that of aluminum oxide. Even when the major constituent analysis is not known and no internal standard is used, a fairly good analysis could be made by

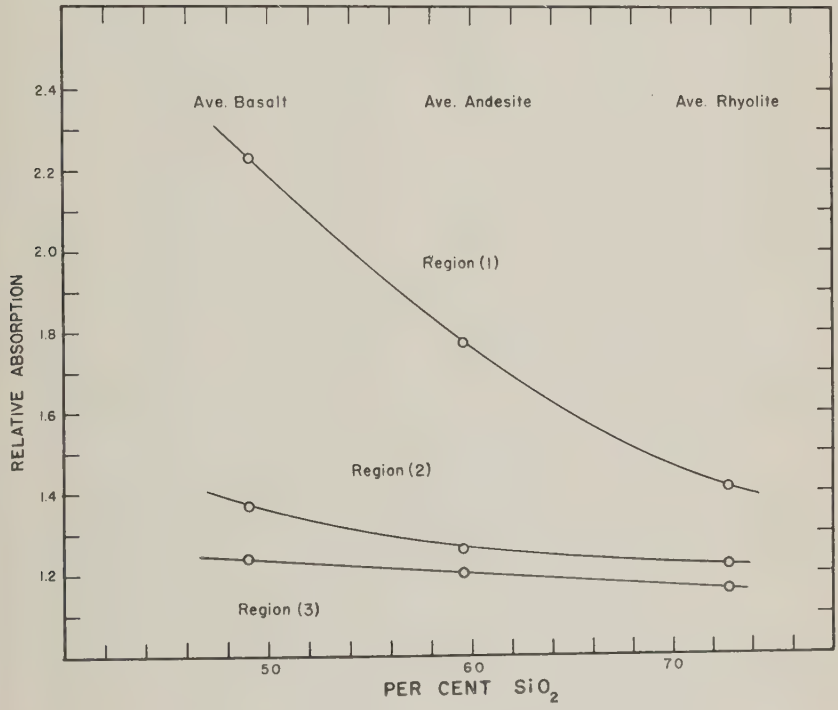

Fig. 6. Relative absorptions, in the three wave-length regions, of average igneous rocks ranging from basalt to rhyolite.

guessing at the absorption of the rock relative to aluminum oxide. Igneous rocks lend themselves well to such estimates. Figure 6 is a plot of the absorption relative to aluminum oxide, for the three regions, of the average igneous rocks ranging from basalt to rhyolite. The compositions used to calculate the points were taken from Daly (1933). By knowing approximately the rock type, the relative absorption can be estimated from the curves.

Quite good corrections can be made by calculation in the trace element analysis of a suite of samples of a mineral with relatively constant and fairly well known major constituent composition. Calcite, dolomite, and many of the simpler ore minerals such as galena and pyrite could be treated in this manner.

Matrix Corrections in G-1 and W-1

The author does not have an x-ray spectograph available with which to present successful analyses following exactly the line of this technique. However, a trace element analysis of the standard granite, G-1, and the standard diabase, W-1, reported by Hower and Fancher (1957) is susceptible to this treatment. Internal standards were used for matrix corrections. The major constituent analyses are also known, so both methods of matrix correction can be illustrated.

The trace elements determined in G-1 and W-1 are Mn, Ni, Cu, Zn, Rb, Sr, and Zr. The Kα radiation of Mn lies above the K absorption edge of Fe (region 2); the K radiation of all the other elements lies below the K absorption edge of Fe. Selenium was used as the internal standard for elements in region (1); the titanium already present in G-1 and W-1 was used as the internal standard for manganese. Standards were prepared by mixing oxides of the trace elements in aluminum oxide.

Tables 4*a* and 4*b* show the absorption corrections in regions (1) and

Table 4*a*. Calculated Absorption of G-1 Relative to Al_2O_3 in Regions (1) and (2)

Oxide	Weight* Fraction	Region (1)		Region (2)	
		$\mu/\rho_{1.0\,\text{Å}}$	Wt. Frac. $\times\mu/\rho_{1.0\,\text{Å}}$	$\mu/\rho_{1.93\,\text{Å}}$	Wt. Frac. $\times\mu/\rho_{1.93\,\text{Å}}$
SiO_2	0.7248	10.1	7.31	65.8	47.6
Al_2O_3	0.1420	9.13	1.30	59.8	8.5
Na_2O	0.0329	7.56	0.25	51.1	1.7
MgO	0.0037	8.36	0.03	55.1	0.2
CaO	0.0135	36.7	0.50	228	3.1
K_2O	0.0552	34.9	1.93	225	12.3
Fe_2O_3	0.0078	70.8	0.55	56.3	0.4
FeO	0.0097	78.5	0.76	60.3	0.6
TiO_2	0.0026	38.7	0.10	248	0.6
Total			12.74		75.0
Absorption relative to Al_2O_3			1.40		1.25

TABLE 4b. CALCULATED ABSORPTION OF W-1 RELATIVE TO Al_2O_3 IN REGIONS (1) AND (2)

Oxide	Weight* Fraction	Region (1)		Region (2)	
		$\mu/\rho_{1.0\ Å}$	Wt. Frac. $\times\mu/\rho_{1.0\ Å}$	$\mu/\rho_{1.93\ Å}$	Wt. Frac. $\times\mu/\rho_{1.93\ Å}$
SiO_2	0.5255	10.1	5.31	65.8	34.6
Al_2O_3	0.1498	9.13	1.35	59.8	9.0
Na_2O	0.0214	7.56	0.16	51.1	1.1
MgO	0.0659	8.36	0.55	55.1	3.6
CaO	0.1098	36.7	4.03	228	25.0
K_2O	0.0062	34.9	0.22	225	1.4
Fe_2O_3	0.0141	70.8	1.00	56.3	0.8
FeO	0.0871	78.5	6.84	60.3	5.3
TiO_2	0.0108	38.7	0.41	248	2.7
Total			19.89		83.5
Absorption relative to Al_2O_3			2.18		1.40

* Analyses taken from Goldich and Oslund (1956).

(2) on the basis of calculation from the known major constituent analysis.

Table 5 shows the absorption corrections in these regions as determined by Se and Ti internal standards. Counting rates are given for the internal standards in Al_2O_3 and in G-1 and W-1. The counting rates given for Ti in G-1 and W-1 are adjusted to a basis of 4000 ppm. The calculated matrix corrections are shown for comparison. The comparison shows that the analyses reported would be substantially the same for either technique. The largest discrepancy is in W-1, which has a high iron content, in region (2), where mutual excitation effects are significant.

TABLE 5. ABSORPTION OF G-1 AND W-1 RELATIVE TO Al_2O_3 IN REGIONS (1) AND (2) BY THE INTERNAL STANDARD METHOD

Counting Rate (counts/second) 500 ppm Se			Counting Rate (counts/second) 4000 ppm Ti			Relative absorption region (1)		Relative absorption region (2)	
Al_2O_3	G-1	W-1	Al_2O_3	G-1	W-1	G-1	W-1	G-1	W-1
720	503	336	237	194	178	1.43	2.14	1.22	1.33
Calculated relative absorption						1.40	2.18	1.25	1.40

Acknowledgments

The writer is particularily indebted to Dr. Hugh D. Burnham of the Shell Research Laboratory, Wood River, Illinois, for introducing him to the quantitative aspects of x-ray spectrography.

References

Beattie, H. J., and Brissey, R. M. (1954) Calibration method for x-ray fluorescence spectrometry: *Anal. Chem.*, **26,** 980–983.

Burnham, H. D., Hower, J., and Jones, L. C. (1957) Generalized x-ray emission spectrographic calibration applicable to varying compositions and sample forms: *Anal. Chem.*, **29,** 1827–1834.

Clarke, F. W. (1924) The data of geochemistry: *U.S.G.S. Bull.* **770,** 468.

Cullity, B. D. (1956) Elements of x-ray diffraction: Addison-Wesley Pub. Co., 11–12.

Daly, R. A. (1933) Igneous rocks and the depths of the earth: McGraw-Hill, 9–28.

Goldich, S. S., and Oslund, E. H. (1956) Composition of Westerly granite G-1 and Centerville diabase W-1: *Bull. Geol. Soc. Am.*, **67,** 811–815.

Hower, J., and Fancher, T. W. (1957) Analysis of standard granite and standard diabase for trace elements: *Science*, **125,** 498.

Murray, H. H. (1954) Genesis of clay minerals in some Pennsylvanian shales of Indiana and Illinois: Clays and Clay Minerals, Second Nat. Conf. on Clay Min., 47–67.

Norton, D. A. (1957), Fluorescence as applied to cyrtolite: *Am. Mineral.*, **42,** 492–505.

Sherman, J. (1955) The theoretical derivation of fluorescent x-rays from mixtures: Pitts. Conf. on Anal. Chem., 1955.

Stevenson, J. S. (1954) Determination of columbian in ores by x-ray fluorescence: *Am. Mineral.*, **39,** 436–443.

Manuscript received April 26, 1958

THE AMERICAN MINERALOGIST, VOL. 44, JANUARY-FEBRUARY, 1959

HARDNESS OF SYNTHETIC AND NATURAL MICAS[1]

F. Donald Bloss,[2] Ebraham Shekarchi,[3] and H. R. Shell,[4] *Bureau of Mines, U. S. Department of the Interior, Norris, Tennessee*

Abstract

The hardness of synthetic fluorphlogopite and of two natural muscovites, as measured on (001) by the Knoop indentation method, is definitely anisotropic. In both types of mica, maximum hardness is observed when the long axis of the indentation parallels the *b*-axis, minimum hardness when it parallels the *a*-axis. The pattern of the anisotropy shows, within the limits of measurement, a bilateral symmetry with respect to the (010) plane. Additional minima also occur on either side of the *a*-axis at an angle of 60° thereto for muscovite but at 75° thereto for fluorphlogopite. Additional maxima for hardness were observed at about 45° to the *b*-axis, not at 60° as had been expected. The anisotropy is interpreted in terms of the ionic structure of the micas involved.

Knoop hardnesses were measured parallel to the *a* and *b* axes for synthetic fluorphlogopites in which the following substitutions had been effected: (1) ferric and boron ions respectively into the tetrahedral aluminum positions, (2) manganese and cobalt respectively into the octahedral magnesium positions and (3) barium and strontium into the potassium positions. The boron mica was slightly softer, and the barium mica was much harder than the normal fluorphlogopite. The Knoop hardnesses of natural phlogopite, muscovite, margarite, and biotite were compared with those of the synthetics. The lesser hardness of these natural micas (excluding margarite) in comparison with the synthetic fluormicas is postulated to result, at least in part, from the greater polarizability of (OH) ion than of F ion.

Introduction

The synthetic fluorphlogopites are generally said to be harder than the comparable natural micas. However, as pointed out by Noda (1956, p. 12) "it is not known whether this hardness is its own property or only an apparent one caused by glassy material which exists between cleavage planes of mica crystals." This paper furnishes sufficient data on the relative hardness of synthetic and natural micas to answer these questions. Answers to several other questions that arose during the investigation, particularly regarding the anisotropy of hardness on (001) in mica, also have been suggested tentatively.

[1] Synthetic Mica Investigations, I–VIII, are listed on pages 78 and 79 of Bureau of Mines Report of Investigations 5337, Synthetic Mica Investigations IX, Review of Progress from 1947 to 1955, by R. A. Hatch, R. A. Humphrey, W. Eitel, and J. E. Comeforo.

[2] Academic address: Department of Geology, Southern Illinois University, Carbondale, Illinois.

[3] Graduate student, University of Tennessee, Knoxville, Tennessee.

[4] Supervisory Physical Chemist, Electrotechnical Experiment Station, United States Department of the Interior, Bureau of Mines, Norris, Tennessee.

Anisotropy of Hardness on (001) in Mica

Any comparison of hardness between two minerals must be prefaced with a determination of possible anisotropy of hardness with respect to crystallographic direction. Considerable anisotropy of hardness in micas was shown to exist by Switzer (1941, p. 316) who noted the Mohs hardness to be 2.5 parallel to (001) and 4.0 perpendicular to (001) for both muscovite and biotite. Consequently even though the hardness of all the micas studied was to be measured on the (001) plane, a preliminary investigation of possible directional variations of hardness on (001) in mica was deemed advisable.

For the study of the possible anisotropy, smooth, relatively flawless, single crystals of three specimens of mica were selected with compositions and identities as noted in Table 1. A reference line was drawn per-

Table 1. Composition of Micas Selected for the Study of Hardness Anisotropy on (001)

Identity	Composition	Analyst
Synthetic fluorphlogopite (Electrotech. Lab)	$K_{0.98}Na_{0.01}Mg_3Al_{1.01}Si_{3.01}O_{10}F_{2.03}$	Shell and Craig
Natural muscovite (Brazil)	$K_{0.88}Na_{0.09}Al_{1.78}Fe_{0.10}^{+++}Fe_{0.04}^{++}Mg_{0.04}Li_{0.04}Al_{0.96}Si_{3.03}O_{9.8}(OH)_{2.03}F_{0.09}$	Craig
Natural muscovite (India)	$K_{0.85}Na_{0.19}Al_{1.88}Fe_{0.05}^{+++}Fe_{0.02}^{++}Mg_{0.02}Al_{0.97}Si_{3.02}O_{10.02}(OH)_{1.81}F_{0.16}$	Craig

pendicular to the optic plane for the phlogopites and parallel to it for the muscovites, thus locating the *b*-crystallographic axis for each. The crystals studied, two of the synthetic fluorphlogopite and one each of the muscovites, were next carefully cemented with Canada balsam or similar material upon the plastic cylinders in which specimens are ordinarily embedded,[5] care being taken to eliminate air bubbles from beneath the mica. The indentation hardness of choice areas of these flakes was next measured with a fully automatic Tukon hardness tester equipped with a Knoop indenter under a load of 100 grams. At each of eight different

[5] The ordinary method of embedding had been previously found unsuitable for this work, primarily because the unequal thermal expansions between mica and plastic caused a bowing up of the embedded mica flakes during cooling of the mount. The resultant free space below the center of the mica flake was found to seriously affect accuracy.

choice locales on the flakes studied, a series of 13 hardness measurements was made, the long axis of the indentation being successively oriented at angles of 0°, 15°, 30° . . . 165°, and 180° to the *b*-axis. Results for the four flakes thus studied are shown in Fig. 1, each point representing the average of eight hardness determinations. The spread of the hardness determinations was statistically distributed about an average deviation of 1.0 to 1.5 $Knoop_{100}$ hardness values.

As may be seen in Fig. 1, a definite anisotropy of hardness on (001) exists for both synthetic fluorphlogopite and the two natural muscovites.

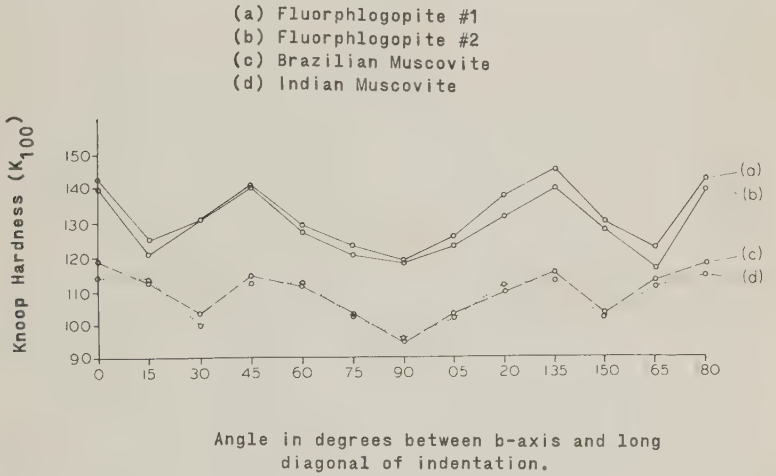

FIG. 1. The anisotropy of Knoop hardness on (001) for two flakes of synthetic fluorphlogopite and for two different muscovites. The bilateral symmetry of the curves around the 90° orientation reflects the plane of symmetry in mica.

The plane of symmetry of mica is clearly reflected in the bilateral symmetry of all curves with respect to the 90° orientation. The two muscovites show remarkable agreement, better in fact than that between the two flakes of fluorphlogopite. For both muscovite and phlogopite minimum hardness is observed parallel to the *a*-axis (i.e. at 90° to *b*). This minimum appears to be slightly less than the other two minima, which for muscovite are at 30° angles to the *b*-axis, whereas for phlogopite they are at only 15° angles to the *b*-axis. Maximum hardness on (001) in mica occurs parallel to the *b*-axis and at 45° thereto for fluorphlogopite; for muscovite the location of the maxima at 45° is less definite, since the hardness at 60° to the *b*-axis is nearly as great.

This observed anisotropy of hardness undoubtedly results from the interplay between (1) the shape of the diamond pyramid of the Knoop

indenter and (2) the atomic structure of the mica investigated. The indenter's shape is important because it produces a diamond-shaped identation, one diagonal of which is much longer than the other. Its penetration, therefore, resembles that of a wedge rather than of a needle. The atomic structure is important since particular directions in the sheet structure may represent lines of weakness by virtue of representing an alignment of weaker bonds or of fewer bonds. The stacking of the mica sheet structures according to the theories elucidated by Smith and Yoder (1956) would distribute these lines of weakness along particular planes parallel to which the wedge action of the Knoop indenter could penetrate more easily.

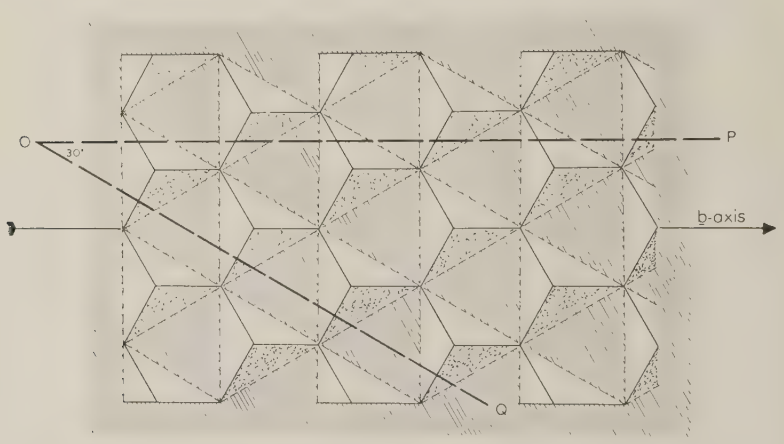

FIG. 2. Schematic drawing of the SiO_4 or AlO_4 tetrahedra in the mica sheet structure. The light, dashed lines represent the bases of the tetrahedra. The heavier solid lines represent the direction of the Si —O (or Al—O) bonds as well as the other three edges of the tetrahedra. A line along OQ cuts the minimum number of bonds per unit length whereas OP cuts 15.5% more per unit length and is one of the directions of maximum density of bonding in the sheet.

Any indentation of the (001) plane of mica is accompanied by (1) breakage of the Si—O or Al—O bonds of the $AlSi_3O_{10}$ sheets, (2) breakage of the K—O bonds linking these sheets, and (3) breakage of the bonds octahedrally coordinating Mg or Al to the surrounding O, OH, or F ions. Considering the $AlSi_3O_{10}$ sheets alone (Fig. 2), the insertion of a wedge along direction OP (or 60° thereto) would involve breakage of 15.5% more Si—O or Al—O bonds than along OQ (or 60° thereto). A similar situation exists for the K—O bonds (Fig. 3), bond breakage along OP again exceeding that along OQ by 15.5%. The octahedral ions have a somewhat different arrangement in phlogopite than in muscovite. In

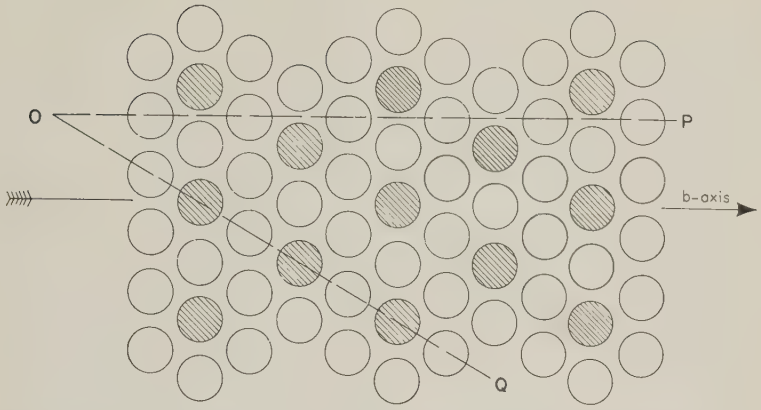

FIG. 3. Location of potassium ions (shaded) with respect to the oxygen ions in the planes above and below them. OQ, and directions at 60° thereto, represent the direction of minimum bond breakage; OP and directions at 60° to it, represent the direction of maximum bond breakage.

phlogopite (Fig. 4), OP represents a minimum for Mg—O or Mg—F, OH bond breakage, OQ exceeding it in this respect by 15.5%. On the other hand in muscovite (Fig. 5), two directions of weakness, OQ and RS,

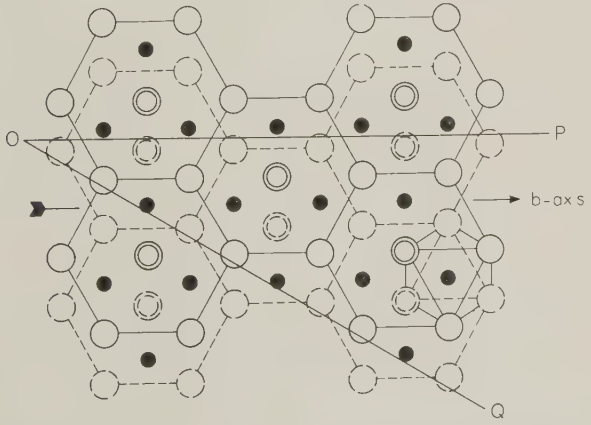

FIG. 4. Projection on (001) of a portion of a phlogopite layer after Hendricks and Jefferson (1939, p. 731). The distribution of the oxygen ions (hollow circles) and the fluorine or hydroxyl ions (double circles) are shown with respect to the magnesium ions (solid black circles). Dashed lines signify the anions to be in a plane slightly below the cations; solid lines signify them to be slightly above. Line OP and directions at 60° thereto here represent the directions of minimum bond density; OQ and associated 60° directions represent lines of maximum bond density.

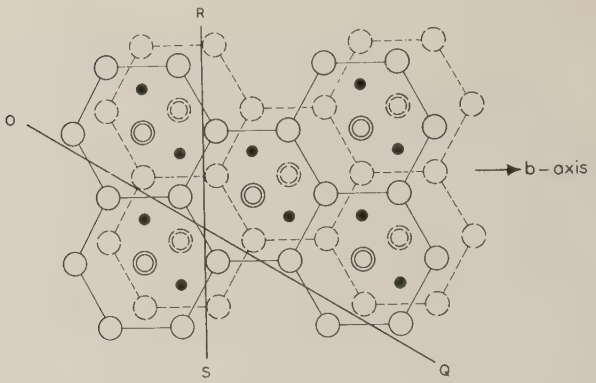

FIG. 5. Projection of a portion of a muscovite layer after Hendricks and Jefferson (1939, p. 731). Ion symbolism as before except solid black circles now represent aluminum ions. Line OQ, in contrast to Fig. 4, now represents a direction of minimum bond density as does RS. The direction at 60° to each of them, however, is not so favored.

are created by the systematic non-filling of one third of the octahedral positions.

By using the terminology of Smith and Yoder (1956), as well as their data and method for identifying the various mica polymorphs, the fluorphlogopite was determined from *x*-ray data to be a 1M type whereas the two muscovites were $2M_1$ types. The manner of alignment of the previously discussed lines of weakness by the 1M and $2M_1$ types of stacking thus becomes of interest in interpreting the observed anisotropy of hardness. To illustrate the relationships more simply, the Smith and Yoder (1956) device of depicting the sheet structure of the mica as hexagons has been adopted (Fig. 6).

The dashed lines in Fig. 6*a* represent the lines of weakness for both the

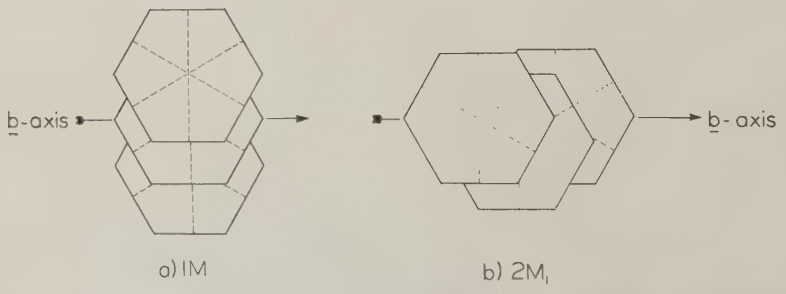

FIG. 6. The relationship of the method of stacking to the directions of presumed weakness (dashed or dotted lines) in the sheet structure of mica for (*a*) phlogopite and (*b*) muscovite. In (*b*) the dotted line is not as favored a direction of weakness as are the dashed lines since it is not as favorably disposed with respect to the distribution of the AlO_6 octahedra.

$AlSi_3O_{10}$ sheets and the K—O arrays; with respect to the Mg—O, F bonds they represent lines of strength. The over-all effect, however, appears to be that they are truly lines of weakness, the identation hardness parallel to the *a*-axis being significantly less than that observed parallel to the *b*-axis. From Fig. 6*a* one would expect Knoop hardness on fluorphlogopite to repeat cyclically every 60°, with minima at 30° and 90° to the *b*-axis. Actually, however, in Fig. 1 the minima are at 15° and 90° to the *b*-axis. Similarly the maxima would be expected (from Fig. 6*a*) to be parallel to and at 60° to the *b*-axis; actually they were observed parallel to and at 45° to the *b*-axis. The explanation thus far found most attractive is that one of the planar arrays of ions composing an individual sheet in the mica structure is not truly hexagonal; the suspicion therefore arises that there is an ordering of the Al ions in the $AlSi_3O_{10}$ sheets.

In muscovite, it may be recalled, two of the three theoretical directions of weakness in the $AlSi_3O_{10}$ and K O arrays actually coincided with the two rather significant directions of weakness produced by the systematic absences in one third of the octahedral positions. In Fig. 6*b* these two weakest directions are shown on the hexagons as dashed lines; the dotted line represents that direction of weakness in the $AlSi_3O_{10}$ and K—O arrays which was not reinforced by the systematic absence of the octahedrally coordinated ions.

The $2M_1$ stacking (Fig. 6*b*) may be seen to maintain a parallelism of the dashed lines in a direction perpendicular to the *b*-axis between the different layers; at 30° to the *b*-axis, however, the dashed and dotted lines are alternately parallel to each other between neighboring layers. This may possibly account for the slightly lesser hardness at 90° than at 30° to the *b*-axis (Fig. 1).

Effect of Ionic Substitution on Hardness

General

Indentation hardness on (001) was measured parallel to the *a*-axis and the *b*-axis, the directions of demonstrated minimum and maximum hardness, for several synthetic and natural micas. The effect of hardness of various ionic substitutions is discussed in the succeeding sections.

Substitution in the tetrahedral positions

Table 2 compares the observed Knoop hardness values for the normal synthetic fluorphlogopite with some substituted analogs. The replacements involve the ferric and boron ions substituting for aluminum in the tetrahedral positions. Each value in this (and succeeding tables) is based on an average of 8 Knoop hardness determinations. "Normal" fluorphlogopite is theoretically $KMg_3AlSi_3O_{10}F_2$. The compositions given in

this and the following tables were determined by calculation from the actual chemical analysis of selected clear single crystals.

Substitution of Fe^{+++} for Al^{+++} in the tetrahedral positions of the $AlSi_3O_{10}$ sheets causes little, if any, increase in hardness. On the other hand, the analogous substitution of B^{+++} for Al^{+++} effects a definite

Table 2. Effect of Tetrahedral Substitutions on Hardness of Synthetic Micas

Mica Type	Composition	Observed Knoop Hardness values for 100 gram indenter load		
		Trial	Orientation of long axis of indentation	
			Parallel to *a*-axis	Parallel to *b*-axis
"Normal" fluorphlogopite	$K_{0.98}Na_{0.01}Mg_3Al_{1.01}Si_{3.01}O_{10}F_{2.03}$	(1)	119	143
		(2)	118	140
Ferric fluorphlogopite, No. 18-47	$K_{0.99} \cdot Fe_{0.29}^{+++}Mg_{2.70} \cdot Fe_{1.03}^{+++}Si_{2.93}O_{10.18}F_{1.82}$	(1)	128	150
		(2)	119	145
Fe-Al fluorphlogopite No. 25-55	$K \cdot Mg_3 \cdot Al_{0.5}Fe_{0.5}^{+++}Si_3 \cdot O_{10}F_2$		129	140
Boron fluorphlogopite No. 25-23	$K_{0.87} \cdot Mg_{2.71} \cdot B_{.34} \cdot Al_{.04}Si_{3.65} \cdot O_{10}F_{2.00}$	(1)	100	125
		(2)	95	122
Boron fluorphlogopite, No. 25-58	$K_{1.00} \cdot Mg_{3.00} \cdot B_{.15}Al_{.83}Si_{3.01} \cdot O_{9.97}F_{4.03}$		114	126
Boron fluorphlogopite No. 25-59	$K_{0.97} \cdot Mg_{2.91} \cdot B_{0.27}Al_{0.61}Si_{3.14} \cdot O_{10}F_{2.01}$		111	120

decrease in hardness. The radii given by Pauling (1940, p. 346) for these ions (i.e. Fe^{+++}, 0.60 Å; Al^{+++}, 0.50 Å; and B^{+++}, 0.20 Å) indicate Fe^{+++} to be larger than B^{+++} as well as closer in size to Al^{+++}. The increased softness of the boron mica may perhaps be due to B^{+++} being rather small for the position it occupies; Fe^{+++}, however, evidently fills it more adequately. If one considers that the radius of Si^{++++} is 0.41 Å, i.e. midway between Fe^{+++} and B^{+++} in size, the interesting conjecture arises that the Al positions in the sheets may differ in size from the Si^{++++} positions.

Substitution in octahedral positions

Table 3 compares the observed Knoop hardness values for the normal synthetic fluorphlogopite with two modifications in which Mn^{++} and Co^{++} respectively are substituted into some of the Mg^{++} positions. The differences appear rather minimal, being within the range of experimental error.

TABLE 3. EFFECT OF OCTAHEDRAL SUBSTITUTIONS ON HARDNESS OF SYNTHETIC MICAS

Mica Type	Composition	Observed Knoop hardness values for 100 gram indenter load		
		Trial	Orientation of long axis of indentation	
			Parallel to *a*-axis	Parallel to *b*-axis
Normal fluorphlogopite	$K_{0.98}Na_{0.01}Mg_3Al_{1.01}Si_{3.01}O_{10}F_{2.03}$	(1)	119	143
		(2)	118	140
Manganese fluorphlogopite No. 18-13	$K_{1.07} \cdot Mg_{2.94}Mn_{0.03} \cdot Mn_{0.11}Al_{0.88}Si_{3.01}O_{10.33}F_{1.97}$	(1)	116	141
		(2)	119	141
Cobalt fluorphlogopite No. 18-24	$K \cdot Mg_{2.03}Co_{0.88}^{++} \cdot Al_{0.12} \cdot Al_{0.76}Si_{3.01}O_{10.15}F_{1.95}$	(1)	103	128
		(2)	114	132

Substitution in the twelve-fold position

Table 4 compares the Knoop hardness on (001) for several micas which differ chiefly as to the ion occupying the twelve-fold coordinated positions. As may be seen from two of the examples, increased substitution of Ba^{++} for K^{+} resulted in a significant increase in hardness. Complete substitution of Ba^{++} for K^{+} resulted in the hardest of all synthetic micas. Sr^{++} in small amounts increased hardness. Synthetic micas containing all Sr^{++} or Ca^{++} in the twelve-fold position could not be made large enough for testing by the methods described. In fact, complete Ca^{++} substitution would yield a fluoramphibole, not a fluormica. Occupancy by Ca^{++} of the twelve-fold positions greatly increases hardness, as shown by the measurements on a natural margarite from Chester, Massachusetts. Results thus bear out the well known hypothesis that the hardness of

mica is strongly affected by the bond strength of the twelve-fold coordination ions.

Samples of otherwise normal fluorphlogopite containing small amounts of Na^+, Li^+, or even Ca^{++} in the twelve-fold position, were apparently slightly softer than an all K^+ fluorphlogopite. Amounts involved were

Table 4. Effect of Twelvefold Coordination Substitutions on Hardness of Micas

Mica Type	Composition	Observed Knoop hardness values for 100 gram indenter load		
		Trial	Orientation of long axis of indentation	
			Parallel to *a*-axis	Parallel to *b*-axis
"Normal" fluorphlogopite	$K_{0.98}Na_{0.01}Mg_3Al_{1.01}Si_{3.01}O_{10}F_{2.03}$	(1)	119	143
		(2)	118	140
Barium fluorphlogopite I 25-28	$K_{0.77}Ba_{0.11} \cdot Mg_3 \cdot AlSi_3 \cdot O_{10}F_2$	(1)	144	176
		(2)	140	172
Barium fluorphlogopite II 25-29	$K_{0.50}Ba_{0.25} \cdot Mg_3 \cdot AlSi_3 \cdot O_{10}F_2$	(1)	173	206
Barium fluormica 18-26X	$Ba \cdot Mg_{2.5} \cdot AlSi_3 \cdot O_{10}F_2$	(1)	241	252
		(2)	232	259
Barium lithium mica 18-34X	$Ba_{0.97} \cdot Mg_{2.23}Li_{0.77} \cdot Al_{1.1}Si_{2.84} \cdot O_{9.90}F_{2.08}$	(1)	235	260
		(2)	225	246
Strontium fluormica 25-33	$K_{0.84}Sr_{0.08} \cdot Mg_3 \cdot AlSi_3 \cdot O_{10}F_2$		122	148
Natural margarite from Chester, Mass.	$Ca_{0.5} \cdot Al_2 \cdot AlSi_3 \cdot O_{10}(OH)_2$	(1)	238	402
		(2)	247	375

$Na^+_{0.1}$ to $_{0.04}$, $Li^+_{0.03}$, and $Ca^{++}_{0.02}$ per unit formula of $KMg_3AlSi_3O_{10}F_2$, and were determined on selected clear crystals by chemical analysis. It was also noted that synthetic fluorphlogopite synthesized from a batch containing feldspar averaged slightly softer than one from a batch containing potassium carbonate. Potassium feldspar of commerce always contains 2 to 3% Na_2O.

Very low hardness values were obtained on some small samples of natural phlogopite which had previously been flexed or bent. Although these apparently were clear and free of air inclusions, Knoop hardness values of 30 to 50 were obtained on the (001) face.

Substitution of F^- for $(OH)^-$

Micas representing various degrees of substitution of F^- for $(OH)^-$ were unavailable at the time of the study. Since this substitution is a chief difference between the natural and synthetic micas, a comparison of their observed hardness (Table 5) should indicate the effect on hardness of substituting fluorine for hydroxyl in the mica structure. (Each value in Table 5 is again the average of eight determinations on a particular flake.) Judged from these results, the synthetic micas apparently are slightly harder than the nearest comparable natural micas. Absolute comparisons, ion for ion, were not obtained, but the trend was definitely for slightly greater hardness in the synthetic than in natural micas. The difference was not sufficiently great, however, to affect the useful properties of the synthetic, nor its substitution for natural when large enough sheets are synthesized. Microscopic examination demonstrated that all flakes tested were free of interlayered glass as well as, in the case of the natural micas, alteration products.

It is here suggested that the substitution of F^- for $(OH)^-$ in the mica structure in general (and in the phlogopite structure in particular) produces increased hardness because of the lesser polarizability of F^- as compared with $(OH)^-$. As may be seen in Fig. 7*a*, an $(OH)^-$ ion would be so polarized (by the three Mg^{++} ions underlying it and by the six

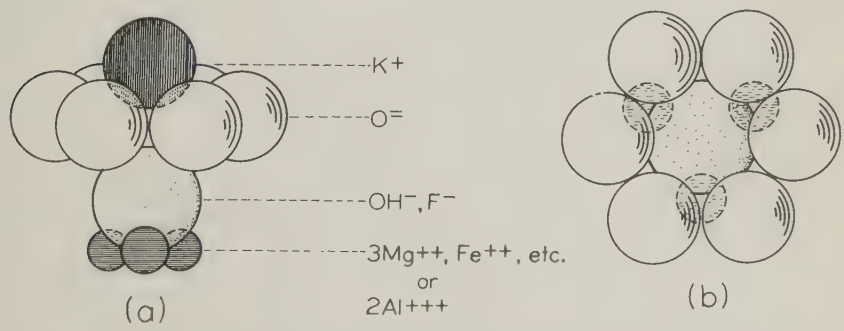

FIG. 7. Structural relationship between the potassium and hydroxyl (or fluorine) ions in mica. (*a*) Side view looking almost edgewise onto (001), (*b*) view looking directly down on (001) with the potassium ion which directly overlies the hydroxyl removed for illustrative purposes. The positive pole of the hydroxyl ions is probably on the side directly underlying the potassium ion.

TABLE 5. HARDNESS OF SOME SYNTHETIC FLUORMICAS AND NATURAL HYDROXY-MICAS FOR COMPARISON OF F^- VS. OH

Mica Type	Composition	Observed Knoop hardness for 100 gram indenter load		
		Trial	Orientation of long axis of indentation	
			Parallel to *a*-axis	Parallel to *b*-axis
Synthetic Fluormicas				
"Normal" fluorphlogopite	$K_{0.98}Na_{0.01}Mg_3Al_{1.01}Si_{3.01}O_{10}F_{2.03}$	(1)	119	143
		(2)	118	143
Manganese fluorphlogopite 18–13	$K_{1.07} \cdot Mg_{2.94}Mn_{0.08} \cdot Mn_{0.11}Al_{0.88}Si_{3.01} \cdot O_{10.13}F_{1.97}$	(1)	116	141
		(2)	119	141
Cobalt fluorphlogopite 18–24	$K \cdot Mg_{2.03}Co_{0.88}^{++}Al_{0.12} \cdot Al_{0.96} \cdot Si_{30.4} \cdot O_{10.13}F_{1.95}$	(1)	103	128
		(2)	114	132
Ferric fluorphlogopite 18–47	$K_{0.99} \cdot Fe_{0.29}^{+++}Mg_{2.70} \cdot Fe_{1.08}^{+++}Si_{2.93} \cdot O_{10.18}F_{1.82}$	(1)	128	150
		(2)	119	146
Natural Micas				
Phlogopite, Canada	—	(1)	98	114
		(2)	84	101
Biotite, Mitchell Co., N. C.	-	(1)	66	69
Lepidomelane, Faraday Twp., Can.	—	(1)	71	84
Muscovite, Brazil	$K_{.83}Na_{.09}Ca_{.005}Al_{1.78}Fe_{.10}^{+++}Fe_{.04}^{++}Mg_{.04}Li_{.04}Al_{.96}Si_{3.03}O_{9.8}(OH)_{2.03}F_{.09}$	(1)	97	116
		(2)	99	126
Muscovite, S. Dakota	$K_{.85}Na_{.19}Ca_{.005}Al_{1.88}Fe_{.05}^{+++}Fe_{.02}^{++}Mg_{.02}Al_{.97}Si_{3.02}O_{10.02}(OH)_{1.81}F_{.16}$	(1)	93	123
		(2)	95	126
Muscovite, India	$(K_{.87}Na_{.10}Ca_{.005})Al_{1.80}Fe_{.06}^{+++}Fe_{.06}^{++}Mg_{.06}Al_{.97}Si_{3.03}O_{9.85}(OH)_{2.09}F_{.05}$	(1)	102	115
		(2)	96	115

oxygen ions overlying it) as to develop a positive pole on its side nearest the potassium. Figure 7*b*, wherein the potassium ion lying directly over the $(OH)^-$ ion has been removed for illustrative purposes, shows this presumed positive region on the hydroxyl to be unscreened by the oxygen ions with respect to the overlying potassium. The resultant mutual repulsion would thereby weaken the K O bonding and consequently cause a decrease in hardness. Substitution of F^- for $(OH)^-$, since fluorine is less polarizable, would reduce this effect and result in increased hardness.

The above hypothesis may also explain, in part, the increased thermal stability and decreased basal spacing (001) of fluorphlogopites as compared to their hydroxyl analogs. As noted by Yoder and Eugster (1954, p. 176), "The substitution of F^- for $(OH)^-$ appears to result in a rise of 575° C. in the upper stability limit at one atmosphere pressure!" A more important factor regulating this increased thermal stability may be the lesser ability of the fluorine ion to escape from the mica structure as an electrically neutral phase. Whereas F^- requires a cation in order to escape, the $(OH)^-$ ion may escape as H_2O simply by combining with an H^+ ion from a second, nearby $(OH)^-$ ion. The resultant $O^=$ remains in the structure, thereby preserving electrical neutrality.

The basal spacing (001) of fluorphlogopite is reported by Noda and Roy (1956, p. 931) to be 0.17 ± 0.02 Å less than for the comparable OH^- phlogopite. Under the hypothesis of increased polarization of the hydroxyl ion, this would be expected.

Effect of Mechanical Pressure on Hardness of Synthetic Fluorphlogopite

Specimens of the "normal" fluorphlogopite were subjected to high pressure at room temperature and at 1250° C. prior to testing their hardness. Such treatment had no striking effect on hardness.

Conversion from Knoop to Mohs

The conversion of Knoop hardness to Mohs hardness is subject to considerable uncertainty, primarily because, as shown by Winchell (1945), the Knoop hardness of some minerals of Mohs' scale depends upon crystallographic orientation. Roughly converted, however, the micas studied possessed Mohs hardnesses as indicated in Table 6.

Conclusions

1. The hardness of synthetic fluorphlogopite and of two natural muscovites, as measured on (001) by the Knoop indentation method, is definitely anisotropic, the pattern possessing a bilateral symmetry with respect to (010).

TABLE 6. KNOOP HARDNESS ROUGHLY TRANSLATED INTO MOHS HARDNESS

Mica	Trial	Mohs Hardness: Parallel to *a*-axis	Mohs Hardness: Parallel to *b*-axis
		Synthetic Fluormicas	
"Normal" fluorphlogopite	(1)	3−	3½
	(2)	3−	3½
Manganese fluorphlogopite No. 18-13	(1)	3−	3½
	(2)	3−	3½
Cobalt fluorphlogopite No. 18-24	(1)	3−	3
	(2)	3−	3
Ferric fluorphlogopite No. 18-47	(1)	3−	4−
	(2)	3−	4−
Boron fluorphlogopite No. 25-23	(1)	3−	3
	(2)	3−	3
Barium fluorphlogopite I No. 25-28	(1)	4	4+
Barium fluorphlogopite II No. 25-29	(1)	4+	4+
		Natural Micas	
Phlogopite (Canadian)	(1)	3−	3−
	(2)	3−	3−
Biotite (Mitchell Co., N. C.)		2½	2½
Lepidomelane (Faraday Twp., Canada)		2½	2½
Muscovite (Brazil)	(1)	3−	3−
	(2)	3−	3
Muscovite (S. Dakota)	(1)	3−	3
	(2)	3−	3
Muscovite (India)	(1)	3−	3
	(2)	3−	3
Margarite	(1)	4+	5
	(2)	4+	5

2. Maximum hardness on (001) in mica is observed when the long axis of the indentation is parallel to the *b*-axis.

3. For synthetic fluorphlogopite the two other directions for minimum hardness are at 15° on either side of the *b*-axis; for muscovite at 30° on either side.

4. For both fluorphlogopite and muscovite, two other maxima exist at 45° to the *b*-axis.

5. Substitution of boron ions into the aluminum positions of fluorphlogopite produced a softer mica; however, substitution of ferric ion for aluminum produced little change.

6. Substitution of Mn for Mg in fluorphlogopite effected little change in hardness; substitution of Co for Mg decreased hardness slightly.

7. Substitution of Ba for K produced a marked increase in the hardness of fluorphlogopite.

8. Except for margarite, the natural micas are softer than the synthetic micas.

9. The natural phlogopite and biotites examined proved softer than the natural muscovites.

10. The increased softness of natural phlogopite and of natural micas in general, as compared to the synthetic fluormicas, is believed partly due to the greater polarizability of the hydroxyl ion as compared to the fluorine ion.

Acknowledgments

The authors thank Mr. Perry Cotter for the time and advice he so generously gave. The encouragement of Dr. John R. Koster is sincerely appreciated.

References

Daniels, F. W. and Dunn, C. G. (1948), The effect of orientation on Knoop hardness of single crystals of zinc and silicon ferrite: *Trans. Am. Soc. Metals*, Preprint No. **14,** [Chem. abstr., **42,** 8565a.]

Hendricks, S. B. and Jefferson, M. E. (1939), Polymorphism of the micas: *Am. Mineral.*, **24,** 729–771.

Kohn, J. A. and Hatch, R. A. (1955), Synthetic mica investigations, VI: *X*-ray and optical data on synthetic fluorphlogopite: *Am. Mineral*, **40,** 10–21.

Noda, Tokiti (1956), Synthetic Mica, its Properties and Applications: *Unpublished report from the Department of Applied Chemistry, Faculty of Engineering, Nagoya University*, Nagoya, Japan.

——— and Roy, Rustum (1956), OH–F exchange in fluorine phlogopite: *Am. Mineral.*, **41,** 929–932.

Pauling, Linus (1940), Nature of the Chemical Bond, 2nd Ed., Cornell University Press, pp. 346–350.

Smith, J. V. and Yoder, H. S. (1956), Experimental and theoretical studies of the mica Polymorphs: *Mineral. Mag.*, **31,** 209–235.

Switzer, George (1941), Hardness of micaceous minerals: *Am. Jour. Sci.*, **239**, 316.

Winchell, Horace (1945), The Knoop microhardness tester as a mineralogical tool: *Am. Mineral.*, **30**, 583–595.

Yoder, H. S. and Eugster, H. P. (1954), Phlogopite synthesis and stability range: *Geochim. Cosmochim. Acta* **6**, 157–185.

Manuscript received April 30, 1958

THE AMERICAN MINERALOGIST, VOL. 44, JANUARY–FEBRUARY, 1959

DISCREPANCIES BETWEEN OPTIC AXIAL ANGLES OF OLIVINES MEASURED OVER DIFFERENT BISECTRICES*

P. J. Wyllie, *Pennsylvania State University, University Park, Pennsylvania.*

Abstract

More than 100 measurements of 2V were made on forsteritic olivines from two picrite sills in Soay, Scotland, using both double and single axis conoscopic methods. The mean of double axis measurements agrees closely with the mean of single axis measurements, but a significant difference exists between the means of double axis measurements made over different bisectrices. Measurements of $(-)2V_\alpha$ are smaller than $(-)2V_\gamma$ by about 2.5°. The difference can be explained if the recorded angles are smaller than the true angles when high radial angles are measured on the universal stage, and calculations show that refraction and displacement of light within the central layers of the sphere could produce this effect. Optical measurements of minerals with 2V near 90° may be unreliable unless corrections are made for the errors introduced by the high angles of tilt which are involved in the measurements.

Introduction

The chemical composition of olivines occurring in igneous rocks is commonly estimated by the measurement of refractive indices or 2V. The measurements of 2V which are recorded in this paper were made in order to compare the results obtained by single axis measurements with the results obtained by double axis measurements made over different bisectrices. The means of double axis measurements are in close agreement with the means of single axis measurements, but a significant difference exists between double axis measurements made over different bisectrices. It is concluded that a single measurement of 2V may be in error by as much as 3°, corresponding to about 6 molecular per cent of fayalite. The errors result from the high angles of tilt of the universal stage which are involved in the measurement of 2V's near 90°.

The olivines measured occur in two picrite sills which outcrop on the Island of Soay in western Scotland. Slight zoning was detected in some crystals but it is restricted to the narrow, outer margins of the olivine.

Previous Observations

Game (1941) measured refractive indices and optic axial angles of olivines from Ubekendt Ejland, West Greenland, and reported that:

"a set of values obtained about one bisectrix usually show fair mutual agreement but differ by as much as 7° or 8° from another set obtained about the other bisectrix (single axis measurements), whereas the mean of the two sets shows good agreement with the value inferred from the measurement of β. . . . no explanation can be offered."

* Contribution No. 57-85, College of Mineral Industries, The Pennsylvania State University, University Park, Pennsylvania.

Frankel (1942), in studies of olivines of Karroo dolerites, found that the sets of single axis 2V measurements made about α and γ varied as much as 7° from each other and that the mean value of each set did not show good agreement with the value suggested from measurement of β. The mean of approximately the same number of single axis measurements taken about both α and γ was in good agreement with double axis measurements and the value obtained from β. He referred to the results of Game and concluded that the two studies demonstrated that single axis measurements of 2V may be quite unreliable.

Johnston (1953), in a study of the olivines of the Garbh Eilean Sill, used the more accurate conoscopic method of Hallimond (1950) and, whenever possible, confined his observations to double axis measurements. This ensured a higher degree of accuracy than is possible with the orthoscopic method. He found that the measurement of $2V_\alpha$ was consistently smaller than $2V_\gamma$, the average difference being 2.4°. The average of an approximately equal number of determinations about each bisectrix was taken as the true 2V of the olivines. The persistence of a difference between sets of double axis measurements using the more precise conoscopic method suggests that the differences noted by Game and Frankel cannot be attributed solely to the inaccuracy of single axis measurements.

Wilkinson (1956) made optical determinations of the olivines from a teschenite sill. Double axis measurements were made always across the acute bisectrix, but the presence of magnesian olivine with large optic axial angles involving high angles of rotation around A_4 discouraged such determinations and in the majority of cases 2V was determined by single axis methods. Agreement was "moderately good" between the mean values of double axis and single axis measurements, and "good correspondence" was found in compositions inferred from refractive indices and 2V. No comparison was possible between double axis measurements made over α and γ, and no discrepancy was found between single axis measurements made over α and γ.

Methods and Measurements

There appears to be no general agreement concerning the use of the terms "direct" and "indirect" as applied to the measurement of 2V. Measurements made about one optic axis are frequently referred to as "indirect" but the writer follows Fairbairn and Podolsky (1951) in describing both single and double axis measurements as direct methods. Indirect methods then include extinction angle procedures and relative retardation methods. Techniques used were as follows:

(A) On suitably orientated grains direct double axis determinations were made using the conoscopic method. In addition, stereographic projections of optical data were completed for each crystal, the orthoscopic method being used to locate the bisectrix (Fig. 1*a*).

(B) Using the stereograms constructed in (A), direct single axis determinations were made on these crystals. The angle between the bisectrix and the optic axis making the smaller radial angle with the center of the projection was doubled to give 2H (Fig. 1*a*).

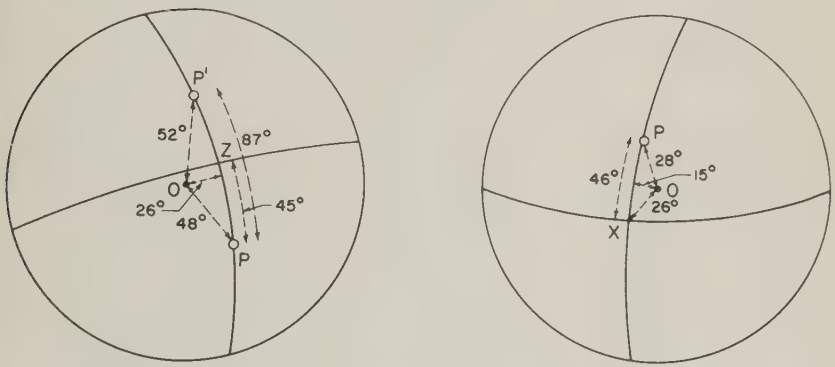

FIG. 1. Stereographic projections of olivine crystals illustrating the measurement of 2H by the three methods (A), (B) and (C).

(*a*) Crystal 50*a* in Table 1. For method (A), $2H_\gamma = PP' = 87°$. For method (B), $2H_\gamma = 2PZ = 90°$.

(*b*) Crystal 50i in Table 1. Method (C), $2H_\alpha = 2PX = 92°$.

(C) On grains not suitably orientated for double axis measurements direct single axis determinations were made using stereographic projections (Fig. 1*b*). Optic axes were located by the conoscopic method.

The measurements, made on 64 crystals in eight specimens from Sills 1 and 1A, are listed in Tables 1 and 2. Two or three thin sections were used from each specimen. Two examples will illustrate the form of tabulation. Figure 1*a* is the stereogram for crystal 50a in Table 1. The tilt of the optic axial plane (OAP) is 26°. In the double axis measurement (group A), $OP' = 52°$ is the greatest radial angle measured and $PP' = 87°$ is the value of $2H_\gamma$. In the single axis measurement (group B) OP is the greatest radial angle measured and $PZ = 45°$ is the value of H_γ, giving $2H_\gamma = 90°$. OP is always less than OP' so that the single axis measurements involve smaller angles of tilt of the universal stage than do the

TABLE 1. MEASUREMENT OF OLIVINES IN SILL 1

Spec.		Tilt of OAP.	2H						(−)2V			
			Double Axis			Single Axis			2-Axis		1-Axis	
			OP′	α	γ	OP	α	γ	α	γ	α	γ
50	a	26	52		87	48		90		94		91
	b	24	52		86	44		86		95		95
	c	10	48		87.5	40		88		93.5		93
	d	21				38		88				93
	e	19				34		90				91
	f	23				33	92				91	
	g	16				30	93				92	
	h	10				30	91				90	
	i	15				28	92				91	
48	a	34	54		85	50		88		96		93
	b	30	54		86	47		86		95		95
	c	20	52	93		47	95		92		94	
	d	4	51.5		85	34		88		96		93
	e	2	45		87	42		87		94		94
	f	4	44.5		87.5	43		88		93.5		93
47	a	5.5	53	93		40	93		92		92	
	b	7	49	93		44	91		92		90	
	c	22.5				32		90				91
	d	5				24		90				91
	e	2				24	90				89	
46	a	7.5	56	92.5		37	92		91.5		91	
	b	10	54	92		38	95		91		94	
	c	11	53		88.5	38		89		92.5		92
	d	4	48	93.5		45.5	95		92.5		94	
	e	13				35		89				92
	f	5				26	93				92	
45	a	22.5	54	92		39	92		91		91	
	b	12	54	92.5		40	93		91.5		92	
	c	27	53	92		49	91		91		90	
	d	15.5	52		86	39		87		95		94
	e	25				38	92				91	
	f	20				32		86				95
	g	19				32		90				91
	h	14				32		88				93
	i	0.5				31.5	94				93	
	j	7				28		88				93
	k	4.5				24		86				95

OAP: optic axial plane. OP′ and OP: the radial angles occurring in each measurement.

TABLE 2. MEASUREMENT OF OLIVINES IN SILL 1A

Spec.	Tilt of OAP.	2H						(−)2V			
		Double Axis			Single Axis			2-Axis		1-Axis	
		OP′	α	γ	OP	α	γ	α	γ	α	γ
73 a	4	55	90		35	92		89		91	
b	13.5	53	93		43	94		92		93	
c	5	53	92		43	92		91		91	
d	5	52	91.5		40	92		90.5		91	
e	2	52		90	39		92		91		89
f	10	51	92		43	94		91		93	
g	28.5				37	90				89	
h	2.5				28.5		87				94
i	10				28	93				92	
j	4				23		90				91
74 a	11	54	91.5		40	92		90.5		91	
b	13	53	92		39	92		91		91	
c	19	53	91.5		44	90		90.5		89	
d	26	50		87.5	48		89		93.5		92
e	0.5	48.5		88.5	40		88		92.5		93
f	12	48		88	43		88		93		93
g	8				26	91				90	
h	1				27		88				93
75 a	2	53.5	91.5		38	94		90.5		93	
b	22	52.5		88	44		89		93		92
c	15	52	91		42.5	92		90		91	
d	4.5	51	91		40	92		90		91	
e	12	51		88	39		90		93		91
f	17.5	49		89.5	45		90.5		91.5		90.5
g	14.5				36	95				94	
h	20.5				35	93				92	
i	5				33		92				89

OAP: the optic axial plane. OP and OP′: the radial angles occurring in a given measurement.

double axis measurements. Figure 1*b* is the stereogram for crystal 50i in Table 1 (group C). The tilt of the optic axial plane (OAP) is 15°. OP is the greatest radial angle measured and PX = 46° is the value of H_α, giving $2H_\alpha = 92°$.

Values of 2H were converted to 2V using the refractive index of the hemispheres (n) and the refractive index β of the olivines. In group (A), the radial angles measured from the centers of the projections to the optic axes were corrected, and 2V was then measured on the great circle passing through the two corrected points (Emmons 1943). By this method

2V was obtained from 2H with an accuracy of $\pm 0.5°$. Conversion of H to V directly using the correction $\sin V = n \cdot \sin H/\beta$ was found to give the same result for 2V within $\pm 0.5°$. Therefore, the simple conversion of H to V was used in groups (B) and (C). The converted value of $2H_\alpha$ gives $(-)2V_\alpha$ and the converted value of $2H_\gamma$ gives $(+)2V_\gamma$. For comparative purposes the supplement of $(+)2V_\gamma$ is listed as $(-)2V_\gamma$. Thus, in Tables 1 and 2, values of $(-)2V$ are listed in four columns for determinations over α and γ by both double and single axis methods.

Angles of tilt of the universal stage were kept as small as possible. In the double axis measurements the tilt of the plane was generally less than 25° and the greatest angle of tilt was 34°. The greatest radial angle involved in a measurement, however, usually exceeded 50°, whereas in the single axis measurements for the same grains the greatest radial angle, with one exception, was always less than 50°. The significance of this fact will be discussed below. In the single axis measurements of group (C) 38° was the greatest tilt of the stage, but most angles were less than 25°.

The accuracy of the measurements varies with the method employed. In group (A) the optic axes may be located with an accuracy of $\pm 0.25°$ by the concoscopic method (Hallimond 1950) giving a possible error of $\pm 0.5°$ for 2H in a given crystal. In groups (B) and (C) the optic axes may be located with an accuracy of $\pm 0.25°$ and the optic symmetry plane containing the optic normal can be found to within $\pm 1°$, using the orthoscopic method. Hallimond (1950) and Turner (1942) state that the accuracy of measurements is variable for different directions within the indicatrix, and some planes were found which appeared to give complete extinction through a range of 4° of tilt, i.e. $\pm 2°$ accuracy. For such planes, the mean of several readings was taken, and the maximum error was probably reduced to $\pm 1°$. The estimated possible error for 2H of a given crystal by this method is therefore $\pm 2.5°$. These experimental errors will be increased slightly by the index correction.

Table 3 compares the values of $(-)2V$ obtained over α and γ for the three groups of measurements. The arithmetic means of $(-)2V$ and the standard deviation of the mean for each column have been calculated. With 99 per cent certainty, the true value of $(-)2V$ lies within the range Arithmetic Mean $\pm 2.6 \times$ Standard Deviation of the Mean, and this may be accepted with confidence as the maximum error of each mean. The values of $2.6 \times$ standard deviation, listed in Table 3, are very close in magnitude to the estimated experimental errors for single measurements.

Discussion of Results

The compositions of the olivines were estimated from the optical data collated by Poldervaart (1950). The molecular percentages of fayalite

TABLE 3. COMPARISON OF (−)2V OBTAINED BY DIFFERENT METHODS

(A) Double axis measurements. (B) Single axis measurements for same grains as in (A). (C) Single axis measurements with no radial angles greater than 40°

	Sill 1						Sill 1A					
	(A)		(B)		(C)		(A)		(B)		(C)	
	α	γ	α	γ	α	γ	α	γ	α	γ	α	γ
		94		91	91	93	89		91		91	89
		95		95	92	93	92		93		91	94
		93.5		93	90	91	91		91		89	91
					91		90.5		91		92	
		96		93		93	91		93			
		95		95				91		89		
		96		93			90.5		91		91	93
		94		94			91		91		91	93
		93.5		93			90.5		89		90	
	92		94					93.5		92		
	92		92		92	91		92.5		93		
	92		90		89	91		93		93		
	91.5		91		91	92	90.5		93		93	91
	91		94		94	92	90		91		91	89
	92.5		94		92		90		91		94	
		92.5		92				93		92	92	
	91		91		91	94		93		91		
	91.5		92		92	95		91.5		90.5		
	91		90		91	91						
		95		94	93	93						
						93						
						95						
$\bar{x}$	91.6	94.5	92	93.3	91.5	92.6	90.5	92.5	91.4	91.5	91.4	91.4
2.6×s	0.5	0.9	1.4	0.9	0.9	1.0	0.6	0.9	0.9	1.4	1.0	2.0
Av.	93.0		92.7		92.1		91.5		91.5		91.4	

$\bar{x}$ Arithmetic mean; s, Standard deviation of the mean; Av., Average of the means of (−)2V obtained by measurements over α and γ.

only are given below. In Sill 1, the average values of (−)2V for groups (A), (B), and (C) respectively correspond to: Fa_7, $Fa_{7.5}$, and Fa_8. Agreement is excellent. In group (A) the mean values for $(-)2V_\alpha$ and $(-)2V_\gamma$ give the compositions $Fa_{9.5}$ and $Fa_{3.5}$, so the discrepancy between the measurements over different bisectrices, 2.9°, corresponds to about 6 molecular per cent of fayalite.

In Sill 1A, the average values of (−)2V for the three groups of measurements give the same composition, namely Fa_{10}. In group (A) the mean values for $(-)2V_\alpha$ and $(-)2V_\gamma$ give the compositions Fa_{12} and Fa_8. The discrepancy between the measurements about different bisectrices,

2.0°, corresponds to about 4 molecular per cent of fayalite, which is smaller than in Sill 1.

A few measurements of β were made on grains pried from thin sections (± 0.003). Two measurements from Sill 1 give compositions $Fa_{6.5}$ and Fa_7, agreeing closely with the mean 2V determinations. Three measurements from Sill 1A give a mean composition of Fa_7 (range $Fa_{5.5}$ to Fa_8), which differs from the mean 2V determination by 3 per cent fayalite. More reliance must be placed upon the 2V determinations because the results of many 2V measurements are consistent, and only five measurements of β were made.

There may be compositional variations among the olivines within each sill but the low values of the errors for the means of 2V measurements indicates that such differences, if present, are too small to be distinguished.

In both sills, the averages of $(-)2V$ obtained by each of the three methods agree within 1°, and the greatest differences between the means of measurements over α and γ are found in columns (A) of Table 3. Yet the latter results were obtained by a more accurate method than those in columns (B) and (C). The significance of the differences may be tested statistically. The variance of the difference between two independent variables is equal to the sum of their variances (Moroney 1951), and the standard deviation of the variables is the square root of the variance. Considering the arithmetic means obtained by different methods as independent variables, the standard errors of the differences of means obtained by measurements over α and γ have been calculated and they are compared with the observed differences in Table 4. A difference of more than two standard errors between means is probably significant and a difference of more than three standard errors between the means is highly significant; the probability that such a difference should arise by chance is less than one half of one per cent. The observed differences between the means obtained by method (A), in both sills, are more than four times the standard errors of the differences and it is very improbable that they are due to chance. In Sill 1A, it is obvious that the differences obtained by methods (B) and (C) are not significant. In Sill 1, the differ-

Table 4. Differences Between the Means of $(-)2V$ Measured over α and γ

	Sill 1			Sill 1A		
Observed Difference Between Means	2.9	1.3	1.1	2.0	0.1	0.0
Standard Error of the Difference	0.4047	0.6799	0.5120	0.4139	0.9536	1.031

ences obtained in methods (B) and (C) are about two standard errors and they may be significant.

The values of (−)2V obtained by method (A) are plotted in Fig. 2 against the greatest radial angle (OP′) involved in the measurement. A statistical test is hardly necessary to prove that a significant difference exists between measurements made over α and γ.

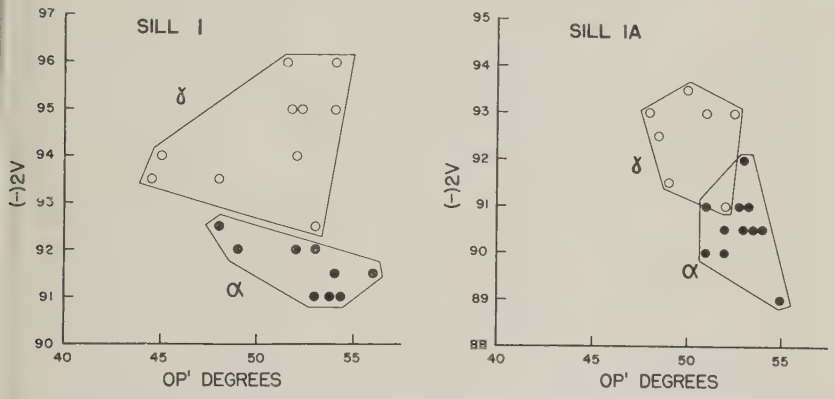

FIG. 2. Measurements of (−)2V obtained by method (A) plotted against the greatest radial angle OP′ involved in the measurement (see Fig. 1*a*). The results are taken from Tables 1 and 2. In both sills, the measurements over α are separated from those over γ.

This confirms that the means of supposedly less accurate single axis measurements (B) give more consistent results *for the same grains* than do the means of the conoscopic double axis measurements (A). The results in columns (B) were obtained from measurements involving smaller angles of tilt of the universal stage than those in columns (A), as were those in columns (C) obtained for different grains. The average values must be regarded as the best values and thus, for higher angles of tilt of the stage $(-)2V_\alpha$ is smaller, and $(-)2V_\gamma$ is larger than the expected value. Since $(-)2V_\gamma$ is the supplement of $(+)2V_\gamma$ it is clear that for higher angles of tilt of the stage (method A) both the measured angles $2H_\alpha$ and $2H_\gamma$ are smaller than the mean value of 2H obtained when lower angles of tilt are involved (methods B and C). The value of 2H within the upper hemisphere depends upon the refractive index of the hemispheres, n, 2V and β, all of which are fixed quantities in a given measurement. Therefore, for large tilts of the stage, the observed angle between the optic axes is smaller than the true 2H, i.e. the angle between the rays in the upper hemisphere. This means that there must be refraction at the surface of the upper hemisphere and the emergent ray cannot be normal to the surface. Since the emergent angle H′ is smaller than the true angle

H, the light rays must be displaced from the center of the sphere as illustrated diagramatically in Fig 3*a*, and it is in the center of the sphere that the cause of the observed discrepancy must have its origin.

The theoretical treatment of the universal stage as a uniform sphere with a thin mineral plate at its center is, of course, simplified and with increasing angles of tilt the treatment becomes less rigorous. When a thin section is mounted on the stage there are seven refracting layers between the stage glass and the upper hemisphere and their effect upon the light rays cannot be neglected for high angles of tilt. The path of a single light ray has been traced through the layers for different angles of tilt of the stage in an attempt to find the cause of the displacement CB (Fig. 3) which could account for the observed discrepancy.

Consider a light ray with angle of incidence i passing through the mount in such a way that without refraction it would pass through the center C of the sphere, i.e. the center of the mineral plate if the stage is correctly adjusted (Fig. 3*b*). In each layer, the light ray will have an angle of refraction r, and $r>i$ for all layers except the mineral plate which, in this example, has a refractive index greater than that of the sphere. In a given layer of thickness t, the ray will be displaced laterally by a distance $\Delta x=t(\tan r-\tan i)$. The total displacement of the ray in passing through the seven layers will be $x=\Sigma t(\tan r-\tan i)$, and this corresponds to CB in Fig. 3. The thickness of the microscope slide is large compared to the other layers, and $x=t_s(\tan r_s-\tan i)$ approximately, where t_s and r_s are the thickness of and the angle of refraction in the glass slide. Knowing that the refractive index of the slide is 1.516 and $t_s=1$ mm., values of x have been calculated for different values of i, which is the angle of tilt of the stage. The calculations are plotted in Fig. 4*a*. From the angles of incidence and the calculated values of x approximate values of θ, the angle of incidence of the emergent ray at the glass-air interface of the upper hemisphere (of radius 12 mm.), are given by the expression:

$$\theta = \frac{180 \cdot x \cdot \cos i}{(12 - x \sin i)} \text{ degrees}$$

(see Fig. 3*a*). The angle of emergence is $\phi=\sin^{-1}(1.649 \sin \theta)$ and from Fig. 3*a* it can be seen that the error of an angular measurement, for an angle of incidence (angle of tilt) i, is $(i-i')=(\phi-\theta)$. Calculated values of $(\phi-\theta)$ have been plotted against i in Fig. 4*b*, and for a given angle of tilt the observed angle i' will be smaller than the true angle i by an amount which can be read from the graph.

When the radial angle from the azimuth of the sphere to the point of measurement is 35°, the calculated error of measurement, $(i-i')$, is 0.25°.

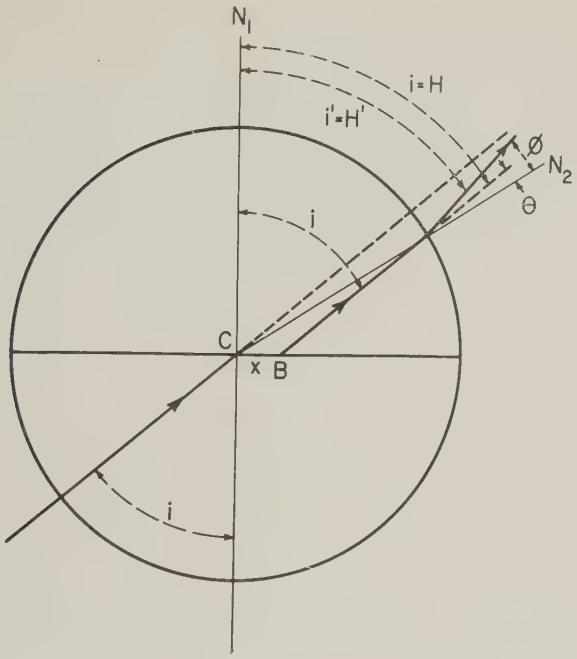

(*a*)

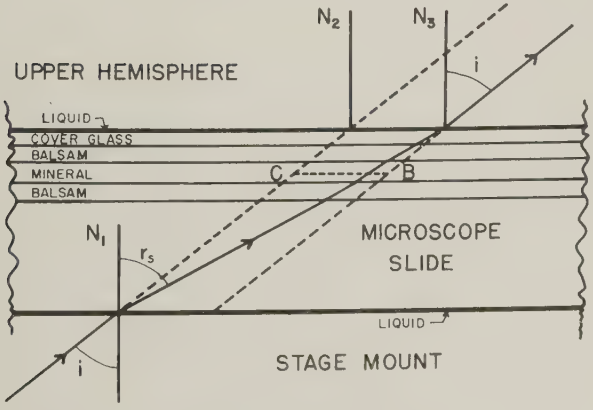

(*b*)

FIG. 3. (*a*) Diagrammatic representation of the path of a light ray through the universal stage. The angle of incidence is $i = H$, and the emergent angle, $i' = H'$ is smaller than i (see text). The emergent ray, therefore, is not normal to the glass-air interface of the upper hemisphere, and there must be a displacement $CB = x$ in the central layers of the sphere.

(*b*) Diagrammatic representation of the seven layers at the center of the universal stage, between the stage mount and the upper hemisphere. The center of the sphere is at the center of the mineral plate, C. r_s is the angle of refraction within the microscope slide, and the distance CB is the displacement of the light ray indicated in Fig. 3*a*. N_1, N_2 and N_3 are normals.

For angles less than 35° the error is negligible but for angles greater than 35° it increases markedly, passing through 0.5° for an angle of tilt of 46° and reaching 1° for an angle of tilt of 56°. These errors are much increased when allowance is made also for the displacive effect of the stage mount. It is tacitly assumed in text books that the stage glass has the same refractive index as the hemispheres, but this is not so. The stage glass used in the present measurements has a refractive index of 1.560 and thickness 2.46 mm. (measured by R. Johnston). If the displacive effect of this

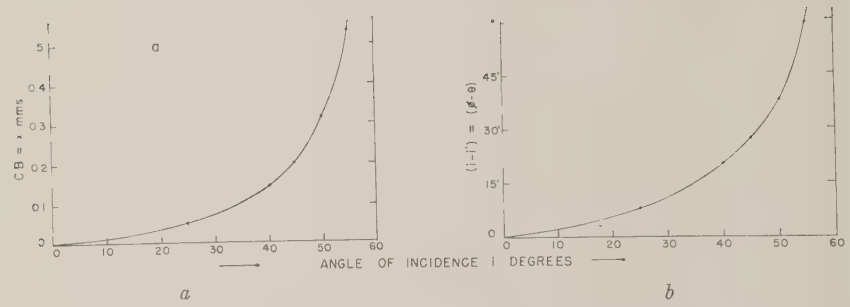

FIG. 4. (*a*) The calculated displacement CB (Fig. 3) plotted against the angle of incidence (angle of tilt) *i*.

(*b*) The calculated angular error $(i-i')$ plotted against the angle of incidence *i*. There is a rapid rate of increase of both values when *i* exceeds 40°.

plate is added to that of the microscope slide, a ray with angle of incidence 45° would have an angular error of 2° when it emerged from the sphere instead of the 27′ which would be produced by the microscope slide alone (Fig. 4*b*).

Examination of the path of a single light ray demonstrates an increasing error with increasing tilt of the stage, but it does not give a realistic picture of what actually happens when a measurement is made on the universal stage. Figure 5 shows a beam of parallel light rays, *abc*, entering the sphere with the central ray, *b*, directed towards the center of the sphere. Only those rays which emerge almost parallel to the incident beam will reach the eye of the observer. The ray *b* is incident normally but the other rays will be refracted slightly on entering the sphere, the amount of refraction increasing towards the edges of the beam, *a* and *c*. The beam as a whole is displaced by refraction within the central layers. Each ray within the beam has a different effective displacement from the center of the sphere and each ray therefore has a different error $(\phi-\theta)$. The rays in the side *c* of the beam will have a value of $(\phi-\theta)$ greater than, and the rays in the side *a* of the beam less than that for the center of the beam, *b*. Figure 5 shows that, except for low angles of tilt of the stage, the rays emerging parallel to the microscope axis are not those which were directed

towards the center of the sphere, i.e. the center of the beam, *b*. The rays emerging parallel to the microscope axis are those from the side *a* of the incident beam. These rays are refracted when they enter the sphere and their angles within the hemispheres do not equal the angle of incidence, which is the measured angle. With increasing angle of tilt, rays further from the center of the incident beam will be received by the microscope

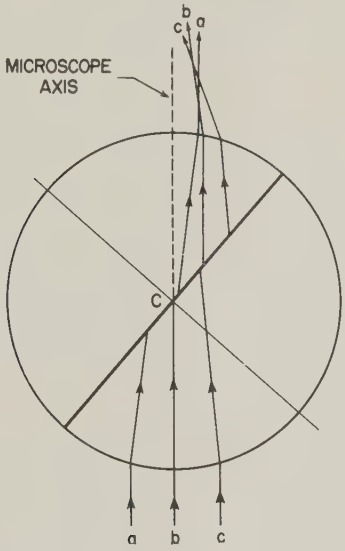

FIG. 5. Diagrammatic representation of the refraction and displacement of a beam of parallel rays entering the universal stage with a high angle of tilt. The center ray *b* is directed towards the center of the sphere, C. The outer rays of the beam are refracted slightly on entering the sphere. The beam as a whole is displaced within the central layers of the sphere (Fig. 3) and the effective displacement of rays in different parts of the beam varies. In the example shown, the ray *a* is displaced the least, and this ray emerges nearly parallel to the microscope axis. The rays *b* and *c* are refracted through successively greater angles on emergence. The angle measured is the angle of tilt, i.e. the angle of incidence of the central ray, *b*. The rays observed will be those most nearly parallel to the microscope axis. i.e. those near *a*. The ray *a* has a different angle within the hemispheres compared to that of *b*.

and the difference between the recorded angle (angle of incidence) and the true angle 2H (the angle of the observed rays within the hemispheres) also increases. The recorded angle is smaller than the true angle (Fig. 5). This is a direct result of the increasing displacement within the central layers of the sphere, and it is clear that accurate universal stage measurements cannot be expected when high angles of tilt are involved unless a correction is made for the displacement within the central layers as well as for refraction within the mineral plate.

Conclusions

(1) No significant difference was found between the means of single axis measurements made over different bisectrices in Sill 1A. In Sill 1, the differences are of the order of the estimated experimental errors and they may be statistically significant. The means of single axis measurements agree closely with the means of double axis measurements.

(2) In double axis measurements a significant difference exists between measurements made over different bisectrices. The average of the means of measurements over α and γ are in close agreement with the single axis measurements.

(3) The discrepancy in the double axis measurements may be explained if the observed angle is smaller than the true angle and it has been shown that refraction within the microscope slide and stage mount could produce this effect for high angles of tilt.

These conclusions are not in accord with those of Game (1941) and Frankel (1942). The difference between the means of $2V_\alpha$ and $2V_\gamma$ is of the same order as that noted by Johnston (1953). Wilkinson (1956) found good agreement between double axis and single axis measurements, and this is probably due to the fact that he avoided double axis measurements involving high angles of rotation.

The results presented emphasize the importance of using low angles of tilt of the universal stage whenever possible, and they demonstrate the nature and magnitude of the error introduced when high angles cannot be avoided. The introduction of errors with high angles of tilt has frequently been noted in the literature. Turner (1942) discussed refractive index corrections and stated that the errors cannot wholly be eliminated if high angles are involved, but according to Hallimond and Taylor (1950) little or nothing has been said in most text books about the refractive effect of the glass-air interfaces of the hemispheres. They discussed the errors arising if the upper hemisphere is not correctly centered. Piller (1957) gives a quantitative treatment of the error which occurs when the specimen or cover-glass is of the wrong thickness, causing a vertical displacement of the upper hemisphere with reference to the horizontal axis.

High angles of tilt of the universal stage, although avoided whenever possible, must frequently be used in optical studies. This is particularly true for the double axis determination of 2V's near 90°. By using the double axis conoscopic method in order to obtain results of higher accuracy, a further error is introduced and this can be detected only because the method is so accurate for a given measurement; the difference between $(-)2V_\alpha$ and $(-)2V_\gamma$ is the only indication that such an error exists. If one measurement made over α or γ were assumed to be correct

the result could be wrong by as much as 3°, corresponding to an error of about 6 molecular per cent of fayalite in the estimated composition of an olivine (see Fig. 2). The accuracy of such measurements is therefore not as high as claimed by Hallimond (1950) unless corrections are made for the high angles of tilt.

Fairbairn and Podolsky (1951) stressed the importance of precision and accuracy in stage measurements and regretted the dearth of published data on the subject. They recorded the compositional variation occurring among plagioclase feldspars within the same rock and concluded that unless accurate determinations are made such variations may not be distinguished. Yet the supposedly accurate measurements plotted in Fig. 2, with estimated experimental errors of $\pm 0.5°$, occupy ranges of 5°. This could be interpreted as due to compositional variations among the olivines, amounting to 10 molecular per cent of fayalite, but the systematization of results indicates that it is due to additional errors produced by the high angles of tilt which had to be used. To the request of Fairbairn and Podolsky for greater precision of measurement may be added a plea for further investigation of the errors involved in measurements.

Acknowledgments

A serial collection of specimens was collected from Soay during a field study of picritic rocks, in collaboration with Dr. H. I. Drever and Mr. R. Johnston, and it was Johnston who drew the writer's attention to the reported discrepancies in the measurement of 2V in forsteritic olivine. Useful criticism of the manuscript was received from Mr. R. Johnston, Dr. H. I. Drever, Professors O. F. Tuttle and H. D. Wright.

References

Emmons, R. C. (1943), The universal stage: *Geol. Soc. Amer. Mem.*, **8**.

Fairbairn, H. W., and Podolsky, T. (1951), Notes on precision and accuracy of optic angle determinations with the universal stage: *Am. Mineral.*, **36**, 823–832.

Frankel, J. J. (1942), Studies on Karroo dolerites. (2). Some younger intrusions of olivine basaltic dolerite: *Trans. Geol. Soc. S. Africa*, **45**, 1–26.

Game, P. M. (1941), Optical properties of olivines from Ubekendt Ejland, West Greenland: *Miner. Mag.*, **26**, 11–15.

Hallimond, A. F. (1950), Universal stage methods: *Mining Mag.*, **83**, 12–22.

Hallimond, A. F., and Taylor, E. W. (1950), An improved polarizing microscope. IV. The federov stage (three axis): *Miner. Mag.*, **29**, 150–162.

Johnston, R. (1953), The olivines of the Garbh Eilean sill, Shiant Isles: *Geol. Mag.*, **90**, 161–171.

Moroney, M. J. (1951), Facts from figures. Penguin Books Ltd.

Piller, H. (1957), Bemerkungen über den Einflüsse der Segment Grösse und Präparatdicke aud die Genauigkeit bei der Messung von Neigungswinkeln mit dem Universal drehtisch: *Mikroskopie*, **12**, 166–174.

Poldervaart, A. (1950), Correlation of physical properties and chemical composition in the plagioclase, olivine, and orthopyroxene series: *Am. Mineral.*, **35,** 1067–1079.

Turner, F. J. (1942), Determination of extinction angles in monoclinic pyroxenes and amphiboles: *Amer. J. Sci.*, **240,** 571–583.

Wilkinson, J. F. G., (1956), The olivines of a differentiated teschenite sill near Gunnedah, New South Wales: *Geol. Mag.*, **93,** 441–455.

Manuscript received May 1, 1958

THE AMERICAN MINERALOGIST, VOL. 44, JANUARY-FEBRUARY, 1959

ABSORPTION AND PLEOCHROISM: TWO MUCH-NEGLECTED OPTICAL PROPERTIES OF CRYSTALS*

JOSEPH A. MANDARINO,† *University of Michigan, Ann Arbor, Michigan.*

ABSTRACT

Certain fundamental relationships of absorption and pleochroism are presented to stimulate interest in the quantitative expression of these two properties. The absorption coefficient (k) is given preference as the absorption constant, while biabsorption is re-emphasized as a quantitative expression for pleochroism. Methods for the determination of the absorption coefficients are briefly discussed. Two methods for the determination of biabsorption are presented in detail.

INTRODUCTION

With the polarizing microscope (probably the most widely used tool in mineralogy today), methods have been evolved which make possible the accurate measurement of many optical properties of crystals. However, investigators have overlooked certain other optical properties. Absorption and pleochroism, although they are sometimes mentioned in a qualitative manner, have been almost entirely ignored.

The purpose of this paper is three-fold. First, it is hoped that interest in absorption and pleochroism will be stimulated among mineralogists and petrographers. Secondly, certain constants for the quantitative expression of these two properties are suggested. Lastly, some methods for measuring these properties are described.

The material presented in this paper stems from a project sponsored by the Office of Naval Research. Their assistance is gratefully acknowledged. Thanks are also extended to Professor Reynolds M. Denning of the University of Michigan, who contributed many suggestions during the course of the project.

HISTORY

The absorption of light in crystals was first investigated early in the 19th century, but it did not progress beyond a rule-of-thumb system until much later. Among the earlier investigators was Babinet (1838), who discovered that the greatest absorption in a crystal generally coincided with the direction of greatest refractive index. He found many exceptions to this rule, however. Laspeyres (1880) pointed out the existence of absorption axes (directions of least, intermediate, and greatest absorption). He investigated certain biaxial crystals and found that the

* Contribution No. 229 from the Department of Mineralogy, University of Michigan, Ann Arbor, Michigan.

† Present address: Department of Geology and Geological Engineering, Michigan College of Mining and Technology, Houghton, Michigan.

absorption axes, although subject to the symmetry of the crystal, did not necessarily coincide with the principal directions of the indicatrix. Between 1880 and 1900, Voigt (1885) and Drude (1900) presented the fundamental theories of absorption in crystals. During this same period, notable experimental work confirming these theories was carried out by Voigt (1885), Becquerel (1887), Ramsay (1888), and Ehlers (1898). Shortly afterwards, Pockels (1906) presented an excellent summary of the work up to that time.

The introduction of photoelectric devices restimulated activity in this field during the 1930's. Vogel (1934) investigated absorption in certain crystals colored by chromium (emerald, natural and synthetic ruby, and synthetic spinel). Unfortunately, his absorption data were given in terms of galvanometer readings and served only to determine the wave lengths at which absorption maxima and minima occurred. He did not specify the orientation of his crystals; nor, apparently, did he measure their absorption for any particular direction. Tromnau (1934) studied the optical properties of synthetic spinel colored by various amounts of cobalt. Again absorption data were presented as galvanometer readings. Tromnau's paper is interesting, however, for the refractive index data presented. It is one of the few tabulations of refractive indices that clearly illustrates the change from normal dispersion to the so-called anomalous dispersion in an inorganic isomorphous series.

Berek's many contributions in the field of absorption are summarized in the book by Rinne and Berek (1953).

In the last ten years much work has been done on the study of light absorption in crystals. However, a great deal of this work includes the same objectionable features of some of the earlier studies: especially, inconsistencies in the choice of absorption constants. Some modern investigators still use terms such as "optical density" [Cohen (1956)] and "absorption modulus" [Vultée and Lietz (1956) and Lietz and Münchberg (1956)].

Bloss (1955) presented a study of absorption in the series $Ni(NH_4)_2(SO_4)_2 \cdot 6H_2O - Mg(NH_4)_2(SO_4)_2 \cdot 6H_2O$, and correlated absorption (optical density and molar absorbance) with composition.

Pleochroism, although included in the titles of many early papers, has been almost completely omitted from any quantitative investigation. Slawson and Thibault (1939) expressed the pleochroism of a tourmaline crystal in terms of the ratio I_ω/I_ϵ. Denning and Mandarino (1955) suggested the term "biabsorption" as a quantitative expression for pleochroism. They defined biabsorption in a uniaxial crystal as the difference between the absorption coefficients for the extraordinary and ordinary rays.

Absorption Terminology

Theory

If light having an initial intensity of I_0 passes through a medium, the initial intensity is reduced by: 1) scattering, 2) reflection at both surfaces of the medium, and 3) the inherent absorbing power of the medium.

In order to convert the measured transmittances I'/I_0 to the correct transmittances I/I_0, the losses due to scattering and reflection must be accounted for. Losses due to scattering can be ignored if the crystal being investigated is relatively free from inclusions and imperfections. Losses due to reflection can be rectified by applying the well-known Fresnel corrections. The relation between the true intensity I and the measured intensity I′ is given by

$$I = I' \left(\frac{1}{1 - R}\right)^2 \tag{1}$$

in which R is the reflecting power. The value of R may be calculated from the following equation:

$$R = \left(\frac{n - 1}{n + 1}\right)^2 \tag{2}$$

in which n is the index of refraction of the crystal for the vibration direction being investigated. Substitution of the value of R in Equation 1 yields

$$I = I'\left[\frac{(n + 1)^2}{4n}\right]^2 \tag{3}$$

Absorption must be expressed in terms of carefully defined constants. A variety of constants have been employed in the past. All of these constants have been based on the following general equation:

$$I/I_0 = e^{-ab} \tag{4}$$

In this equation, I_0 is the intensity of the incident light, I is the intensity of the emergent light corrected for reflection losses, e is the base of the natural logarithms, a is the absorption constant, and b is a constant dependent on the conditions of measurement. The value of I/I_0 is determined and the value of a is then calculated from the equation to yield the desired absorption constant. The numerous absorption constants found in the literature are due to various expansions of the exponent b in Equation 4.

Table 1 is a compilation of terms which have been used to express absorption. Many of these terms over-simplify the process of absorption; others, although suitable for special applications (i.e., colorimetry) are unsuitable for fundamental absorption studies. A term for the ex-

Table 1. Various Terms Used to Express Absorption

In the equations, l = optical path length in the medium, c = concentration of the coloring material, M = molecular weight of the coloring material, λ = wave length of the light used, n = refractive index of the medium, I_0 = the intensity of the incident light, and I = the intensity of the emergent light corrected for reflection losses.

Symbol	Term	Equation
T	Transmission = Transmittancy	$T = I/I_0$
A	Absorption = Absorbancy	$A = 1 - T$
D	Optical density	$D = \log_{10} (I_0/I)$
E	Extinction	$E = \log_{10} (I_0/I)$
K	Extinction coefficient	$K = \frac{\log_{10} (I_0/I)}{l}$
k	Specific extinction	$k = \frac{\log_{10} (I_0/I)}{cl}$
α	Specific absorption coefficient	$\alpha^{-cl} = I/I_0$
ϵ	Molecular extinction	$\epsilon = \frac{M \log_{10} (I_0/I)}{cl}$
m	Absorption modulus	$I/I_0 = e^{-ml}$
k	Absorption coefficient	$I/I_0 = e^{-k(4\pi l/\lambda)}$
X	Absorption index	$I/I_0 = e^{-X(4\pi ln/\lambda)}$

pression of absorption should be based on the following precepts: 1) an absorption constant, like index of refraction, should be mathematically dimensionless; 2) it should be based on accepted physical theories, thus lending itself to the calculation of special constants for special absorption problems; and 3) it should be easily measurable or easily calculable from an easily measurable quantity.

An expression such as "absorption modulus," because of its dimensions (cm^{-1}), gives the erroneous impression of "absorption per centimeter." But more important: it has very little significance in the concept

of the complex index of refraction for absorbing media. Simply stated, the complex index is a combination of the refractive index and the absorption ($N = n - ik$). Consequently, both properties should be expressed as dimensionless quantities.

In analyzing the terms found in Table 1, it can be seen that two terms meet the first two requirements stated above. In addition, they may both be calculated from easily measurable quantities. These terms are: the "absorption index" (X) and the "absorption coefficient" (k). They are related by the following equation:

$$k = nX \tag{5}$$

in which n is the index of refraction.

In this paper the nomenclature of Berek (1953) is used. Absorption is expressed in terms of the absorption coefficient k. Consequently, only equations dealing with k are presented here. The basic equation relating the absorption coefficient to the intensities of the incident and emergent light is as follows:

$$I/I_0 = e^{-4\pi tk/\lambda} \tag{6}$$

In this equation, k is the absorption coefficient, I_0 is the intensity of the incident light, I is the intensity of the transmitted light corrected for reflection losses, t is the path length in the absorbing medium, e is the base of the natural logarithms, and λ is the wave length of the light used.

If a plate of a uniaxial crystal cut parallel to the c-axis is used for the specimen, the absorption coefficients for the ordinary and extraordinary rays are derived from the following equations:

$$I_\omega/I_o = e^{-4\pi tk_\omega/\lambda} \tag{7}$$

$$I_\epsilon/I_o = e^{-4\pi tk\epsilon/\lambda} \tag{8}$$

in which I_ω is the intensity of the transmitted ordinary ray, corrected for reflection losses; and I_ϵ is the same for the extraordinary ray. If the specimen is mounted in the usual type of petrographic thin-section, the measured intensities must also be corrected for the reflection losses due to the glass and balsam. The absorption coefficients for the ordinary and extraordinary rays are

$$k_\omega = -\frac{\lambda \ln (I_\omega/I_0)}{4\pi t} \tag{9}$$

$$k_\epsilon = -\frac{\lambda \ln (I_\epsilon/I_0)}{4\pi t} \tag{10}$$

In like manner, similar equations can be derived for k_α, k_β, and k_γ for biaxial crystals.

These absorption coefficients are independent of thickness and can

be used to calculate any of the special absorption constants previously mentioned.

Methods of Measurement

All absorption measurements, regardless of the constant desired, require a measurement of the ratio I/I_0. In some methods of measurement this quantity is measured directly (that is, I'/I_0 is measured, and then corrected for reflection losses to I/I_0). However, in many methods, a function of this quantity is measured instead. There are three common spectrophotometric methods of measuring I/I_0 or some function thereof: visual, electronic, and photographic.

Typical instruments for all three types of measurement are fully described by Gibb (1942), Mellon et al. (1950), Judd (1952), Brode (1943), and the Committee on Colorimetry of the Optical Society of America (1953). These references also include comprehensive bibliographies of the literature on spectrophotometry.

The choice of the instrument to be used in absorption work usually depends on the instrument available. For this reason, descriptions of individual instruments will not be presented here.

Pleochroism Terminology

Theory

Although the study of absorption in crystals has been complicated by the use of many different constants, few attempts have been made to apply a quantitative term for the expression of pleochroism. The use of the ratio I_ω/I_ϵ has been suggested (for uniaxial crystals), but this has the objectionable feature of being dependent on the thickness of the sample. Since pleochroism is the difference between the extraordinary absorption and the ordinary absorption in a uniaxial crystal, the quantity $k_\epsilon - k_\omega$ could be used to express pleochroism quantitatively. This quantity, like the individual absorption coefficients, is independent of thickness. It follows, then, that pleochroism can be calculated from the values of k_ϵ and k_ω. This method of calculating pleochroism is analogous to the method of calculating birefringence from the indices of refraction. By using various compensators, birefringence can be measured directly without recourse to the values of the refractive indices; similarly, pleochroism can be measured directly.

The equation for $k_\epsilon - k_\omega$ can be derived from Equations 7 and 8 for the ordinary and extraordinary rays. Division of the ordinary equation (Eq. 7) by the extraordinary equation (Eq. 8) yields

$$I_\omega/I_\epsilon = e^{(4\pi t/\lambda)(k_\epsilon - k_\omega)} \tag{11}$$

Solution for $k_\epsilon - k_\omega$ yields

$$k_\epsilon - k_\omega = \frac{\lambda \ln (I_\omega / I_\epsilon)}{4\pi t} \tag{12}$$

The similarity of this equation to that for birefringence ($n_\epsilon - n_\omega = \Gamma/t$) led to the expression of $k_\epsilon - k_\omega$ as *biabsorption*. Calculation of biabsorption can be accomplished by measuring the ratio I_ω/I_ϵ directly. Just as in the measurement of I/I_0, reflection corrections must be applied to the measured value I_ω'/I_ϵ'. If the birefringence is relatively small, the correction is negligible. For specimens in ordinary thin-sections, no correction is necessary for reflection losses due to the glass slide, balsam, and cover glass.

Methods of Measurements

There are two generally applicable methods of measuring I_ω/I_ϵ directly. One method uses a standard retardation compensator and a rotatable analyzer. The other method depends on visually matching the brightness of two images formed by a double-image plate.

Double-Image Method

This method employs a double-image plate above or below a pleochroic plate so oriented that the vibration directions of the crystal plate are parallel to the vibration directions of the double-image plate. The double-image plate may be a Wollaston plate, Rochon plate, or simply a calcite cleavage plate. When monochromatic light is passed through both plates and observed by means of a suitable optical system, two images are seen. The light forming both images is linearly polarized such that the vibration direction of one image is normal to the vibration direction of the other image. Thus, one image represents the intensity of the light transmitted by the ordinary ray of the pleochroic crystal and the other image represents the intensity of the light transmitted by the extraordinary ray. A linear polar placed between the plates and the eye can be rotated until the two images have the same brightness. Figure 1 shows the relations of the amplitudes of the two transmitted rays. OA is the amplitude of the ordinary ray and OB is the amplitude of the extraordinary ray. When the polar is rotated to a position such that its vibration direction is OP, the two images have the same brightness. If angle AOP is designated as α,

$$\frac{OA}{OB} = \tan \alpha = \frac{A_\omega}{A_\epsilon} \tag{13}$$

Squaring both sides of this equation produces

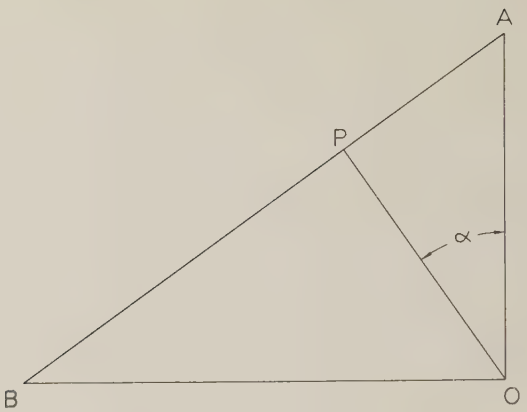

FIG. 1. Relationship between the amplitudes of the transmitted rays of a pleochroic crystal plate.

$$I_\omega/I_\epsilon = \tan^2 \alpha \tag{14}$$

Thus the ratio of I_ω to I_ϵ can be measured directly. Very often the two images have different brightnesses before the pleochroic plate is placed in the system. If such is the case, the ratio between these two incident intensities must be determined and applied as a correction to the measured value of I_ω/I_ϵ. This correction is determined by rotating the polar to a position of equal brightness when the pleochroic plate is out of the system. If this angle is designated as β, the equation for I_ω/I_ϵ becomes:

$$I_\omega/I_\epsilon = \tan^2 \alpha \cot^2 \beta \tag{15}$$

When a calcite cleavage plate is used as a double-image plate, the value of $\cot^2 \beta$ may vary considerably from unity due to the extreme difference between the refractive indices. The use of a Wollaston or Rochon plate greatly reduces the correction.

The double-image method was used to determine biabsorption in synthetic ruby and the resulting data will be presented in a later paper.

Compensator-Analyzer Method

In general, when a non-pleochroic, optically anisotropic crystal plate is placed between crossed linear polars such that the vibration directions of the crystal are at 45° to those of the polars, elliptically polarized light is produced. The axes of the resultant ellipse are parallel to the vibration directions of the crystal plate and their ratio is a function of the phase-difference between the two rays transmitted by the crystal. The solid curve in Fig. 2 represents the trace of the elliptically polarized light pro-

duced by a crystal plate whose two rays were subjected to a phase-difference of thirty degrees ($\lambda/6$ linear path difference).

If the crystal is pleochroic, an entirely different ellipse is traced by the resultant elliptically polarized light. Not only is the ratio of the axes of the ellipse changed, but the axes are inclined to the vibration directions of the crystal. The dotted curve in Fig. 2 is the trace of the resultant elliptically polarized light from a pleochroic crystal whose two rays are subjected to the same phase-difference as before (thirty degrees).

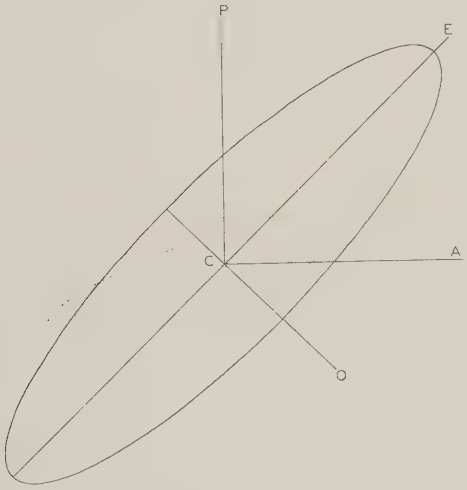

FIG. 2. Traces of the elliptically polarized light produced from crystal plates with a phase-difference of thirty degrees. Solid curve, non-pleochroic crystal; dotted curve, pleochroic crystal.

The angle through which this second ellipse has been rotated is a function of the ratio of the intensities of the ordinary and extraordinary rays. Measurement of this angle makes possible the calculation of I_ω/I_ϵ and, subsequently, $k_\epsilon - k_\omega$. The problem is very similar to the determination of birefringence discussed by Berek (1953) and Hallimond (1953).

In order to develop the mathematical relations upon which this method is based, the dotted ellipse of Fig. 2 has been redrawn in Fig. 3. The vibration directions of the polarizer and analyzer are represented by CP and CA, respectively. CO is the ordinary vibration direction of the crystal and CE is the extraordinary vibration direction. CO_0 and CE_0 are the components of the incident light resolved along the ordinary and extraordinary vibration directions of the crystal, respectively. CO_1 is the amplitude of the transmitted ordinary ray and CE_1 is the amplitude of

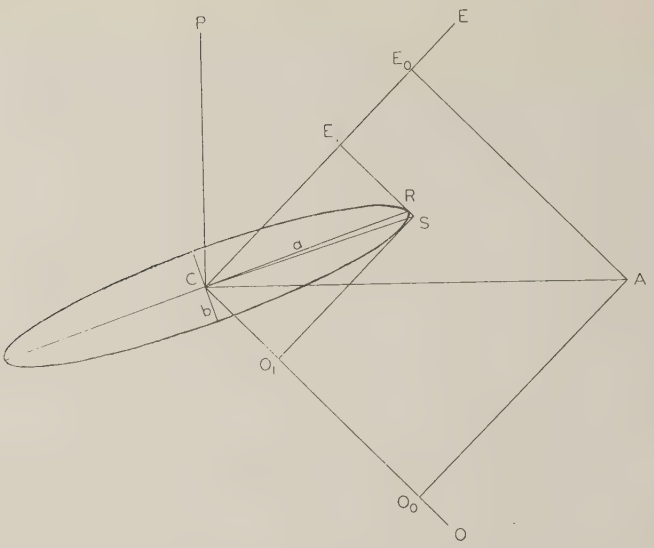

FIG. 3. Geometrical relationships of the elliptically polarized light produced by a pleochroic crystal plate.

the transmitted extraordinary ray. It can be seen that CO_1/CE_1 equals the square root of I_ω/I_ϵ. Because $CO_1/CE_1 = \tan$ ECS, it is necessary to determine the value of angle ECS.

The relationships between angle ECS, angle ECR, and Δ are given by the following equations from Hallimond (1953). Proofs of these equations are given by Schuster and Nicholson (1924).

$$\tan 2 \text{ ECS} = \frac{\tan 2 \text{ ECR}}{\cos \Delta} \tag{16}$$

$$\tan \Delta = \frac{\tan 2(\tan^{-1} b/a)}{\sin 2 \text{ ECR}} \tag{17}$$

Angle ECR is the angle between the extraordinary vibration direction of the crystal and the major axis of the ellipse. Δ is the angular phase-difference between the ordinary and extraordinary rays.

From Equations 16 and 17, it can be seen that measurements of b/a and angle ECR are necessary for the determination of I_ω/I_ϵ.

Procedures for the measurement of both of these quantities are described by Hallimond. The measurement requires a microscope so constructed that the analyzer may be rotated. In addition, an accessory slot must be provided at 45° to the analyzer vibration direction and must rotate with the analyzer.

If a compensator is placed in the accessory slot, the crystal plate can be compensated only when the vibration directions of the compensator

are parallel to the axes of the ellipse. Thus, in the case of a non-pleochroic crystal, the elliptically polarized light can be resolved into linearly polarized light by adjusting the compensator when the vibration directions of the compensator are parallel to the vibration directions of the crystal plate. In the case of a pleochroic crystal plate, however, the axes of the ellipse are not parallel to the vibration directions of the crystal. Therefore, the compensator and analyzer must be rotated until the vibration directions of the compensator are parallel to the axes of the ellipse. This angle of rotation is equal to the angle ACR which is equal to 45°-ECR.

Many compensators yield values of retardation in terms of linear path-difference, Γ. The angular phase-difference at 45° to the ellipse is designated ϕ. The relation between ϕ and Γ is

$$\phi = \frac{2\pi\Gamma}{\lambda} \tag{18}$$

in which λ is the wave length of the light employed. ϕ is related to the quantity b/a as follows:

$$\phi = 2(\tan^{-1} b/a) \tag{19}$$

From Equations 16 and 17 it follows that

$$\tan 2\ \mathrm{ECS} = \frac{\tan 2(45° - \mathrm{ACR})}{\cos \Delta} \tag{20}$$

$$\tan \Delta = \frac{\tan \phi}{\sin 2(45° - \mathrm{ACR})} \tag{21}$$

Substitution of the measured values of ACR and ϕ in the preceding equations yields a solution for the value of ECS. The value of I_ω/I_ϵ is determined from the following equation:

$$I_\omega/I_\epsilon = \tan^2 \mathrm{ECS}$$

Biabsorption can then be calculated in the usual manner from the value of I_ω/I_ϵ.

The compensator-analyzer method is subject to one serious limitation: it can only be used for substances that show appreciable pleochroism in relatively thin plates (more specifically, in plates of relatively low retardation). The double-image method, however, can be used on plates of relatively high retardation.

Comments

It can be seen, from the foregoing discussion of measurement methods, that rather expensive equipment is necessary for the determination of absorption coefficients. Unless a suitable spectrophotometer is available to interested workers, it is doubtful whether the absorption coefficient

will become a commonly noted constant in mineralogical literature. However, the measurement of biabsorption requires very little equipment not already present in most mineralogical or petrographic laboratories.

The emphasis in this paper has been on uniaxial crystals. However, these same methods, with appropriate changes in equations, may also be applied to biaxial crystals. It is proposed that k_α, k_β, and k_γ refer to the absorption associated with the directions of the refractive indices α, β, and γ, respectively. *It should be noted that* $k_\alpha < k_\beta < k_\gamma$ *will not necessarily hold true.*

References

Babinet, M. (1838), Sur l'absorption dans les milieux colores birefringents: *Compt. Rend. Acad. Sci. Paris*, **7**, 832–833.

Becquerel, H. (1887), Sur l'absorption de la lumiere au travers des cristaux: *Bull. Soc. Fran. Min.*, **10**, 120–124.

Berek, M. (Rinne-Berek) (1953), Anleitung zu optischen Untersuchungen mit dem Polarisationsmikroskop. Stuttgart.

Bloss, F. (1955), Relationship between light absorption and composition in a solid solution series: *Am. Mineral.*, **40**, 371–397.

Brode, W. (1943), Chemical Spectroscopy. John Wiley and Sons, New York.

Cohen, A. (1956), Color centers in the α-quartz called amethyst: *Am. Mineral.*, **41**, 874–891.

Committee on Colorimetry of the Optical Society of America (1953), The Science of Color. Thomas Y. Crowell, New York.

Denning, R., and Mandarino, J. (1955), Pleochroism in synthetic ruby: *Am. Mineral.*, **40**, 1055–1061.

Drude, P. (1900), Lehrbuch der Optik. S. Hirzel, Leipzig.

Ehlers, J. (1898), Die Absorption des Lichtes in einigen pleochroitischen Krystallen: *Neues Jahrb.*, **11**, 259–317.

Gibb, T. (1942), Optical Methods of Chemical Analysis. McGraw-Hill Book Company, Inc., New York.

Hallimond, A. (1953), Manual of the Polarizing Microscope. Cooke, Troughton, and Simms, York, England.

Judd, D. (1952), Color in Business, Science, and Industry. John Wiley and Sons, New York.

Laspeyres, H. (1880), Mineralogische Bemerkungen: *Zeit. Kryst.*, **4**, 433–467.

Lietz, J., und Münchberg, W. (1956), Über Symmetrie und Pleochroismus von Amethyst: *Neues Jahrb.*, **88**, 217–232.

Mellon, M. (Editor) (1950), Analytical Absorption Spectroscopy. John Wiley and Sons, New York.

Pockels, F. (1906), Lehrbuch der Kristalloptik. Leipzig-Berlin.

Ramsay, W. (1888), Ueber die Absorption des Lichtes im Epidot vom Sulzbachthal: *Zeit. Kryst.*, **13**, 97–134.

Schuster, A., and Nicholson, J. (1924), Theory of Optics. Arnold, London.

Slawson, C., and Thibault, N. (1939), Quantitative measurement of dichroism in tourmaline: *Am. Mineral.*, **24**, 492–498.

Tromnau, H. (1934), Chemische und physikalische Untersuchungen an synthetischen mit Kobalt gefärbten Spinellen: *Neues Jahrb.*, **68**, 349–376.

Vogel, P. (1934), Optische Untersuchungen am Smaragd und einigen anderen durch Chrom gefarbten Mineralien: *Neues Jahrb.*, **68**, 401–438.

Voigt, W. (1885), Erklärung der Farbenerscheinungen pleochroitischer Krystalle: *Neues Jahrb.*, **1**, 119–141.

Vultée, J., und Lietz, J. (1956), Über die Rolle des Titans als Färbungsursache von Blau- und Rosenquarz: *Neues Jahrb.*, **88**, 49–58.

Manuscript received April 18, 1958

THE AMERICAN MINERALOGIST, VOL. 44, JANUARY–FEBRUARY, 1959

MORPHOLOGY AND CRYSTAL CHEMISTRY OF 1:1 LAYER LATTICE SILICATES*

THOMAS F. BATES, *The Pennsylvania State University, University Park, Pennsylvania.*

ABSTRACT

Sixty-four chemical analyses of sheet structure silicates with a 1:1 type layer lattice have been evaluated in order to demonstrate certain interrelationships between chemistry, structure and morphology within and between the following mineral groups: kaolin, serpentine and "other 1:1" layer lattice silicates (amesite, cronstedtite and ferrous and ferric chamosite). The analyses of five synthetic 1:1 compounds and seven representative chlorites are also included and discussed.

The morphological characteristics of the minerals relate directly to the nature and amount of cation substitution in tetrahedral and octaheral sheets, and to the amount of H_2O+. The former is evaluated in terms of a morphological index, M, which gives a measure of the amount of misfit of the two sheets within the layer. The effect of the latter is shown in ternary composition diagrams.

Structural formulas are computed on the basis of a lattice of 18 oxygens but using the premise that oxygen and (OH) allocation between the two sheets will be proportioned in accord with the cation distribution. The allocation of cations, in turn, is based on the assumption that substitutions or additions of Fe''' and Al in the octahedral sheet will equal substitutions of these ions for silicon in the tetrahedral sheet.

The kaolin, serpentine and "other 1:1" groups differ from each other chiefly with respect to the amount of cation substitution and therefore the amount of misfit of the two sheets in the 1:1 layer. In terms of the morphological index, serpentines range from +73.53 to+ 60.09, other 1:1 from +35.35 to −60.09 and kaolins from −72.11 to −84.13.

Within the serpentine and kaolin groups cation substitutions play an important role but the amount of hydrogen provides the most important distinction between platy and tubular varieties. Analyses of chrysotile and halloysite ($2H_2O$) contain significantly more H_2O+ than those of their platy counterparts. Although the position of the "excess" hydrogen and oxygen ions in or on the lattice is not known, the effect of these elements is apparently to weaken interlayer bonds to the extent that misfit of the sheets produces tubes or curved laths rather than plates.

The evaluation of the chlorite analyses yields results similar to those obtained for amesite, chamosite and cronstedtite in that cation substitution provides for much less misfit than in kaolins or serpentines, and H_2O+ is nearly equal to or less than that to be expected in the O and (OH) of the properly proportioned structural formulas.

INTRODUCTION

Research during the past eight years on morphological details of kaolin, serpentine and related minerals has led to an evaluation of the relationship of morphology to chemical composition in those compounds which combine a "gibbsite" or "brucite" sheet with a Si-O sheet to give a so-called 1:1 layer structure. Meanwhile studies of others on crystal structure, density and other characteristics of the minerals have pro-

* Contribution No. 57-81 from the College of Mineral Industries, The Pennsylvania State University.

vided additional information as to the relationship of the minerals to each other and to other members of the sheet structure silicate group.

In the present study the minerals of major interest are those of the kaolin and serpentine groups but, in order to obtain a more complete picture of overall chemical-morphological relationships, amesite, cronstedtite, chamosite and several synthetic compounds having the 1:1 structure are included. In addition, the relationship of the chlorites to these minerals is considered.

Summary of Morphological Data

Amesite and cronstedtite both occur in small but megascopic crystals, amesite in the form of hexagonal plates, cronstedtite in hexagonal pyramids and diverging groups having perfect basal cleavage.

Chamosite normally is massive or oolitic. Deudon (1955) points out that in electron micrographs platy particles are commonly irregular but sometimes show hexagonal corners.

In the kaolin group, nacrite, dickite and kaolinite are platy and show poor to well-developed hexagonal outlines depending on the source and type of material and the manner of preparation of the material for observation in the electron microscope. Flat laths of well-crystallized kaolinite with hexagonal terminations are not uncommon, particularly from areas where hydrothermal solutions have led to the formation of clay minerals.

At the other extreme in the kaolin group are the irregular nodules and spherical particles considered typical of allophane (Davis, et al., 1950, p. 9; Sudo and Takahashi, 1956). The latter authors have shown that there may be a morphological and chemical transition between amorphous spherules of allophane and the tubes of halloysite ($4H_2O$). Replicas of fractured surfaces of samples of the latter (Bates and Comer, 1955) demonstrate that tubes are the characteristic crystal form of this clay mineral, and show that the cross sections of the cylinders are circular or elliptical in outline.

The occurrence of tubes with polygonal outlines (Bates, 1955) plus evidence of the existence of lath-shaped particles in a mixture of equidimensional kaolinite plates and halloysite tubes (Brindley and Comer, 1956), led to a more critical re-evaluation of hundreds of electron micrographs of halloysite, and to a detailed study of certain clay samples using replicas of fractured surfaces in order to minimize disturbance of the particles during sample preparation. The results of this study were presented at the Sixth National Clay Conference and are published in the proceedings thereof (Bates and Comer, 1959) but may be briefly summarized as follows. Replicas of fractured surfaces of halloysite

($2H_2O$) clay from the Fox deposit, Utah County, Utah, and of a halloysite ($2H_2O$)-kaolinite clay from the Raddatz deposit near Eureka, Utah, show that most of the halloysite particles are lath-shaped and possess crystallographic terminations and angles which indicate a higher degree of crystallinity than that commonly attributed to halloysite ($4H_2O$) tubes.* Figure 1, an electron micrograph of a fracture surface of the Fox Clay, illustrates these features. Electron micrographs of dispersions of this clay show that the laths have a tendency to bend along lines approximately parallel to the long axis of the particle thus giving rise to tubes with the polygonal outlines of the type referred to above. This evidence indicates that there is a complete morphological transition in the kaolin group from the well-crystallized hexagonal plates of kaolinite to elongate plates to laths with crystallographic terminations to curved laths to tubes of halloysite ($4H_2O$). If the halloysite-allophane transition suggested by Davis, *et al.* and discussed in more detail by Sudo and Takahashi is correct, the morphological transition may be said to extend all the way from the amorphous allophane to the well-ordered kaolinite.

FIG. 1. Halloysite ($2H_2O$), Fox deposit, Utah County, Utah. Replica of fracture surface showing laths with angular projections along edges. Scale represents one micron.

* This was observed and illustrated by Alexander, Faust, Hendricks, Insley and McMurdie (1943).

The analogy between the kaolin and serpentine groups is striking. Fibrous serpentine, or chrysotile, ranges morphologically from tubes of remarkable uniformity in inner and outer diameter and very high length /width ratio to elongate splintery laths many of which are associated with and genetically related to tubes. These give way to the broader curved laths and irregular sheets characteristic of antigorite and other structural varieties of the platy serpentine group. The rectified wave or corrugated structure postulated by Onsager (1952) and elaborated on by Zussman (1954) would appear to be morphologically intermediate between the curved laths of chrysotile and the well-developed plates of irregular outline but uniform thickness characteristic of the serpentine from Kennack Cove described by Midgely (1951) and later by Zussman, Brindley, and Comer (1957, p. 142), and referred to as lizardite by Whittaker and Zussman (1956). This material may represent the closest approach made by a natural serpentine mineral to the well-formed hexagonal crystals of synthetic serpentine such as those made by Tu (1950), Yoder (1952), and Roy and Roy (1954) by introducing Al into the serpentine structure.

Detailed morphological features of chrysotile tubes and halloysite laths and tubes, and the relationship of morphology to bulk density determinations have been dealt with in the paper referred to previously (Bates and Comer, 1959).

Chemical Data

Analyses Employed

Table I lists the analyses evaluated and their sources. In most cases the analyses used were those from recent literature wherein *x*-ray and other data were also reported for the samples. Chrysotile analysis #5 and platy serpentine analysis #5 are exceptions and represent the average of 29 and 14 analyses, respectively, labeled as chrysotile and antigorite in earlier literature. Dickite analyses D-1 to D-6, kaolinites K-5 to K-14, and halloysites H-2 to H-13 inclusive are taken from the reports by Ross and Kerr (1930, 1934) and the numbers used herein are those assigned in these papers.

The following synthetic compositions studied and described by Roy and Roy (1954) are also discussed and are designated in the figures by the numbers given below:

1) $Si_4Mg_6O_{10}(OH)_8$
2) $Si_4Ni_6O_{10}(OH)_8$
3) $Ge_4Mg_6O_{10}(OH)_8$
4) $Ge_4Ni_6O_{10}(OH)_8$
5) $(Si_3Al)(Mg_5Al)O_{10}(OH)_8$

In addition, characteristic compositions of penninite and corundo-

phyllite are used to help represent certain limits of chlorite composition. The formulas and the symbols used to represent them are:

P Penninite $(Si_{3.2}Al_{.8})(Al_{.8}Mg_{1.6}Fe''_{3.6})O_{10}(OH)_8$
Co Corundophyllite $(Si_{2.6}Al_{1.4})(Al_{1.4}Mg_{2.8}Fe''_{1.8})O_{10}(OH)_8$

Calculation of Structural Formulas

In calculating from the analyses the structural formulas which will be used as a basis for pointing out some of the chemical-morphological relationships it is appreciated that experimental evidence is insufficient to permit a decision as to which of many possible arrangements of ions is most nearly correct. The procedure followed here was chosen primarily on the basis of simplicity and consistency with current concepts.

In making the assignments of cations to specific lattice sites the basic premise is somewhat different from that usually employed. Because of the layer structure of this particular group of minerals and because of the

TABLE 1. CHEMICAL ANALYSES

	C-1	C-2	C-3	C-4	C-5	C-6	C-7	C-8	P-1(M)	P-2(M)	P-3(M)	P-4(M
SiO_2	41.70	42.50	41.80	41.88	41.84	42.02	41.33	41.24	41.52	42.40	41.80	42.0
Al_2O_3	.24	.32	.11	.19	.36	.52	.80	.06	.57	.74	.19	.4
Fe_2O_3	.30	.50	.68	.81	.52	.19	1.29	2.40	.36	.48	.93	1.5
MgO	42.85	42.50	42.82	41.38	40.83	41.44	41.39	38.43	42.80	42.70	42.67	42.0
FeO	.05	.01	.05	.05	2.00	.11	.08	2.16	.06	.043	.06	.0
MnO	.02	.02	.04	.05	—	.03	.04	.14	.04	.02	.04	.0
NiO	.00	.00	.00	.00	—	—	—	—	.00	.00	.00	.0
H_2O+	14.23	13.46	14.04	14.22	14.02	14.04	13.66	13.42	14.36	13.52	13.88	13.7
TiO_2	.03	.021	.05	.036	—	none	.02	trace	.06	.070	.10	.0
Cr_2O_3	.005	.004	.003	.005	—	—	—	—	.01	.008	.003	.0
CaO	.05	.04	.10	.47	—	none	trace	—	.11	.01	.19	.2
CuO	.02	.01	.00	.00	—	—	—	—	.05	.05	.00	.0
Na_2O	.07	.04	.03	.06	—	—	—	—	.03	.03	.02	.0
K_2O	.01	.02	.01	.023	—	—	—	—	.02	.02	.01	.0
P_2O_5	—	—	—	—	—	—	—	trace		—	—	—
SO_3	.02	.00	.09	.31	—	—	—	.37	.02	.00	.08	.0
CO_2	.07	.14	.01	.02	—	—	—	.10	.00	.11	.04	.0
H_2O-	.83	.65	.28	.60	—	1.64	1.57	—	.60	.26	.24	.3
Total	100.495	100.235	100.113	100.104	99.57	99.99	100.18	98.32	100.61	100.461	100.253	100.1

	P-5	P-6	P-7	P-8	P-9	P-10	P-11	P-12	P-13	P-14	P-1
SiO_2	41.26	40.75	41.30	43.45	43.60	38.40	41.65	44.25	44.50	43.53	44.
Al_2O_3	2.38	2.51	1.59	.81	1.03	.10	.10	.24	1.41	1.89	..
Fe_2O_3	2.01	3.47	3.61	.88	.90	3.42	2.88	1.34	none	.49	.(
MgO	38.40	36.94	36.30	41.90	41.00	41.91	41.06	39.02	41.56	37.52	42.(
FeO	3.31	3.12	4.51	.69	.81	none	.16	.60	.35	4.21	..
MnO	—	—	.11	none	.04	.05	.05	.02	none	.04	—
NiO	—	—	.26	—	.16	—	—	—	.095	.20	—
H_2O+	12.70	11.74	11.19	12.29	12.18	15.03	13.10	12.54	12.36	11.69	12.
TiO_2	—	.06	.15	.02	.01	none	none	.07	none	none	nor
Cr_2O_3	—	—	.30	—	.02	—	—	—	.06	.01	—
CaO	—	1.62	.43	.04	.05	none	none	—	.02	none	.
CuO	—	—	—	—	—	—	—	—	—	—	—
Na_2O	—	—	.04	.05	.01	—	—	—	none	none	—
K_2O	—	—	.02	.02	.03	—	—	—	none	none	—
SO_3	—	—	.06	—	—	—	—	—	—	—	—
CO_2	—	—	.03	—	—	—	—	—	—	—	—
H_2O-	—	.31	—	.04	.08	1.26	1.12	2.06	none	.55	.
Total	100.06	100.52	99.90	100.19	99.92	100.17	100.12	100.14	100.355	100.13	100.

TABLE 1. (*Continued*)

	Am	Cr	Fe''-Ch	Fe'''-Ch	Sh	Ri	Ap	Th	Cl	Pe	Da
SiO_2	20.95	16.42	23.81	24.69	27.12	26.50	23.47	24.18	31.18	34.06	22.0
Al_2O_3	35.21	.90	23.12	23.61	27.68	20.85	21.03	18.23	18.28	11.75	27.6
Fe_2O_3	—	29.72	.23	45.61	.20	1.90	1.86	10.56	2.00	1.92	4.7
MgO	22.88	—	2.72	2.74	30.96	19.85	6.72	5.40	31.11	33.90	4.7
FeO	8.28	41.86	39.45	.47	1.24	18.73	35.14	29.75	4.85	2.78	30.2
MnO	trace	—	—	—	.54	.52	.05	.48	.03	—	—
H_2O+	13.02	10.17	10.67	2.88	12.82	11.65	11.23	9.54	12.73	13.08	10.6
TiO_2	—	—	—	—	—	.03	—	—	.10	—	—
Cr_2O_3	—	—	—	—	—	—	—	—	—	4.31	—
CaO	.58	1.32	—	—	—	—	.40	.24	—	—	—
K_2O	—	—	—	—	—	—	—	—	—	2.45	—
P_2O	—	—	—	—	—	—	—	—	—	.39	—
V_2O_5	—	—	—	—	—	—	—	—	—	—	—
H_2O-	.23	—	—	—	.01	.12	.80	1.07	.10	—	.1
	101.15	100.39	100.00	100.00	100.57	100.15	100.70	99.45	100.38	104.64	99.9

	D-1	D-2	D-3	D-4	D-5	D-6	D-7	K-5	K-6	K-7	K-8	K-9
SiO_2	43.10	44.64	45.04	46.35	46.53	46.55	45.4	45.56	44.81	45.44	44.70	44.74
Al_2O_3	40.10	40.42	40.70	39.59	38.93	38.90	39.2	37.65	37.82	38.52	38.64	37.97
Fe_2O_3	.64	.32	trace	.11	—	—	.2	1.35	.92	.80	.96	1.44
MnO	none	—	—	—	—	—	none	none	none	—	none	none
MgO	.20	.05	trace	—	—	—	.3	.07	.35	.08	.08	.06
CaO	.24	.34	.22	—	—	—	trace	.10	.43	.08	.24	.09
TiO_2	—	—	trace	—	—	—	none	.19	.37	.16	.22	.27
H_2O-	1.08	.04	none	13.93	14.54	14.04	.4	.76	1.10	.60	.64	.58
H_2O+	14.82	13.98	14.08	—	—	—	13.4	13.66	14.27	13.60	13.88	13.98
CO_2	—	—	—	—	—	—	trace	—	—	—	—	—
P_2O_5	—	—	—	—	—	—	none	—	—	—		
K_2O	—	—	—	—	—	—	.2	.11	—	.14	.14	.16
Na_2O	—	—	—	—	—	—	trace	1.16	—	.66	.62	.76
	100.18	99.79	100.04	99.98	100.00	99.49	100.1*	100.61	100.07	100.08	100.12	100.05

Includes 1.0 carbonaceous matter.

	K-10	K-11	K-12	K-13	K-14	K-15	K-16	H-2	H-3	H-4	H-5	H 6
SiO_2	43.64	44.92	44.06	44.26	43.78	43.1	45.1	44.75	40.26	43.67	44.34	44.08
Al_2O_3	38.33	40.22	39.44	40.22	40.06	34.0	37.7	36.94	37.95	37.91	37.39	39.20
Fe_2O_3	1.43	.54	.80	.30	.64	.67	.7	.31	.30	.26	.42	.10
MnO	—	—	trace	none	—	—	—	—	—	—	—	—
MgO	1.02	.14	.26	.18	.16	—	—	—	—	trace	.04	.05
CaO	1.48	.08	.06	.32	.36	—	—	.11	.22	—	.17	none
K_2O	—	—	—	—	—	—	—	.60	.74	—	.04	.20
Na_2O	—	—	—	—	—	—	—			—	.17	
TiO_2	—	—	—	none	—	5.73	1.4	—	—	—	—	
H_2O-	.60	.08	1.06	.64	1.02	3.00	.9	2.53	4.45	3.79	2.00	1.44
H_2O+	13.64	14.22	14.16	14.16	14.08	12.30	13.9	14.89	15.94	14.50	15.09	14.74
FeO	—	—	—	—	—	—	—	—	—	—	—	none
P_2O_5	—	—	—	—	—	—	—	—	—	.12	—	—
	100.14	100.20	99.84	100.08	100.10	98.80	99.7	100.13	99.86	100.25	99.66	99.81

	H-7	H-8	H-9	H-10	H-11	H-12	H-13	H-21	H-22	H-23	H-24	H-25	H-26
	44.08	41.62	44.68	44.50	39.84	44.18	43.10	45.20	44.51	44.35	39.22	43.6	44.3
O_3	38.60	38.66	38.50	38.68	39.70	39.34	40.10	38.96	39.90	40.35	34.22	40.3	39.1
O_3	.32	.62	.39	.24	.64	.32	.64	.21	.21	.21	.10	.4	.4
	—	—	—	—	—	—	—	—	—	—	—	—	—
O	.22	.08	.08	.05	.14	.03	.20	.08	.05	.04	.29	—	—
	.12	.10	.18	none	.40	.30	.24	—	—	—	.18	—	—
O	—	—	.11	1.19	—	—	—	—	—	—	.10	—	—
	—	—	.05	.14	—	—	—	—	—	—	.09	—	—
—	2.34	4.26	1.55	1.17	1.76	.96	1.08	—	—	—	13.00	2.5	4.0
+	14.72	14.64	14.90	14.38	17.52	14.96	14.82	15.35	15.44	15.54	13.00	14.7	13.4
O	—	—	—	—	—	—		—	—	—	.01	—	—
								—	—	—	<.0001	.1	.1
	100.40	99.98	100.53	100.35	100.00	100.09	100.18	99.80	100.11	100.49	100.21	101.6	101.3

Source Data for Analyses

Chrysotile:

C-1 Fiber, Quebec, Canada. Kalousek and Muttart (1957).
C-2 Fiber, Delaware County, Pa. Kalousek and Muttart (1957).
C-3 Fiber, Aboutville, N. Y. Kalousek and Muttart (1957).
C-4 Fiber, Montville, N. J. Kalousek and Muttart (1957).
C-5 Chrysotile, average of 29 analyses.
C-6 Chrysotile, Gila County, Arizona. J. J. Fahey, analyst. Nagy and Faust (1956).
C-7 Silky Chrysotile, Transvaal. W. A. Deer, analyst. Brindley and Zussman (1957).
C-8 Chrysotile, Woodsreef, Barraba, New South Wales. W. A. Greig, analyst. Proud and Osborne (1952).

Platy serpentine:

P-1(M) Matrix, Quebec Canada. Kalousek and Muttart (1957).
P-2(M) Matrix, Delaware County, Pa. Kalousek and Muttart (1957).
P-3(M) Matrix, Aboutville, N. Y. Kalousek and Muttart (1957).
P-4(M) Matrix, Montville, N. J. Kalousek and Muttart (1957).
P-5 Antigorite, average of 14 analyses.
P-6 Antigorite, Val Antigorio, Piedmont, Italy. S. Caillere (1936).
P-7 Matrix, Val Antigorio, Italy. Kalousek and Muttart (1957).
P-8 Antigorite, Mikonui, New Zealand. R. A. Howie, analyst. Zussman (1954).
P-9 Antigorite, Caracas, Venezuela. L. C. Peek, analyst. Hess, Smith and Dengo (1952).
P-10 Antigorite No. 2, Nikka Vord Quarries, Shetland Islands. O. v. Knorring, analyst. Brindley and v. Knorring (1954).
P-11 Antigorite No. 1, Nikka Vord Quarries, Shetland Islands. O. v. Knorring, analyst. Brindley and v. Knorring (1954).
P-12 Deweylite, near Murfreesboro, Pike County, Ark. J. J. Fahey, analyst. Nagy and Faust (1956).
P-13 Williamsite, State Line pits, Cecil County, Md. J. J. Fahey, analyst. Nagy and Faust (1956).
P-14 Baltimoreite, Baltimore County, Md. J. J. Fahey, analyst. Nagy and Faust (1956).
P-15 "Yu-Yen Shi Stone," Liaoning Province, Manchuria. J. J. Fahey, analyst. Nagy and Faust (1956).

Other 1:1

Am Amesite, Chester, Mass. E. V. Shannon (1921)
Cr Cronstedtite, Kisbanya, Hungary. B. Gossner (1935).
Fe''-Ch Ferrous chamosite, Northamptonshire, England. R. F. Youell, analyst. Brindley and Youell (1953).
Fe'''-Ch Ferric chamosite prepared from Fe'''-chamosite by heating in air at 400° C. for two hours. Brindley and Youell (1953).

Chlorites:

Sh Sheridanite, Savoie, France. Orcel (1937).
Ri Ripidolite, Androta, Madagascar. Orcel (1927).
Ap Aphrosiderite, Weilburg, Nassau, Germany. Orcel (1927).
Th Thuringite, Evisa, Corsica. Orcel (1927).

SOURCE DATA (*continued*)

Cl Clinochlore, Besafotre, Madagascar. Orcel (1927).
Pe Pennine, Zermatt, Switzerland. R. Schlaepfer, analyst. Orcel (1927).
Da Daphnite, Cornwall, England. R. F. Youell, analyst. Brindley and Gillery (1954).

Dickites:

D-1 Dickite, Neurode, Silesia. F. A. Gonyer, analyst. Ross and Kerr (1930).
D-2 Dickite, Greenwood, Ark. F. A. Gonyer, analyst. Ross and Kerr (1930).
D-3 Dickite, Cusihuiriachic, Chihuahua. J. G. Fairchild, analyst. Ross and Kerr (1930).
D-4 Dickite, National Belle mine, Colo. W. F. Hillebrand, analyst. Ross and Kerr (1930).
D-5 Dickite, Island of Anglesey. Ross and Kerr (1930).
D-6 Dickite, Backbone Mountain, Okla. R. K. Bailey, analyst. Ross and Kerr (1930).
D-7 Dickite, Durham, England. C. O. Harvey, analyst. Dunham, Claringbull and Bannister (1948).

Kaolinites:

K-5 Kaolinite, Sand Hill station, Pontiac, S. C. F. A. Gonyer, analyst. Ross and Kerr (1930).
K-6 Kaolinite, Mexia, Tex. F. A. Gonyer, analyst. Ross and Kerr (1930).
K-7 Kaolinite, Roseland, Va. F. A. Gonyer, analyst. Ross and Kerr (1930).
K-8 Kaolinite, Ione, Amador County, Calif. F. A. Gonyer, analyst. Ross and Kerr (1930).
K-9 Kaolinite, Ione, Amador County, Calif. F. A. Gonyer, analyst. Ross and Kerr (1930).
K-10 Kaolinite, Abatik River, Alaska. F. A. Gonyer, analyst. Ross and Kerr (1930).
K-11 Kaolinite, Jerome, Ariz. F. A. Gonyer, analyst. Ross and Kerr (1930).
K-12 Kaolinite, Saline County, Ark. F. A. Gonyer, analyst. Ross and Kerr (1930).
K-13 Kaolinite, Franklin, N. C. F. A. Gonyer, analyst. Ross and Kerr (1930).
K-14 Kaolinite, Saline County, Ark. F. A. Gonyer, analyst. Ross and Kerr (1930).
K-15 Kaolinite, St. Ives, New South Wales. G. T. See, analyst. Loughnan (1957).
K-16 Kaolinite, Huber, Georgia. G. T. See, analyst. Loughnan (1957).

Halloysites:

H-2 Halloysite, Liege, Belgium. L. T. Richardson, analyst. Ross and Kerr (1934).
H-3 Halloysite, Huron County, Ind. L. T. Richardson, analyst. Ross and Kerr (1934).
H-4 Halloysite, Huron County, Ind. L. T. Richardson, analyst. Ross and Kerr (1934).
H-5 Halloysite, Peppers, N. C. E. T. Erickson, analyst. Ross and Kerr (1934).
H-6 Halloysite, Hickory, N. C. J. G. Fairchild, analyst. Ross and Kerr (1934).
H-7 Halloysite, Hickory, N. C. F. A. Gonyer, analyst. Ross and Kerr (1934).
H-8 Halloysite, Adams County, Ohio. F. A. Gonyer, analyst. Ross and Kerr (1934).
H-9 Halloysite, Brandon, Rankin County, Miss. Charles Milton, analyst. Ross and Kerr (1934).

Source Data (*continued*)

H-10 Halloysite, Leakey, Real County, Tex. R. K. Bailey, analyst. Ross and Kerr (1934).
H-11 Halloysite, Sneeds Creek, Newton County, Ark. F. A. Gonyer, analyst. Ross and Kerr (1934).
H-12 Halloysite, Franklin, N. C. F. A. Gonyer, analyst. Ross and Kerr (1934).
H-13 Halloysite, Myeline, Saxony. F. A. Gonyer, analyst. Ross and Kerr (1934).
H-21 Endellite, Djebal Deber, Libya dried at 110° C. L. T. Alexander, analyst. Alexander et al. (1943).
H-22 Endellite, Anamosa, Iowa dried at 110° C. L. T. Alexander, analyst. Alexander et al. (1943).
H-23 Endellite, Eureka, Utah dried at 110° C. L. T. Alexander, analyst. Alexander et al. (1943).
H-24 Hydrated halloysite, Ness County, Kansas. Swineford et al. (1954).
H-25 Halloysite, Eureka, Utah. G. T. See, analyst. Loughnan (1957).
H-26 Halloysite, Bedford, Indiana. G. T. See, analyst. Loughnan (1957).

fact that misfit of the two sheets that make up the layer can and apparently does occur, the ratio of the number of cation positions in the tetrahedral versus the octahedral sheet may vary from the commonly accepted value of 2:3. Any resulting departure from electrostatic balance may be corrected by appropriate distribution of H^+ in the layer. In addition to this underlying premise the following assumptions are made:

1) of the elements listed in the chemical analyses only Si, Al, Fe, Mg, Mn, Ni, O, and H are considered for positions in the mineral structures discussed here;

2) the total cation charge is adjusted to balance a negative charge resulting from 18 oxygen ions;

3) all silicon is allocated to the tetrahedral sheet (IV) and all divalent cations are placed in the octahedral sheet (VI);

4) except in the case of kaolin minerals, Al and Fe''' are divided equally between IV and VI independent of the amount of Si and Mg present (see Zussman, 1954, p. 510; and Roy, 1952); in the kaolin minerals any Al and Fe''' in excess of the number of Si ions is divided equally between IV and VI. Neglecting small amounts of divalent cations in the kaolin minerals this is the equivalent of assuming that any excess negative charge resulting from substitution for silicon in the tetrahedral sheet will be balanced by an equal positive charge due to substitution in the octahedral sheet.

The resulting procedure yields structural formulas of the usual type in which all the cations except hydrogen are appropriately allocated. Although much of the following discussion pertains only to the distribution of cations other than hydrogen, two additional steps have been added to

the calculations in order to provide information as to a logical distribution of H^+, $(OH)^-$, and $O^=$ in the lattice. 1) Oxygen and hydroxyl ions are proportioned to correspond with the following ideal structural proportions by simply assigning the proper number to account for the sum of the cation charges in each sheet:

$$\underset{\text{IV}}{\underline{\mid O_6Si_4O_2 \mid}} \qquad \underset{\text{VI}}{\underline{\mid O_2(OH)_2Mg_6(\text{or } Al_4)(OH)_6 \mid}}$$

2) Since the amount of O and OH required for this procedure is usually less than and sometimes greater than that available from the analysis, a final adjustment is required involving either a) the subtraction of H^+ and consequent adjustment of associated oxygen in the octahedral sheet or b) the addition of the extra H^+ and associated oxygen. The latter is accomplished by adding the H to the tetrahedral sheet as $(H_4)^{4+}$ simply because, in the opinion of the author, this is the least involved procedure to follow until experimental data reveal the actual proton positions.

The examples in Table II illustrate the complete procedure. Table III gives the number of each of the various cations in a structure unit containing 18 oxygens. Table IV gives the structural assignments prior to readjustments for excess or deficient hydrogen and oxygen. Table V records the complete structural formula after all adjustments have been made.

Relationships of Morphology to Chemistry

General Statement

The factors that determine the degree of curvature and therefore the shape of the minerals considered here are: 1) the misfit of the tetrahedral and octahedral sheets which make up the 1:1 layer; and 2) the strength of the interlayer bonds. These factors, in turn, are affected by: a) the number of cations (and associated oxygens) in the tetrahedral sheet relative to those in the octahedral sheet; b) the size and polarizing power of the cations; and c) the distribution of H^+ ions.

With these factors in mind certain general observations are pertinent. First, interlayer bonds are stronger in the dioctahedral minerals than in the trioctahedral varieties because the Al has a greater effect than Mg on the adjacent OH and therefore on the resulting creation of hydroxyl bonds.

Second, subsitution of Al or Fe''' for Si tends to make the tetrahedral sheet larger, whereas substitution of the same ions for Mg will make the octahedral sheet smaller and at the same time tend to strengthen interlayer bonds in accord with the reasoning in the preceding paragraph. Because cation substitution is more common in the trioctahedral than in

TABLE II. EXAMPLES OF FORMULA CALCULATIONS

Example #1: Kaolinite #10, Abatik River, Alaska.

Analysis:	SiO_2 43.64	Al_2O_3 38.33	Fe_2O_3 1.43	MgO 1.02	H_2O+ 13.64	H_2O- 0.60
Cationic equivalents:	3.874	3.992	.096	.135	8.038	
Cation allocation: IV:	$Si_{3.874}$	$Al_{.059}$	$Fe_{.048}'''$	(charge=15.748)		
VI:	$Al_{3.874+.059}$		$Fe_{.048}'''$	$Mg_{.135}$	(charge=12.214)	

Allocation of H^+ and O:

A. Proportioning in accord with cation distribution:

IV: Oxygens in proportion 6:2 to account for 15.748 positive charge: $O_{5.905}:O_{1.968}$

VI: Oxygens and (OH) in proportion $O_2:(OH)_2:(OH)_6$ to account for 12.214 positive charge: $O_{2.036}:(OH)_{2.036}:(OH)_{6.107}$

Total oxygen used: 18.052. Resulting oxygen deficiency: 18.052−18.00=.052 ions

Total hydrogen used: 8.143. Resulting hydrogen deficiency: 8.143−8.038=.105 ions

B. Adjustment in octahedral sheet to account for deficiencies: Removal of .105 H^+ and .052 $O^=$ from VI gives $O_{2.088}:(OH)_{2.010}:(OH)_{6.028}$

Complete structural formula:

$$O_{5.905}(Si_{3.874}Al_{.059}Fe_{.048}''')O_{1.968+2.088}(OH)_{2.010}(Al_{3.874+.059}Fe_{.048}'''Mg_{.135})(OH)_{6.028}$$

Example #2: Chrysotile #6, Gila County, Arizona.

Analysis:	SiO_2 42.02	Al_2O_3 0.52	Fe_2O_3 0.19	MgO 41.44	FeO 0.11	MnO 0.03	H_2O+ 14.04	H_2O- 1.64
Cationic equivalents:	3.901	.058	.013	5.733	.008	.003	8.694	
Cation allocation: IV:	$Si_{3.901}$	$Al_{.029}$	$Fe_{.006}'''$	(charge=15.711)				
VI:	$Mg_{5.733}$	$Al_{.029}$	$Fe_{.007}'''$	$Fe_{.008}''$	$Mn_{.003}$	(charge=11.595)		

Allocation of H^+ and O:

A. Proportioning in accord with cation distribution:

IV: Oxygens in proportion 6:2 in account for 15.711 positive charge: $O_{5.892}:O_{1.964}$

VI: Oxygens and (OH) in proportion $O_2:(OH)_2:(OH)_6$ to account for 11.595 positive charge: $O_{1.932}:(OH)_{1.932}:(OH)_{5.797}$

Total oxygen used: 17.517. Resulting oxygen excess: 18.000−17.517=.483 ions

Total hydrogen used: 7.729. Resulting hydrogen excess: 8.694−7.729=.965 ions

B. Adjustment in tetrahedral sheet to account for excess:

Addition of excess H^+ gives: $Si_{3.901}Al_{.029}Fe_{.007}'''(H_4)_{.241}$

Addition of excess O in proportion 6:2 gives: $O_{6.254}:O_{2.085}$

Complete structural formula:

$$O_{6.254}(Si_{3.901}Al_{.029}Fe_{.007}'''(H_4)_{.241})O_{2.085+1.932}(OH)_{1.932}(Mg_{5.733}Al_{.029}Fe_{.007}'''Fe_{.008}''Mn_{.003})(OH)_{5.797}$$

TABLE III. CATIONS PER STRUCTURE UNIT OF 18 OXYGENS

	C-1	C-2	C-3	C-4	C-5	C-6	C-7	C-8	P-1(M)	P-2(M)	P-3(M)	P-4(M)
	3.840	3.936	3.854	3.883	3.905	3.901	3.859	3.924	3.809	3.891	3.860	3.877
e'''	.026	.035	.011	.020	.037	.058	.088	.006	.062	.081	.030	.054
g	.020	.035	.048	.056	.037	.013	.089	.171	.026	.033	.065	.103
e''	5.876	5.863	5.881	5.717	5.654	5.733	5.756	5.445	5.849	5.887	5.870	5.778
n	.003	—	.003	.003	.056	.008	.050	.170	.005	.005	.005	.005
i	.001	.003	.003	.003	—	.003	.003	.012	.003	.008	.003	.003
+	—	—	—	—	—	—	—	—	—	—	—	—
	8.739	8.312	8.633	8.794	8.734	8.694	8.501	8.514	8.784	8.290	8.547	8.449

	P-5	P-6	P-7	P-8	P-9	P-10	P-11	P-12	P-13	P-14	P-15
i	3.855	3.909	4.019	4.047	4.082	3.574	3.914	4.172	4.094	4.131	4.133
l	.262	.284	.183	.089	.114	.011	.011	.026	.153	.211	.054
e'''	.224	.250	.265	.062	.064	.239	.203	.094	—	.340	.006
Mg	5.355	5.277	5.262	5.811	5.718	5.811	5.743	5.481	5.694	5.303	5.791
Fe''	.252	.250	.368	.053	.064	—	.011	.048	.027	.333	.022
Mn	—	—	.008	—	.003	.003	.003	.003	—	.003	—
Ni	—	—	.021	—	.011	—	—	—	.069	.031	—
H+	7.906	7.708	7.258	7.630	7.545	9.325	8.199	7.883	7.581	7.398	7.663

	Am	Cr	Fe''-Ch	Fe'''-Ch	Sh	Ri	Ap	Th	Cl	Pe	Da
	2.000	2.160	2.656	2.836	2.259	2.703	2.590	2.760	2.958	3.269	2.390
l	3.960	.129	3.036	3.197	2.717	2.505	2.736	2.453	2.043	1.330	3.532
e'''	—	2.941	.020	3.942	1.253	.145	.155	.908	.142	.138	.385
g	3.254	—	.452	.569	3.843	3.017	1.104	.919	4.394	4.849	.760
e''	.662	4.600	3.678	.045	.085	1.595	3.242	2.839	.384	.222	2.744
n	—	—	—	—	.037	.046	.003	.048	.003	—	—
i	—	—	—	—	—	—	—	—	—	—	—
+	8.286	8.917	7.933	2.208	7.121	7.920	8.267	7.263	8.049	8.373	7.680

	D-1	D-2	D-3	D-4	D-5	D-6	D-7	K-5	K-6	K-7	K-8	K-9
	3.738	3.868	3.880	3.988	3.982	4.015	3.978	4.004	3.923	3.983	3.922	3.930
l	4.099	4.127	4.132	4.013	3.925	3.955	4.046	3.899	3.902	3.979	3.994	3.930
e'''	.042	.031	—	.007	—	—	.014	.090	.061	.053	.063	.095
g	.026	.005	—	—	—	—	.039	.008	.044	.010	.010	.008
+	8.571	8.076	8.086	7.988	8.296	8.077	7.829	8.002	8.329	7.951	8.120	8.188

	K-10	K-11	K-12	K-13	K-14	K-15	K-16	H-2	H-3	H-4	H-5	H-6
	3.874	3.866	3.844	3.841	3.781	4.125	3.980	3.933	3.603	3.872	3.881	3.838
	3.992	4.078	4.054	4.112	4.077	3.835	3.920	3.826	4.004	3.961	3.857	4.021
'''	.096	.034	.052	.019	.041	.048	.046	.021	.020	.018	.028	.007
g	.135	.018	.034	.023	.205	—	—	—	—	—	.005	.005
+	8.038	8.161	8.238	8.193	8.108	7.849	8.178	8.727	9.516	8.575	8.807	8.554

	H-7	H-8	H-9	H-10	H-11	H-12	H-13	H-21	H-22	H-23	H-24	H-25	H-26
	3.849	3.724	3.870	3.895	3.427	3.820	3.738	3.859	3.791	3.763	3.862	3.775	3.931
	3.971	4.075	3.938	3.990	4.026	4.008	4.099	3.920	4.003	4.035	3.970	4.112	4.088
''	.021	.041	.026	.016	.041	.021	.042	.014	.014	.014	.008	.026	.027
	.029	.010	.010	.005	.018	.002	.026	.010	.005	.005	.041	—	—
	8.569	8.733	8.605	8.390	10.051	8.627	8.571	8.740	8.770	8.791	8.534	8.486	7.931

the dioctahedral minerals considered here, the effect of cation substitution on morphology is more pronounced in the serpentines than in the kaolinites.

Third, with or without substitution of the type considered above, the amount of misfit is affected by the number of ions in the tetrahedral sheet

TABLE IV. STRUCTURAL ASSIGNMENTS

(Prior to adjustment for excess or deficient O and H)

Sample	Tetrahedral Sheet					Octahedral Sheet									Excess or Deficient (−)	
	O	Si	Al	Fe'''	O	O	(OH)	Al	Fe'''	Mg	Fe''	Mn	Ni	(OH)	O	H
Chrysotile:																
C-1	5.785	3.840	.013	.010	1.928	1.972	1.972	.013	.010	5.876	.003	.001	—	5.915	.428	.852
C-2	5.943	3.936	.009	.010	1.981	1.973	1.973	.010	.009	5.863	—	.003	—	5.919	.211	.420
C-3	5.814	3.854	.006	.024	1.938	1.977	1.977	.005	.024	5.881	.003	.003	—	5.931	.363	.725
C-4	5.868	3.883	.010	.028	1.956	1.926	1.926	.010	.028	5.717	.003	.003	—	5.779	.545	1.089
C-5	5.900	3.905	.018	.019	1.966	1.922	1.922	.019	.018	5.654	.056	—	—	5.766	.526	1.046
C-6	5.892	3.901	.029	.006	1.964	1.932	1.932	.029	.007	5.733	.008	.003	—	5.797	.483	.965
C-7	5.888	3.859	.044	.044	1.963	1.966	1.966	.044	.045	5.756	.005	.003	—	5.898	.319	.637
C-8	5.986	3.924	.003	.085	1.995	1.920	1.920	.003	.085	5.445	.170	.012	—	5.760	.419	.838
Platy Serpentine:																
P-1(M)	5.763	3.809	.031	.013	1.921	1.975	1.975	.031	.013	5.849	.005	.003	—	5.924	.442	.885
P-2(M)	5.901	3.891	.041	.016	1.967	1.996	1.996	.040	.017	5.887	.005	.008	—	5.986	.154	.308
P-3(M)	5.838	3.860	.015	.032	1.946	1.981	1.981	.015	.033	5.870	.005	.003	—	5.942	.312	.624
P-4(M)	5.904	3.877	.015	.028	1.968	1.968	1.968	.014	.028	5.778	.005	.003	—	5.904	.288	.577
P-5	6.056	3.855	.131	.112	2.019	1.990	1.990	.131	.112	5.355	.252	—	—	5.971	−.026	−.055
P-6	6.164	3.909	.142	.125	2.054	1.976	1.976	.142	.125	5.277	.250	—	—	5.928	−.098	−.196
P-7	6.282	4.019	.091	.133	2.094	1.998	1.998	.092	.132	5.262	.368	.008	.021	5.995	−.367	−.735
P-8	6.156	4.047	.045	.031	2.052	1.993	1.993	.044	.031	5.811	.053	—	—	5.978	−.172	−.341
P-9	6.222	4.082	.057	.032	2.074	1.977	1.977	.057	.032	5.718	.064	.003	.011	5.930	−.180	−.362
P-10	5.502	3.574	.005	.119	1.834	2.001	2.001	.006	.120	5.811	—	.003	—	6.002	.660	1.322
P-11	5.986	3.914	.006	.101	1.995	1.973	1.973	.005	.102	5.743	.011	.003	—	5.919	.154	.307
P-12	6.327	4.172	.013	.047	2.109	1.874	1.874	.013	.047	5.481	.048	.003	—	5.623	.193	.386
P-13	6.228	4.094	.076	—	2.076	1.969	1.969	.077	—	5.694	.027	—	.069	5.906	−.148	−.294
P-14	6.334	4.131	.105	.170	2.111	1.952	1.952	.106	.170	5.303	.333	.003	.031	5.855	−.204	−.409
P-15	6.232	4.133	.027	.003	2.077	1.953	1.953	.027	.003	5.791	.022	—	—	5.858	−.073	−.148
Other 1:1																
Am	5.227	2.000	1.980	—	1.742	2.295	2.295	1.980	—	3.254	.662	—	—	6.886	−.445	−.895
Cr	4.974	2.160	.070	1.470	1.658	2.303	2.303	.070	1.471	—	4.600	—	—	6.910	−.148	−.296
Fe''-Ch	5.706	2.656	1.518	.010	1.902	2.142	2.142	1.518	.010	.452	3.678	—	—	6.425	−.317	−.634
Fe'''-Ch	6.052	2.836	1.599	—	2.017	2.942	2.942	1.598	3.942	.569	.045	—	—	8.825	−4.778	−9.559
Chlorite:																
Sh	5.622	2.259	1.359	.626	1.874	2.314	2.314	1.358	.627	3.843	.085	.037	—	6.943	−1.067	−2.136
Ri	5.544	2.703	1.253	.072	1.848	2.215	2.215	1.252	.073	3.017	1.595	.046	—	6.646	−.468	−.941
Ap	5.511	2.590	1.368	.077	1.837	2.172	2.172	1.368	.078	1.104	3.242	.003	—	6.517	−.209	−.422
Th	6.030	2.760	1.227	.454	2.010	2.109	2.109	1.226	.454	.919	2.839	.048	—	6.327	−.585	−1.173
Cl	5.667	2.958	1.022	.071	1.889	2.140	2.140	1.021	.071	4.394	.384	.003	—	6.421	−.257	−.512
Pe	5.730	3.269	.665	.069	1.910	2.058	2.058	.665	.069	4.849	.222	—	—	6.173	.071	.142
Da	5.788	2.390	1.766	.192	1.929	2.147	2.147	1.766	.193	.760	2.744	—	—	6.442	−.453	−.909

TABLE IV (*Continued*)

Sample	Tetrahedral Sheet					Octahedral Sheet						Excess or Deficient (−)	
	O	Si	Al	Fe‴	O	O	(OH)	Al	Fe‴	Mg	(OH)	O	H
Dickite:													
D-1	5.835	3.738	.181	.021	1.945	1.978	1.978	3.738+.180	.021	.026	5.934	.330	.659
D-2	5.958	3.868	.129	.010	1.986	2.006	2.006	3.868+.130	.011	.005	6.017	.027	.053
D-3	5.961	3.880	.126	—	1.987	2.003	2.003	3.880+.126	—	—	6.009	.037	.074
D-4	6.000	3.988	.013	.003	2.000	2.002	2.002	3.988+.012	.004	—	6.005	−.009	−.019
D-5	5.973	3.982	—	—	1.991	1.963	1.963	3.925	—	—	5.888	.222	.445
D-6	6.022	4.015	—	—	2.007	1.977	1.977	3.955	—	—	5.932	.085	.168
D-7	6.012	3.978	.034	.007	2.004	2.023	2.023	3.978+.034	.007	.039	6.068	−.130	−.262
Kaolinite:													
K-5	6.006	4.004	—	—	2.002	1.997	1.997	3.899	.090	.008	5.991	.007	.014
K-6	5.907	3.923	—	.020	1.969	1.986	1.986	3.902	.021+.020	.044	5.959	.193	.384
K-7	6.003	3.983	—	.024	2.001	2.007	2.007	3.979	.004+.025	.010	6.022	−.040	−.078
K-8	5.958	3.922	.036	.031	1.986	1.998	1.998	3.922+.036	.032	.010	5.995	.065	.127
K-9	5.949	3.930	—	.047	1.983	1.992	1.992	3.930	.048	.008	5.975	.109	.221
K-10	5.905	3.874	.059	.048	1.968	2.036	2.036	3.874+.059	.048	.135	6.107	−.052	−.105
K-11	5.937	3.866	.106	.017	1.979	2.001	2.001	3.866+.106	.017	.018	6.002	.080	.158
K-12	5.913	3.844	.105	.026	1.971	1.999	1.999	3.844+.105	.026	.034	5.997	.121	.242
K-13	5.925	3.841	.135	.010	1.975	2.001	2.001	3.841+.136	.009	.023	6.003	.095	.189
K-14	5.862	3.781	.148	.020	1.954	2.043	2.043	3.781+.148	.021	.205	6.129	−.031	−.064
K-15	6.189	4.125	—	—	2.063	1.942	1.942	3.835	.048	—	5.825	−.039	−.082
K-16	5.970	3.980	—	—	1.990	1.983	1.983	3.920	.046	—	5.949	−.125	−.246
Halloysite:													
H-2	5.899	3.933	—	—	1.966	1.923	1.923	3.826	.021	—	5.770	.519	1.034
H-3	5.643	3.603	.201	.010	1.881	1.906	1.906	3.603+.200	.010	—	5.719	.945	1.891
H-4	5.868	3.872	.045	.009	1.956	1.962	1.962	3.872+.044	.009	—	5.887	.365	.726
H-5	5.824	3.881	—	.002	1.941	1.943	1.943	3.857	.024+.002	.005	5.830	.519	1.034
H-6	5.865	3.838	.092	.003	1.955	1.968	1.968	3.838+.091	.004	.005	5.904	.340	.682
H-7	5.853	3.849	.061	.010	1.951	1.970	1.970	3.849+.061	.011	.029	5.910	.346	.689
H-8	5.805	3.724	.175	.021	1.935	1.964	1.964	3.724+.176	.020	.010	5.891	.441	.878
H-9	5.869	3.870	.034	.013	1.953	1.962	1.962	3.870+.034	.013	.010	5.886	.378	.757
H-10	5.907	3.895	.048	.008	1.969	1.977	1.977	3.895+.047	.008	.005	5.930	.240	.483
H-11	5.502	3.427	.299	.021	1.834	1.880	1.880	3.427+.300	.020	.018	5.639	1.265	2.532
H-12	5.847	3.820	.094	.010	1.949	1.963	1.963	3.820+.094	.011	.002	5.889	.389	.675
H-13	5.835	3.738	.181	.021	1.945	1.978	1.978	3.738+.180	.021	.026	5.934	.330	.659
H-21	5.832	3.859	.031	.007	1.944	1.951	1.951	3.859+.030	.007	.010	5.854	.468	.935
H-22	5.814	3.791	.106	.007	1.938	1.954	1.954	3.791+.106	.007	.005	5.861	.479	.955
H-23	5.805	3.763	.136	.007	1.935	1.955	1.955	3.763+.136	.007	.005	5.864	.486	.972
H-24	5.859	3.862	.054	.004	1.953	1.974	1.974	3.862+.054	.004	.041	5.921	.319	.639
H-25	5.868	3.775	.169	.013	1.956	1.978	1.978	3.775+.168	.013	—	5.934	.286	.574
H-26	6.000	3.931	.079	.013	2.000	2.011	2.011	3.931+.078	.014	—	6.034	−.056	−.114

TABLE V. STRUCTURAL FORMULAS

Chrysotile:		
C-1	$O_{6.106}Si_{3.840}Al_{.013}Fe_{.010}'''(H_4)_{.213}O_{2.035}$	$O_{1.972}(OH)_{1.972}Mg_{5.876}Al_{.013}Fe_{.010}'''Mn_{.001}Fe_{.003}''(OH)_{5.915}$
C-2	$O_{6.101}Si_{3.936}Al_{.009}Fe_{.010}'''(H_4)_{.105}O_{2.034}$	$O_{1.973}(OH)_{1.973}Mg_{5.863}Al_{.010}Fe_{.009}'''Mn_{.003}(OH)_{5.919}$
C-3	$O_{6.086}Si_{3.854}Al_{.006}Fe_{.024}'''(H_4)_{.181}O_{2.029}$	$O_{1.977}(OH)_{1.977}Mg_{5.881}Al_{.005}Fe_{.024}'''Mn_{.003}Fe_{.003}''(OH)_{5.931}$
C-4	$O_{6.227}Si_{3.883}Al_{.010}Fe_{.028}'''(H_4)_{.272}O_{2.092}$	$O_{1.926}(OH)_{1.926}Mg_{5.717}Al_{.010}Fe_{.028}'''Mn_{.003}Fe_{.170}''(OH)_{5.779}$
C-5	$O_{6.295}Si_{3.905}Al_{.018}Fe_{.019}'''(H_4)_{.261}O_{2.097}$	$O_{1.922}(OH)_{1.922}Mg_{5.654}Al_{.019}Fe_{.018}'''Fe_{.056}''(OH)_{5.766}$
C-6	$O_{6.254}Si_{3.901}Al_{.029}Fe_{.006}'''(H_4)_{.241}O_{2.085}$	$O_{1.932}(OH)_{1.932}Mg_{5.733}Al_{.029}Fe_{.007}'''Mn_{.003}Fe_{.008}''(OH)_{5.797}$
C-7	$O_{6.127}Si_{3.859}Al_{.044}Fe_{.044}'''(H_4)_{.159}O_{2.043}$	$O_{1.966}(OH)_{1.966}Mg_{5.756}Al_{.044}Fe_{.045}'''Mn_{.003}Fe_{.005}''(OH)_{5.898}$
C-8	$O_{6.300}Si_{3.924}Al_{.003}Fe_{.085}'''(H_4)_{.209}O_{2.100}$	$O_{1.920}(OH)_{1.920}Mg_{5.445}Al_{.003}Fe_{.085}'''Mn_{.012}Fe_{.170}''(OH)_{5.760}$
Platy Serpentine:		
P-1(M)	$O_{6.095}Si_{3.809}Al_{.031}Fe_{.013}'''(H_4)_{.221}O_{2.031}$	$O_{1.975}(OH)_{1.975}Mg_{5.849}Al_{.031}Fe_{.013}'''Mn_{.003}Fe_{.005}''(OH)_{5.924}$
P-2(M)	$O_{6.017}Si_{3.891}Al_{.041}Fe_{.016}'''(H_4)_{.077}O_{2.005}$	$O_{1.996}(OH)_{1.996}Mg_{5.887}Al_{.040}Fe_{.017}'''Mn_{.008}Fe_{.005}''(OH)_{5.986}$
P-3(M)	$O_{6.072}Si_{3.860}Al_{.015}Fe_{.032}'''(H_4)_{.156}O_{2.024}$	$O_{1.981}(OH)_{1.981}Mg_{5.870}Al_{.015}Fe_{.033}'''Mn_{.003}Fe_{.005}''(OH)_{5.942}$
P-4(M)	$O_{6.120}Si_{3.877}Al_{.015}Fe_{.028}'''(H_4)_{.144}O_{2.040}$	$O_{1.968}(OH)_{1.968}Mg_{5.774}Al_{.014}Fe_{.028}'''Mn_{.003}Fe_{.005}''(OH)_{5.904}$
P-5	$O_{6.056}Si_{3.855}Al_{.131}Fe_{.112}'''O_{2.019}$	$O_{2.045}(OH)_{1.976}Mg_{5.355}Al_{.131}Fe_{.112}'''Fe_{.252}''(OH)_{5.930}$
P-6	$O_{6.164}Si_{3.909}Al_{.142}Fe_{.125}'''O_{2.054}$	$O_{2.074}(OH)_{1.927}Mg_{5.277}Al_{.142}Fe_{.125}'''Fe_{.250}''(OH)_{5.781}$
P-7	$O_{6.282}Si_{4.019}Al_{.091}Fe_{.133}'''O_{2.094}$	$O_{2.365}(OH)_{1.814}Mg_{5.262}Al_{.092}Fe_{.132}'''Mn_{.008}Fe_{.368}''Ni_{.021}(OH)_{5.444}$
P-8	$O_{6.156}Si_{4.047}Al_{.045}Fe_{.031}'''O_{2.052}$	$O_{2.224}(OH)_{1.908}Mg_{5.811}Al_{.044}Fe_{.031}'''Fe_{.053}''(OH)_{5.722}$
P-9	$O_{6.222}Si_{4.082}Al_{.057}Fe_{.032}'''O_{2.074}$	$O_{2.157}(OH)_{1.887}Mg_{5.718}Al_{.057}Fe_{.032}'''Mn_{.003}Fe_{.064}''Ni_{.011}(OH)_{5.658}$
P-10	$O_{5.997}Si_{3.574}Al_{.005}Fe_{.119}'''(H_4)_{.330}O_{1.999}$	$O_{2.001}(OH)_{2.001}Mg_{5.811}Al_{.006}Fe_{.120}'''Mn_{.003}(OH)_{6.002}$
P-11	$O_{6.102}Si_{3.914}Al_{.006}Fe_{.101}'''(H_4)_{.077}O_{2.033}$	$O_{1.973}(OH)_{1.973}Mg_{5.743}Al_{.005}Fe_{.102}'''Mn_{.003}Fe_{.011}''(OH)_{5.919}$
P-12	$O_{6.472}Si_{4.172}Al_{.013}Fe_{.047}'''(H_4)_{.096}O_{2.057}$	$O_{1.874}(OH)_{1.874}Mg_{5.481}Al_{.013}Fe_{.047}'''Mn_{.003}Fe_{.048}''(OH)_{5.623}$
P-13	$O_{6.228}Si_{4.094}Al_{.076}O_{2.076}$	$O_{2.117}(OH)_{1.896}Mg_{5.694}Al_{.077}Fe_{.027}''Ni_{.069}(OH)_{5.685}$
P-14	$O_{6.334}Si_{4.131}Al_{.105}Fe_{.170}'''O_{2.111}$	$O_{2.156}(OH)_{1.850}Mg_{5.503}Al_{.106}Fe_{.170}'''Mn_{.003}Fe_{.333}''Ni_{.031}(OH)_{5.548}$
P-15	$O_{6.232}Si_{4.133}Al_{.027}Fe_{.003}'''O_{2.077}$	$O_{2.026}(OH)_{1.916}Mg_{5.791}Al_{.027}Fe_{.003}'''Fe_{.022}''(OH)_{5.747}$
Other 1:1		
Am	$O_{5.227}Si_{2.000}Al_{1.980}O_{1.742}$	$O_{2.740}(OH)_{2.071}Al_{1.980}Mg_{3.254}Fe_{.662}''(OH)_{6.215}$

Table V (*continued*)

Cr	$O_{4.974}Si_{2.160}Al_{.070}Fe_{1.470}'''O_{1.658}$	$O_{1.806}(OH)_{2.229}Al_{.070}Fe_{1.471}'''Fe_{4.600}''(OH)_{6.688}$
Fe''-Ch	$O_{5.706}Si_{2.656}Al_{1.518}Fe_{.010}'''O_{1.902}$	$O_{2.459}(OH)_{1.984}Al_{1.518}Fe_{.010}'''Mg_{.452}Fe_{3.678}''(OH)_{5.949}$
Fe'''-Ch	$O_{6.052}Si_{2.836}Al_{1.599}O_{2.017}$	$O_{1.699}(OH)_{.552}Al_{1.598}Fe_{3.942}'''Mg_{.569}Fe_{.045}''(OH)_{.656}O_{4.096}$
Chlorites:		
Sh	$O_{5.622}Si_{2.259}Al_{1.359}Fe_{.626}'''O_{1.874}$	$O_{3.381}(OH)_{1.780}Mg_{3.843}Al_{1.358}Fe_{.627}'''Mn_{.037}Fe_{.085}''(OH)_{5.341}$
Ri	$O_{5.544}Si_{2.703}Al_{1.253}Fe_{.072}'''O_{1.848}$	$O_{2.683}(OH)_{1.980}Mg_{3.017}Al_{1.252}Fe_{.073}'''Fe_{1.595}''Mn_{.046}(OH)_{5.940}$
Ap	$O_{5.511}Si_{2.590}Al_{1.368}Fe_{.077}'''O_{1.837}$	$O_{2.381}(OH)_{2.067}Mg_{1.104}Al_{1.368}Fe_{.078}'''Fe_{3.242}''Mn_{.003}(OH)_{6.200}$
Th	$O_{6.030}Si_{2.760}Al_{1.227}Fe_{.454}'''O_{2.010}$	$O_{2.694}(OH)_{1.816}Fe_{2.839}''Al_{1.226}Fe_{.454}'''Mg_{.919}Mn_{.048}(OH)_{5.447}$
Cl	$O_{5.667}Si_{2.958}Al_{1.022}Fe_{.071}'''O_{1.889}$	$O_{2.397}(OH)_{2.012}Mg_{4.394}Al_{1.021}Fe_{.071}'''Fe_{.334}''Mn_{.003}(OH)_{6.037}$
Pe	$O_{5.783}Si_{3.269}Al_{.665}Fe_{.069}'''(H_4)_{.035}O_{1.928}$	$O_{2.058}(OH)_{2.058}Mg_{4.849}Al_{.665}Fe_{.069}'''Fe_{.222}''(OH)_{6.173}$
Da	$O_{5.788}Si_{2.390}Al_{1.766}Fe_{.192}'''O_{1.929}$	$O_{2.600}(OH)_{1.920}Fe_{2.744}''Al_{1.766}Fe_{.193}'''Mg_{.760}(OH)_{5.760}$
Dickite:		
D-1	$O_{6.083}Si_{3.738}Al_{.181}Fe_{.021}'''(H_4)_{.165}O_{2.027}$	$O_{1.978}(OH)_{1.978}Al_{3.738+.180}Fe_{.021}'''Mg_{.026}(OH)_{5.934}$
D-2	$O_{5.978}Si_{3.868}Al_{.129}Fe_{.010}'''(H_4)_{.013}O_{1.993}$	$O_{2.006}(OH)_{2.006}Al_{3.868+.130}Fe_{.011}'''Mg_{.005}(OH)_{6.017}$
D-3	$O_{5.989}Si_{3.880}Al_{.126}(H_4)_{.018}O_{1.996}$	$O_{2.003}(OH)_{2.003}Al_{3.880+.126}(OH)_{6.009}$
D-4	$O_{6.000}Si_{3.988}Al_{.013}Fe_{.003}'''O_{2.000}$	$O_{2.011}(OH)_{1.997}Al_{3.988+.012}Fe_{.004}'''(OH)_{5.991}$
D-5	$O_{6.140}Si_{3.982}(H_4)_{.111}O_{2.046}$	$O_{1.963}(OH)_{1.963}Al_{3.925}(OH)_{5.888}$
D-6	$O_{6.086}Si_{4.015}(H_4)_{.042}O_{2.028}$	$O_{1.977}(OH)_{1.977}Al_{3.955}(OH)_{5.932}$
D-7	$O_{6.012}Si_{3.978}Al_{.034}Fe_{.007}'''O_{2.004}$	$O_{2.107}(OH)_{1.958}Al_{3.978+.034}Fe_{.007}'''Mg_{.039}(OH)_{5.871}$
Kaolinite:		
K-5	$O_{6.011}Si_{4.004}(H_4)_{.003}O_{2.004}$	$O_{1.997}(OH)_{1.997}Al_{3.899}Fe_{.090}'''Mg_{.008}(OH)_{5.991}$
K-6	$O_{6.052}Si_{3.923}Fe_{.020}'''(H_4)_{.096}O_{2.017}$	$O_{1.986}(OH)_{1.986}Al_{3.902}Fe_{.021+.020}'''Mg_{.044}(OH)_{5.959}$
K-7	$O_{6.003}Si_{3.983}Fe_{.024}'''O_{2.001}$	$O_{2.041}(OH)_{1.988}Al_{3.979}Fe_{.004+.025}'''Mg_{.010}(OH)_{5.963}$
K-8	$O_{6.017}Si_{3.922}Al_{.036}Fe_{.031}'''(H_4)_{.032}O_{2.002}$	$O_{1.995}(OH)_{1.995}Al_{3.922+.036}Fe_{.032}'''Mg_{.010}(OH)_{5.995}$
K-9	$O_{6.031}Si_{3.930}Fe_{.047}'''(H_4)_{.055}O_{2.010}$	$O_{1.992}(OH)_{1.992}Al_{3.930}Fe_{.048}'''Mg_{.008}(OH)_{5.975}$
K-10	$O_{5.905}Si_{3.874}Al_{.059}Fe_{.048}'''O_{1.968}$	$O_{2.088}(OH)_{2.010}Al_{3.874+.059}Fe_{.048}'''Mg_{.135}(OH)_{6.028}$

Table V (*Continued*)

K-11	$O_{6.097}Si_{3.866}Al_{.106}Fe_{.017}'''(H_4)_{.039}O_{1.999}$	$O_{2.001}(OH)_{2.001}Al_{3.866+.106}Fe_{.017}'''Mg_{.013}(OH)_{6.002}$
K-12	$O_{6.004}Si_{3.844}Al_{.105}Fe_{.026}'''(H_4)_{.060}O_{2.001}$	$O_{1.999}(OH)_{1.999}Al_{3.844+.105}Fe_{.026}'''Mg_{.034}(OH)_{5.997}$
K-13	$O_{5.996}Si_{3.841}Al_{.135}Fe_{.010}'''(H_4)_{.047}O_{1.999}$	$O_{2.001}(OH)_{2.001}Al_{3.841+.136}Fe_{.009}'''Mg_{.053}(OH)_{6.003}$
K-14	$O_{5.862}Si_{3.781}Al_{.148}Fe_{.020}'''O_{1.954}$	$O_{2.074}(OH)_{2.027}Al_{3.781+.148}Fe_{.021}'''Mg_{.205}(OH)_{6.081}$
K-15	$O_{6.219}Si_{4.125}(H_4)_{.020}O_{2.073}$	$O_{1.942}(OH)_{1.942}Al_{3.835}Fe_{.048}'''(OH)_{5.825}$
K-16	$O_{6.064}Si_{3.980}(H_4)_{.061}O_{2.021}$	$O_{1.983}(OH)_{1.983}Al_{3.920}Fe_{.046}'''(OH)_{5.949}$
Halloysite:		
H-2	$O_{6.288}Si_{3.933}(H_4)_{.258}O_{2.096}$	$O_{1.923}(OH)_{1.923}Al_{3.826}Fe_{.021}'''(OH)_{5.770}$
H-3	$O_{6.352}Si_{3.603}Al_{.201}Fe_{.010}'''(H_4)_{.473}O_{2.117}$	$O_{1.906}(OH)_{1.906}Al_{3.603+.200}Fe_{.010}'''(OH)_{5.719}$
H-4	$O_{6.142}Si_{3.872}Al_{.045}Fe_{.009}'''(H_4)_{.181}O_{2.047}$	$O_{1.962}(OH)_{1.962}Al_{3.872+.044}Fe_{.009}'''(OH)_{5.887}$
H-5	$O_{6.213}Si_{3.881}Fe_{.002}'''(H_4)_{.258}O_{2.072}$	$O_{1.943}(OH)_{1.943}Al_{3.857}Fe_{.024+.002}'''Mg_{.005}(OH)_{5.836}$
H-6	$O_{6.120}Si_{3.838}Al_{.092}Fe_{.003}'''(H_4)_{.170}O_{2.040}$	$O_{1.968}(OH)_{1.968}Al_{3.838+.091}Fe_{.004}'''Mg_{.005}(OH)_{5.904}$
H-7	$O_{6.113}Si_{3.849}Al_{.061}Fe_{.010}'''(H_4)_{.173}O_{2.021}$	$O_{1.970}(OH)_{1.970}Al_{3.849+.061}Fe_{.011}'''Mg_{.029}(OH)_{5.910}$
H-8	$O_{6.136}Si_{3.724}Al_{.175}Fe_{.021}'''(H_4)_{.219}O_{2.045}$	$O_{1.964}(OH)_{1.964}Al_{3.724+.176}Fe_{.020}'''Mg_{.010}(OH)_{5.891}$
H-9	$O_{6.139}Si_{3.870}Al_{.034}Fe_{.013}'''(H_4)_{.189}O_{2.047}$	$O_{1.962}(OH)_{1.962}Al_{3.870+.034}Fe_{.013}'''Mg_{.010}(OH)_{5.886}$
H-10	$O_{5.967}Si_{3.895}Al_{.048}Fe_{.008}'''(H_4)_{.121}O_{2.009}$	$O_{1.977}(OH)_{1.977}Al_{3.895+.047}Fe_{.008}'''Mg_{.005}(OH)_{5.930}$
H-11	$O_{6.451}Si_{3.427}Al_{.299}Fe_{.021}'''(H_4)_{.633}O_{2.150}$	$O_{1.880}(OH)_{1.880}Al_{3.427+.300}Fe_{.020}'''Mg_{.018}(OH)_{5.639}$
H-12	$O_{6.139}Si_{3.820}Al_{.094}Fe_{.010}'''(H_4)_{.169}O_{2.046}$	$O_{1.963}(OH)_{1.963}Al_{3.820+.094}Fe_{.011}'''Mg_{.002}(OH)_{5.889}$
H-13	$O_{6.083}Si_{3.738}Al_{.181}Fe_{.021}'''(H_4)_{.165}O_{2.027}$	$O_{1.978}(OH)_{1.978}Al_{3.738+.180}Fe_{.021}'''Mg_{.026}(OH)_{5.934}$
H-21	$O_{6.183}Si_{3.859}Al_{.031}Fe_{.007}'''(H_4)_{.234}O_{2.063}$	$O_{1.951}(OH)_{1.951}Al_{3.859+.030}Fe_{.007}'''Mg_{.010}(OH)_{5.854}$
H-22	$O_{6.173}Si_{3.791}Al_{.106}Fe_{.007}'''(H_4)_{.239}O_{2.058}$	$O_{1.954}(OH)_{1.954}Al_{3.791+.106}Fe_{.007}'''Mg_{.005}(OH)_{5.861}$
H-23	$O_{6.170}Si_{3.763}Al_{.136}Fe_{.007}'''(H_4)_{.243}O_{2.056}$	$O_{1.955}(OH)_{1.955}Al_{3.763+.136}Fe_{.007}'''Mg_{.005}(OH)_{5.864}$
H-24	$O_{6.098}Si_{3.862}Al_{.054}Fe_{.004}'''(H_4)_{.160}O_{2.033}$	$O_{1.974}(OH)_{1.974}Al_{3.862+.054}Fe_{.004}'''Mg_{.041}(OH)_{5.921}$
H-25	$O_{6.083}Si_{3.775}Al_{.169}Fe_{.013}'''(H_4)_{.143}O_{2.027}$	$O_{1.978}(OH)_{1.978}Al_{3.776+.168}Fe_{.013}'''(OH)_{5.934}$
H-26	$O_{6.000}Si_{3.931}Al_{.079}Fe_{.013}'''O_{2.000}$	$O_{2.067}(OH)_{1.933}Al_{3.931+.078}Fe_{.014}'''(OH)_{5.948}$

relative to a given number in the octahedral sheet. Thus, a deficiency or excess of silicon relative to aluminum or magnesium (electrostatic balance being achieved by appropriate H^+ distribution) may play a very important role in affecting morphology.

Fourth, the amount and distribution of H^+ may be very important in affecting the strength of interlayer bonds.

The fact that the greatest chemical variation accompanying the morphological change from kaolinite to halloysite ($4H_2O$) to allophane is that of H^+ content suggests that factor four plays the predominant role in determining the morphology of kaolin-group minerals. On the other hand, factors two and three as well as four are important in the case of the serpentines. Obviously, interaction of all four factors is involved in all cases.

Unfortunately, data are not sufficient to permit a detailed evaluation of these factors and all possible interactions. For this discussion the chemical-morphological relationships have been evaluated in two ways which are believed to relate most directly to the concepts expressed above and which involve the minimum number of assumptions. These two evaluations are demonstrated 1) by plotting the position of the various platy and fibrous minerals with respect to the average size of the cations in the tetrahedral sheet as compared to the average size of those in the octahedral sheet; and 2) by plotting the position of the kaolin group minerals on a SiO_2-Al_2O_3-H_2O diagram and the serpentine minerals on a SiO_2-R″O-H_2O diagram (where R″ = Mg, Fe″, Mn, and Ni).

Morphology in Relation to Average Radii of Octahedral and Tetrahedral Cations

Figure 2 illustrates the relationship of morphology to the size of the cations in the octahedral versus the tetrahedral sheets of the 1:1 layer structure. The points for chrysotile (C) and kaolinite (K) represent the ideal serpentine and kaolinite compositions whereas those for platy serpentine (PS) and halloysite (H) represent average values obtained from all the analyses of these minerals. Variation within the two groups will be discussed later. The radii used are those of Goldschmidt. The symbols denote whether the compound has tubular or platy crystals.

The position of each compound is determined from the structural assignments in Table IV by plotting the average size of the cations in the tetrahedral sheet against the average size of those in the octahedral sheet. It is, of course, appreciated that "size" does not pertain to misfit of the sheets in the sense of "space occupied by the cation" but is used as a convenient index of the effect of cations of differing polarizing power on the anions which make up the lattice framework.

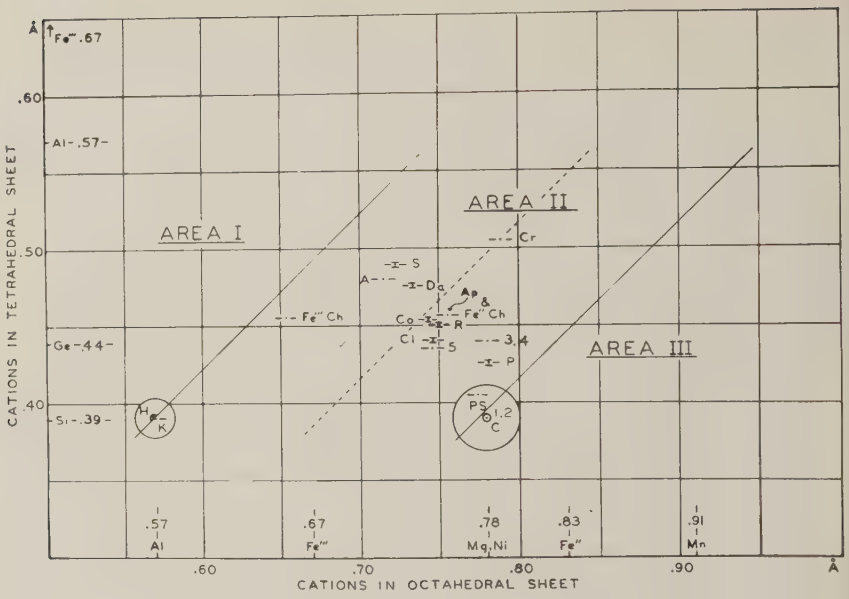

FIG. 2. 1:1 minerals plotted on the basis of the average radius of tetrahedral versus average radius of octahedral cations. (Radii of Goldschmidt.)

A: amesite; Co: corundophyllite (characteristic composition); P: penninite (characteristic composition); PS: platy serpentine; S: sheridanite; Ri: ripidolite. Other initials are the same as those given in the tables.

The figure can be divided into three areas on the basis of the morphology of the compounds. Since there are not enough compounds to determine the precise boundaries, the light lines are arbitrarily drawn from points adjacent to the positions of Si vs. Al and Si vs. Mg at an angle of 45° to the horizontal. It is important to note that the utility of the graph is not dependent upon the validity of the assumptions as to the distribution of cations in the two sheets of the layer. For example, the addition of Al or Fe''' to the ideal serpentine composition will place the position of the resulting compound in area II independent of whether these ions substitute in the tetrahedral sheet, the octahedral sheet, or both.

Area II contains those compounds that occur as platy to flaky crystals. This characteristic morphology is attributed to the fact that in most of this area the size, charge, and number of the ions in octahedral as opposed to tetrahedral coordination is such that misfit between the two sheets of the 1:1 layer is at a minimum and there is little tendency for curvature. On approaching the edges of this region, interlayer bond strength, which is not taken direct account of in this graph, plays an increasingly dominant role.

In the region designated as area I, the chemical composition is such that the "gibbsite" sheet becomes too small for the silicon-oxygen sheet and therefore when interlayer bonds are sufficiently weak tubes having a "negative"* curvature result (silicon-oxygen sheet outside, gibbsite sheet inside). Halloysite ($4H_2O$) is the only natural tubular mineral known from this area and thus far efforts to synthesize this and other tubes in this composition region have been unsuccessful. Indeed it is unlikely that other 1:1 minerals exist in this region because 1) aluminum represents the smallest ion commonly found in the octahedral sheet, and 2) a dioctahedral mineral having appreciable aluminum or ferric iron substituting for silicon in the tetrahedral sheet would be likely to have a 2:1 structure with interlayer cations to compensate for the excess negative charge.

In area III, as a result of the increase of size of "octahedral" as opposed to "tetrahedral" ions, the "brucite" sheet is too large for the silicon-oxygen sheet and tubes having a "positive" curvature result. Natural and synthetic chrysotile and nickel chrysotile ($Si_4Ni_6O_{10}(OH)_8$) represent the only compounds definitely known to occur in this area. (Sufficiently detailed chemical and morphological data on greenalite ($Si_4Fe'''Fe_{4\text{-}5}O_{10}(OH)_8$) have not been obtained.) Replacement of part of the Mg or Ni by Fe'' or Mn would result in a still greater misfit of tetrahedral and octahedral sheets and therefore finer tubes of smaller radii of curvature. On the basis of similar reasoning, it is unlikely that many other 1:1 layer silicates occur in area III for, as the radius of curvature is decreased, physical and chemical instability of the extremely thin tubes would result. Previous studies (Nagy and Bates, 1952) have demonstrated that chrysotile itself is very much more susceptible to chemical attack than platy serpentine.

On the basis of present knowledge the two circled areas on the graph encompassing the kaolin and serpentine groups are the only locations where both tubes and plates occur. It seems evident that in both situations naturally-occurring lath-shaped crystals with varying "tendencies to curve" and of varying length/width ratio occupy the area between platy and tubular morphological "end-members." It has already been shown in the case of serpentine (Zussman, 1954; Whittaker and Zussman, 1956; Zussman, Brindley and Comer, 1957; Zussman and Brindley, 1957), and to a lesser extent in the kaolinites (Honjo, Kitamura and Mihama, 1954), that various "structure states" may exist in this transition region.

In order to provide a measure of the relative position of the various

* The terms positive and negative have no significance except to designate opposite directions of curvature.

compounds on the graph, Table VI lists the calculated perpendicular distance of each from the dashed line which divides area II in half. The resulting value "M" is referred to as the morphological index of the compound. Assuming that the line represents the locus of all cation combinations producing best fit of tetrahedral and octahedral sheets, the greater the value of M, the greater the misfit and therefore the greater the tendency of the layer to curve (other factors being equal). A value of +74.23* for the ideal chrysotile composition represents sufficient misfit to cause formation of tubes with "positive" curvature. Negative values indicate a tendency for the layers to curve in the opposite direction, as in the case of halloysite ($4H_2O$).

Analysis of the data reveals some interesting relationships. Cronstedtite lies directly on the line while (3) $Ge_4Mg_6O_{10}(OH)_8$, (4) $Ge_4Ni_6O_{10}(OH)_8$, (5) $(Si_3Al)(Mg_5Al)O_{10}(OH)_8$, ferrous chamosite and amesite all lie within 40 units of it. The position of ferric chamosite (Brindley and Youell, 1953) was determined on the basis of the assumption that the oxidation of the ferrous to ferric iron produced no change in the distribution of the cations in the tetrahedral and octahedral sheets.

Since areas in Fig. 2 encompassing the kaolin and serpentine minerals fall in borderline situations with respect to fields I, II, and III, the amount of misfit produced by cation substitution leads to a sensitive situation such that the resultant morphology will be easily affected by and dependent upon the role of other factors such as interlayer bond strength, proportion of tetrahedral to octahedral cations and distribution of H^+. Nevertheless, the M values in Table VI reveal interesting differences between the minerals within each group.

In the serpentines the mean value for chrysotile is +71.94 as compared to +67.96 for all the platy varieties and +62.96 for material labeled antigorite. The fact that the highest value is given by one of the best examples of tubular chrysotile, and the lowest value is that of the megascopically platy, type antigorite, indicates that the method of evaluation is meaningful. The analyses of fiber (C-1 to C-4) and adjoining matrix (P-1(M) to P-4(M)) from the same specimens (Kalousek and Muttart, 1957) are of particular interest in that the difference in M values between the two portions of each sample is in the expected direction but very small. Thus, as might be expected in situations where matrix and fiber are intimately associated, the formation of one type rather than the other may hinge on differences in chemistry which are very slight and related to factors such as temperature, pressure, stress,

* The perpendicular distance to the line is calculated from the formula: $M = \sin 45° (X - Y - .285)(1000)$.

TABLE VI. RADII OF TETRAHEDRAL AND OCTAHEDRAL CATIONS, AND MORPHOLOGICAL INDEX: *M*

Sample	Average Cation Radius		M	Sample	Average Cation Radius		M
	IV	VI			IV	VI	
Ideal Serpentine	.390	.780	74.23	*Ideal Kaolinite*	.390	.570	−74.23
Chrysotile:				Dickite:			
C-1	.391	.779	72.82	D-1	.400	.572	−79.89
C-2	.391	.780	73.53	D-2	.396	.570	−78.48
C-3	.392	.779	72.11	D-3	.396	.570	−78.48
C-4	.392	.779	72.11	D-4	.391	.570	−74.94
C-5	.392	.779	72.11	D-5	.390	.570	−74.23
C-6	.391	.780	73.53	D-6	.390	.570	−74.23
C-7	.395	.778	69.29	D-7	.392	.572	−74.23
C-8	.396	.780	69.99				
				Kaolinite:			
Platy Serpentine:				K-5	.390	.572	−72.82
P-1(M)	.393	.779	71.40	K-6	.391	.573	−72.82
P-2(M)	.393	.778	70.70	K-7	.392	.571	−74.94
P-3(M)	.393	.779	71.40	K-8	.394	.571	−76.36
P-4(M)	.393	.779	71.40	K-9	.393	.571	−75.65
P-5	.403	.775	61.51	K-10	.396	.578	−72.82
P-6	.404	.774	60.09	K-11	.396	.571	−77.77
P-7	.402	.777	63.63	K-12	.396	.572	−77.06
P-8	.394	.778	69.99	K-13	.397	.571	−78.48
P-9	.394	.778	69.99	K-14	.397	.580	−72.11
P-10	.399	.778	66.46	K-15	.390	.571	−73.53
P-11	.397	.778	67.87	K-16	.390	.571	−73.53
P-12	.393	.779	71.40				
P-13	.393	.777	69.99	Halloysite:			
P-14	.405	.776	60.80	H-2	.390	.570	−74.23
P-15	.391	.779	72.82	H-3	.400	.570	−81.30
				H-4	.393	.570	−76.36
Other 1:1				H-5	.390	.571	−73.53
Am	.480	.715	−35.35	H-6	.394	.571	−76.36
Cr	.505	.789	−00.70	H-7	.394	.572	−75.65
Fe″-Ch	.456	.756	10.60	H-8	.399	.571	−79.89
Fe‴-Ch	.455	.655	−60.09	H-9	.392	.571	−74.94
				H-10	.393	.570	−76.36
Synthetic 1:1				H-11	.405	.571	−84.13
1	.390	.780	74.23	H-12	.395	.570	−77.77
2	.390	.780	74.23	H-13	.400	.572	−79.89
3	.440	.780	38.88	H-21	.392	.571	−74.94
4	.440	.780	38.88	H-22	.395	.570	−77.77
5	.435	.745	17.67	H-23	.397	.571	−78.48
				H-24	.393	.573	−74.23
Chlorite:				H-25	.399	.571	−79.89
Sh	.489	.722	−36.76	H-26	.394	.570	−77.06
Ri	.451	.749	9.19				
Ap	.456	.757	11.31	Group Averages:			
Th	.471	.751	− 3.53	Chrysotile	.393	.779	71.94
Cl	.441	.746	−14.14	Platy serpentine	.397	.778	67.96
Pe	.425	.756	32.52	Matrix (M)	.393	.779	71.23
Da	.476	.733	−19.80	Excluding (M)	.398	.777	66.78
P	.426	.782	50.20	Other 1:1	.474	.729	−21.39
Co	.453	.746	5.66	Chlorite	.454	.749	3.85
				Dickite	.394	.571	−76.35
				Kaolinite	.394	.573	−74.82
				Halloysite	.395	.571	−77.38

etc. which influenced crystallization at the time of formation or subsequent alteration of the rock.

In considering the significance of the M values, it is important to appreciate that most of the so-called platy varieties and massive specimens contain varying amounts of fibrous material. This has been demonstrated by Zussman, Brindley and Comer (1957) and by work by the author and Nagy as reported in the paper by Nagy and Faust (1956). Therefore, whereas the range in M values for the relatively homogeneous fibrous specimens is only from +69.29 to +73.53, that for the platy material is much greater (+60.09 to +72.82) due not only to a greater compositional range of the platy component but also to the probability that many of the analyzed specimens contained admixed, submicroscopic fibers which may approach the ideal composition. Until precise evaluations can be made of the chemical composition of individual submicroscopic plates, laths and tubes, it cannot be said which of these two factors plays the more important role.

In the kaolin group the range in M values is not quite as large as in the serpentines and the averages for kaolinites (−74.82), dickites (−76.35) and halloysites (−77.38) are not greatly different. Since, with one or two exceptions, the role of Mg is minor, the variation in M values is a result of the variation in the amount of Al and Fe‴ in excess of Si.

The M values indicate that, although the difference for platy (kaolinite and dickite) versus lath-shaped and tubular varieties (halloysite) is in the right direction, variation in misfit due to cation distribution in octahedral and tetrahedral sheets is probably not the major cause of variation in morphology within the group.

Morphology in Relation to Proportions of Major Components

In order to show the relationships of bulk composition to morphology each analysis was recalculated so that the sum of the major components would be equal to 100. The resulting compositions are plotted on Figs. 3 and 4. It is apparent in the case of both the serpentine and kaolin groups that the chief difference between platy and tubular varieties lies in the greater amount of hydrogen and associated oxygen in the latter.

In the serpentines (Fig. 3) the three components evaluated are SiO_2, H_2O+ and R″O where R″ = Mg, Fe″, Mn and Ni. If the assumption is correct that Al and Fe‴ are divided equally between tetrahedral sites (substitution for Si) and octahedral sites (substitution for R″), the effect of these ions would be to move each point to the left in a direction parallel to the dotted line which, if extended, would terminate at the H_2O corner of the diagram. Since, as shown in Fig. 2, the platy varieties contain more Al and Fe‴ than chrysotile, the result of including these

components would be to increase the separation of the two groups.

As in the case of the data recorded in Table VI, the samples of adjoining matrix and fiber described by Kalousek and Muttart are very similar in composition suggesting that 1) the matrix is a mixture containing a large percentage of fiber, 2) the platy component of the matrix has a composition very similar to the fiber, 3) or both factors are involved.

Of the remaining eleven platy samples, eight differ markedly from the chrysotiles by having a greater SiO_2:R″O ratio. It is significant in this respect, that the greatest departure from the ideal serpentine composition is made by varieties labeled deweylite, williamsite, baltimoreite and Yu Yen Stone; whereas analyses of material labeled antigorite (Nos. 5, 6, 7, 8, 9) plot closer to the line which indicates the ideal proportion of the components in question. The "anomalous" character of sample P-10 (one of two antigorites from Nikka Vord quarry, Shetland Islands) has been discussed previously by Brindley and von Knorring (1954), McConnell (1954) and Zussman (1956).

The relationships of composition and structure of sample P-9 have been considered by Hess, *et al.* (1952) and Brindley (1954); and of samples P-8 and P-9 by Zussman (1954).

The relationships shown diagrammatically in Fig. 3 indicate that on the whole, platy crystals are favored over fibrous material if there is 1)

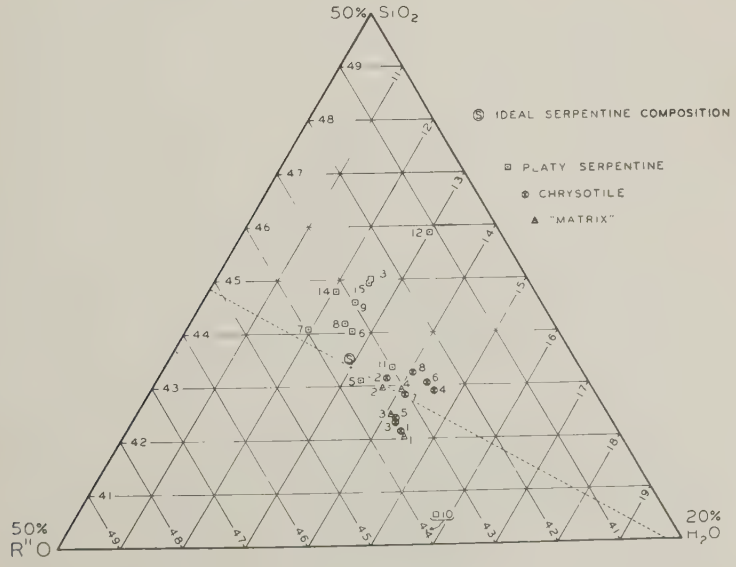

FIG. 3. SiO_2-(Mg, Fe″, Ni, Mn)O-H_2O composition of serpentine samples.

an increase of SiO_2 with respect to R″O, and 2) a decrease in H_2O+. The role of H^+ will be considered later. If the assumption is correct that Al and Fe‴ are equally divided between tetrahedral and octahedral positions, the evidence with respect to SiO_2:R″O ratio is in line with the observation made earlier that the amount of misfit is affected by the number of ions in the tetrahedral sheet relative to a given number in the octahedral sheet. In this case, the increase in proportion of Si to divalent ions will improve the fit between the larger "ideal" brucite sheet and smaller "ideal" Si-O sheet and thereby promote the formation of platy crystals.

In the kaolin group (Fig. 4) the range in the ratio of SiO_2:Al_2O_3 shown by kaolinites and dickites is similar to that shown by most of the halloysite samples. However, as indicated by the work of others, the average SiO_2:Al_2O_3 ratio of halloysites is lower than that of kaolinites and dickites, being in this case 192:100 (excluding samples 3, 11 and 26) as compared with 196:100. Granting that the difference may be due to undetectable impurities in the samples analyzed, the fact remains that the lath-shaped and tubular material has 1) a lower SiO_2:Al_2O_3 ratio and 2) a higher H_2O+ content than the platy varieties. It is important to bear in mind that most if not all of the interlayer water found in halloysite ($4H_2O$) is presumably not included in the H_2O+ value of the analysis.

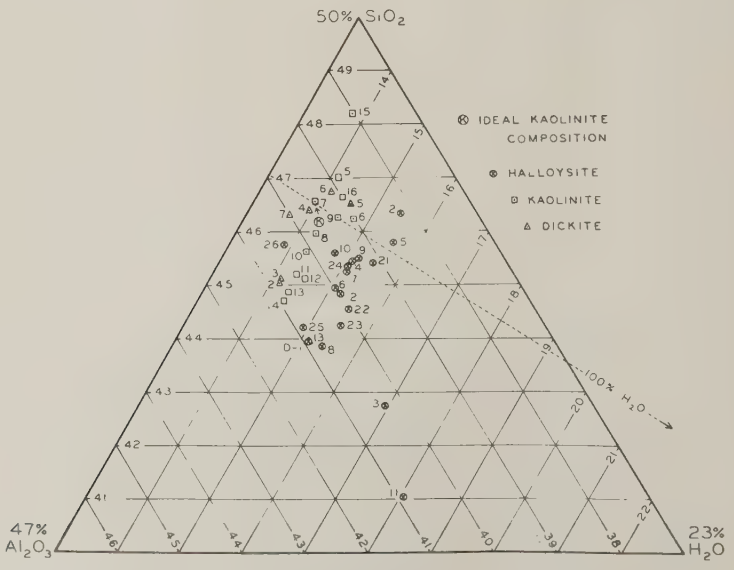

FIG. 4. SiO_2-Al_2O_3-H_2O composition of kaolin samples.

Other Pertinent Relationships

General Statement

The morphological-chemical relationships discussed thus far are considered to be particularly significant because they involve a minimum number of assumptions. Thus, the general relationships graphed in Figs. 2, 3, and 4 pertain regardless of the choice of radii used to represent the ions, of the means of proportioning of cations between tetrahedral and octahedral positions, and of the problem as to the exact disposition of hydrogen. The writer, therefore, wishes to draw a sharp distinction between the previous discussion and the points made in this section in that the latter rely more directly upon the assumptions used in making the structural calculations. Although these points are more subject to question, the calculations have resulted in a number of interesting relationships which, in the opinion of the author, should be considered by other workers in this area. Two things, in particular, deserve attention. These are: 1) the number of cations (excluding H^+) assigned to tetrahedral as opposed to octahedral positions; and 2) the amount of H_2O+ given in the analysis as compared with that needed to provide the "proper" proportion of (OH) and oxygen with respect to the postulated cation distribution in the formulas.

Number of Tetrahedral versus Octahedral Cations

Table VII lists the pertinent cation distribution data for all minerals except those of the kaolin group. These are not included because the method of allocating ions to tetrahedral versus octahedral positions in the formulas for this group results in equal distribution except in those few cases where appreciable divalent ions are present. Column 1 gives the number of cations allocated to tetrahedral positions, column 2 those in octahedral positions, and column 3 the number of tetrahedral ions on the basis of six in the octahedral sheet.

In the serpentines the distribution corroborates the evidence presented in Fig. 3 to the effect that, assuming equal amounts of Al and Fe''' in the two sheets of each layer, there are appreciably more tetrahedral cations per six octahedral cations in the platy than in the fibrous specimens. Thus, the average chrysotile has 4.041 tetrahedral ions for every six octahedral ions whereas in the platy serpentines (omitting the matrix specimens and the anomalous specimen from Unst, P-10) the ratio is 4.291:6.0. If correct, this would require nearly one extra tetrahedral position for every three octahedral units of structure* in the layer. Ob-

* Using a formula unit with six octahedral positions.

TABLE VII. CATION DISTRIBUTION DATA

Sample	No. of Cations: IV	VI	Cat IV per Cat. VI =6	Sample	No. of Cations: IV	VI	Cat IV per Cat. VI =6
Chrysotile:				Other 1:1:			
C-1	3.863	5.903	3.926	Am	3.980	5.896	4.050
C-2	3.955	5.885	4.032	Cr	3.700	6.141	3.615
C-3	3.884	5.916	3.939	Fe''-Ch	4.184	5.658	4.437
C-4	3.921	5.928	3.969	Fe'''-Ch	4.435	6.154	4.324
C-5	3.942	5.747	4.116				
C-6	3.936	5.780	4.086	Chlorite:			
C-7	3.947	5.853	4.046	Sh	4.244	5.950	4.280
C-8	4.012	5.715	4.212	Ri	4.028	5.983	4.039
				Ap	4.035	5.795	4.178
Platy Serpentine:				Th	4.410	5.486	4.823
P-1(M)	3.853	5.901	3.918	Cl	4.051	5.873	4.139
P-2(M)	3.948	5.957	3.976	Pe	4.003	5.805	4.138
P-3(M)	3.907	5.926	3.956	Da	4.348	5.463	4.775
P-4(M)	3.920	5.828	4.036				
P-5	4.098	5.850	4.203	Group Averages:			
P-6	4.176	5.794	4.324	Chrysotile	3.933	5.841	4.041
P-7	4.243	5.883	4.327	Platy serpentine	4.075	5.868	4.169
P-8	4.123	5.939	4.165	Excluding (M)			
P-9	4.171	5.885	4.253	and P-10	4.180	5.846	4.291
P-10	3.698	5.940	3.735	Chlorite	4.160	5.765	4.339
P-11	4.021	5.864	4.114				
P-12	4.232	5.592	4.541				
P-13	4.170	5.857	4.265				
P-14	4.406	5.946	4.446				
P-15	4.163	5.843	4.275				

viously this would be one way in which the misfit between the smaller Si-O and larger "brucite" sheets might be partially adjusted.

Although the presence of more than four filled tetrahedral positions for every six in the octahedral sheet involves a departure from the "classical" picture of the serpentine structure, it is in accord with the structural data presented by Zussman (1954) as evidence in support of an alternating or rectified wave structure for some varieties of platy serpentine. The cation assignments he gives as the result of detailed structural analysis of antigorites from Venezuela and New Zealand are compared in Table VIII with those calculated by the author from the same analyses. The ratios obtained for the number of tetrahedral ions per six octahedral ions are given at the bottom of the table. The close agreement indicates that the method used herein for calculating the formulas from the analyses is meaningful.

Amesite and ferrous and ferric chamosite also have ratios greater than 4:6 whereas cronstedtite gives a value of 3.6:6.0.

As in the other evaluations the matrix and fiber pairs give very similar values.

TABLE VIII. STRUCTURAL ASSIGNMENTS FOR NEW ZEALAND AND VENEZUELA ANTIGORITES (P-8 AND P-9)

Ions		Ideal structure*	Mikonui, New Zealand		Caracas, Venezuela	
			Zussman	calculated	Zussman	calculated
IV	O	48.9	51.0	50.2	51.0	50.7
	Si, etc.	32.6	33.9	33.6	34.1	34.0
VI	O	32.6	34.4	33.0	33.9	33.0
	(OH)	16.3	15.0	16.2	15.0	16.1
	Mg, etc.	48.9	48.9	48.4	48.2	48.0
	(OH)	48.9	47.6	48.7	47.4	48.3
$Cat._{IV}$ per $Cat._{VI}=6$		4.00	4.16	4.16	4.24	4.25

* Proportioned to Zussman's structural unit of 8.15 "cells" along "a" axis.

Excess or Deficiency of Hydrogen and Oxygen

With respect to item 2 of the preceding "general statement," it is of interest that the amount of oxygen and hydrogen provided by each analysis is not equal to that needed if these elements are proportioned with respect to the cation distribution in octahedral and tetrahedral sheets as indicated by the ideal structural formula.

Thus, in the kaolinite example given in Table II, 0.052 more oxygen ion and 0.105 more H^+ is needed for the properly proportioned structural formula than the H_2O+ of the analysis provides. In the serpentine example, on the other hand, the analysis provides an excess of 0.483 oxygen and 0.965 H^+ over that needed in a "properly proportioned" structure. Although in writing the structural formulas in Table V it is convenient to add "excess" hydrogen to the tetrahedral sheet as H_3 or to account for a deficiency by subtracting the element (with appropriate oxygen) from the octahedral sheet, the author feels that correct assignments must await procurement of better experimental data. The following discussion, therefore, relates only to the amount of these ions present and not to the possible structural positions. The data are presented in the last two columns of Table IV. For each analysis the amount of excess or deficient hydrogen should be twice that of the corresponding oxygen. The slight discrepancies are due to rounding-off errors in the calculations.

Because of the uncertainty as to the temperature at which H_2O+ was measured for many of the analyses, the precision of the values is uncertain. However, an analysis of variance shows that the differences between chrysotiles as opposed to platy serpentines (including matrix

samples), and between kaolinites and dickites as opposed to halloysites are significant at the 1% level. The chrysotiles have a mean value of +.821 H^+ as compared to +.125 for platy serpentines, and halloysites give a mean of +.889 compared to +.099 for kaolinites and dickites.

Again it will be noted that the values for the "matrix" analyses from the matrix and fiber pairs (numbers P-1(M) to P-4(M)) are very different from those of the platy serpentines and very similar to those of the adjacent fiber material. The anomalous position of sample P-10 from Unst is apparent.

Data on Chlorites

The relationship of serpentine to chlorite has been discussed by many workers, among the most recent being Nelson and Roy (1954), Brindley and Gillery (1954 and 1956), Bradley (1955) and Gillery (1958). The purpose of including the subject in this paper is to point out that morphological and other relationships between the two groups of minerals can be satisfactorily explained on the basis of the same parameters as those used to evaluate the 1:1 layer minerals. The pertinent data are presented in this section and will be discussed in the next.

A number of chlorite analyses considered by Orcel (1927) to be characteristic of various chlorite sub-groups have been evaluated on the same basis as the other analyses considered here, and the various compositions are represented on the graph in Fig. 2. In addition characteristic compositions of corundophyllite and penninite are also represented, as is that of the daphnite specimen discussed by Brindley and Gillery (1954). It is apparent that the chlorites represented fall well within area II and do not overlap the serpentine compositions. The relative positions are brought out by the M values in Table VI. Those for chlorite compositions range from −36.76 for sheridanite to +50.20 for penninite. The lowest value for a platy serpentine is +60.09 for the Val Antigorio antigorite.

It is also instructive to consider the amount of hydrogen present in the H_2O+ of the analysis as compared with that "required" to provide the proper proportion of OH as given by the ideal chlorite formula. The values are recorded in Table IV (the amounts given are for one half of the usual formula unit in order that the values may be more easily compared with those of the 1:1 minerals). In marked contrast to the chrysotiles and all but one of the platy serpentines, the chlorite analyses have appreciably less hydrogen than that needed if the proportions are to be similar to those in the formula.

Discussion

The Role of Hydrogen

In those minerals, such as amesite, cronstedtite, chamosite, platy serpentines and chlorites, where the analysis provides less H^+ and $O^=$ than is appropriate to the ideal formula, it is apparent that the lattice must contain oxygens in place of some of the hydroxyls and either have an occasional oxygen or hydroxyl position vacant or have a structural modification, such as the rectified layers postulated by Zussman (1954), which involves fewer oxygen and hydroxyl positions than the ideal structure.

In the opposite situation, namely in hallosysite and chrysotile, where the analysis provides an excess of hydrogen and oxygen, either 1) some interlayer water is so tightly held as to be included in the H_2O+ value, or 2) the ions occupy structural positions in the 1:1 lattice. Independent of whether the hydrogen ions are present between the layers in H_2O or $(H_3O)^+$ or are in the tetrahedral sheet as OH in place of or in addition to oxygen, a very probable and important result of their presence is a weakening of interlayer bonds. This is evidenced by the difference in the (001) spacings of halloysite (7.3–7.9 Å) as compared with kaolinite (7.15 Å) and dickite (7.15 Å), and of chrysotile (7.3 Å) as compared with platy serpentine (7.26 Å).

Interrelationships of Chemistry, Structure and Morphology

Some of the relationships between the mineral groups with respect to the parameters discussed herein are shown in Fig. 5. The figures in parentheses give the (001) and a_o values for the various structures. Some observations of a general nature are as follows:

1) The halloysites, kaolinites and dickites, chrysotiles, and platy serpentines fall in distinct groups. The matrix specimens closely associated with serpentine fiber fall within the chrysotile area as in Fig. 3. Platy serpentine P-10 and halloysite H-26 are anomalous.
2) With respect to both "amount of misfit" and "excess or deficient hydrogen" the analogy between platy serpentine and kaolinite and dickite, and between chrysotile and halloysite is very apparent.
3) The compounds with the greatest amount of misfit have the largest amount of H^+ and the smallest amount of substitution of other cations. These compounds crystallize in the form of tubes or curved laths.
4) The gap between kaolins and serpentines is bridged, in the lower half of the diagram only, by the other 1:1 minerals and the chlorites.
5) On the left and right sides of the diagram, the (001) spacing characteristic of the minerals of each group increases with increasing H^+ content.
6) The a_o spacing increases from that of the kaolins to a maximum for cronstedtite at the center of the diagram and then decreases again to that of chrysotile.

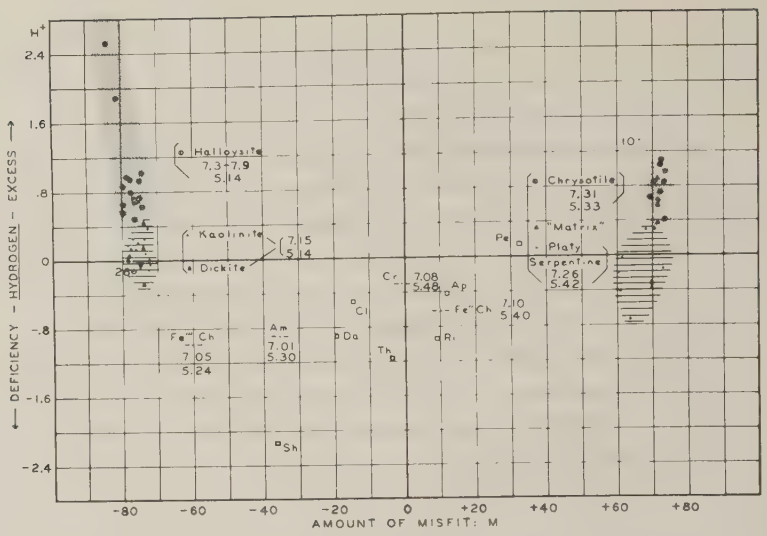

FIG. 5. Relationship of excess or deficient hydrogen content to the amount of misfit of tetrahedral and octahedral sheets. The top number is the (001) spacing whereas the bottom number is a_o.

7) Platy crystals are either deficient in H^+ or have enough to approach the correct proportions of the structural formula. Theoretically, compounds having the largest platy crystals have the least amount of misfit and fall nearest the center of the diagram.

These relationships all support the contention that, in this group of the sheet structure silicates, details of structure and morphology are a function of the amount of misfit and the strength of interlayer bonds. These latter factors are interdependent and are a function of chemical composition. Interlayer bonds are strongest in amesite, cronstedtite, chamosite and the chlorites where excess H^+ is not present and where excess negative charges produced by substitution in the tetrahedral sheet form bonds not only with positive charges produced by substitution in the octahedral sheet of the same layer, but also with those produced in the neighboring octahedral sheet in the adjacent layer.

Toward the left side of the diagram, as the amount of substitution decreases, the role of hydroxyl bonds becomes more important. In kaolinite and dickite these bonds are presumably strong enough to "stretch" the gibbsite sheet of one layer to fit the Si-O sheet of the adjacent layer thereby overcoming the misfit and producing platy crystals of limited size. Oberlin and Tchoubar (1957) have shown that when thin enough plates of kaolinite are produced either naturally or synthetically, interlayer bonds are weakened and the plates curl.

With an increase in excess H^+ above that found in kaolinites and dickites, interlayer bonds become too weak to overcome the misfit and curved laths and tubes are to be expected. Where excess H^+ is sufficient in amount ($=+6.546$) to combine with associated oxygen in a continuous sheet of interlayer water, tubes of halloysite ($4H_2O$) are formed. For the specimens shown in Fig. 5 only H_2O+ was considered and consequently only compositions approaching halloysite ($2H_2O$) are represented. Although it was formerly believed that all $2H_2O$ halloysite probably formed by dehydration of the $4H_2O$ material, present evidence (Bates and Comer, 1959) indicates that $2H_2O$ halloysite such as that pictured in Fig. 1 may form directly where there is enough excess H^+ to cause sufficiently weak interlayer bonds for the production of curved laths but not enough to make the bonds so weak that tubes result.

Toward the right side of Fig. 5 the situation differs from that just discussed in that hydroxyl bonds are formed only where Al and Fe''' substitute for Mg. In the platy serpentines, as compared with chrysotile, the decrease in amount of misfit and the OH bond formation produced by Al and Fe''' substitution is sufficient to produce crystals which are characteristically platy but show irregular rather than crystallographic outlines. However, interlayer bonds are significantly weaker than in kaolinite and it is not surprising that plates may exist that may be made up of alternating or rectified waves of varying periodicity giving rise to varying a_o dimensions (Zussman, Brindley and Comer, 1957).

In chrysotile, with practically no Al and Fe''' substitution and with a large amount of excess H^+, interlayer bonds are so weak and the misfit so great that tubes are the logical result.

Finally, the minerals lying between the kaolin and serpentine groups have the maximum amount of Al and Fe''' substitution and therefore 1) relatively strong interlayer bonds, 2) the least amount of misfit of octahedral and tetrahedral sheets, 3) greater order perpendicular to (001) and consequently 4) larger platy crystals with crystallographic outlines.

Summary

Because of their 1:1 layer structure the kaolin and serpentine groups, and certain other structurally associated minerals and synthetic compounds, have morphological and structural characteristics which are particularly sensitive to slight changes in chemical composition. In order to demonstrate the nature of the interrelationships of chemistry, structure and morphology and their bearing on similarities and differences within and between the mineral groups, 64 analyses have been evaluated and compared.

The evaluation has been made in terms of four parameters: 1) a

morphological index, M, which is a measure of the amount of misfit of tetrahedral and octahedral sheets; (2) the proportions of the major components, SiO_2, Al_2O_3 (or R″O) and H_2O, as represented on ternary diagrams; 3) the number of cations assigned to the tetrahedral sheet in relation to a standard number in the octahedral sheet; and 4) the amount of deficient or excess hydrogen and oxygen recorded as H_2O+ in the chemical analysis as related to that required to provide the correct number of properly proportioned O and OH ions in the structural formulas.

Conclusions resulting from the use of parameters one and two are considered particularly significant because they do not depend on the validity of assumptions that must be made in the calculation of structural formulas. Parameters three and four involve the assumption that the Al and Fe‴ in excess of the amount of silicon in the dioctahedral minerals and all Al and Fe‴ in the trioctahedral minerals is divided equally between the tetrahedral and octahedral sheets.

The use of these parameters helps to clarify the differences within and between mineral groups. With respect to the overall group of 1:1 minerals, the two major chemical differences are: 1) the nature and number of cations substituting for Si in the tetrahedral sheet and for Al or Mg in the octahedral sheet; and 2) the amount of H_2O+.

Variation in the amount of misfit of octahedral and tetrahedral sheets brings out not only the expected distinction among the kaolin group, the serpentine group, and the other 1:1 minerals (amesite, cronstedtite and chamosite) but also reveals a smaller but distinct difference between chrysotiles and platy serpentines. It is of interest that the difference between chrysotile and the type antigorite from Val Antigorio is greater than that between chrysotile and any other platy serpentine. Of the other 1:1 minerals cronstedtite has the least amount of misfit and all three have much less than kaolin minerals or serpentines. The morphological and misfit relationships of several synthetic silicates and germanates fit nicely in the pattern set by the natural materials.

The amount of H_2O+ varies considerably in the analyses studied and serves particularly well to distinguish platy from lath-shaped and tubular varieties in the kaolin and serpentine groups since analyses of platy minerals contain significantly less H_2O+ than those of the non-platy specimens.

Calculation of structural formulas is based on a structural unit of 18 oxygens, but the distribution of the oxygens is determined not in terms of an ideal structural formula but on the basis of the distribution of cations in the two sheets of the layer. This approach is used in the belief that the number of cations (and accompanying oxygens) in the tetra-

hedral sheet, per standard number in the octahedral sheet, may vary in order to reduce the amount of misfit between sheets. Thus, whereas the chrysotiles have, on the average, 4.041 tetrahedral cations for every six octahedral cations the ratio in the platy serpentines (excluding anomalous sample P-10 and matrix samples) is 4.291. Obviously, this excess could increase the size of the tetrahedral sheet and thereby produce a better fit with the larger "brucite" sheet.

The method of formula calculation also provides a measure of the amount of excess or deficient hydrogen and oxygen in the H_2O+ value of the chemical analysis as related to that required by properly proportioning O and OH in accord with the formula distribution of cations other than hydrogen. The results bear out the bulk-composition evidence to the effect that tubular and lath-shaped varieties in both kaolin and serpentine groups have a significant excess of hydrogen and oxygen in the H_2O+ value of the analysis as compared to that "required" by the cations. On the other hand platy varieties of these groups have either a deficiency or nearly the correct amount of H_2O+, and the other 1:1 minerals have a deficiency.

Since H_2O+ content, which bears directly on interlayer bond strength, and cation nature and distribution in the two sheets of each layer are probably interrelated, both factors must be considered in explaining structural and morphological details. Figure 5 represents an attempt to do this and thus place the individual specimens and various groups in proper perspective relative to one another. When viewed in this way distinctions between groups become sharply defined and relationships between morphology and chemistry become more apparent. The picture also serves to suggest that the transition from kaolinite to halloysite ($2H_2O$) is simply the first part of the series leading to halloysite ($4H_2O$) and allophane as H_2O content is increased. In the serpentines the difference between chrysotile and the platy varieties is distinct but the variation within the platy group is probably due in part to mechanical mixtures of fiber and platy material in the samples analyzed.

A few typical chlorite analyses have been included to demonstrate the relationship of these minerals to the 1:1 group. On the basis of the parameters used herein, the chlorites characteristically have a deficiency in the H_2O+ content of the analyses and show a much smaller "amount of misfit" than serpentines or kaolins. In general they have similar characteristics to the 1:1 minerals amestie, chamosite and cronstedtite thus indicating the very close chemical and structural relationships of the two mineral groups. The fact that there is no overlap of chlorites and serpentines is logical in that a chlorite structure would be expected only

where there is sufficient substitution of trivalent ions for Si and Mg to keep the amount of misfit small and to promote the formation of relatively strong interlayer bonds.

Acknowledgment

Much of the morphological data collected by the author and used as a background for this paper was obtained as part of a research program sponsored by the Office of Naval Research entitled "Investigation of morphology, structure and origin of fine-grained minerals." Former graduate students who contributed much to the aspects of the program dealt with herein include John F. Mink, Leonard B. Sand, and Bartholomew Nagy. Research on halloysite sponsored by the Filtrol Corporation and performed by M. A. Rosenfeld, J. C. Griffiths and the author provided large amounts of data on the morphology of numerous samples of this mineral.

The excellent electron microscope work of Mr. J. J. Comer has provided the essential information upon which many of the observations and concepts recorded herein are based.

References

Alexander, L. T., Faust, G. T., Hendricks, S. B., Insley, H. and McMurdie, H. F. (1943), Relationship of the clay minerals halloysite and endellite: *Am. Mineral.*, **28,** 1–18.

Bates, Thomas F. (1955), Electron microscopy as a method of identifying clays: in Clays and Clay Technology, *Calif. Div. Mines Bull.* **169,** 130–150.

——— and Comer, J. J. (1955), Electron microscopy of clay surfaces: in Clays and Clay Minerals, *Natl. Acad. Sci.—Natl. Res. Council Publ.* **395,** 1–25.

——— and Comer, J. J. (1959), Further observations on the morphology of chrysotile and halloysite: *Proc. Sixth Natl. Clay Conf.*, in press.

Bradley, W. F. (1955), Structural irregularities in hydrous magnesium silicates: Proc. Third National Clay Conference, *Natl. Acad. Sci.—Natl. Res. Council Publ.*, **395,** 94–102.

Brindley, G. W. (1954), The structural formula of an antigorite from Venezuela: *Am. Mineral.*, **39,** 391–393.

——— and Comer, J. J. (1956), The structure and morphology of a kaolin clay from Les Eyzies, France: in Clays and Clay Minerals, *Natl. Acad. Sci.—Natl. Res. Council Publ.* 456, 61–66.

——— and Gillery, F. H. (1954), A mixed-layer kaolin-chlorite structure: Proc. Second National Clay Conference, *Natl. Acad. Sci.—Natl. Res. Council Publ.* **327,** 349–354.

——— and Gillery, F. H. (1956), *X*-ray identification of chlorite species: *Am. Mineral.*, **41,** 169–186.

——— and von Knorring, O. (1954), A new variety of antigorite (ortho-antigorite) from Unst, Shetland Islands: *Am. Mineral.*, **39,** 794–804.

——— and Youell, R. F. (1953), Ferrous chamosite and ferric chamosite: *Min. Mag.*, 30, 57–70.

Caillère, S. (1936), Contribution a l'étude des mineraux de serpentines: *Bull. Soc. Fr. Min.*, **59,** 163–373.

Davis, D. W., Rochow, T. G., Rowe, F. G., Fuller, M. L., Kerr, P. F. and Hamilton, P. K. (1950), Electron micrographs of reference clay minerals: A.P.I. Proj. 49, Prelim. Rep't. #6.

Deudon, Madeleine (1955), La chamosite orthorhombique du minerai de Sainte-Barbe, Couche grise: *Bull., Fr. Min. Soc.*, **78,** 475–480.

Dunham, K. C., Claringbull, G. F. and Bannister, F. A. (1948), Dickite and collophane in the magnesian limestone of Durham: *Min. Mag.*, **28,** 338–342.

Gillery, F. H. (1958), *X*-ray study of synthetic Mg-Al serpentines and chlorites, in press.

Hendricks, S. B. (1939), Random structures of layer minerals as illustrated by cronstedite ($2FeO \cdot Fe_2O_3 \cdot SiO_2 \cdot 2H_2O$). Possible iron content of kaolin: *Am. Mineral.*, **24,** 529–539.

Hess, H. H., Dengo, G. and Smith, R. J. (1952), Antigorite from the vicinity of Caracas, Venezuela: *Am. Mineral.*, **37,** 68–75.

Honjo, G., Kitamura, N. and Mihama, K. (1954), A study by means of single crystal electron diffraction diagrams—the structure of tubular kaolin: *Clay Minerals Bull.*, **2,** 133–140.

Kalousek, G. L. and Muttart, L. E. (1957), Studies on the chrysotile and antigorite components of serpentine: *Am. Mineral.*, **42,** 1–22.

Loughnan, F. C. (1957), A technique for the isolation of montmorillonite and halloysite: *Am. Mineral.*, **42,** 393–398.

McConnell, D. (1954), Ortho-antigorite and the tetrahedral configuration of hydroxyl ions: *Am. Mineral.*, **39,** 830–831.

Midgley, H. G. (1951), A serpentine mineral from Kennack Cove, Lizard, Cornwall: *Min. Mag.*, **29,** 526–530.

Nagy, B. and Bates, T. F. (1952), Stability of chrysotile asbestos: *Am. Mineral.*, **37,** 1055–1058.

Nagy, B. and Faust, G. T. (1956), Serpentines: natural mixtures of chrysotile and antigorite: *Am. Mineral.*, **41,** 817–837.

Nelson, B. W. and Roy, R. (1954), New data on the composition and identification of chlorites: Proc. Second Clay Conference, *Natl. Acad. Sci.—Natl. Res. Council Publ.* **327,** 335–353.

Oberlin, A. M. and Tchoubar, C. (1957), Etude en microscopie électronique de l'alteration des cristaux de kaolinite: *Acad. Sci., Compt. rend.*, **244,** 1624–1626.

Onsager, L. (1952), in conference report by Robinson, K. and Shaw, E. R. S., *Brit. J. Appl. Phys.*, **3,** 281–282.

Orcel, J. (1927), Chemical composition of chlorites: *Bull. Soc. Fr. Min.*, **50,** 75–454.

Proud, J. S. and Osborne, G. D. (1952), Stress-environment in the genesis of chrysotile, with special reference to the occurrence at Woodsreef, near Barraba, New South Wales: *Econ. Geol.*, **47,** 13–23.

Ross, C. S. and Kerr, P. F. (1930), The kaolin minerals: *U. S. Geol. Surv. Prof. Paper* **165-E,** 151–180.

Ross, C. S. and Kerr, P. F. (1934), Halloysite and allophane: *U. S. Geol. Surv. Prof. Paper* **185-G,** 135–148.

Roy, D. M. (1952), Phase equilibria in the system MgO-Al_2O_3-H_2O and in quaternary systems derived by the addition of SiO_2, CO_2 and N_2O_5: Ph.D. thesis, The Pennsylvania State University, Jan. 1952.

Roy, D. M. and Roy, R. (1954), An experimental study of the formation and properties of synthetic serpentines and related layer silicate minerals: *Am. Mineral.*, **39,** 957–975.

Shannon, E. V. (1921), Some minerals from the old tungsten mine at Long Hill in Trumbull, Conn.: *Proc. U. S. Nat. Mus.*, **58,** 469–482.

Sudo, T. and Takahashi, H. (1956), Shapes of halloysite particles in Japanese clays: Clays and Clay Minerals, *Natl. Acad. Sci.—Natl. Res. Council Publ.* **456,** 67–79.

Swineford, A., McNeal, J. D. and Crumpton, C. F. (1954), Hydrated halloysite in Blue Hill shale: *Natl. Acad. Sci.—Natl. Res. Council Publ.* **327,** 158–171.

Tu, K. C. (1950), Ph.D. Thesis, Department of Geology, University of Minnesota.

Whittaker, E. J. W. and Zussman, J. (1956), The characterization of serpentine minerals by *x*-ray diffraction: *Min. Mag.*, (233), **31,** 107–127.

Yoder, H. S. (1952), The MgO-Al_2O_3-SiO_2-H_2O system and the related metamorphic facies: *Am. J. Sci.* (Bowen vol.), 569–627.

Zussman, J. (1954), Investigation of the crystal structure of antigorite: *Min. Mag.*, **30,** 498–512.

Zussman, J. (1956), Antigorite: superlattice and structural formula: *Am. Mineral.*, **41,** 148–152.

Zussman, J. and Brindley, G. W. (1957), Serpentines with 6-layer orthohexagonal cells: *Am. Mineral.*, **42,** 666–670.

Zussman, J., Brindley, G. W. and Comer, J. J. (1957), Electron diffraction studies of serpentine minerals: *Am. Mineral.*, **42,** 133–153.

Manuscript received May 5, 1958

THE AMERICAN MINERALOGIST, VOL. 44, JANUARY–FEBRUARY, 1959

CHEVKINITE, PERRIERITE AND EPIDOTES

STEFANO BONATTI, *Pisa University, Pisa, Italy.*

ABSTRACT

The relationship between perrierite and chevkinite and between these and the epidotes are here re-examined and illustrated on the basis of new data obtained by Jaffe, Evans, Jr. and Chapman on a chevkinite in New Hampshire.

INTRODUCTION

On the basis of research conducted by myself and G. Gottardi [3], [4] on a new mineral, perrierite, found in the sands of the shore at Nettuno (Roma), we showed that chevkinite represents a family of minerals possessing orthorhombic and monoclinic members with close morphological and structural relationships to the family of epidote. A morphological character common to epidote and chevkinite is shown by the very close angular values in the planes of the zone [010]; a structural character in common is the presence of oxygen chains which develop, in the monoclinic group, along the axis of symmetry; thus the two families of minerals acquire a value of b very close to 5.6 Å (twice the diameter of oxygen). Other minerals such as rinkite, mosandrite and related silicates which show morphological analogies to epidote and have $c \sim 5.6$ Å, belong to this category of silicates.

An interesting article by Howard W. Jaffe, Howard T. Evans Jr. and Randolph W. Chapman [6] supplies important new data on chevkinite which support the conclusions of our research [3], [4] and supply experimental evidence for our earlier speculative, though strongly motivated, conclusions.

These authors made an exhaustive study of a chevkinite found in a New Hampshire fayalite-quartz syenite; there is no doubt that this chevkinite is the same mineral described by Boldireff [1], [2] for the Urals. The report by these authors refers several times to the data in our two notes on perrierite; however while the authors concede that many of our statements are convincing (see [6], p. 478 and others), they maintain that our conclusions are not clear to them. That some misunderstanding exists is apparent, apart from the explicit declaration of the authors, by the fact that they still admit the possibility, although with strong reservations, that perrierite and chevkinite might be the same mineral. This is in spite of the fact that, with their own determination of the elementary cell of the New Hampshire chevkinite, different from the perrierite cell, they have proved beyond any doubt that chevkinite and perrierite belong to different mineralogical species.

Most certainly credit must be given to the afore-mentioned authors

for having furnished, after accurate observations, the means for a complete and very interesting clarification of the relationship between epidote, perrierite and chevkinite. I will now try to put this interesting subject of descriptive mineralogy in final and complete form by reexamining our results, adding new data and comparing them with those of the quoted authors.

Morphological Crystallography of Perrierite

Perrierite [3] bears a very close morphological analogy to the epidotes and in particular to allanite. By projecting the most common and frequent forms of allanite stereographically, and by superimposing those of perrierite, thereby identifying poles when they are not more than two degrees apart, we obtain the diagram shown in Fig. 1.

The very close isogonal relationships are evident. Due to the presence of the same zone (112) (012) (indices of allanite), in both minerals, we could have given perrierite an axial ratio almost identical to that of allanite. The crystallographic argument which I consider not worthwhile repeating and to which I refer in the note [3] led us to use the following axial ratio for perrierite:

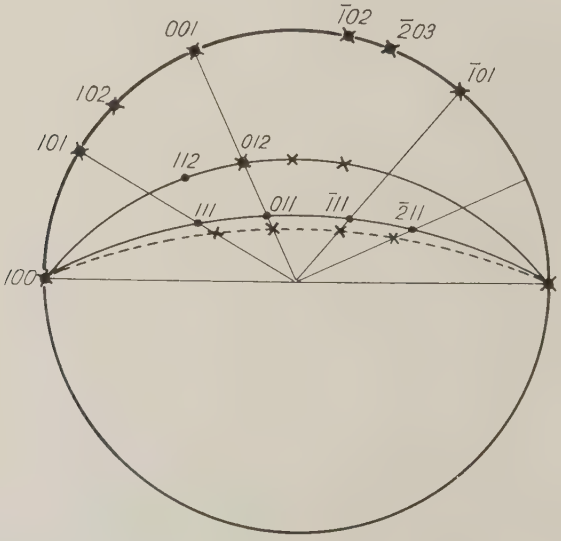

Fig. 1. Allanite and perrierite.
Points = poles of the faces of allanite with relative indices.
Crosses = poles of the faces of perrierite without indices.
Points with crosses = poles of the faces of allanite and perrierite which fall within two degrees of each other. Indices of allanite.

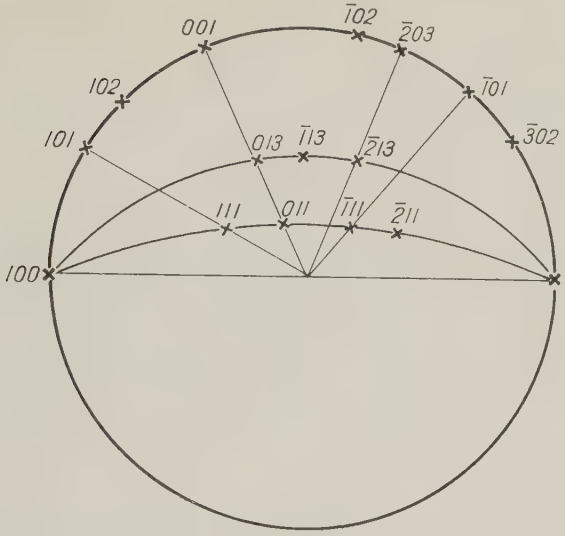

FIG. 2. Crystallographic interpretation of perrierite.

$$a:b:c = 2.047:1:2.380 \qquad \text{with } \beta = 113°28'$$

in respect to the axial ratio for allanite:

$$a:b:c = 1.551:1:1.769 \qquad \text{with } \beta = 115°11'.$$

In addition we showed that, if A:B:C is the axial ratio of allanite, then that of perrierite is almost exactly:

$$\frac{4A}{3}:B:\frac{4C}{3}.$$

We predicted that such ratios should apply also to the unit cell of allanite and that of perrierite. Succeeding research permitted the determination of the unit cell of perrierite which, when compared to that of epidote[1] was found to be:

	$a = 8.96$ Å	$(\frac{4}{3}a = 11.94)$
epidote: $\beta = 115°24'$	$b = 5.63$ Å	$(1b = 5.63)$
	$c = 10.30$ Å	$(\frac{4}{3}c = 13.73)$
	$(a = 11.63$ Å$)$	
perrierite[2]: $\beta = 113°28'$	$b = 5.62$ Å	
	$(c = 13.61$ Å$)$.	

[1] The lattice of allanite was not yet known, but it was assumed to be almost identical to that of the common epidote as it actually turned out [14].

[2] The data which in note [4] are expressed in kX are changed here to Å.

The values for perrierite, a and c, are expressed in parentheses since the inversion of a and c was made necessary by the fact that the crystallographic plane (100) was found to be centered. Therefore the final unit cell of perrierite became:

perrierite: $\beta = 113°28'$ $a = 13.61$ Å, $b = 5.62$ Å, $c = 11.63$ Å.

Notwithstanding the fact that the inversion of a with c became structurally necessary, I believe that the orientation used by us must be preserved for the macroscopic crystallography of perrierite; for it demonstrates the close relationship of isogonism between it and the monoclinic epidotes. Other reasons for preserving the orientation given will be formulated in the paragraph where I will give particular treatment to the structural data of perrierite.

Morphological Crystallography of Chevkinite

In 1915–16 Ungemach and Lacroix [11], [12], [15] described chevkinite as a rare earths silico-titanate, and they positively assigned it to the orthorhombic system. They also suggested the possibility of the occurrence of a chevkinite with monoclinic symmetry.

In 1924 Boldireff [1], [2] comprehensively described a monoclinic chevkinite of the Urals and ventured a very reserved opinion that the orthorhombic chevkinite found by Ungemach and Lacroix might be the same monoclinic chevkinite he described. For reasons already given [4] and others to be presented in this paper, the above conjecture cannot be defended. Therefore, to distinguish it from the monoclinic chevkinite of Boldireff, I will call "orthochevkinite" the Ungemach and Lacroix mineral, whose existence must be accepted until new evidence to the contrary.

Boldireff describes the chevkinite of the Urals as monoclinic and gives the following crystallographic elements [1]:

$$a:b:c = 2.426:1:1.955 \quad \text{with } \beta = 79°52',$$

where $79°52'$ is the angle between the positive crystallographic axes, x and z. This is clearly indicated by the angular values and stereographic projections reported by the above author.

In his crystals Boldireff finds a very frequent and unique twinning with union and twin-plane (001). By applying the method of Fedoroff for the determination of the "symbols of the complex" he finds that allanite is the only mineral similar to chevkinite in form and chemical composition. Consequently, he tries an iso-orientation of the two minerals by bringing (100), the larger face of chevkinite in coincidence with (100) of

allanite (also found very large in a crystal at Moriah, N. Y., as reported in Dana's System [5]), as shown in Fig. 3.

In Fig. 3 the dashed line connects the two faces selected by Boldireff for the iso-orientation; therefore, the faces of both minerals have the same

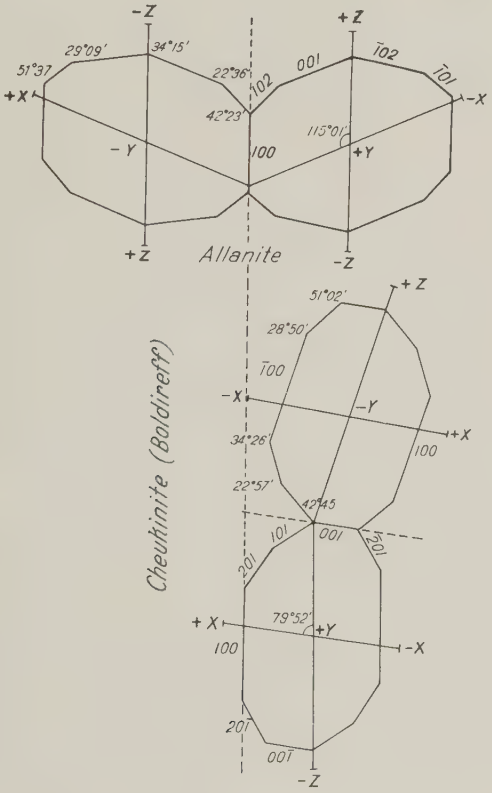

FIG. 3. Orthogonal projections on the (010) plane of the faces of the zone [010] of allanite and chevkinite with their common twinning and iso-oriented according to Boldireff. For chevkinite the indices are those of Boldireff ($\beta = 79°52'$).

index (100). With this iso-orientation the two twin-planes change to (100) for allanite and (001) for chevkinite. The angular sequences, though extremely close, develop different indices. It seemed to us that the crystallographic orientation could be modified by superimposing the two planes of common twinning, transforming (001) into (100), and assuming the face marked (201) by Boldireff to be (001).

The angular coincidences are listed below:

Allanite Indices of allanite	Chevkinite Indices of Boldireff	Difference
(100) : (101) = 30°06′	face corresponding (101) missing	
(100) : (102) = 42°23′	42°45′ = (001) : (101)	0°22′
(102) : (001) = 22°36′	22°57′ = (101) : (20$\bar{1}$)	0°21′
(001) : ($\bar{1}$02) = 34°15′	34°26′ = (201) : (100)	0°11′
($\bar{1}$02) : ($\bar{1}$01) = 29°09′	28°50′ = (100) : (20$\bar{1}$)	0°19′
($\bar{1}$01) : ($\bar{3}$02) = 17°00′	16°14′ = (20$\bar{1}$) : (10$\bar{1}$)	0°46′
($\bar{3}$02) : ($\bar{1}$00) = 34°37′	34°48′ = (10$\bar{1}$) : (00$\bar{1}$)	0°11′

Bearing in mind that even perrierite repeats the same series of angles almost exactly, we then have *three minerals which develop a zone around* [010] *in perfect syngony; they are allanite* (monoclinic epidotes in general), *perrierite*, and *chevkinite*. The only difference worth noting is that chevkinite lacks the form corresponding to the (101) of perrierite and allanite.

Let us now examine the faces of the other zones. We have already spoken of the relationship between perrierite and allanite; it led us to assign to perrierite an axial ratio, as referred to the parameters of allanite (we call A : B : C) nearly equal to 4A/3 : B : 4C/3, β being almost the same.

Next we shall compare the morphology of perrierite to that of chevkinite. In the stereographic projection of Fig. 4, the iso-orientation used by us is that which clearly shows the morphological relationships between chevkinite and perrierite, and, consequently, monoclinic epidotes.

For chevkinite we have added, to the forms determined by Boldireff, four new forms reported by Jaffe, *et al.* [6] (indices according to Boldireff), {010}, {012}, {021}, {112}.

In spite of the presence in perrierite of a zone (100) (111) with an inclination almost equal to that of chevkinite, Fig. 4 reveals that only the forms belonging to the zone around [010] find correspondence in the two minerals. *Evidently perrierite is much closer* to allanite than to chevkinite, according to what has already been said and illustrated in Fig. 1.

We started from crystallographic considerations fully given in [4], and which I do not deem worthwhile to repeat here, also because the results of the later investigations of Jaffe, Evans Jr., and Chapman [6] have given us all the relevant facts, where we were only trying to make a forecast. We inferred that for the chevkinite of Boldireff it would also be preferable to adopt the same orientation chosen by us for perrierite, namely by superposing the face of habitual twinning (see Fig. 4). We deemed it would be advisable to assume , for the axial ratio of chevkinite, values very close to those of perrierite, but with *a* about twice as great. We thought that this morphological interpretation might have a struc-

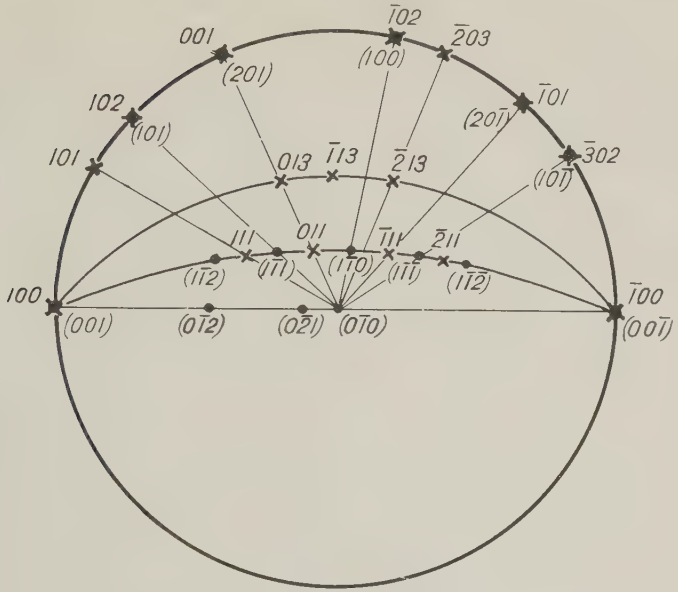

FIG. 4. Stereographic projection on (010) of perrierite and chevkinite with the iso-orientation indicated.

Crosses = poles of the faces of perrierite.

Points = poles of the faces of chevkinite.

Crosses with points = poles of the faces of perrierite and chevkinite which fall within a degree of each other.

hkl = indices of perrierite.

(*hkl*) = indices of chevkinite according to Boldireff ($\beta = 79°62'$).

tural correspondence. More in detail: having found the cell of perrierite, with respect to that of epidote, to be 4A/3, B, 4C/3, with β almost the same, we thought that chevkinite with respect to epidote would have the values: 8A/3, B, 4C/3, with β almost equal and, consequently, with respect to perrierite: 2*a*, *b*, *c* with β almost equal.

Recently Jaffe, Evans Jr. and Chapman [6] have determined the unit cell of chevkinite. As will be explained in the following paragraphs, the unit cell predicted by us, as compared with the one determined by the said authors, corresponds closely to a double cell, with the planes (010) centered. The unit cell determined by the above authors repeats the morphological interpretation given by Boldireff [1], [2] ($\beta = 100°45'$) with centered base corresponding to the (001) of Boldireff.

In view of this I believe that the crystallographic interpretation of Boldireff must be retained, even if it does not show clearly the zone of isogony [010] with the epidotes, and leads to different indices for the planes of twinning.

It should be clear therefore that, on the basis of the new data now available, the morphological orientation of chevkinite formerly suggested by us, is not acceptable any more; it would be based on a structural cell which is twice the unit one. In this connection however, I wish to make the two following remarks:

1) If one wants to stress the morphological relationships between chevkinite, perrierite and monoclinic epidotes, one has always to keep in mind that (100) and (001) of perrierite and of the epidotes correspond to (001) and (201) of chevkinite.

2) Boldireff, in his crystallographic description of chevkinite, accepted as true β (angle between $+x$ and $+z$) 79°52′, and chooses indices accordingly. Jaffe, Evans Jr. and Chapman [4], on the contrary, adopt an obtuse angle for β, for the unit cell, and most probably also for the external morphology. They do not make any mention of this change. There is, however, no possibility of ambiguity, as in chevkinite, for each positive and negative form there exists the corresponding negative and positive; according to Boldireff the negative form corresponding to {112} was missing, but it has now been found by the American authors. I believe that the interpretation of the American authors is the one to be accepted, as it conforms to current usage. Therefore the crystallographic constants of chevkinite are the following:

2.329:1:1.926, $\beta = 100°45'$ (according to Jaffe, Evans Jr., Chapman).

They are derived from structural data, surely more reliable than the very imprecise crystallographic measurements of Boldireff (see [1] and [2], 2.426:1:1.955, $\beta = 79°52'$, Boldireff).

Unit Cell and Structural Data of Perrierite and Chevkinite

The unit cell [4] determined by us for perrierite, conforms to the unit cell of monoclinic epidotes, with the already mentioned change in the lengths of a and of c. Moreover it has been necessary to exchange a and c, because it has been found that the plane (100) is centered. This gives:

$a = 13.61$ Å, $b = 5.62$ Å, $c = 11.63$ Å, $\beta = 113°28'$.

It should be emphasized that the lattice of perrierite has been found to be of the monoclinic centered type, whereas the lattice of epidote and allanite is of the primitive monoclinic type. In this connection I should like to point out, that:

1) In epidote some of the atoms (e.g. Al, O) are present not only at the corners of unit cell, but also in 0, $\frac{1}{2}$, $\frac{1}{2}$; for these atoms, the cell would be with (100) centered. This does not happen for all atoms, and therefore the cell must be considered primitive monoclinic.

2) It seems that something similar may be the case with perrierite.

On account of the small size of the crystals, the x-ray photographs are very faint and therefore reveal only the arrangement of the heaviest atoms (mainly the rare earths and titanium). The observed absences could therefore become meaningless if stronger photographs should reveal the arrangement of the lighter atoms also. In such a case perrierite would also have a primitive cell.

At the present stage of the investigations, the unit cell has to be considered as centered. For a correct iso-orientation with the lattices of epidote and of chevkinite, it should be kept in mind that the centered basal plane (structurally (001)) is morphologically the crystallographic plane of very frequent twinning (100).

Jaffe, Evans Jr. and Chapman have determined the unit cell of chevkinite as:

$$a = 13.56 \text{ Å}, \quad b = 5.82 \text{ Å}, \quad c = 11.21 \text{ Å}, \quad \beta = 100°45'.$$

Also in this unit cell the centered base is the plane of very frequent twinning, the plane which, for chevkinite, is also morphologically the plane (001).

These two cells, although substantially different, are closely related as far as angles and of translations lengths. The relationships, with the iso-orientation as revealed by macroscopic crystallography, are illustrated in Fig. 5.

The centered basal planes are, in both minerals, planes of the usual twinning.

Let us now examine the relationships between these two unit cells and those of epidote, superposing the common planes of usual twinning, in conformity with the morphological iso-orientation suggested by us. See Fig. 6.

Figure 6 is only approximate, because slightly divergent lines are drawn as coincident, and the same is the case for very near points. The approximation is very close. In the case of perrierite and chevkinite this is brought out by the following computation: $a = 13.56$ Å, $b = 5.82$ Å, $c = 11.21$ Å, $\beta = 100°45'$ being, according to Jaffe etc. [6], the unit cell of chevkinite; the values for the double cell as drawn on the figure in prolongation (dotted lines) of the cell of perrierite are $a = 13.56$ Å, $b = 5.82$ Å, $c = 23.94$ Å, $\beta = 113°04'$. After doubling c in the unit cell of perrierite, one obtains $a = 13.61$ Å, $b = 5.62$ Å, $c = 23.26$ Å, $\beta = 113°28'$; this is in excellent agreement with the computed values, and with what we had predicted. In our note [4], on account of an obvious printing error, there is $a = 29$ Å. One should read 24 Å (8/3 of a of epidote is equal to 23.89 Å) and should take into account the exchange between a and c.

We are faced here with a singular case of relationship between the unit cells of different mineralogical species, which opens new vistas on

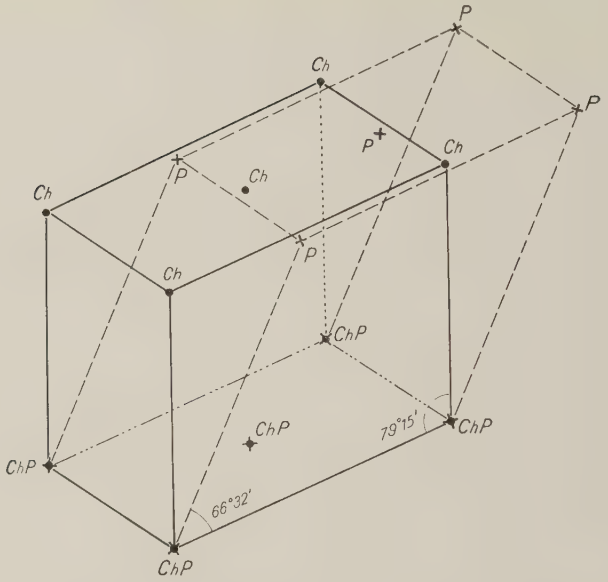

FIG. 5. Relationship between the unit cell of chevkinite (full lines) and of perrierite (dashed lines).

Points *Ch* = equivalent points of chevkinite.

Crosses *P* = equivalent points of perrierite.

polymorphism. It becomes therefore necessary to make an accurate examination of the experimental results, and of the interpretation of the morphological and structural data. The following points are given in confirmation:

(1) On the basis of *x*-ray photographs, the two lattices are clearly different. Equator and first level Weissenberg or Buerger precession photographs about [010] are sufficient to distinguish them. As a consequence of the (001) centering, the patterns for the zero level are almost identical (see dashed lines in Figs. 7 and 8), but the *h*1*l* photograph clearly differentiates them.

Figures 9 and 10 show precession photographs of perrierite around [010], equator and first level.

Figure 11 combines the reflections observed in Figs. 9 and 10, thus showing both the zero and first levels. There is no possibility of confusing the unit cell of perrierite with that of chevkinite [6].

(2) We shall examine next the evidence which can be obtained from the macroscopic crystallographic characters of chevkinite.

Let us compare the stereographic projection of the faces of zone $(1\bar{1}0)$ $(1\bar{1}1)$ of chevkinite with the set $(1\bar{1}0)$ $(11\bar{1})$ of the first layer $[0\bar{1}0]$ of the

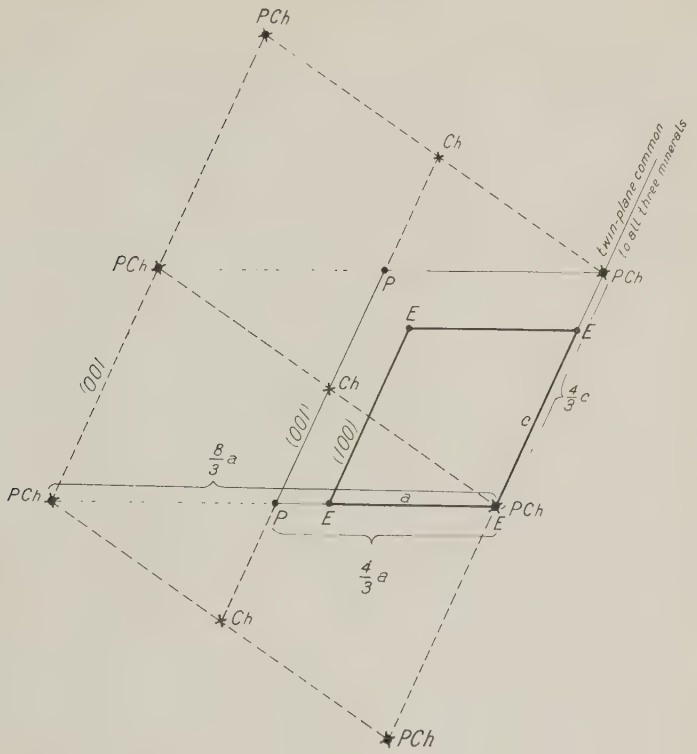

FIG. 6. This scheme gives very closely the relationship, on the plane (010), between the unit cell of epidote (heavy full lines), of perrierite (light full lines), and of chevkinite (dashed lines: four unit cells (010)). Structural indices.

Points E = equivalent points of epidote.

Points P = equivalent points of perrierite.

Crosses Ch = equivalent points of chevkinite.

reciprocal lattice of chevkinite (see Fig. 12). On this figure, besides the crystallographic planes of chevkinite, shown with dots and their indices, are represented also, with crosses, the crystallographic planes of perrierite.

It is clear from the foregoing that the morphological crystallography reflects exactly the relationship of the two lattices. It was on account of this morphological relationship that we had predicted for chevkinite a unit cell which, although of double size, did closely correspond to the real one.

(3) Powder photographs. Data on perrierite from Nettuno, Italy, obtained with a Philips diffractometer, are compared with data for chevkinite from New Hampshire and Arizona, and for a specimen from Japan, called chevkinite, but actually perrierite, in Table 1.

TABLE 1. POWDER PHOTOGRAPH DATA

I Perrierite of Kobe-mura, Japan [13] (called chevkinite)		II Perrierite of Nettuno, Italy			III Chevkinite, New Hampshire [6]			IV Chevkinite, Arizona [10]	
d, Å	I	*hkl*	*d*, Å	I	*hkl*	*d*, Å	I[1]	*d*, Å	I[1]
5.399	20	002	5.34	65	002	5.50	W		
5.195	30	110	5.13	25					
4.834	10				$\bar{1}11$	4.92	MW	4.97	M
					111	4.67	M	4.71	M
4.104	20		4.06	20					
3.566	40	003	3.56	20	003	3.67	W	3.68	W
		$31\bar{1}$	3.53	15	$\bar{3}10$	3.51	MW	3.52	M
3.462	40		3.43	20					
3.405	40								
3.217	20	400	3.15	15	*$\bar{3}12$*	*3.20*	Sb	*3.20*	S
3.045	50		3.03	20	$\bar{4}02$	3.11	M	3.11	W
2.983	*100*	*$31\bar{3}$*	*2.96*	*100*	203	2.98	W	3.04	M
2.956	*100*	*311*	*2.93*	*55*					
2.841	*70*	*020*	*2.82*	*65*	020	2.90	M	2.91	M
					312	2.79	MW	2.77	W
		113	2.73	15	*004*	*2.74*	VS	*2.74*	S
2.699	60	004	2.675	20					
					022	2.60	W		
2.579	20	220	2.550	15					
2.513	30	022	2.488	15					
2.458	40							2.38	W
2.247	20		2.229	50					
2.231	20								
2.176	*50*		*2.166*	*25*		2.19	W	2.19	W
2.158	*40*		*2.156*	*25*					
2.108	20		2.095	15					
		600	2.088	15					
1.952	*30*	*024*	*1.941*	*50*		1.99	MW	1.98	M
			1.779	15					
1.723	20		1.719	10					
1.659	30		1.658	10					
1.612	30		1.649	15					
1.597	20		1.585	15					

[1] VS = Very strong; S = Strong; M = Medium; MW = Medium weak; W = Weak; F = Faint; VF = Very faint; b = Broad.

For perrierite the indices given have been obtained from a comparison of Weissenberg and precession data with powder data.

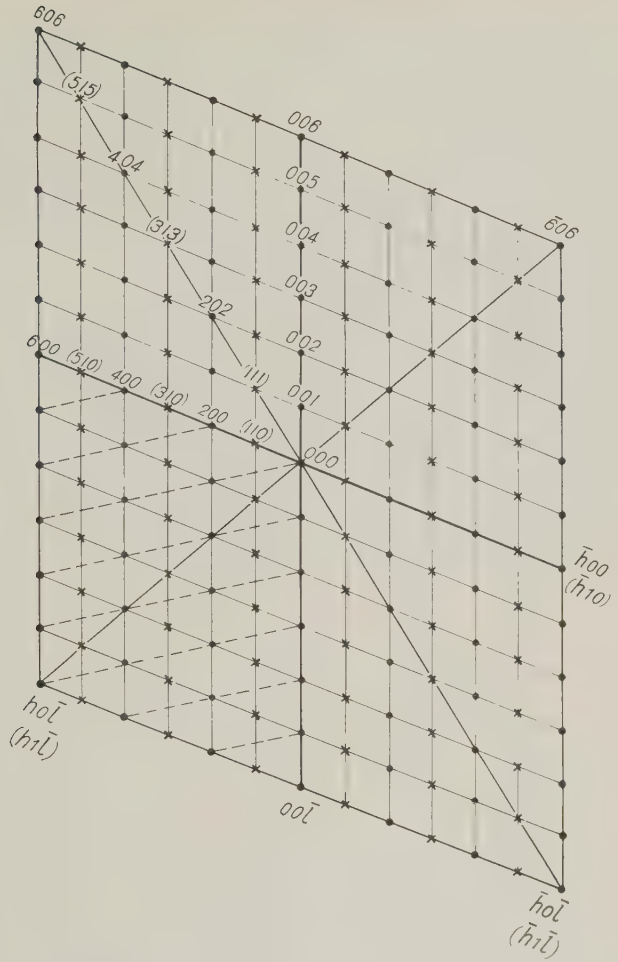

FIG. 7. Reciprocal lattice around [010] of perrierite, equator (dots) and first layer (crosses).

Let us note in the first place that now we are in possession of powder both of perrierite and of chevkinite, which are definitely different; even without morphological data, they allow one to distinguish clearly one mineral from the other, unless these chevkinites be hopelessly metamictic. The chevkinite of Arizona (column IV) is undoubtedly chevkinite; the so-called chevkinite of Kobe-mura (column I) is perrierite.

Now let us examine the powder data of perrierite (column II) and of chevkinite (column III). If the unit cells of perrierite and of chevkinite have been correctly interpreted, we should find the same analogies and

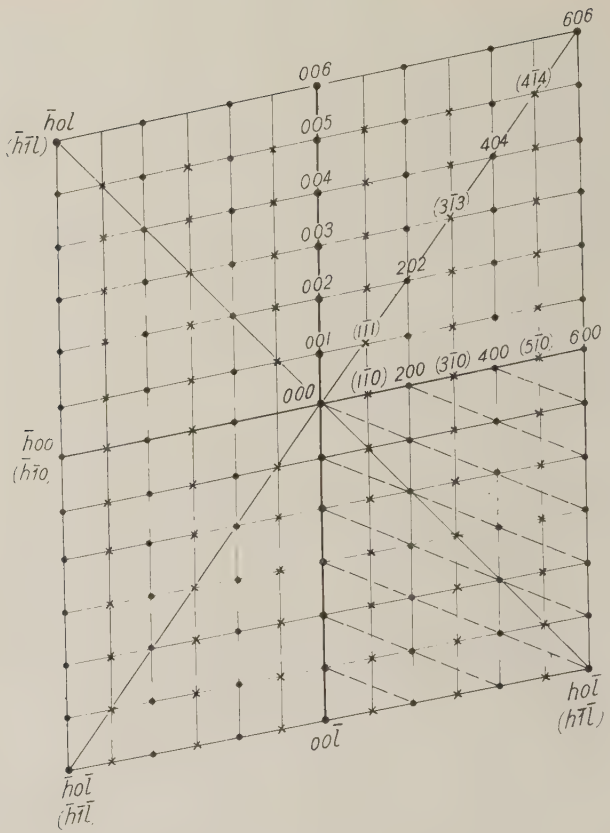

Fig. 8. Reciprocal lattice around [010] of chevkinite, equator (dots) and first layer (crosses).

the same differences pointed out in respect of their morphological characters. This means, coincidence of the lattice planes ($h0l$) and ($00l$), and mutual exclusion for the lattice planes ($h1l$). This is evident from the powder data. Consider for instance , the absence in perrierite of the lines which would correspond to ($\bar{1}11$) and (111) of chevkinite; and the presence, in perrierite, of three near and strong lines belonging to the lattice planes ($31\bar{3}$), (311) (see also Buerger precession 1st layer) and (020). In chevkinite the lines corresponding to ($31\bar{3}$) and (311) are missing, but (020) appears.

There is no doubt whatever that both the unit cell, determined by us for perrierite, and the unit cell determined by Jaffe, Evans Jr. and Chapman for chevkinite, are correct. Structurally also, on the basis of the unit cells, the analogies between perrierite and epidotes seem closer

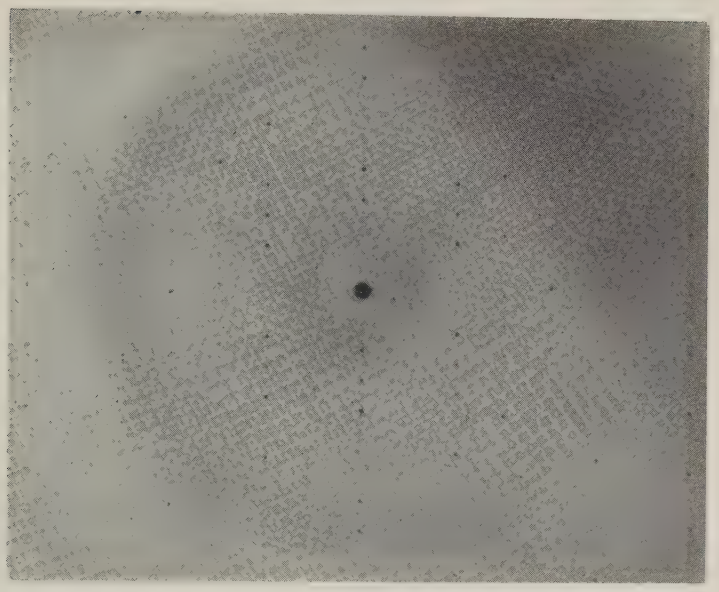

FIG. 9. Buerger precession, 0-level; [010] of perrierite.

than the analogies between chevkinite on one hand, and epidotes and perrierite on the other.

As far as the space group is concerned, the quoted authors [6] give as probable for chevkinite the group $C2/m$; they do not exclude however, the possibility that it may belong to $C2$ or Cm, these being groups without a symmetry center. I may add to their convincing remarks, that the analogies with perrierite and epidotes seem to me to exclude the latter possibility. We had assigned perrierite to group $C2/m$. In fact, the detailed and easily interpretable morphological crystallography of perrierite does not offer any indication of the lack of a center of symmetry; moreover, repeated endeavors to detect with an extremely sensitive device, any piezoelectricity, have always led to negative results. These data, and the crystallographic relationship with epidote, allow one to conclude with almost absolute certainty that perrierite has a symmetry center.

Optical Properties of Perrierite and of Chevkinite

Perrierite and chevkinite do not lend themselves to easy optical determinations, on account of their very strong absorption, with exceptional pleochroism. We feel however that the data we have obtained for perrierite deserve confidence; on account of its rather young age (quaternary) [3], it also does not show strong signs of metamict transformations.

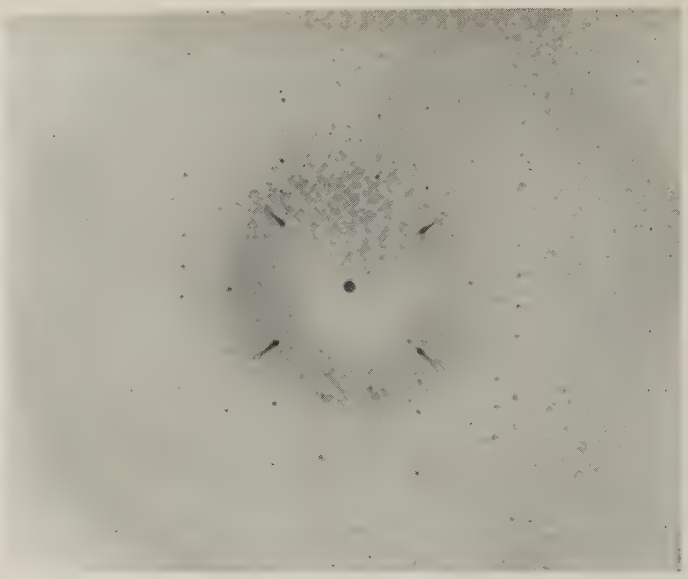

FIG. 10. Buerger precession, first layer [010] of perrierite.

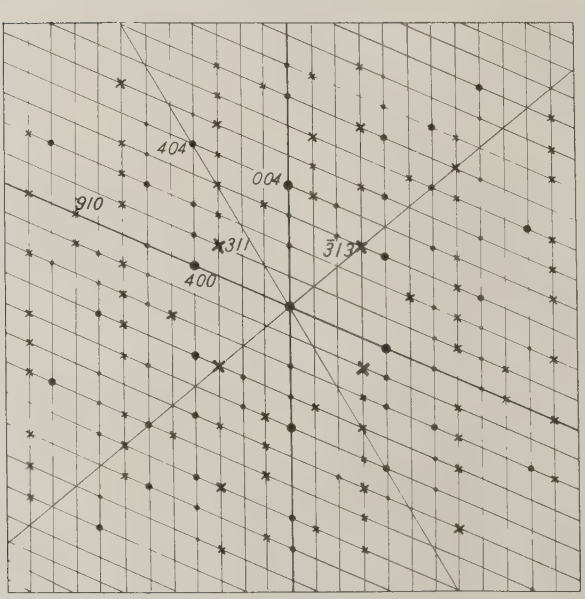

FIG. 11. Diffraction spots observed in the Buerger precession [010] of perrierite, equator (dots) and first layer (crosses).

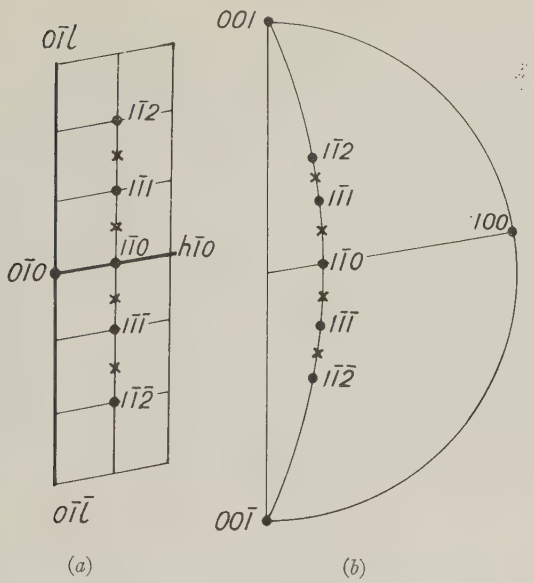

FIG. 12. *a*) Reciprocal lattice first layer of chevkinite (dots with indices), with added lattice planes of perrierite (crosses only).

b) Stereographic projection of the corresponding faces of chevkinite (dots with indices) and of perrierite (crosses only).

On the other hand, on account of the quoted difficulties, I have nothing to add to what has already been published in note [4].

Perrierite: Very strong absorption, with $Z \geqq Y \gg X$; X = yellow; Y = opaque to violet red; Z = opaque to deep brown; $\alpha = 1.90$–1.95; $\beta = 2.01$ (computed); $\gamma = 2.02 - 2.06$.

Orientation: $Z = b$; $X \wedge a$ = about 24° in the obtuse angle; 2V = about 60°, with negative birefringence.

For chevkinite we have Boldireff's data, which however were obtained on strongly metamict material. Therefore he found birefringence around 0.001–0.002, which surely does not fit unaltered material. Boldireff gives: intense pleochroism in reddish brown shades, with $Z > Y > X$; orientation $Z = b$, $X \wedge c$ from 11°30′ to 25°45′ in the acute angle.

Jaffe, Evans Jr. and Chapman who have studied the chevkinite of New Hampshire, recognized, in the same sample, definitely metamict zones near other more fresh ones. For the latter, they found a minimum index of refraction of 1.97 and a maximum of 2.05, with 2V variable from medium to large and optic sign negative. As orientation they give $Z \wedge$ elongation (*b*) 6°–9°. This last data, for an undoubtedly monoclinic crystal, seems perplexing.

From the examination of these optical characters it is however evident, that it is practically impossible to distinguish between perrierite and chevkinite under the microscope in thin sections. It is also difficult, especially in thin sections, to distinguish the chevkinites from allanite, although, in the unusual case of fresh mineralizations, the chevkinites should be recognizable through higher indices and the stronger birefringence. The diagnostic character which, in my opinion, is easiest to ascertain, is the stronger absorption in violet shades of the chevkinites as compared with allanite. It is very likely that perrierite and chevkinite are far more widespread in rocks than commonly believed, and that in petrographical analyses they have been determined as allanite. The fact that in petrographical treatises one finds, besides the normal data for allanite, also anomalous data (e.g., much higher indices of refraction and an orientation $Z = b$), could be fittingly explained by this possibility of confusion between allanite and the chevkinites.

Chemistry

None of the attempts made to assign a chemical formula to the chevkinites, have led to fully satisfactory results. It can be foreseen that it will not be possible to gather under a single formula all the chevkinites for which chemical analyses are available, on account of the wide range of their compositions; this range appears to me to exceed very much the limits of possible isomorphic substitutions. I do not wish to insist on the subject, because I hope to be able to soon give the complete structure of perrierite, which is being studied at present in the Mineralogy Institute of Pisa. It would therefore serve no purpose to offer unwarranted hypotheses, since the knowledge of the structure of at least one mineral of the chevkinite group will be put on a sure basis.

I shall limit myself therefore to a few remarks on crystallochemical criteria, which will have to be respected also when we know the complete structure of chevkinite.

In the first place, I believe that the general crystallochemical rule, according to which calcium is in isomorphic substitution with cerium and with the other rare earths, shall not admit exception in the chevkinites. Keeping together those elements which have the same coordination (8, 6, 4), we gave a formula of the following type:

$$Ce_2O_3 \cdot 2TiO_2 \cdot 2SiO_2$$

or more in detail

$$(Ce, La, Y, Ca, Th, Na)_2O_3 \cdot 2(Ti, Fe'', Mg)O_2 \cdot 2(Si, Al, Fe''')O_2.$$

I admit that this formula is not very satisfactory. On account of the great quantity of titanium, and of the difficulty of maintaining the electrical neutrality, it is not easy to accept the association of tetravalent

titanium with bivalent iron and magnesium. On this point the decision will have to be left to the analysis of the structure; should it confirm this grouping, it would contribute valuable data on the possibilities of isomorphic substitution. I believe, however, that it is preferable to the earlier formulas, which by rather naively grouping bivalent, trivalent and quadrivalent elements, lead to results not in harmony with the principles of crystal chemistry.

Also Jaffe, Evans Jr. and Chapman have tried to assign to chevkinite a new formula, while declaring the previously suggested ones are not supported by any convincing evidence ([6], p. 480). Considering that a structural basis would be of help in reaching an exact formula, they have tried to find in their determination of the unit cell the starting point for the solution of the problem. Starting from the assumption that in such compounds the volume is accounted for by the oxygen atoms alone, and taking the value of the oxygen volume as 18.1 Å^3, as in epidote, they come to the result that the number of oxygen atoms in chevkinite (unit cell volume 873 Å^3) is 48. On this assumption they give the following formula:

$$R_3^{2+}R_3^{3+}AlSi_4Ti_5O_{22}(OH)_2.$$

Even omitting other crystallochemical considerations, it is perplexing to note, that in this formula, calcium and rare earths are separated. As far as the 48 atoms of oxygen are concerned, I wish to point out that applying the same procedure to perrierite[3] (unit cell volume 812 Å) the number of atoms in the unit cell should be 44.86, nearly equal to the 44 required by our formula. I do not intend, however, to make use of this computation as a support for our interpretation, because it leads to a rough approximation only, with an uncertainity of a few units. For example, assuming as the unit volume of chevkinite the volume found after heat-treatment, the number of oxygen atoms which ought to be present is reduced to 46.

The chemical formula put forward by us for perrierite seems to me the most acceptable, until the day the determination of the structure will supply further data. It should then be possible to decide if perrierite and chevkinite are polymorphs, or if they have to be considered two distinct minerals.

Orthochevkinite from Madagascar

Ungemach [15], and Lacroix [12] described for the first time the morphology of a chevkinite on samples from Madagascar. They stated

[3] Some of the chemical data and the density of perrierite have been incorrectly reported in the paper by Jaffe, Evans Jr. and Chapman [6].

definitely that it is orthorhombic, although expressing the possibility that a monoclinic form may also exist. In describing chevkinite from the Ural, Boldireff [1], [2] admits, although very doubtfully, the possibility that the orthorhombic crystals described by Ungemach and Lacroix may be morphologically the same as the ones described by himself, simulating through twinning an orthorhombic symmetry. We have already shown in detail why the hypothesis of Boldireff seems indefensible. Let me state three fundamental points in confirmation:

1) The twinning which, according to Boldireff, would transform the monoclinic chevkinite described by him into the orthorhombic chevkinite of Ungemach, would be; twinning plane (100) not coincident with the composition plane. Therefore, a parallel twinning with irrational twinning axis and with composition plane equally irrational (no plane containing the normal to (100), can have a rational index, with the exception naturally of (100)). Such a twinning does not seem acceptable.

2) Even if one admits this strange twinning, one does not obtain the orthorhombic crystals of Ungemach [15] which show, for instance, the association of the three orthogonal pinacoids {100}, {010}, {001}.

3) This twinning has never been found either in the chevkinite of the Urals, in that of New Hampshire, in perrierite, in allanite, or in other monoclinic epidotes. It would therefore be specific, and very common, only in orthochevkinite of Madagascar. One would make use, for proving the crystallographic identity of two minerals, of an evident and important differential character.

I owe to the kindness of Mme. Jérémine of the Minéralogical Laboratory of the Museum of Paris the opportunity to examine three of the original crystals from Madagascar, described by Ungemach and Lacroix. My crystallographic examination fits perfectly the orthorhombic interpretation of the said authors.

With the kind permission of Mme. Jérémine I have broken off a small fragment from a big crystal; with this I have made some Debye-Scherrer photographs. Those obtained with this material before heat treatment are very faint, with broad lines; this confirms the advanced metamict transformation of the mineral. The photographs after heat treatment are more sharp and rich in diffraction lines; but it has been easy to ascertain that, besides the faint lines which correspond almost exactly to the untreated material, there appears the powder pattern of Ce_2O_3, some of the lines being very strong. Table 2 gives the data so obtained.

With all the uncertainties due to the fact that the material is strongly altered, one can assume as specific for the chevkinite of Madagascar those diffractions common to the spectrograms both of the untreated and

TABLE 2. ORTHOCHEVKINITE OF MADAGASCAR

Untreated		Heat-treated[2]	
d, Å	I[1]	*d*, Å	I[1]
4.15	VS	4.13	W
3.78	S	3.72	F
3.54	M	3.50	W
		(3.12)	(VS)
		2.96	W
2.875	S	2.831	W
2.699	S	(2.706)	(M)
2.527	M	2.505	W
		2.232	F
		2.159	MW
		2.085	W
		1.959	W
		(1.911)	(S)
		1.738	VF
1.692	S	1.689	F
		(1.632)	(S)
		(1.565)	(W)
1.488	M	1.413	W
		(1.353)	(MW)
		(1.241)	(M)
		(1.210)	(MW)
		(1.104)	(M)
		(1.041)	(M)
		(0.956)	(MW)

[1] VS = Very strong; S = Strong; M = Medium; MW = Medium weak; W = Weak; F = Faint; VF = Very faint.

[2] Spacings in parentheses pertain to the Ce_2O_3 produced by heating.

of the heat-treated material. There is no possibility of correlation with the powder spectrograms of perrierite and of chevkinite (cf. Table 1).

I do not wish to deny that it may be possible to identify the orthorhombic chevkinite with monoclinic chevkinite or with perrierite, through a mimetic twinning (but surely not of the kind suggested by Boldireff). I am more inclined to believe in a structural twinning within the lattice, in keeping with what is already well known in the case of orthorhombic zoisite, with respect to monoclinic epidotes. The close analogies between epidotes and chevkinites hint of the possibility of this further kinship; should this be proved, it would complete in a very satisfactory way the picture of the relationship between epidotes and chevkinites.

Conclusions

1) Epidotes and chevkinites form two groups of minerals with close morphological and structural ties. The most significant common character is the development of oxygen chains along the symmetry axis in the monoclinic members ($b \sim 5.6$ Å). Other minerals, like mosandrite, rinkite, etc., are related to these two groups.

2) The chevkinites are not a single mineral species. Well identified are perrierite and monoclinic chevkinite; probably there is also a orthorhombic chevkinite.

3) Perrierite has to be referred to the following crystallographic elements, which give it the same orientation as for the monoclinic epidotes:

Monoclinic system, prismatic class,

$$a:b:c = 2.047:1:2.380, \qquad \beta = 113°28' \text{ (Bonatti and Gottardi).}$$

The values of the unit cell are the following:

$$a = 13.61 \text{ Å}, \qquad b = 5.62 \text{ Å}, \qquad c = 11.63 \text{ Å}, \qquad \beta = 113°28'$$

where a and c are interchanged in respect to the morphological interpretation, the lattice being centered.

Space group: $C2/m$.

4) Chevkinite has to be referred to the following elements, in iso-orientation with its unit cell:

Monoclinic system, prismatic class,

$$a:b:c = 2.329:1:1.926, \qquad \beta = 100°45' \text{ (Jaffe, Evans Jr., Chapman)}$$

remembering that, for stressing the isogonal relations with perrierite and with the monoclinic epidotes, the face (001) must be assumed as (100), and (201) as (001).

The values of the unit cell are the following:

$$a = 13.56 \text{ Å}, \qquad b = 5.82 \text{ Å}, \qquad c = 11.21 \text{ Å}, \qquad \beta = 100°45'$$

in iso-orientation with the morphological elements.

Space group: $C2/m$.

5) The unit cell of chevkinite as given above, with c doubled and with (010) centered, gives:

$$a = 13.56 \text{ Å}, \qquad b = 5.82 \text{ Å}, \qquad c = 23.94 \text{ Å}, \qquad \beta = 113°04'$$

which repeats with great accuracy the unit cell of perrierite with c doubled; therefore it is in the following relationship with the unit cell of monoclinic epidotes:

$$\frac{4}{3}\,c,\ 1b,\ \frac{8}{3}\,a, \text{ with } \beta \text{ similar.}$$

This confirms what had been anticipated, through the morphological comparison of perrierite with chevkinite and the epidotes, by Bonatti and Gottardi [4].

References

1. Boldireff, A. (1924), Note crystallographique sur la tchevkinite: *Bull. Ac. de Sc. de Russie*, série 6, **18,** 257–288.
2. ——— (1925), Etude cristallographique de la tscheffkinite de l'Oural: *Bull. Soc. Franc. de Minéralogie*, **48,** 120–127.
3. Bonatti, S. and Gottardi, G. (1950), Perrierite, nuovo minerale ritrovato nella sabbia di Nettuno (Roma): *Rend. Acc. Naz. Lincei*, serie 8, **9,** 361–368.
4. ——— (1954), Nuovi dati sulla perrierite. Relazioni tra perrierite, chevkinite ed epidoti: *Rend. Soc. Mineral. Ital.*, **10,** 208–225.
5. Dana, J. D. (1882), The System of Mineralogy, p. 522, New York.
6. Jaffe, H. W., Evans, H. T., Jr. and Chapman, R. W. (1956), Occurrence and age of chevkinite from the Devil's slide fayalite-quartz syenite near Stark, New Hampshire: *Am. Mineral.*, **41,** 474–487.
7. Ito, T. (1947), The structure of epidote: *Am. Mineral.*, **32,** 309–321.
8. Ito, T., Morimoto, N. and Sadanaga, R. (1954), On the structure of epidote: *Acta Cryst.*, **7,** 53–59.
9. Kaufman, L. (1924), Sur la composition chimique de la tscheffkinite: *Bull. Ac. de Sc. de Russie*, série 6, **18,** 315–320.
10. Kauffman, A. J., Jr. and Jaffe, H. W. (1946), Chevkinite from Arizona: *Am. Mineral.*, **31,** 582–588.
11. Lacroix, A. (1915), La bastnaésite et la tscheffkinite de Madagascar, etc.: *Bull. Soc. Franc. de Minéralogie*, **38,** 106–125.
12. ——— (1922), Minéralogie de Madagascar, **1,** 585–588; **3,** 313–314, Paris.
13. Takubo, J. and Nishimura, S. (1953), On Tscheffkinite from Kobe-mura, Kyoto Prefecture, Japan: *Mem. Coll. Science, Univ. of Kyoto*, series B, **20,** 323–328.
14. Ueda, T. (1955), The crystal structure of allanite: *Mem. Coll. de Science, Univ. of Kyoto*, series B, **22,** 145–163.
15. Ungemach, H. (1916), Contribution à la Minéralogie de Madagascar: *Bull. Soc. Franc. de Minéral.*, **39,** 5–37.

Manuscript received May 29, 1958

X-RAY STUDIES OF ALUMINUM AND IRON PHOSPHATES CONTAINING POTASSIUM OR AMMONIUM

JAMES P. SMITH AND WALTER E. BROWN, *Division of Chemical Development, Tennessee Valley Authority, Wilson Dam, Alabama.*

ABSTRACT

Lattice constants and space groups are reported for several complex iron and aluminum phosphates containing potassium or ammonium: $H_6(K, NH_4)_3Al_5(PO_4)_8 \cdot 18H_2O$ (taranakite), $H_2(K, NH_4)(Al, Fe)(PO_4)_2 \cdot H_2O$, $H_2(K, NH_4)(Al, Fe)(PO_4)_2$, $(K, NH_4)(Al, Fe)_2(PO_4)_2(OH) \cdot 2H_2O$ (leucophosphite) and $H_8(K, NH_4)(Al, Fe)_3(PO_4)_6 \cdot 6H_2O$. A new formula given for tarankite is consistent with the chemical composition, density and space-group requirements. In a layer structure postulated for taranakite, aluminum phosphate sheets are separated by water molecules.

INTRODUCTION

An interest in phosphate-soil relations led Haseman *et al.* (1950, 1951) to the preparation of several groups of complex iron and aluminum phosphates from reagent chemicals or through treatment of soil minerals with phosphate solutions. Their work included determinations of the chemical compositions, optical properties and *x*-ray powder diffraction spacings of the compounds, three of which have been shown to be identical with the minerals taranakite (Haseman, *et al.*, 1950), minyulite (Haseman *et al.*, 1951) and leucophosphite (Axelrod *et al.*, 1952).

Single-crystal *x*-ray studies of representative members of these groups of compounds are reported here. To facilitate cross reference, Haseman's designations of compounds are included.

X-RAY MEASUREMENTS

The results of the *x*-ray studies* are summarized in Table 1. Densities were calculated on the basis of theoretical chemical compositions instead of those obtained by chemical analyses.

Taranakite, $H_6(K, NH_4)_3Al_5(PO_4)_8 \cdot 18H_2O$ (Group 1, Product A)

Bannister and Hutchinson (1947) concluded that the minerals minervite, palmerite and taranakite are identical and on the basis of priority should be called taranakite. A synthetic mineral obtained upon treatment of kaolinite with potassium phosphate solution at 50° C. was assumed by Stout (1940) to be a product of the exchange of phosphate ions for hydroxyl ions of the kaolinite lattice. The mineral was shown by

* Diameter of Weissenberg camera, 57.3 mm. Filtered copper radiation ($\lambda = 1.541$ Å) used for aluminum compounds –filtered iron radiation ($\lambda = 1.936$ Å) for iron compounds. With the exception noted, diffraction data were obtained from at least two axial settings of the crystals. Where possible, reciprocal angles were determined by the method of triangulation (Buerger, 1942). Axial measurements are considered reliable to $\pm 0.3\%$—interaxial angles to $\pm 20'$.

TABLE 1. LATTICE CONSTANTS OF SYNTHETIC IRON AND ALUMINUM PHOSPHATES CONTAINING POTASSIUM OR AMMONIUM IONS

Designation*		Unit-Cell Contents	Crystal System	Probable Space Group	Lattice Constants				Density, g./cc.	
Group	Product				*a*	*b*	*c*	β	*X*-Ray	Pycnometric
1	A	$6[H_6K_3Al_5(PO_4)_8 \cdot 18H_2O]$	Hexagonal (rhombohedral)	C_{3v}^6 or D_{3d}^6	8.71	—	96.1	—	2.11	2.09
2	C	$8[H_2KAl(PO_4)_2 \cdot H_2O]$	Monoclinic	C_{2h}^5—$P2_1/c$	10.04	9.10	16.34	101°18′	2.49	2.52
2	D	$8[H_2KFe(PO_4)_2 \cdot H_2O]$	Monoclinic	C_{2h}^5—$P2_1/c$	10.22	9.23	16.56	99°20′	2.61	2.63
3	E	$3[H_2KFe(PO_4)_2]$	Triclinic	C_1^1 or C_i^1	9.26	9.49	7.20	—†	2.87	2.90
4	I	$4[(KFe_2(PO_4)_2(OH) \cdot 2H_2O]$	Monoclinic	C_{2h}^5—$P2_1/n$	9.76	9.65	9.70	102°54′	2.92	2.93
4	J	$4[(NH_4)Al_2(PO_4)_2(OH) \cdot 2H_2O]$	Monoclinic	C_{2h}^5—$P2_1/n$	9.63	9.59	9.58	103°19′	2.42	—
5	—	$2[(H_8(NH_4)Al_3(PO_4)_6 \cdot 6H_2O$	Hexagonal	D_{6h}^4, C_{6v}^4, D_{3h}^4	8.90	—	16.50	—	2.29	—
5	K	$2[H_5(NH_4)Fe_3(PO_4)_6 \cdot 6H_2O]$	Hexagonal	D_{6h}^4, C_{6v}^4, D_{3h}^4	9.14	—	16.88	—	2.36	2.36

* Haseman *et al.* (1951).

† $\alpha = 110°11'$ *et al*, $\beta = 117°7'$, $\gamma = 97°56'$.

Low and Black (1948), however, to be a complex aluminum phosphate. Haseman *et al.* (1951) grew tarankite crystals as single hexagonal plates or as stacks of plates resembling kaolinite worms, too small to give good interference figures. The crystals appeared to be biaxial and were reported to be monoclinic.

A redetermination of the optical and morphological properties showed the crystals to be uniaxial negative (see also Murray and Dietrich, 1956). The uniaxial character and the alternate undercut-overcut $\{10\bar{1}1\}$ lateral faces of the plates are clearly consistent with the rhombohedral symmetry indicated by the *x*-ray study. The observed reflections conform to the conditions $hk\bar{i}l$ present when $-h+k+l=3n$, $hh2\bar{h}l$ present when $l=3n$, and $h\bar{h}0l$ present when $h+l=3n$ and $l=2n$, which are characteristic of the space groups C_{3v}^6—$R3c$ and D_{3d}^6—$R\bar{3}c$.

The empirical formula $H_4K_2Al_3(PO_4)_5 \cdot 11H_2O$, reported by Haseman *et al.* (1951) from chemical analyses, and the space-group multiplicities lead to density values of 2.61 and 1.30, which differ greatly from the pycnometric value, 2.09. An alternative formula, $H_6K_3Al_5(PO_4)_8 \cdot 18H_2O$, agrees equally well with the chemical analyses, gives a density of 2.11, and is considered to be a more probable formula for taranakite.

A lower hydrate (group 1, product B), obtained at 95° C., has the empirical composition $H_6K_3Al_5(PO_4)_8 \cdot 13H_2O$. Crystals in sizes suitable for single-crystal *x*-ray study were not obtained. The powder diffraction pattern has an intense line at 13.8 Å. One preparation contained relatively large crystals which individually comprised both hydrates. The diffraction pattern revealed that the plane giving rise to the 13.8 Å spacing of the lower hydrate is parallel to that giving rise to the 16.0 Å spacing of the higher hydrate. This is known to be the 006 reflection in the higher hydrate. Certain lines, identified as the $h00$ reflections of the higher hydrate, are common to diffraction patterns of both hydrates. Apparently, the unit-cell dimensions of the two hydrates are the same in the *a* direction and the cell shrinks in the *c* direction on loss of water. This is consistent with a view that taranakite has a layer structure with water molecules disposed between sheets comprising aluminum, phosphate, and perhaps potassium or ammonium ions, there being six such layers in a unit cell normal to the *c* axis. The platy habit and the greater increase in the refractive index normal to the plate than in the index parallel to the plate on dehydration are also in accord with this view.

The portion of a given layer lying in one unit cell contains five aluminum atoms and eight phosphorus atoms. The space-group multiplicities are such that at least two of the five aluminum atoms and at least two of the eight phosphorus atoms must lie in special positions. These conditions, along with the possibility of close packing of oxygens and the usual spatial restrictions on the coordination of oxygens by aluminum and phos-

phorus atoms, indicate that a trial-and-error approach to the crystal structure may be practical, once a choice can be made between the two space groups.

$H_2(K, NH_4)(Al, Fe)(PO_4)_2 \cdot H_2O$ (Group 2, Products C and D)

The synthetic minerals of group 2 have a tabular prismatic form and monoclinic symmetry. Their natural occurrence has not been reported. All four end members of the series were prepared, but only two, the potassium aluminum and the potassium iron combinations, were studied by single-crystal methods. The observed reflections for both materials conformed to the conditions *hkl* present in all orders, *h0l* present when $l=2n$, and *0k0* present when $k=2n$. The most probable space group is C_{2h}^5—$P2_1/c$.

The equatorial Weissenberg photograph for the *c*-axis rotation displayed a pseudohexagonal symmetry that was lacking in the photographs of higher levels. This suggests that the crystal structure, when projected on the *c* face, will reveal a hexagonal framework.

$H_2(K, NH_4)(Al, Fe)(PO_4)_2$ (Group 3, Product E)

Only the potassium iron member of group 3 was obtained in crystals suitable for single-crystal *x*-ray study. The lattice constants were determined from a single setting. A rotation photograph, zero-, first- and second-layer line Weissenberg photographs, and composites of zero-layer with first-layer and with second-layer line photographs were taken about the *c*-axis. The primitive cell of three formula weights (Table 1) is somewhat unusual; if the crystal is centrosymmetric, at least one iron and one potassium must occupy centers of symmetry.

The dispersion formula given by Haseman *et al.* (1951) is reversed.

Leucophosphite, $(K, NH_4)(Al, Fe)_2(PO_4)_2(OH) \cdot 2H_2O$ (Group 4, Products I and J)

Powder diffraction data on a naturally occurring potassium iron phosphate, leucophosphite, from Bambuta, Liberia, showed it to be identical with one of the members of group 4 (Axelrod *et al.*, 1952). The lattice constants, space group and optical properties of a leucophosphite from Minas Gerais, Brazil, were reported by Lindberg (1957). The extinction angles ($z \wedge c$) given by Lindberg and by Haseman (1951) are consistent, since Lindberg refers to the *b*-centered cell and Haseman to obtuse β in the primitive cell. The dispersion formula given by Haseman *et al.* (1951) is reversed.

The potassium iron and ammonium aluminum isomorphs were used in this study. The observed reflections, *hkl* present in all orders, *h0l* present only when $h+l=2n$, and *0k0* present only when $k=2n$, agree

with those reported by Lindberg. The most probable space group for both compounds is C_{2h}^5 -$P2_1/n$. The lattice constants for the natural and the synthetic potassium iron materials agree within the expected experimental errors.

$H_8(K, NH_4)(Al, Fe)_3(PO_4)_6 \cdot 6H_2O$ (Group 5, Product K)

The synthetic compounds of group 5 crystallize in the hexagonal system as thin plates or short rods. They are formed readily in acid solutions containing iron and phosphate. The ammonium or potassium content is variable; they apparently can be formed with few, perhaps even none, of these ions in the lattice. Only the ammonium iron compound was obtained in crystals suitable for Weissenberg study. The respective powder diffraction patterns indicate that the potassium iron compound has essentially the same unit-cell dimensions. The lattice parameters listed in Table 1 for the ammonium aluminum compound were derived from an indexing of the first 27 lines of the powder diffraction pattern.

The observed reflections in the Weissenberg patterns, $hk\bar{i}l$ and $h\bar{h}0l$ present in all orders, $hh2\bar{h}l$ present only when $l = 2n$, correspond with the possible space groups D_{6h}^4—$P6_3/mmc$, C_{6v}^4—$P6_3mc$ and D_{3h}^4—$P\bar{6}2c$. The most probable space group could not be decided from etch experiments and morphology. Once the correct space group is established, a determination of the structure should be straightforward, in view of the many restrictions imposed by the symmetry elements on the positions of the atoms.

References

Axelrod, J. M., Carron, M. K., Milton, C., and Thayer, T. P. (1952), Phosphate mineralization at Bomi Hill and Bambuta, Liberia, West Africa: *Am. Mineral.*, **37,** 883–909.

Bannister, F. A., and Hutchinson, G. E. (1947), Identity of minervite and palmerite with taranakite: *Mineral. Mag.*, **28,** 31–35.

Buerger, M. J. (1942), X-Ray Crystallography: John Wiley & Sons, Inc., New York.

Haseman, J. F., Brown, E. H., and Whitt, C. D. (1950), Some reactions of phosphate with clays and hydrous oxides or iron and aluminum: *Soil Sci.*, **70,** 257–271.

Haseman, J. F., Lehr, J. R., and Smith, J. P. (1951), Mineralogical character of some iron and aluminum phosphates containing potassium and ammonium: *Soil Sci. Soc. Amer. Proc.* (1950), **15,** 76–84.

Lindberg, Marie Louise (1957), Leucophosphite from the Sapucaia pegmatite mine, Minas Gerais, Brazil: *Am. Mineral.*, **42,** 214–221.

Low, P. F., and Black, C. A. (1948), Phosphate-induced decomposition of kaolinite: *Soil Sci. Soc. Amer. Proc.* (1947), **12,** 180–184.

Murray, J. W., and Dietrich, R. V. (1956), Brushite and taranakite from Pig Hole Cave, Giles County, Virginia: *Am. Mineral.*, **41,** 616–626.

Stout, P. R. (1940), Alterations in the crystal structure of clay minerals as a result of phosphate fixation: *Soil Sci. Soc. Amer. Proc.* (1939), **4,** 177–182.

Manuscript received May 24, 1958

THE *X*-RAY STUDY OF SYNTHETIC Mg-Al SERPENTINES AND CHLORITES*

F. H. GILLERY
(Hydrothermal experimentation by *V. G. Hill*),† *The Pennsylvania State University, University Park, Pennsylvania.*

ABSTRACT

The effect of the hydrothermal conditions of synthesis on the production of the Mg-Al chlorite and the serpentine polytypes has been examined. The results show that temperature has the greatest effect on which mineral is produced and composition the greatest effect on which of three serpentine polytypes is produced.

The stability relations of the serpentines and chlorites are discussed.

INTRODUCTION

This investigation was undertaken in order to determine how the composition and the conditions of hydrothermal synthesis affect the polytypic variety of synthetic serpentines and chlorites. Detailed study of the serpentines and chlorites up to the present time has been concerned largely with natural specimens and several problems concerning the formation of these specimens may be elucidated by a study of the conditions of formation of the synthetic specimens. Roy and Roy (1954) and Yoder (1952) showed that two structures could be synthesized at the clinochlore ($5MgO \cdot Al_2O_3 \cdot 3SiO_2$) composition and that the 14 Å chlorite structure was in all cases the high temperature structure, while the 7 Å kaolin-type mineral variously called a serpentine, antigorite or septechlorite was formed at low temperatures. Nelson and Roy (1954) established that solid solution extended from near chrysotile to amesite ($4MgO \cdot 2Al_2O_3 \cdot 2SiO_2$) but were still unable to establish unequivocally whether or not the serpentines had any true stability range. The synthetic specimens were all made from gels of the general composition $(6-x)MgO$, $(4-x)$ SiO_2, x Al_2O_3, which gives the formula $(Si_{4-x}Al_x)(Mg_{6-x}Al_x)O_{10}(OH)_8$ for the serpentines and chlorites produced by complete reaction. x had the values 0, 0.25, 0.50, 0.75, 1.00, 1.50, 2.00, 2.25, 2.50 for this particular investigation.

The temperatures used were between 400° C, and 620° C., hydrothermal pressures between 15,000 p.s.i. and 56,000 p.s.i., and times of treatment from a few minutes to about 30 days.

The procedure for preparing the gels has been described by Roy (1956) and the apparatus for treating the gels described by Roy and Roy (1954)

* Contribution No. 57-55 from the College of Mineral Industries, The Pennsylvania State University, University Park, Pennsylvania.

† At the time of this work V. G. Hill was a Research Associate in Geochemistry, The College of Mineral Industries, The Pennsylvania State University. He is now with the Ghana Geological Survey.

and Nelson and Roy (1954). In the present investigation the gels were reacted both in gold capsules with a buffering envelope, and in sealed gold capsules.

The treated specimens were examined by means of a North American Philips Wide Range Diffractometer, using a scanning speed of 1° (2θ)/min for routine identification, but for more accurate work, such as indexing, a scanning speed of $\frac{1}{4}$° (2θ)/min was used and the results were usually independently checked by means of powder photographs taken with a 114.6 mm diam. Norelco camera. The accurate cell parameters from indexed patterns were derived by a least squares procedure. using all the available reliable reflections and the indexing was finally rechecked using the accurate cell parameters.

The electron micrographs and electron diffraction patterns were taken by Mr. J. J. Comer, using an R.C.A. Model E.M.U.-2D electron microscope.

The conditions of the synthesis and phases produced by the compositions examined are shown in Table 1. Anomalies in the products of some of the treatments are due to incomplete reaction. The percentages of 6-layer serpentine given for some of the specimens are rough estimates and are given with respect to the total serpentine content and not the total of all components present.

The Polytypic Varieties Produced

Chlorites were produced from compositions with $x>0.5$ treated at temperatures above about 500° C. at all the pressures examined, and for times exceeding a few days. Compositions with $x=0$, 0.25 and 0.5 produced a mixed phase of brucite or talc and forsterite with some chlorite. No polytypic varieties were observed within the chlorite species, but many of these varieties can be distinguished only by using single crystal methods, a technique not possible in the present investigation due to the small particle size of the synthetic specimens.

The serpentine-type structure was produced by treating the starting gels at temperatures below about 500° C. and with all the pressures and compositions examined. Three polytypic varieties of serpentines were distinguished and their occurrence was found to depend mainly upon the composition of the gel. One of the polytypes was shown by the electron microscope to be of the fibrous type and was only produced by the composition with $x=0$. This type of serpentine can almost certainly exist with values of $x>0$ but evidently not with x as great at 0.25 which was the next composition examined.*

* Nagy and Faust (1956), carried out a survey of natural serpentines and stated that natural fibrous serpentines can contain up to about 4% Al_2O_3 in the structure which corresponds to $x=0.2$ in the present nomenclature.

TABLE 1. DATA FOR THE SPECIMENS EXAMINED

Comp.	Temp. ° C.	Pres. p.s.i.	Time days	Phases present	c_0(Å)	% 6-layer
0.25	610	50,000	4	Fors., Bru.	—	—
0.50	610	50,000	4	Fors., Bru.	—	—
0.75	610	50,000	4	Chl., l Serp.	—	—
1.00	610	50,000	4	Chl.	—	—
1.50	610	50,000	4	Chl.	—	—
2.00	610	50,000	4	Serp., Chl., l. Spin.	—	—
2.25	610	50,000	4	Serp., Spin., l. Chl.	—	—
2.50	610	50,000	4	Serp., Spin., l. Chl.	—	—
0.25	445	40,000	18	Fors., Bru., l. Serp.	7.226 Å	—
0.50	445	40,000	18	Serp.	7.258 Å	—
0.75	445	40,000	18	Serp.	7.208 Å	—
1.00	445	40,000	18	Serp.	7.152 Å	—
1.50	445	40,000	18	Serp.	7.096 Å	—
2.00	445	40,000	18	Serp.	7.048 Å	—
0.25	450	15,000	41	Serp., Chl., Bru., Fors.	—	—
0.50	450	15,000	41	Serp., Fors.	7.228 Å	0%
0.75	450	15,000	41	Serp.	7.238 Å	5%
1.00	450	15,000	41	Serp.	7.156 Å	25%
1.50	450	15,000	41	Serp.	7.102 Å	85%
2.00	450	15,000	41	Serp.	7.052 Å	90%
2.25	450	15,000	41	Serp., l. Spin., l. Cor.	7.054 Å	—
2.50	450	15,000	41	Serp., l. Spin., l Cor.	7.054 Å	—
0	450	45,000	15	Serp.	—	—
0.25	450	45,000	15	Serp., l. Fors.	7.162 Å	10%
1.00	450	45,000	15	Serp.	7.140 Å	50%
2.25	450	45,000	15	Serp., Cor.	7.042 Å	—
2.50	450	45,000	15	Serp., Spin., Cor.	7.044 Å	—
0	400	5,000	15	Serp.	—	—
1.00	600	35,000	19	Chl.	—	—
1.50	600	35,000	19	Chl.	—	—
2.00	600	35,000	19	Chl.	—	—
0	620	40,000	0.2	Talc., Fors.	—	—
0.25	620	40,000	0.2	Fors., Bru., Talc, Spin.	—	—
0.50	620	40,000	0.2	Fors., Serp.	7.220 Å	—
0.75	620	40,000	0.2	Serp., Fors., Talc	7.176 Å	10%
1.00	620	40,000	0.2	Serp.	7.140 Å	25%
1.50	620	40,000	0.2	Serp.	7.084 Å	85%
2.00	620	40,000	0.2	Serp., Spin.	7.060 Å	100%
0	620	50,000	0.4	Talc, Fors.	—	—
0.25	620	50,000	0.4	Fors., Bru., Spin.	—	—
0.50	620	50,000	0.4	Fors., Bru.	7.186 Å	0%
0.75	620	50,000	0.4	Serp., Fors.	7.180 Å	5%
1.00	620	50,000	0.4	Serp.	7.134 Å	35%
1.50	620	50,000	0.4	Serp.	7.076 Å	90%
2.00	620	50,000	0.4	Serp., Spin.	7.068 Å	100%

TABLE 1 (*continued*)

Comp.	Temp. ° C.	Pres. p.s.i.	Time days	Phases present	c_0(Å)	% 6-layer
0	400	35,000	16	Serp., Bru.	7.308 Å	—
0.75	400	35,000	16	Serp., Fors.	7.202 Å	5%
1.00	400	35,000	16	Serp.	7.140 Å	25%
1.50	400	35,000	16	Serp.	7.082 Å	95%
2.00	400	35,000	16	Serp., Spin.	7.040 Å	75%
0	400	56,000	19	Serp., Fors., Bru.	—	—
0.75	400	56,000	19	Serp.	—	—
1.00	400	56,000	19	Serp., l. Bru.	—	—
1.50	400	56,000	19	Serp.	—	—
2.00	400	56,000	19	Serp., l. Spin.	—	—
1.00	600	20,000	12 min.	Serp.	—	—
1.00	600	25,000	15 min.	Serp.	—	—
1.00	600	40,000	20 min.	Serp.	—	—
1.00	600	40,000	60 min.	Serp.	—	—
1.00	600	40,000	120 min.	Serp.	—	—
1.00	600	40,000	240 min.	Serp.	—	—
1.00	600	40,000	960 min.	Serp.	—	—
1.00	600	40,000	0.75	Serp.	—	—
1.00	600	40,000	1	Serp.	—	—
1.00	600	40,000	2	Serp., Chl.	—	—
1.00	600	40,000	4	Chl., Serp.	—	—

Chl.—Chlorite, Cor.—Corundum, Bru.—Brucite, Fors.—Forsterite, Serp.—Serpentine, Spin.—Spinel, l.—little.

The other two polytypic varieties are shown by electron micrography to be platy. One which is produced in the low aluminum compositions (x small) can be indexed on the basis of a 1-layer ortho cell (Table 2) and shows much disorder in the b direction. The other is produced in the high aluminum compositions (x large) and can be indexed on the basis of a 6-layer ortho cell (Table 3). The two structures occur together in the medium aluminum compositions.

The cell parameters of the two platy structures show a progressive decrease as x increases (see Table 1). The amount of the 6-layer structure produced increases slightly in relation to the 1-layer as the hydrothermal pressure is increased and further, the basal spacing decreases with increased hydrothermal pressure. The two platy structures must be closely interrelated when they occur together, since despite the different conditions of formation and related change in parameters of the different specimens examined, the x-ray reflections common to the two structures are never resolved into two components or even broadened. The interatomic distances must therefore be almost the same in the two structures. The findings are summarized in Fig. 1.

TABLE 2. LATTICE SPACINGS, INDICES AND INTENSITIES FOR 1-LAYER ORTHO SERPENTINE

d, Å camera	*d*, Å diffractometer	*d*, Å calc.	I/I_0	*hkl*
7.22	7.25	7.25	60	001
4.61	4.61	4.62	20	020
3.89	3.91	3.90	5	021
3.617	3.619	3.624	60	002
2.659	2.655	2.669	5	200
2.504	2.503	2.505	100	201
	2.415	2.416	10	003
2.148	2.148	2.149	35	202
	1.807	1.812	5	004
1.791	1.788	1.791	15	203
1.745	1.744	1.747	5	310
1.543	1.541	1.541	25	060
1.510	1.507	1.507	20	061
1.497	1.496	1.499	15	204
1.447	1.448	1.450	5	005
1.420	1.418	1.418	5	062
1.332	1.329	1.334	5	400
1.313	1.312	1.312	10	401
1.299	1.299	1.299	5	063
1.272	1.274	1.274	5	205
1.253	1.254	1.252	5	402
1.168	1.163		5	

Specimen composition 21 $MgO.3Al_2O_3.13SiO_2$ treated hydrothermally for 41 days at 450° C. and 15,000 psi.

Cell parameters $a=5.338$ Å, $b=9.245$ Å, $c=7.249$ Å, (CuKα radiation 1.54178 Å).

THE PROCESS OF CRYSTALLIZATION OF A GEL

The growth of crystallization of a gel with composition $x=1$, treated at 600° C. and 40,000 p.s.i. for times varying from 10 min to several days has been studied. Under the conditions employed, a gel should produce a chlorite when stability is reached and this is the product after several days treatment. However, after several hours the product is not a chlorite in any state of crystallization but a mixture of 1- and 6-layer serpentines such as would be expected by treating this composition at temperatures less than 500° C. The increase in crystallization is rapid and after about 20 minutes the pattern given by a mixture of 1- and 6-layer serpentines can be recognized although the reflections are broad. After about 50 hours the reflections of a well-crystallized serpentine mixture begin to decrease in intensity and those of a well-crystallized chlorite to appear. From the first appearance of the serpentine reflections

TABLE 3. LATTICE SPACINGS, INDICES AND INTENSITIES OF 6-LAYER ORTHO SERPENTINE

d, Å Camera	*d*, Å Diffractometer	*d*, Å calc.	I/I_0	*hkl*
7.08	7.09	7.10	100	006
4.59	4.59	4.597, 4.570	35	020, 021
4.493	4.511	4.493	5	022
4.212	4.236	4.221	5	024
3.842	3.857	3.859	5	026
	3.658	3.669	5	027
3.544	3.551	3.552	100	00, 12
	3.474	3.480	5	028
3.289		3.299	5	029
3.127		3.125	5	02, 10
2.816		2.811	5	02, 12
	2.655	2.654	15	200
2.635	2.635	2.634	55	202
	2.613	2.609	25	203
2.571	2.576	2.575	40	204
2.531	2.534	2.534	15	205
2.486	2.487	2.486	35	206
	2.429	2.433	15	207
2.379	2.377	2.375	80	208
2.315	2.315	2.315	10	209
2.250	2.254	2.253	15	20, 10
2.126	2.125	2.126	5	20, 12
2.001	2.001	2.001	30	20, 14
1.937	1.939	1.940	10	20, 15
1.881	1.881	1.880	5	20, 16
1.769	1.768	1.767	5	20, 18
1.735	1.735	1.737, 1.736, 1.731	5	310, 311, 312
1.661	1.662	1.662	15	20, 20
1.608	1.609	1.611	5	20, 21
1.562	1.561	1.561, 1.565	10	31, 12, 20, 22
1.533	1.534	1.532	65	060
1.500	1.499	1.498	10	066
1.470	1.474	1.472, 1.476	5	068, 20, 24
	1.422	1.421	5	00, 12
1.407	1.408	1.407	10	06, 12
	1.392	1.395	5	20, 26
1.352	1.352		5	
1.321	1.325	1.327	10	400
	1.318		10	
1.287		1.286	10	06, 18
1.269			5	

Specimen of composition 9 $MgO.3Al_2O_3.5SiO_2$ treated hydrothermally for 41 days at 450° C. and 15,000 psi.

Cell parameters $a=5.308$ Å; $b=9.193$ Å; $c=42.62$ Å (CuKα radiation 1.54178 Å).

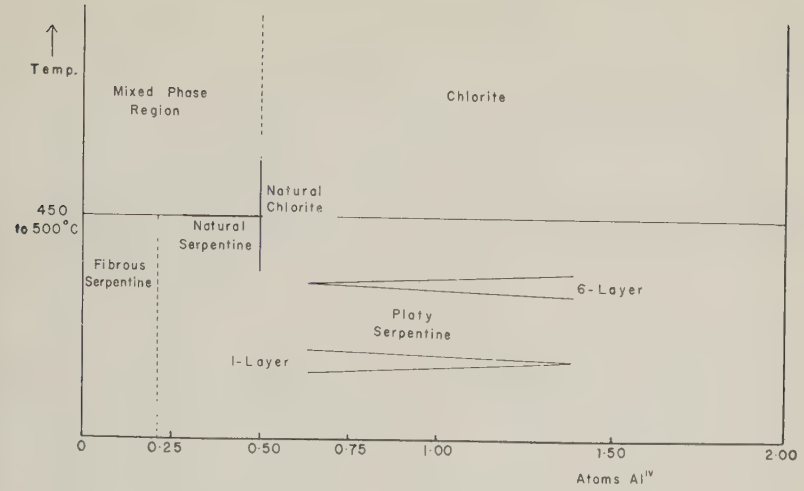

FIG. 1. The relation of the phases found.

to their complete disappearance, the relative amounts of 1- and 6-layer materials remain fixed.

COMPARISON OF THE SYNTHETIC MINERALS WITH THEIR NATURAL EQUIVALENTS

The x-ray powder diagrams of the synthetic chlorites appear to be essentially identical with those of natural chlorites. Comparison of careful measurements of the basal spacings of the natural and the synthetic specimens indicate the difference shown in Fig. 2.

The x-ray diagrams of the fibrous serpentines appear to be identical with the corresponding natural chrysotiles examined in detail by Whittaker and Zussman (1956). The electron micrographs, however, show the peculiar cone-in-cone effect (Bates, Sand, and Mink, 1950), which has not been noticed in natural specimens.

Several 1-layer specimens of platy serpentines were also described by Whittaker and Zussman (1956) and called lizardites. These appear to be identical with the synthetic 1-layer serpentines. It appears that two types of 6-layer structure exist, one which approximates to a 3-layer cell with hkl, $l=2n$ usually more intense than $l=2n\pm1$ (6(3) layer structure), and one which approximates to a 2-layer cell with hkl, $l=3n$, usually more intense than $l=3n\pm1$ (6(2) layer structure). The 6(3) layer structure is found in the synthetic specimens investigated. The 6(2) layer structure has been produced hydrothermally in the MgO-GeO_2-H_2O system (Roy and Roy 1954) and has been found naturally (see Brindley and von Knorring, 1954, and Zussman and Brindley, 1957). It approxi-

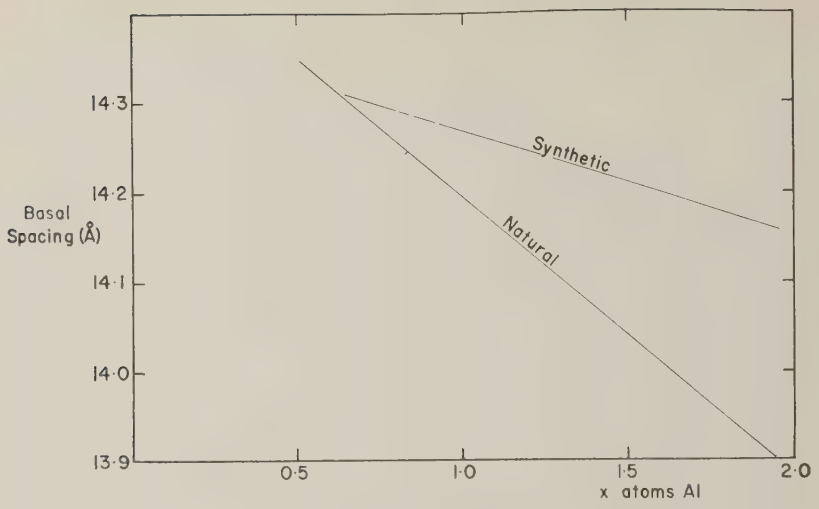

FIG. 2. The variation of the basal spacing of chlorites with composition. (The curve for the natural chlorites is taken from Brindley and Gillery, 1956.)

mates closely the amesite structure reported by Brindley, Oughton and Youell (1951) and by Steinfink and Brunton (1956), amesite having the ideal composition $x = 2.0$. S. W. Bailey, Department of Geology, University of Wisconsin kindly supplied films of four natural serpentines found in rock drillings and two of these showed the 6(3)-layer structure and the other two showed the 6(2)-layer structure. Both were mixed with the 1-layer structure.

DISCUSSION

At first sight temperature appears to control whether a chlorite or a serpentine is produced. It may be, however, that serpentines of a possible chlorite composition are metastable. This is suggested by the observations on the crystallization of the gel. Chlorites are formed hydrothermally by way of a serpentine structure and if this process does not reach stability a serpentine will result. Stability takes several days to attain even at 600° C. so that below 500° C. it may take a much longer time than has been allowed in this series of experiments. Hence the serpentines of a possible chlorite composition which appear to be stable below 500° C. may be metastable with respect to chlorite. This point of view may be correlated with the rarity of serpentines with an appreciable aluminum content in nature. An examination of natural chlorite and serpentine analyses indicates that their chemical compositions rarely overlap. The boundary of Al substituted for 4Si atoms is about 0.5 atoms or about 10% Al_2O_3 in the chemical analysis.

The difference in the basal-spacing versus composition curves given by natural and synthetic chlorites could be due to an uneven distribution of cations in the two types of octahedral layer in the latter. If the tetrahedral charge is more than half balanced in the 'talc' octahedral layer, the interlayer charge and the resultant interlayer ionic bonding decrease, hence the basal spacing would increase. This situation existing in the synthetic specimens would explain their generally larger basal spacing. This hypothesis is supported by the tendency of the two curves to converge at the lower Al content where the effect would be expected to be smaller.

It is evident that the amount of Al present in the gel has an overruling effect on the serpentine polytype produced. The formation of fibers rather than plates has been ascribed to the misfit between the octahedral and tetrahedral type layers (See Bates, Hildebrand, and Swineford, 1950, and Roy and Roy, 1954), but the aluminum also controls the amount of 6-layer material present which does not appear to be affected by time or temperature and only slightly by pressure. No explanation can be offered for this observation, though the answer could probably be given if the exact structure of the polytypes were known. The decrease in basal spacing with aluminum content is easily explained by the way the charge on the serpentine layers changes with the substitution of Al. The surplus charge caused by the substitution of Al in the octahedral part of the serpentine layers is balanced by the corresponding substitution of Al for Si in the tetrahedral part. Thus the octahedral part acquires a positive charge and the tetrahedral a negative charge and the layer as a whole is neutral. The layer surfaces which face each other have opposite charges and this provides a force of attraction between them which increases with increasing aluminum content. Hence the basal spacing decreases with increasing aluminum content.

The increased amount of 6-layer structure in relation to the amount of 1-layer structure and the decrease of the basal spacing, both with increase in hydrothermal pressure of formation can be explained by supposing that the 6-layer structure occupies a slightly smaller volume than the 1-layer structure. Increase in the pressure of formation will constrain the system and the equilibrium will move in a direction which will tend to occupy a smaller volume. This can be done by the production of more 6-layer material which will also decrease the basal spacing.

Since the difference in spacing is never noticeable in the mixtures, the difference must be either very small or the mixture must be on almost unit cell scale when the *x*-ray spacing will be a compromise between the two individual spacings.

The important conclusions to be drawn from the study are that:

1. The temperature controls the mineral family produced.
2. The composition is the predominant factor in determining the polytype.

Acknowledgments

This investigation forms part of A.P.I. Project 55 sponsored by the American Petroleum Institute.

References

Bates, T. F., Hildebrand, F. A., and Swineford, A., (1950), *Am. Mineral.*, **35,** 463–484.
Bates, T. F., Sand, L. B., and Mink, J. F., (1950), *Science,* **111,** 512–513.
Brindley, G. W., and Gillery, F. H., (1956), *Am. Mineral.*, **41,** 169–186.
Brindley, G. W., Oughton, B. M., and Youell, R. F., (1951), *Acta Cryst.*, **4,** 552–557.
Brindley, G. W., and von Knorring, O., (1954), *Am. Mineral.*, **39,** 794–804.
Nagy, B., and Faust, G. R., (1956), *Am. Mineral.*, **41,** 817–838.
Nelson, B. W., and Roy, R., (1954), in Clays and Clay Minerals, *Nat. Acad. Sci.—Nat. Res. Council Publ.* **327,** 335–348.
Roy, R., (1956), *Jour. Amer. Cer. Soc.*, **39,** 145–146.
Roy, R., and Osborn, E. F., (1952), *Econ. Geol.*, **47,** 717–721.
Roy, D. M., and Roy, R., (1954), *Am. Mineral.*, **39,** 957–975.
Steinfink, H., and Brunton, G., (1956), *Acta Cryst.*, **9,** 487–492.
Whittaker, E. J. W., and Zussman, J., (1956), *Min. Mag.*, **31,** 107–126.
Yoder, H. S., (1952), *Amer. J. Sci.*, **Bowen Volume,** 569–627.
Zussman, J., and Brindley, G. W., (1957), *Am. Mineral.*, **42,** 666–670.

Manuscript received May 31, 1958

THE AMERICAN MINERALOGIST, VOL. 44, JANUARY-FEBRUARY, 1959

ORIENTED PENETRATION OF IONIC COMPOUNDS BETWEEN THE SILICATE LAYERS OF HALLOYSITE

Koji Wada, *Kyushu University, Fukuoka, Japan.*

Abstract

Drying hydrated halloysite from certain salt solutions results in reversible lattice expansion ranging from 5 to 45 per cent of the basal spacing. The reaction occurred with K^+, NH_4^+, Rb^+ and Cs^+, whose ionic diameters are of the order of 2.7 Å or more, whereas smaller cations such as Li^+ and Na^+, and divalent cations Mg, Ca and Ba gave no evidence of the reaction. The increase in the basal spacing of halloysite is clearly related to the kind of anion. There was no evidence of this type of expansion for montmorillonite. About 200 to 300 m. mols. of the ionic compound were estimated to be retained on the basal plane surfaces per 100 gm. of the air-dried clay.

It is concluded that the cation and anion penetrate between the silicate layers of halloysite, probably forming a unimolecular layer of the ionic compound, replacing the interlayer water.

Introduction

The phenomenon described here is concerned with oriented penetration of ionic compounds between the silicate layers of halloysite, resulting in reversible one-dimensional swelling. Similar phenomena are known with halloysite and some minerals of the montmorillonite group in the formation of interlayer complexes with certain organic and inorganic liquids. Although a type of complex of montmorillonite with inorganic molecules, e.g., $Mt^-NH_4^+(AgCl)$ was reported by Bloch (2); a chlorite-like mineral, $Mt^-NH_4^+Mg(OH)_2$ was obtained on treating Mg-montmorillonite with NH_4OH by Caillère and Hénin (3), relatively little is known of the oriented penetration of ionic compounds between the layers of clay minerals. It is suggested, however, from a study by the author on the reaction of halloysite with phosphates (10), that $(NH_4)_2HPO_4$ orients between the silicate layers of halloysite and forms a type of interlayer complex.

The first aim of the present study is to show that this type of reaction is possible between halloysite and some ionic compounds under certain conditions. The second is to study the factors affecting the reactions, to determine the stability of the resulting complexes and to assess the mechanism of the reaction. The technique used in this study is direct *x*-ray examination of the air-dried specimens obtained by treating clay minerals with salt solutions, without removing the excess salt.

Materials and Methods

The clay minerals employed were hydrated halloysite from Yoake, Oita, Japan (1), and montmorillonite from Osage, Wyoming, U.S.A. One-half gram samples of the clay (<150 mesh, saturated predominantly with Na^+) were soaked in 1 ml. H_2O with 0.5 to 2.5 m. mols of an ap-

propriate salt, allowed to dry at 30° C. (R.H. 36.5 to 60%) for several days, and ground in an agate mortar for *x*-ray analysis. Some specimens were subjected to ethylene glycol (E.G.) treatment; wetting with E.G. for 24 hours and heating at 100° C. for an appropriate time to remove the excess liquid.

X-ray diffraction patterns were obtained using Co radiation with Fe filter and a camera with a diameter of 80 mm., and employing a fine rod of the specimen in an *oblate* tube. Reported spacings were probably accurate to ±0.1 Å in the *d*-values higher than 10 Å, and intensity was measured visually.

Experimental Results

Sodium, potassium, and ammonium chloride, nitrate, sulfate, phosphate, and acetate were tentatively divided into the following two groups on the basis of the effect of the treatment on the 10.1 Å spacing of hydrated halloysite (Table 1):

(1) The treatment of the first group with the salts did not affect the basal spacing of hydrated halloysite. After heating at 100° C., the basal spacing of halloysite was reduced to the 7.2–7.4 Å spacing of metahalloysite.

(2) The treatment of the second group with the salts clearly affected the basal spacing of hydrated halloysite, and after heating at 100° C. the basal spacing of halloysite was not reduced to 7.2–7.4 Å.

The interaction of halloysite with the salts belonging to the second group was shown by alteration in spacing between the layers and in the relative intensities of higher order basal reflections, excepting for the KCl and KNO_3 treated halloysites, where the basal spacing of hydrated halloysite was not significantly affected (Table 2 and 3). No essential alteration was found apart from these basal reflections.*

Table 1. Effect of the Treatment with Salts on the Basal Spacing of Hydrated Halloysite

(5.0 m.mols of the salt per gm. of clay)

Cation	Anion					
	Cl	NO_3	SO_4	H_2PO_4	HPO_4	CH_3COO
Na	−	−	−	−	−	−
K	+	+	−	−	+	+
NH_4	+	+	+	−	+	+

* Recently it has been shown by *x*-ray diffractometer methods that (*hk*) bands of halloysite are a little affected as the result of the reaction in some cases (unpublished).

On heating at 100° C., the basal reflections of all specimens treated with these salts, except for NH_4CH_3COO which sublimates at this temperature, were either not affected at all or merely diffused (Table 2 and 3). In either case the 7.2–7.4 Å spacing corresponding to that of metahalloysite was not shown. On the other hand, on washing with excess water, the 10.1 Å spacing of hydrated halloysite was readily restored in every specimen.

Factors Affecting the Reaction

(*a*) *Kind of cation*

No alteration in the basal spacing of halloysite was found with the specimens treated with the sodium salts in contrast to those with the potassium and ammonium salts (Table 1). The similarity in the behavior of some of the latter is noted in view of the similarity of the ionic radii of K^+ and NH_4^+. This suggests the importance of the size of the cation in relation to the structure of the interlayer surface of halloysite in allowing the reaction, although the absence of the reaction with some ammonium and potassium salts should also be noted.

Table 2. *X*-Ray Diffraction Patterns of Halloysite Treated with Potassium Salts

(5.0 m.mols of the salt per gm. of clay)

(00*l*) or (*hk*)	Salt									
	None		KCl		KNO_3		K_2HPO_4		KCH_3COO	
	d	I	*d*	I	*d*	I	*d*	I	*d*	I
001	10.1	vs	10.2	s	10.1	s	13.3	m	14.3	vs
002							6.9	bv	7.2	bv
02, 11	4.42	s	4.38	ms	4.38	ms	4.42	w	4.33	mw
003	3.36	m	3.46	vw	3.38	bv				
004									3.51	mw
20, 13	2.56	m	2.55	w	2.53	w	2.55	vw	2.55	mw
	2.34	vw	2.34	bv			2.34	bv	2.34	bv
04, 22	2.23	vw	2.20	bv	2.16	bv	2.21	bv	2.23	vw
24, 31, 15	1.68	bv	1.69	bv	1.68	bv	1.67	bv	1.67	vw
	1.64	vw	1.65	bv	1.65	bv	1.64	bv	1.64	vw
33, 06	1.48	ms	1.48	w	1.48	w	1.48	mw	1.48	m
001*	7.4	m	10.1	s	10.1	w	diffuse		14.3	vs
					7.2	w				

d in Å.

Reflections due to the presence of the excess salt were omitted.

* (001) reflection after heating at 100° C.

TABLE 3. *X*-RAY DIFFRACTION PATTERNS OF HALLOYSITE TREATED WITH AMMONIUM SALTS

(5.0 m.mols of the salt per gm of clay)

(00*l*) or (*hk*)	Salt									
	NH_4Cl		NH_4NO_3		$(NH_4)_2HPO_4$		$(NH_4)_2SO_4$		NH_4CH_3COO	
	d	I	*d*	I	*d*	I	*d*	I	*d*	I
001	10.5	vs	11.6	vs	13.2	vs	13.4	s	14.4	vs
002					6.65	w	7.1	bv	7.2	w
02, 11	4.43	mw	4.43	s	4.43	s	4.45	vs*	4.45	s
003	3.51	m	3.87	m						
004									3.57	w
20, 13	2.57	w	2.58	w	2.58	w*	2.56	vw*	2.58	w
			2.34	vw	2.30	bv*	2.34	vw*	2.36	bv
04, 22	2.23	vw	2.22	vw			2.20	vw*	2.23	vw
24, 31, 15	1.69	bv	1.68	bv	1.69	bv	1.69	bv	1.69	bv
	1.65	bv	1.64	bv	1.64	bv	1.64	bv	1.64	bv
33, 06	1.48	m	1.48	w	1.48	m	1.48	m	1.48	mw
001†	10.5	vs	11.6	vs	diffuse		diffuse		7.4	m

d in Å.

Reflections due to the presence of the excess salt were omitted.

* Reflection due to the presence of the excess salt was superposed.

† (001) reflection after heating at 100° C.

In order to clarify the relation of the size and the valence of the cation to the nature of the reaction, the following experiment with some alkali and alkaline earth chlorides, nitrates, and acetates was carried out. The specimens treated with the salts were placed in a desiccator over $CaCl_2$, heated at 100° C., washed with H_2O, air-dried, and then *x*-rayed. It is assumed that if the altered spacing is maintained on heating at 100° C., and the 10.1 Å spacing is readily obtained by washing with H_2O as was shown above with some specimens, the resulting 10.1 Å spacing may be considered an evidence that the reaction occurred, and the 7.2–7.4 Å spacing that it did not (Table 4). This procedure was adopted because of difficulties in obtaining clear *x*-ray diffraction patterns with some treated specimens, due to the deliquescent nature of some salts and the strong *x*-ray absorption of some cations.

The occurrence of the reaction seems to depend on the size of the cation involved. No reaction on halloysite was found with any salt involving a cation smaller than Na^+. A limiting value of ionic size might

be estimated at approximately that of K^+. This is of interest in relation to the size of the cavity in the oxygen network of the silicate layer, because K^+ is assumed to fit into this cavity. Thus, so far as the monovalent cation is concerned, the reaction seems to occur only with the salt involving a cation not falling into the cavity of the oxygen network, suggesting a positive role of the cation for allowing the reaction. That is, the geometrical fitting of the cation into the surface structure of the oxygen layer of clay minerals seems to have prime importance in the reaction. The salts involving the divalent cation give no evidence of the reaction,

Table 4. Effect of the Treatment with Chlorides, Nitrates, and Acetates of Alkali and Alkaline Earth Metals on the Basal Spacing of Halloysite

(5.0 m.mols of salt per gm. of clay)

Anion	Cation								
	Li	Na	K	NH_4	Rb	Cs	Mg	Ca	Ba
Cl	−	−	+	+	+	+	−	−	−
NO_3	−	−	+	+			−	−	−
CH_3COO		−	+	+				−	−

in spite of the similarity of Ba^{++} to K^+ in ionic radii. These limitations in size and valency of cation are noted from the viewpoint of the mechanism of the reaction.

Observed differences in the behavior between some corresponding potassium and ammonium salts—generally the latter are clearly liable to induce the reaction—would be accounted for by either the minor difference in the geometry of K^+ and NH_4^+, or the effect of hydrogen bonding that might be assumed between the H atom of NH_4 and the oxygen atom of the silicate layer. Also, it would be considered that the difference in solubility is of importance.

(*b*) *Kind of anion*

The variation in the basal spacing of halloysite between the specimens treated with some ammonium salts, or those treated with the potassium salts, and the similarity between the specimens treated with some corresponding ammonium and potassium salts indicate clearly the existence of anions between the silicate layers (Tables 2 and 3). Here, again, the absence of the reaction with some ammonium and potassium salts should be noted, because the occurrence is supposed to be limited by the type

of anion involved in the reaction. However, there is no evidence to show the specific relation between the type of anion and the absence of the reaction or to suggest the positive role of the anion for causing the reaction, as was shown with the cation.

The effect on the basal spacing of halloysite treated with ammonium salts of different anions is shown in Table 5. The resulting variation in basal spacing may be due to the difference in the geometry of the anions. The validity of this view is also supported by the striking similarity in the basal spacing of halloysite treated with phosphate, sulfate, and ar-

Table 5. Basal Spacing of Halloysite Treated with Ammonium Salts

Anion	Basal spacing in Å	Δ-value* in Å
Without treatment	10.1	2.9
H_2PO_4	10.1	2.9
$(COO)_2$	10.1	2.9
Cl	10.5	3.3
Br	10.6	3.4
NO_3	11.6	4.4
HCOO	11.6	4.4
$HC_6H_5O_7$	13.0	5.8
$HAsO_4$	13.1	5.9
HSO_4	13.2	6.0
HPO_4	13.2	6.0
SO_4	13.4	6.2
CH_3COO	14.4	7.2

* Δ-value = basal spacing − 7.2 Å.

senate, suggesting that the size and shape of the tetrahedra affect the basal spacing of the treated halloysite.

While HPO_4^{--} and CH_3COO^- afford practically the same increments of basal spacing associated either with K^+ or NH_4^+, Cl^- and NO_3^- do not, although the reason for this is not clear at present. Rather small clearance space for the KCl and KNO_3 treated halloysites is of interest, because it raises the question whether the anions penetrate between the silicate layers.

(c) Amount of salt

Up to a certain point, the basal spacing obtained with the treated specimens increased with the amount of the added salt, but above this,

showed a definite value (Fig. 1). The shift of the (001) reflection position followed approximately what would be expected from random interlayer stratification. That is, the movement of the position of the (001) reflection relates to the separation in basal spacing between the reaction product and the original halloysite. When the separation is smaller, such as in the case of hydrated halloysite and NH_4Cl, the reflection position moves almost linearly; widely separated ones, as NH_4NO_3 and NH_4HCOO, show S-shaped curves. When they are far apart, $(NH_4)_2HPO_4$ and $(NH_4)_2HC_6H_5O_7$, the reflection position follows a markedly S-shaped curve with a steep central portion, where the reflection itself becomes very diffuse, and an almost horizontal end portion. Finally the separation becomes still greater, and with KCH_3COO the two reflections cease to form a pair and become isolated. This suggests the random interlayer stratification of the layers with a hydrated halloysite spacing and one with a unique spacing of the reaction product.

The rate of the salt addition required for the development of a unique spacing of the reaction product is 300 to 400 m. mols per 100 gm. of clay and seems not to depend so critically on the kind of the salt (Fig. 1). The reflections due to the excess salt were barely perceptible unless the salt was added at the above rate or more. The rate was found to be 50 to 100 m. mols per 100 gm. of clay in the corresponding experiment with the baked clay. Thus, it might be estimated roughly that 200 to 300 m. mols or more of the salt per 100 gm. of clay participates in the reaction. Since the cation exchange capacity of this clay is about 20 m.e. per 100 gm. of clay, the rather high figure of 200 to 300 m. mols is significant from the viewpoint of the forces exerted on the interlayer surface of halloysite.

(d) Kind of clay minerals

In view of a common peculiarity in the crystal structure in connection with interlayer swelling, it was of interest to determine whether montmorillonite also gives the same reaction. No evidence of variation in basal spacing was found with montmorillonite treated with some ammonium salts in contrast with halloysite (Table 6). The rather uniform 12.8 Å spacing may be attributed to the presence of the interlayer NH_4^+ and water. The difference between montmorillonite and halloysite is ascribed to the difference in the charge density on the interlayer surface and the atomic configuration of the exposed silicate layer. The higher interlayer charge and the lack of the exposed hydroxyl layer of the former would induce a stable configuration of NH_4^+ and a contraction of the silicate layers, that probably hinder further absorption of cation and anion With halloysite, on the contrary, the low interlayer charge and the existence of the exposed oxygen and hydroxyl layers seem to favor the

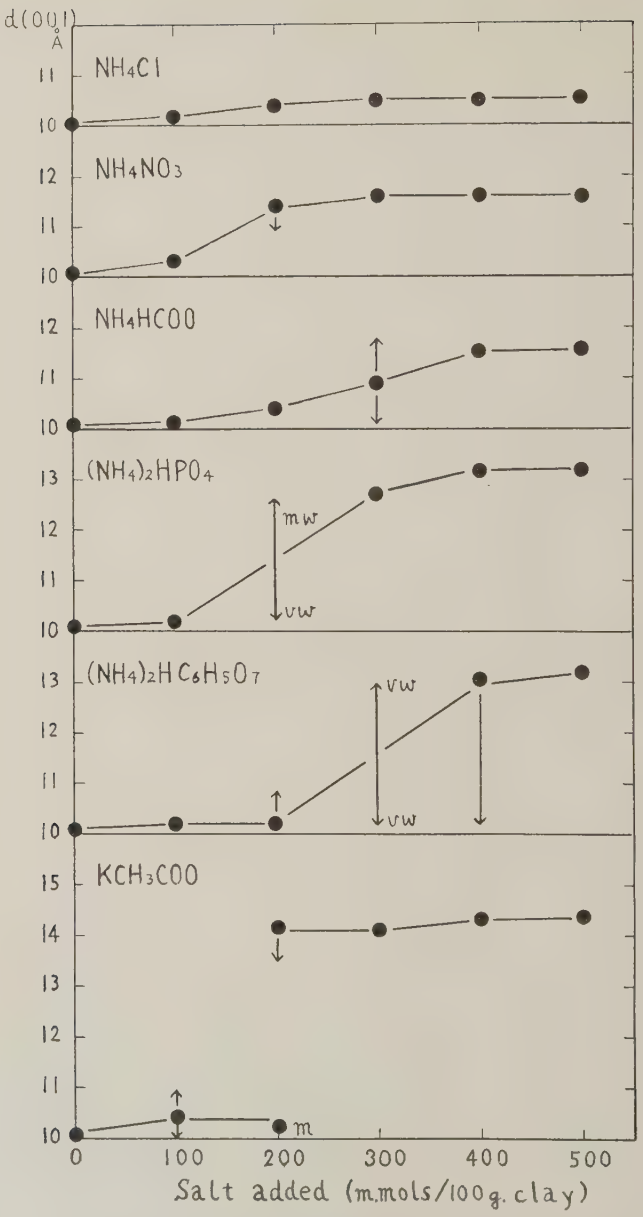

FIG. 1. Variation of basal spacing of halloysite with the amount of salt added.

Table 6. Basal Spacing of Montmorillonite and Halloysite Treated with Ammonium Salts

(5.0 m.mols of salt per gm. of clay) in Å

Mineral	Anion				
	Cl	NO_3	HPO_4	SO_4	CH_3COO
Montmorillonite	12.7	13.8 ~11.7	12.8	12.8	12.8
Halloysite	10.5	11.6	13.2	13.4	14.4

reaction. Besides this, a possible weak polarizability of the silicate layer itself would support the reaction.

Stability of the Reaction Products

The reversibility of the reaction is ascertained from the ready restoration of the 10.1 Å spacing of hydrated halloysite by washing the reaction product with water. It is suggested that the progress of the reaction depends on the moisture condition of the salt-halloysite system. The reaction may occur appreciably only after some diminution of moisture in the system.

In connection with this, the effect of the following tests of dry intimate mixing of hydrated halloysite and salt on the basal spacing of halloysite is of interest. On grinding hydrated halloysite with NH_4Cl, NH_4NO_3, NH_4HCOO, or KCH_3COO in an agate mortar for 5 to 10 minutes, the resulting alteration in the basal spacing of halloysite was identical with that observed previously by drying from these salt solutions (Table 7).

Table 7. Relative Stability of the Reaction Product Obtained by Treating Halloysite with Salts

Salt	Basal spacing of halloysite dried from salt solution in Å	Basal spacing of halloysite after dry mixing in Å	Basal spacing of the reaction product after E.G. treatment in Å
NH_4Cl	10.5	10.5	10.5
NH_4NO_3	11.6	11.6	11.6
NH_4HCOO	11.6	11.6	11.1
NH_4CH_3COO	14.4	—	11.1
KCH_3COO	14.3	14.4	14.3
$(NH_4)_2SO_4$	13.4	Not clear	11.1
$(NH_4)_2HPO_4$	13.2	Not clear	11.1

However, with $(NH_4)_2HPO_4$ and $(NH_4)_2SO_4$, no clear basal reflection was obtained on this treatment, suggesting some difference in the stability of the reaction product.

As regards the relative stability of the reaction product, the result of the E.G. treatment shows a tendency similar to that observed above. Under this experimental condition, the resulting spacing may be considered a manifestation of the stability of the reaction product relative to the E.G.-halloysite complex. That is, the NH_4Cl, NH_4NO_3, or KCH_3COO treated halloysite each showed its own spacing after this treatment (Table 7). On the contrary, with $(NH_4)_2HPO_4$ or $(NH_4)_2SO_4$, the resulting spacings were identical with that of the E.G.-halloysite complex, indicating interlayer penetration of E.G. molecules, because these treated halloysites have shown only diffuse basal reflections on heating without E.G. at 100° C. (Table 3). Although the 11.1 Å spacing of the E.G.-halloysite complex was observed with NH_4HCOO and NH_4CH_3COO, it could be interpreted as the result of the sublimation of these salts at this temperature, not as the manifestation of their relative stability to the E.G.-halloysite complex.

Discussion

Several possible explanations for the alteration of hydrated halloysite observed in *x*-ray patterns may be listed as follows:

a. Cation exchange reaction between halloysite and salt.
b. Anion exchange reaction between halloysite and salt.
c. Chemical combination of salt with halloysite, resulting in a breakdown of halloysite, as has been shown by several workers for the phosphate fixation by clay minerals (4, 5, 6, 7, 9).
d. Oriented penetration of neutral ionic compounds between the silicate layers of halloysite resulting in a type of the interlayer complex.

Explanations (a) and (b) would not account for the dependence of the reaction on the kind of cation and anion. Explanation (c) could be applied to the alteration in *x*-ray pattern as the result of the reaction of halloysite with ammonium phosphate in acidic solution, as was found by Stout (9) and by the present author in his preceding study (10). However, it seems very difficult to account for many results obtained here, particularly for the following:

(1) The alteration in *x*-ray pattern was found only on (00*l*) reflections of halloysite, essentially not on (*hk*) bands.
(2) There was no specific relation between the type of anion and the

reaction, that is expected from the viewpoint of the breakdown of the silicate layers.

(3) On washing with excess water, the complete x-ray pattern of the original halloysite, and only that, reappeared.

(4) Merely by intimately mixing halloysite and salt, similar alteration in x-ray pattern was found with certain salts.

The results obtained, including the ones just described, are overwhelmingly in favor of the oriented penetration of neutral ionic compounds between the silicate layers.

The limitation in geometry and valence of cation associated with those of the anion for the reaction may be interpreted in terms of the stability of the resulting configuration of the salt layer at the interlayer region. The difference between montmorillonite and halloysite can also be accounted for by this supposition

The increment in basal spacing suggests two-dimensional one or two molecular salt layer formation as was shown in Table 4. If the cation is trapped in the cavity of the oxygen network at the interlayer surface, as is presupposed from the geometrical fitting into that cavity, the position of the anion which orients to balance the excess positive charge, and consequently the configuration of the salt layer would also be fixed to the silicate layer of halloysite, indicating that the orienting force is sufficiently strong to induce the polymorphism of the salt.

Although the obtained spacings give no conclusive evidence on the disposition of the anion, some information would be obtained (Table 5). For example, a packing effect of Cl^- and Br^- into the hollows of the interlayer surface is suggested from comparison of the Δ-value for each NH_4Cl- and NH_4Br-halloysite complex (3.3 and 3.4 Å) with the diameter of each anion (3.6 and 3.9 Å). Also, since the Δ-value is obviously too high for a single anion layer formation of the tetrahedral type of anion ($\Delta = 13.4 \sim 13.4 - 7.2 = 6.0 \sim 6.2$ Å, the height of the tetrahedra = 4.9 Å), a triple cation-anion-cation layer formation is likely to occur, though the spacing of NH_4HSO_4-halloysite complex is not accounted for. The organic anion may dispose itself in some complicated manner. Further study is needed on this point.

It was estimated roughly that 200 to 300 m. mols or more of the salt orients onto 100 gm. of clay. The magnitude of this value is comparable with the theoretically expected value, 330 m. mols per 100 gm. of clay, assuming the formation of mono-molecular layer of the salt and the orientation of two molecules of the salt per unit cell of halloysite. Also, the random interlayer stratification of the layer with a hydrated halloy-

site spacing and one with a unique complex spacing was suggested, so that the salt is supposed to become regular within any one given interlayer region, rather than partially filling all the interlayer regions to an equal extent. This is also expected from the concept of the layer formation of the ionic compound.

If nearly 300 m. mols of the salt orients between the silicate layers, the interlayer water, or a part of it at least, should be replaced with the penetrating ions. Hence it might be considered from the view of the bond energy that the added stability of the system consisting of the halloysite, water, and salt, due to the salt halloysite bond formation, is greater than that due to the water-halloysite bond formation at least in the condition of air-drying . This also seems to be evident from the positive penetration of some salts, as the result of the intimate mixing in air-dry state.

It might be concluded from the experiments on the stability of the salt-halloysite complex, that the strength of the bond between the oriented salt and halloysite depends on the kind of the ionic compounds, particularly of the type of anion, suggesting the importance of the geometrical relationship between the interlayer material and the surface structure of clay minerals, and is much the same as that of the bond between water or E.G. and halloysite, in which the hydrogen bond is usually assumed to have prime importance. The small activation energy expected from this small bond energy agrees with the observed reversible complex formation occurring readily at normal temperature. The weak electrostatic forces may act between the ionic compound and the silicate layers of halloysite with a weak polarizability, as has been indicated by MacEwan for the formation of the interlayer complex between halloysite and some polar organic molecules (8), but the van der Waals forces may act mainly in the complex formation. Besides this, with ammonium salts, one may consider the effect of NH-O hydrogen bond formation.

Summary and Conclusion

Variation in the basal spacing of halloysite results from the interaction of halloysite with some K^+, NH_4^+, Rb^+, and Cs^+ salts. The alteration in *x*-ray pattern was found only in the (00*l*) reflections and was reversible. Although the increment in basal spacing varied with the type of anion, there was no specific relation between the type of anion and the occurrence of the reaction. The reaction has not been shown for montmorillonite. It is concluded that the neutral ionic compound penetrates and orients between the silicate layers of halloysite.

Through this mechanism, halloysite would be able to retain 200 to 300 m. mols of the ionic compound on the basal plane surfaces per 100 gm. of air-dried clay state, and it is probable that the interlayer water is re-

placed. The stability of the resulting complex may be determined by the geometry and valency of anion in combination with those of the cation. The geometrical fitting between the interlayer material and halloysite as substrate is of prime importance in this type of complex formation.

The observed phenomenon is important in that it presupposes a type of physical adsorption peculiar to the surface structure of clay minerals and to the combination of ion species in solution. The technique used in this work should permit more positive identification and characterization of hydrated halloysite with *x*-ray diffraction.

Acknowledgments

The author is greatly indebted to Dr. S. Aomine and to Dr. R. E. Grim for valuable suggestions, and for generous help in the preparation of this manuscript. The research was supported in part by a grant from the Science Research Fund of the Japanese Ministry of Education.

References

1. Aomine, S. and Higashi, T. (1956), Clay minerals of decomposed andesitic agglomeratic lava at Yoake. *Mineral. Jour.* (Japan), **1,** 278–289.
2. Bloch, J. M. (1954), Fixation des halogènures d'argent sur la montmorillonite. *Fourth Int. Congr. Soil Sci.*, **III,** 32–34.
3. Caillère, S. and Hénin, S. (1949), Experimental formation of chlorite from montmorillonite. *Min. Mag.*, **28,** 612–620.
4. Ensminger, L. R. (1948), The relationship between water lost and PO_4 adsorbed on phosphating clay minerals and soil colloids. *Soil Sci. Soc. Amer. Proc.*, **13,** 170–174.
5. Haseman, J. F., Brown, E. H., and Whitt, C. D. (1950), Some reaction of phosphate with clays and hydrous oxides of iron and aluminum. *Soil Sci.*, **70,** 257–271.
6. Kittrick, J. A. and Jackson, M. L. (1954), Electron microscope observations of the formation of aluminum phosphate crystals with kaolinite as the source of aluminum. *Science*, **120,** 508–509.
7. Kittrick, J. A. and Jackson, M. L. (1956), Electron microscope observations of the reaction of phosphate with minerals leading to a unified theory of phosphate fixation in soils. *J. Soil Sci.*, **7,** 81–89.
8. MacEwen, D. M. C. (1948), Complexes of clays with organic compounds. I. Complex formation between montmorillonite and halloysite and certain organic liquids. *Trans. Faraday Soc.*, **44,** 349–367.
9. Stout, P. R. (1939), Alterations in the crystal structure of clay minerals as a result of phosphate fixation. *Soil Sci. Soc. Amer. Proc.*, **4,** 177–182.
10. Wada, K. (1959), Reactions of phosphate with allophane and halloysite. *Soil Science*, in press.

THE NATURAL OCCURRENCE OF GALENA-CLAUSTHALITE SOLID SOLUTION SERIES*

ROBERT G. COLEMAN, *U. S. Geological Survey, Menlo Park, California.*

ABSTRACT

A study of the sulfides associated with the vanadium-uranium deposits of the Colorado Plateau has revealed that a complete natural solid solution series exists between galena (PbS) and clausthalite (PbSe). Twenty analyzed samples range in composition from 0.04 to 93.7 molecular per cent PbSe in PbS with a concomitant variation of the unit cell from 5.930 Å to 6.127 Å. A plot of these values using the $a_o = 5.936$ Å for PbS and $a_o = 6.140$ Å for PbSe indicates an almost straight line variation of the cell edge between galena and clausthalite. Mineragraphic and *x*-ray study shows these minerals to be true solid-solution phases; exsolution of one end member in the other was not found. Semiquantitative spectrographic analyses indicate that the minor elements in these sulfides are similar to those found in galena with some variations resulting from the environment of deposition.

INTRODUCTION

Recent studies (Coleman and Delevaux, 1957) of the sulfides associated with sedimentary-type uranium deposits from the western United States indicate that selenium is commonly present in the sulfide structures substituting for sulfur. A systematic study of these various sulfides shows that galena usually contains more selenium than the associated sulfides, particularly where these minerals have crystallized from selenium-rich solutions.

Earley (1950) has shown that a complete solid solution series, PbS-PbSe, can be produced by pyrosyntheses. The fusions were made at intervals of 20 atomic per cent between the end members, galena and clausthalite. A plot of the unit cell dimension against composition produces an almost linear variation illustrating that the two isostructural compounds could form a continuous series.

The presence of selenium has often been reported in galena (Fleischer, 1955); however, the combined analytical and *x*-ray data were insufficient to definitely establish the natural occurrence of the PbS-PbSe solid solution series.

Bergenfelt (1953) has reported 50 ppm to 1.5 per cent Se in galena from the Boliden mine, Sweden, but the unit cell was not determined on these samples. Heier (1953) has used the unit cell size of galena to determine its selenium content from Earley's synthetic data. He determined the molecular per cent of PbSe as 80, 79, and 93 per cent on three samples from Norway. Since chemical analyses were not made on Heier's samples, these may not be used to further illustrate the series as other elements may have been substituting in the PbS structure.

* Publication authorized by the Director, U. S. Geological Survey.

Within the collection of sulfides from the Colorado Plateau uranium-vanadium deposits analyzed for selenium it was found that 19 samples ranged in composition between galena and clausthalite. Fortunately, these specimens exhibited enough range in selenium content to illustrate the existence of a galena-clausthalite series in nature.

Location and Description of Samples

The majority of the galena-clausthalite samples were obtained from the vanadium deposits in the Entrada sandstone of Jurassic age (Table 1). In most of these layered deposits thin sulfide bands asymmetrically border the tabular ore bodies. These bands may be continuous along strike for several hundred feet.

The galena-clausthalite within the thin sulfide bands forms as interstitial grains concentrated in a thin zone to produce a continuous banding effect (Coleman and Delevaux, 1957). The bands are well developed in the Rifle and Garfield mines, Garfield County, Colorado, where the majority of the samples were obtained through the cooperation of R. P. Fischer and Theodore Botinelly, U. S. Geological Survey. Similar galena-clausthalite bands are developed in the Bear Creek mine, San Miguel County, and Good Hope mine, La Plata County, Colorado (Table 1).

The almost pure clausthalite was obtained by A. D. Weeks and Lee Eicher, U. S. Geological Survey, from the Corvusite mine, Grand County, Utah, a uranium-vanadium deposit in the Morrison formation of Jurassic age. Here the clausthalite formed a quarter-inch layer bordering an uranium-rich coalified log. The seleniferous galena, from the Darwin mine, California, was collected by Wayne E. Hall, U. S. Geological Survey.

Analytical Procedures

Each sample was treated in a similar manner in its purification. The rock containing the sulfide-selenide was crushed to pass through a 100-mesh sieve and concentrated by the use of a superpanner. The superpanned concentrate was further purified by centrifuging in methylene iodide. The abundance of heavy minerals in these sulfide-bearing sandstones along with alteration of the sulfide-selenide to secondary lead minerals contribute impurities to the concentrates.

Each purified sample was then analyzed for selenium by the distillation method described by Robinson and others (1934). The selenium content was determined gravimetrically except in the one sample (74-D) where selenium was determined colorimetrically. The analytical error estimated for the gravimetric determination of selenium by this method is ± 5

Table 1. Location and Description of Samples[1]

AW-165-52	—Corvusite mine, Grand County, Utah; selenide rimming coalified log associated with uranium ore. Morrison formation. U. S. National Museum No. 112933.
306-RGC-56	—Rifle mine, Garfield County, Colorado; single sulfide band in No. 1 vein. Navajo (?) sandstone.
303-RGC-56	—Rifle mine, Garfield County, Colorado; single sulfide band in No. 1 vein. Navajo (?) sandstone.
302-RGC-56	—Rifle mine, Garfield County, Colorado; single sulfide band in No. 1 vein. Navajo (?) sandstone.
305-RGC-56	—Rifle mine, Garfield County, Colorado; single sulfide band in No. 1 vein. Navajo (?) sandstone.
73A-RGC-55	—Rifle mine, Garfield County, Colorado; single sulfide band in No. 2 vein. Entrada sandstone.
74-RGC-55	—Rifle mine, Garfield County, Colorado; single sulfide band in No. 1 vein. Navajo (?) sandstone.
300-RGC-56	—Rifle mine, Garfield County, Colorado; single sulfide band near junction of No. 1 and No. 2 veins. Entrada sandstone.
304-RGC-56	—Rifle mine, Garfield County, Colorado; multiple sulfide bands in No. 1 vein. Navajo (?) sandstone.
74C-RGC-55	—Rifle mine, Garfield County, Colorado; single sulfide band in No. 1 vein. Navajo (?) sandstone.
69-RGC-55	—Rifle mine, Garfield County, Colorado; thin multiple bands in No. 1 vein. Navajo (?) sandstone.
72-RGC-55	—Rifle mine, Garfield County, Colorado; single broad band in No. 2 vein. Entrada sandstone.
452-RGC-56	—Good Hope mine, La Plata County, Colorado; multiple fine bands in Entrada sandstone.
75-RGC-55	—Bear Creek mine, San Miguel County, Colorado; broad zone of disseminated sulfide in Entrada sandstone.
65-RGC-55	—Garfield mine, Garfield County, Colorado; single sulfide band in No. 2 vein. Entrada sandstone.
301-RGC-56	—Rifle mine, Garfield County, Colorado; extremely finely disseminated band in No. 1 vein. Navajo (?) sandstone.
66-RGC-55	—Garfield mine, Garfield County, Colorado; double sulfide band in No. 3 vein. Entrada sandstone.
68-RGC-55	—Garfield mine, Garfield County, Colorado; broad double banding in No. 2 vein. Entrada sandstone.
H-2	—Darwin mine, Inyo County, California; sulfide in lead-zinc vein type deposit, massive galena in Essex vein.
74D-RGC-55	—Rifle mine, Garfield County; galena in brecciated fracture zone, probably hydrothermal in origin. Entrada sandstone.

[1] Exact locations for samples from the Rifle and Garfield mines are plotted on mine maps compiled by R. P. Fischer (personal communication), U. S. Geological Survey.

per cent of the reported value. When large amounts of selenium are present (> 20 per cent Se) the error may be higher, possibly ± 10 per cent.

The unit cell dimensions were determined from *x*-ray diffractometer charts, using the method described by Parrish, *et al.* (1953).

A split of the original sample was then analyzed by the semiquantitative spectrographic method described by Waring and Annell (1953).

Each sample was carefully checked by mineragraphic techniques to establish the presence of a single phase. Exsolution of PbSe in PbS or PbS in PbSe was not observed in any of the samples. This was verified by the *x*-ray examination as all the peaks of the important reflections are well defined; no doublets were observed. To check the possibility that the diffractometer was not sensitive enough to distinguish exsolved phases, several mechanical mixtures of galena and clausthalite were made. In all these mixtures it was possible to distinguish the individual peaks of the two end members.

Results

The 20 analyzed samples range from 0.04 to 93.7 molecular per cent PbSe in PbS with a variation in the unit cell from 5.930 Å to 6.127 Å (Table 2). To establish the ideal linear curve between the two end members, the precise unit cell of pure galena (PbS) and clausthalite (PbSe) should be known. Earley (1950) used 5.923 kX for pure galena and 6.110 kX for pure clausthalite. These values (converted from kX to Å) along with those determined for the intermediate synthetic members produce an almost linear variation. However, it is not clear on what type of material Earley determined the unit cell of galena PbS—synthetic or natural. The value used for clausthlalite is somewhat open to question as it was not analyzed and the density is low. A small amount of sulfur substituting for selenium in clausthalite would produce a marked change in the unit cell determination.

The value used in this study for galena (PbS) is $a_o = 5.924$ kX, determined by Wasserstein (1951) on pure analyzed material from Joplin, Missouri. As pointed out by Wasserstein, bismuth may enter the galena and proxy for Pb producing a concomitant decrease in cell size, thus unit cell parameters on unanalyzed material are of no value in establishing the cell size of end members.

The true cell size of PbSe is difficult to establish as there are many conflicting values reported in the literature. Unit cell measurements for synthetic PbSe have been reported as $a_o = 6.14$ Å (Ramsdell, 1925), $a_o = 6.128$ Å (Nozato and Igaki, 1955), $a_o = 6.135$ Å (Goldschmidt, 1926), and for natural clausthalite the values reported are $a_o = 6.162$ Å (Olshausen, 1925), $a_o = 6.124$ Å (Swanson and others, 1955).

The values given by Ramsdell and Goldschmidt are in fairly close

Table 2. Unit Cell and Selenium Determinations of the Galena-Clausthalite Series

Sample No.	Per cent Se[1]	Molecular per cent PbSe in PbS	Unit cell in Å[2]
AW-165-52	25.6	93.7	6.127±.003
306-RGC-56	25.1	89.4	6.099±.003
303-RGC-56	22.5	78.8	6.120±.003
302-RGC-56	21.9	76.4	6.116±.003
305-RGC-56	21.1	73.0	6.103±.006
73A-RGC-55	18.0	61.1	6.048±.008
74-RGC-55	17.0	56.7	6.099±.008
300-RGC-56	16.1	54.0	6.043±.003
304-RGC-56	15.9	53.2	6.068±.005
74C-RGC-55	15.1	50.3	6.048±.008
69-RGC-55	14.2	47.6	6.044±.008
72-RGC-55	11.8	38.5	6.033±.008
452-RGC-56	11.7	38.1	6.029±.003
75-RGC-55	10.0	32.2	6.003±.008
65-RGC-55	8.66	27.7	5.996±.008
301-RGC-56	8.24	26.2	5.981±.008
66-RGC-55	8.10	25.8	5.996±.008
68-RGC-55	7.09	22.4	5.981±.008
H-2	2.11	6.5	5.924±.005
74D-RGC-55	0.009	0.04	5.930±.008

[1] Relative error of the Se analyses is approximately ±5 per cent of the reported value. Analysts, Maryse Delevaux and Esma Campbell, U. S. Geological Survey.

[2] CuKα radiation; calculations from x-ray spectrometer charts. The estimated error of the unit cell measurement was established from the average of five a_0 determinations from reflections in the high angle region. The extremes on either side of the average give the estimated error. Measurements by R. G. Coleman and J. R. Houston, U. S. Geological Survey.

agreement and since these were determined on synthetic PbSe, the cell size $a_o = 6.140$ Å seems to be the best figure.

Using $a_o = 5.936$ Å for galena and $a_o = 6.140$ Å for clausthalite as the best values for the end members, a graph was constructed with molecular per cent plotted against unit-cell size. The assumption was made that the relationship was linear. The naturally occurring galena-clausthalites were plotted on the same graph along with Earley's (1950) data on synthetic materials (Fig. 1). In the majority of cases the values determined seem to follow the hypothetical linear trend. The greatest divergence is found near PbSe where the analytical problem of accurate Se determinations becomes critical because of the great difference in atomic weight between sulfur and selenium. In addition to this, impure samples tend to decrease the amount of total selenium (for example , 74-RGC-55, Fig. 1). Only one complete analysis was made (AW-165-52, Table 3), and from

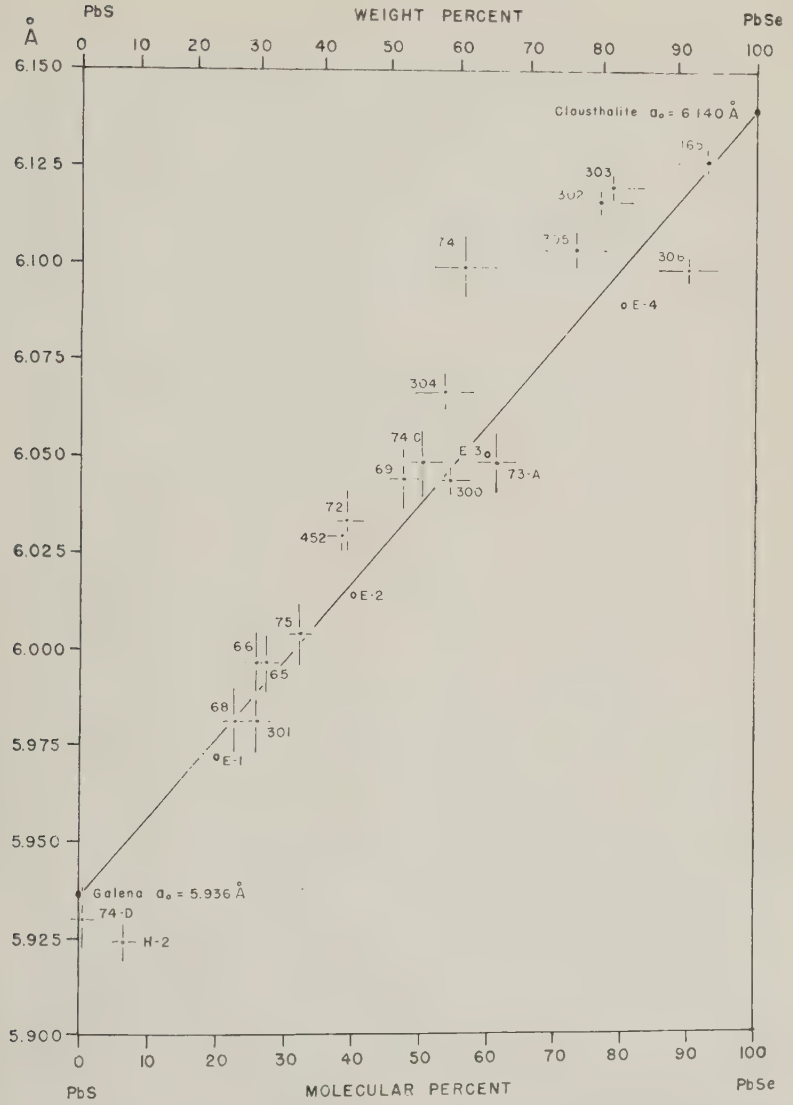

FIG. 1. Plot of unit cell against molecular per cent PbSe in PbS for galena clausthalite series. Relative error of the unit cell and selenium determinations are expressed as bars. The points labeled E-1 to E-4 represent the synthetic material made by Earley (1950). Weight per cent PbSe in PbS is given on the top abscissa.

this PbS and PbSe were calculated directly. For the other points in Fig. 1 the molecular per cent PbSe was calculated from the selenium analyses and the remainder was taken as PbS. When using this type of calculation to determine PbSe-PbS values, impurities will give a lower apparent weight per cent PbSe with the same a_o. The strong divergence of H-2 can be explained by its high bismuth content. *X*-ray spectrometer analysis on this sample indicates several per cent Bi; and as shown by Wasserstein (1951), substitution of Bi for Pb causes a decrease in cell size. A complete analysis of clausthalite (AW-165-52) shows that small amounts of sulfur may greatly affect the unit-cell determination (Table 3).

The calculation of the molecular per cent of PbS and PbSe in the

Table 3. Chemical Analysis of Clausthalite, (AW-165-52)[1]
(Analyst, A. M. Sherwood, U. S. Geological Survey)

	Weight per cent	Molecular per cent clausthalite-galena
Pb	72.0	PbSe—93.7
Se	25.6	PbS—5.9
S	0.4	Density 25° C.=8.01±0.005 (Berman balance)
As	0.6	Density =8.09 (calculated)
Total	98.6	

[1] Corvusite mine, Grand County, Utah. Material used for analysis and *x*-ray determination is in the U. S. National Museum, No. 112933.

clausthalite from the Corvusite mine illustrates that only 0.4 per cent S in clausthalite accounts for 5.9 per cent galena (PbS). Thus, one must be cautious in selecting natural material for true end members unless a complete analysis has been made.

The pyrosyntheses of the galena-clausthalite solid solution series by Earley (1950) was accomplished at fusion temperatures; however, data on the PbS-PbSe system at various pressures and temperatures is not available. The majority of these samples were taken from sandstone-type uranium-vanadium deposits suggesting that the formation of this series can be accomplished at fairly low temperatures. Estimates of the temperature of formation of these particular deposits have shown that they may have formed at temperatures similar to that of the enclosing host rock (Coleman, 1957).

Spectrographic Analyses

Each sample was analyzed by a semiquantitative spectrographic method described by Waring and Annell (1953) to ascertain the minor element content of this group of specimens (Table 4).

TABLE 4. SEMIQUANTITATIVE SPECTROGRAPHIC ANALYSES OF GALENA-CLAUSTHALITE SERIES

(Analysts: Charles Annell, Joseph Haffty, and Katherine V. Hazel, U. S. Geological Survey)

Sample No.	Element											
	As	Ni	Co	Cu	Mn	Zn	Mo	Ag	Mg	Fe	Sr	Impurities[1]
AW-165-52	0.5 –1	0.01 0.05	0.01 0.05	0.1 0.5	0.001–0.005	—	0.001 0.005	0.1 –0.5	0.05 –0.1	0.5 –1	—	V.
306-RGC-56	0.1 0.5	0.01 –0.05	0.005 –0.01	0.01 –0.05	0.01 0.05	0.05 0.1	0.005 –0.01	0.001 0.005	0.1 - 0.5	1 5	0.01 - 0.05	Py. dol.
303-RGC-56	—	0.001 0.005	0.001 0.005	0.005 0.01	0.01 –0.05	—	—	0.001–0.005	0.05 –0.1	1–5	0.005–0.01	Py. qtz.
302-RGC-56	–	0.01 0.05	0.001 –0.005	0.005–0.01	0.01 –0.05	—	0.005 0.01	0.001–0.005	0.05 - 0.1	1 5	0.001 0.005	Py. qtz.
305-RGC 56	0.1 –0.5	0.01 –0.05	0.0001–0.0005	1–5	0.01 0.05	0.05–0.1	0.005 –0.01	0.001 0.005	0.05 –0.1	0.5 –0.1	0.001–0.005	Ccp. qtz.
73A-RGC-55	—	–	0.001 0.005	0.001–0.005	0.001 0.005	—	0.001 - 0.005	0.001 0.005	0.01 –0.05	0.01–0.05	—	Zr. qtz. clay
74-RGC-55	–	0.001–0.005	0.001 - 0.005	0.001–0.005	0.005–0.01	—	0.001 0.005	0.001 0.005	0.1 –0.5	1 5	0.005–0.01	Py. dol. zr.
300-RGC-56	0.1 –0.5	0.01 –0.05	0.01 –0.05	0.005–0.01	0.001–0.005	—	0.01 –0.05	0.05 –0.1	0.05 –0.1	0.05 0.1	0.001 0.005	Qtz.
304-RGC-56	0.1 0.5	0.01 0.05	0.001 - 0.005	0.01 –0.05	0.05 0.1	5–10	1–5	0.005–0.01	0.1 –0.5	0.5 –1	0.05 –0.1	Dol. v. sp.
74C-RGC 55	–	0.01 0.05	0.01 0.05	0.01 –0.05	0.01 0.05	0.01–0.05	0.01 - 0.05	0.01 0.05	0.1 –0.5	0.5 –1	0.001–0.005	Dol. v. sp.
69-RGC-55	0.01–0.05	0.01 0.05	0.01 0.05	0.01 –0.05	0.005 0.01	0.01–0.05	0.001 - 0.005	0.01 –0.05	0.1 0.5	0.1 –0.5	0.001–0.005	Qtz. zr. dol.
72-RGC 55	—	0.005–0.01	0.001 0.005	0.005–0.01	0.01 0.05	0.01–0.05	0.01 0.05	0.01 - 0.05	0.05 0.1	1–5	—	Py. zr. qtz.
452-RGC-56	0.5 –1	0.01 –0.05	0.001 0.005	5–10	0.01 0.05	1–5	0.001 - 0.005	1–5	0.005 0.01	0.5 1	0.01 –0.05	Ccp. sp.
75-RGC 55	—	0.001–0.005	0.001 0.005	0.001–0.005	0.005 0.01	—	—	0.1 0.5	0.01 0.05	0.1 - 0.5	0.5 –1	Qtz. dol.
65-RGC 55	—	0.001–0.005	—	0.01 –0.05	0.005 0.01	-	0.0005 0.001	0.001 0.005	0.1 0.5	0.1 - 0.5	0.005–0.01	Zr. qtz. dol.
301-RGC-56	—	0.001–0.005	0.001 0.005	0.01 0.05	0.01 –0.05	—	—	0.01 –0.05	0.05 - 0.1	1–5	0.1 –0.5	Py.
66-RGC 55	0.01–0.05	0.01 –0.05	0.01 0.05	0.01 0.05	0.001–0.005	—	-	0.01 –0.05	0.1 - 0.5	0.05–0.1	0.001 0.005	Qtz. dol.
68-RGC-55	-	0.001 0.005		0.01 –0.05	0.001 0.005	—	0.001 0.005	0.001–0.005	0.05 –0.1	0.1 –0.5	0.005–0.01	Zr.
H-2	—	0.001	—	0.003	0.0003	0.01	—	1.0	0.00003	0.03	0.001	
74D-RGC-55	1–5	0.1 –0.5	0.1 0.5	0.01 0.05	0.01 –0.05	0.1 - 0.5		0.5 –1	0.01 - 0.05	0.1 - 0.5	0.001–0.005	Sp.
Sensitivity	0.05	0.001	0.001	0.0005	0.0005	0.02	0.0005	0.0001	0.001	0.001	0.001	

[1] Recognized impurities are listed without relative amounts; in most instances these do not exceed 10 per cent of the sample. V.—vanadium oxide, Sp.—sphalerite, Py. pyrite, Qtz.- quartz, Ccp.—chalcopyrite, Zr.– zircon, Dol.—dolomite.

In general, the minor element content of these galena-clausthalites is similar to those elements present in galenas as summarized by Fleischer (1955). However, several notable differences were observed and it is assumed that unique environment of deposition of the galena-clausthalites may account for these variances in minor element content. Bismuth and antimony are almost completely absent whereas both these elements are commonly reported in galenas from typical hydrothermal deposits. Antimony was found in the samples from the Good Hope and Darwin mines.

The iron, copper, and zinc reported are considered as impurities in the samples, as pyrite, chalcopyrite, and sphalerite were present in many of the sulfide concentrates. Nickel and cobalt are consistently present in about equal amounts ranging from 10 to 500 ppm and it is assumed that these elements must enter the galena-clausthalite structure. One might suspect that the small amount of iron sulfide present could contribute the necessary Ni and Co. However, the Ni-Co content does not vary sympathetically with the iron content.

The silver content of these specimens is similar to what has been reported in the literature (Fleischer, 1955) for galenas. The strong variations are probably related more to the local geochemistry of the sample rather than a function of temperature as suggested by Tischendorf (1955).

Molybdenum is a common element in these sediments and shows a marked affinity for sulfides. The amount of Mo reported is small in the samples but it undoubtedly has been captured in the sulfide-selenide lattice. Insufficient data are at hand to compare this with other galenas.

Magnesium and iron are probably present as impurities, the iron resulting from pyrite and chalcopyrite and the magnesium from dolomite.

Strontium has not been reported as a minor element in galena up to this time; however, in the galena-clausthalites from sedimentary rocks, Sr was found to be present in amounts up to 1 per cent. As the element is strongly lithophile one would not expect it to be present in sulfides. However, SrS has a NaCl type structure and Sr^{2+} has an ionic radius 1.27 Å which is very similar to the ionic radius of Pb^{2+} (1.32 Å). Strontium bearing minerals were not observed in the host rocks or in the purified concentrates; however, further analytical work is necessary to establish the substitution of Sr for Pb in the galena-clausthalite minerals.

There is no apparent difference in the kind of minor elements found in the PbS-PbSe series when compared to those characteristic of galena. It seems that the minor elements substituting for Pb are not strongly controlled by the sulfur-selenium ratio.

Conclusions

The close adherence of naturally occurring galena-clausthalites to the hypothetical linear variation of unit cell plotted against composition

strongly suggests that a complete isomorphous series PbS-PbSe does exist in nature.

The minor element content of these galena-clausthalites reflects, in part, their peculiar environment, but, in general, the minor element suites are comparable to those found in other galenas.

Acknowledgments

This work is part of a program being conducted by the U. S. Geological Survey on behalf of the Division of Raw Materials of the U. S. Atomic Energy Commission.

References

Bergenfelt, Sven (1953), Om förekomsten av selen i Skelleftefältets sulfidmalmer: *Geol. Fören. Stockholm Förh.*, **75,** 327–359.

Coleman, R. G. (1957), Mineralogical evidence on the temperature of formation of the Colorado Plateau uranium deposits: *Econ. Geology*, **52,** 1–4.

Coleman, R. G. and Delevaux, Maryse (1957), Occurrence of selenium in sulfides from some sedimentary rocks of the Western United States: *Econ. Geology*, **52,** 499–527.

Earley, J. W. (1950), Description and synthesis of the selenide minerals: *Am. Mineral.*, **35,** 356–358.

Fleischer, Michael (1955), Minor elements in some sulfide minerals: *Econ. Geology*, **50th Anniversary Volume,** 1905–1955, pt. 2, 970–1024.

Goldschmidt, V. M. (1926), Geochemische Verteilungsgesetze der Elemente VII. Die Gesetze der Kristallochemie: *Skrifter Norske Vidensk.—Akad. I. Nat. Kl., Oslo*, No. **2,** 117 p.

Heier, Knut (1953), Clausthalite and selenium-bearing galena in Norway: *Norsk. Geol. Tidsskr.*, **32,** 228–231.

Nozato, Royichi, and Igaki, Kenzo (1955), The equilibrium diagram of the lead-selenium system: *Bull. Naniwa Univ.* **A3,** 125–133.

Olshausen, S. v. (1925), Strukturuntersuchungen nach der Debye-Scherrer-Methode: *Zeit. Krist.*, **61,** 463–514.

Parrish, W., Ekstein, M. G., and Irwin, B. W. (1953), Data for *X*-ray analysis. v. II. Tables for computing the lattice constant of cubic crystals: Irvington-on-Hudson, N. Y., Philips Tech. Library, 81 p.

Parrish, W., and Irwin, B. W. (1953), Data for *X*-ray analysis, v. I. Charts for solution of Bragg's equation: Mount Vernon, N. Y., North American Philips Company.

Ramsdell, L. S. (1925), The crystal structure of some metallic sulfides: *Am. Mineral.*, **10,** 281–304.

Robinson, W. O., Dudley, H. C., Williams, K. T., and Byers, H. G. (1934), Determination of selenium and arsenic by distillation: *Indus. and Eng. Chemistry, Anal. Ed.*, **6,** 274–276.

Swanson, H. E., Gilfrich, Nancy, T., and Ugrinic, G. M. (1955), Standard *X*-ray diffraction powder patterns: *Natl. Bur. Standards Circ. 539*, **5,** 75 p.

Tischendorf, G. (1955), Paragenetische und tektonische Untersuchungen auf Gangen des Fluorbarytischen Bleiformation Freibergs: *Freiberger Forschungshefte*, **18,** 1–129.

Waring, C. L., and Annell, C. S. (1953), Semiquantitative spectrographic method for analysis of minerals, rocks, and ores: *Anal. Chemistry*, **25,** 1174–1179.

Wasserstein, B. (1951), Precision lattice measurement of galena: *Am. Mineral.*, **36,** 102–115.

Manuscript received June 2, 1958

NOTES AND NEWS

GARRELSITE AND THE DATOLITE STRUCTURE GROUP*

C. L. CHRIST, *U. S. Geological Survey, Washington 25, D. C.*

The fact that the *x*-ray powder diffraction patterns of datolite, bakerite, herderite, and homilite are very similar led Frondel (Palache, Berman, and Frondel, 1951) to postulate that a structural resemblance exists among these minerals. He expressed the chemical formulas in the following way:

Datolite	$Ca_4B_4(SiO_4)(SiO_4)_3(OH)_4 = CaB(SiO_4)(OH)$
Bakerite	$Ca_4B_4(BO_4)(SiO_4)_3(OH)_3.H_2O$
Herderite	$Ca_4Be_4(PO_4)(PO_4)_3(F, OH)_4 = CaBe(PO_4)(F, OH)$
Homilite	$(Ca, Fe)_4B_4(SiO_4)(SiO_4)_3(OH)_4 = (Ca, Fe)B(SiO_4)(OH)$ (?)

Recently, Milton, Axelrod, and Grimaldi (1955) described the new mineral garrelsite, $(Ba_{.65}Ca_{.29}Mg_{.06})_4H_6Si_2B_6O_{20}$, and postulated that it also is related to datolite. Following Frondel, these authors write the following chemical formulas:

Datolite	$Ca{\cdot}B_4(SiO_4)_4(OH)_4$
Bakerite	$Ca_4B_4(BO_4)(SiO_4)_3(OH)_3.H_2O$
Garrelsite	$(Ba, Ca, Mg)_4B_4(BO_4)_2(SiO_4)_2(OH)_2.2H_2O$

This way of writing and comparing the formulas implies that the bakerite and garrelsite structures may be derived from the datolite structure by the replacement of one-fourth and one-half, respectively, of the SiO_4 content of datolite, by BO_4, with concomittant decrease in the hydroxyl content in order to maintain the charge balance.

Ito and Mori (1953) have determined the crystal structure of datolite; Pavlov and Belov (1957) have verified their results, and, in addition, have analyzed the crystal structure of herderite. An examination of these crystal structures permits a more detailed assessment to be made of the structural relations existing among all of the minerals listed above. Datolite contains infinite sheets of composition $[BSiO_4(OH)]_n^{-2n}$. In forming a sheet, SiO_4 tetrahedra and $BO_3(OH)$ tetrahedra link at corners so that each SiO_4 shares three corners and has one unshared corner, and each $BO_3(OH)$ shares three corners, with the unshared (OH) at the fourth corner (see Fig. 5 of the paper of Ito and Mori (1953)). Thus, it appears that in deriving bakerite or garrelsite from datolite the SiO_4 should be replaced by $BO_3(OH)$ rather than BO_4. To make this relationship explicit the formulas involved can be written in the following way:

Datolite	$Ca_4[B(OH)SiO_4]_4 = Ca_4B_4(SiO_4)_4(OH)_4$
Bakerite	$Ca_4[B(OH)SiO_4]_3[B(OH)BO_3(OH)] = Ca_4B_4(SiO_4)_3(BO_3OH)(OH)_4$
Garrelsite	$M_4[B(OH)SiO_4]_2[B(OH)BO_3(OH)]_2 = M_4B_4(SiO_4)_2(BO_3OH)_2(OH)_4$ (M = Ba, Ca, Mg)

* Publication authorized by the Director, U. S. Geological Survey.

With this formulation none of the minerals contain water molecules as such. The next possible member of the series would have the formula $M_4B_4(SiO_4)(BO_3OH)_3(OH)_4$, and the end-member the formula $M_4B_4(BO_3OH)_4(OH)_4 = MB(BO_3OH)(OH)$.

In herderite, $CaBe(PO_4)(F, OH)$, PO_4 and $BeO_3(F, OH)$ tetrahedra play the same roles as do the SiO_4 and $BO_3(OH)$ tetrahedra in datolite (Pavlov and Belov, 1957).

References

Ito, T., and Mori, H. (1953), The crystal structure of datolite: *Acta Cryst.*, **6**, 24–32.

Milton, Charles, Axelrod, J. M., and Grimaldi, F. S. (1955), New mineral, garrelsite, $(Ba_{.65}Ca_{.29}Mg_{.06})_4H_6Si_2B_6O_{20}$, from the Green River formation, Utah: *Geol. Soc. Am. Bull.*, **66**, 1597.

Palache, C., Berman, H., and Frondel, C. (1951), *The System of Mineralogy, 5th Ed.*, vol. 2, John Wiley and Sons, Inc., N. Y.

Pavlov, P. V., and Belov, N. V. (1957), Crystal structure of herderite, datolite, and gadolinite: *Doklady Akad. Nauk S.S.S.R.*, **114**, 884–887. [*Chem. Abstr.*, **52**, 176 (1958)].

THE AMERICAN MINERALOGIST, VOL. 44, JANUARY–FEBRUARY, 1959

SINE TABLE FOR INDEXING POWDER PATTERNS

J. D. H. Donnay, *Crystallographic Laboratory, The Johns Hopkins University, Baltimore, Md.*

and

Gabrielle Donnay, *Geophysical Laboratory, Carnegie Institution of Washington, Washington, D. C.*

The indexing of a line on a powder pattern rests on the comparison of an observed with a calculated quantity, such as the interplanar distance d or some related function.

Tables giving d in Å in terms of θ at every 0.01° (or 2θ at every 0.02°) have been published for the six most commonly used x-ray wave lengths (ref. 1). The calculation of $d(hkl)$, on the other hand, is tedious,[1] even if d is expressed as a function of the reciprocal-cell dimensions a^*, b^*, c^*, α^*, β^*, γ^*.

The easiest function to calculate is

$$Q(hkl) = h^2a^{*2} + k^2b^{*2} + l^2c^{*2} + 2klb^*c^* \cos\alpha^* + 2lhc^*a^* \cos\beta^* + 2hka^*b^* \cos\gamma^* = 1/d^2(hkl),$$

which is the square of the length of the reciprocal-lattice vector. It is probable that, if the powder-data card catalogue could be compiled all

[1] We have in mind the workers who use desk calculators, not the lucky ones who have access to electronic computers.

over again, the Q's rather than the d's would be listed on the cards. At the present time, however, there exists only one table (ref. 2) that gives $Q(2\theta)=\sin^2\theta/(\lambda/2)^2$, *at every 0.01° in* 2θ, but it covers only the range 10° to 70° for copper radiation. This table would have to be extended to higher 2θ values and to all the other useful wave lengths, if Q values were to be listed instead of the customary d's. But until such a decision is reached, and for the more restricted purpose of indexing a pattern, other functions can be used which are independent of wave length and for which tables already exist, for example $(\lambda/2)^2Q(2\theta)=\sin^2\theta$. The reciprocal-cell dimensions must be multiplied by $\lambda/2$ before calculations are performed. Tables of $\sin^2\theta$ are available (ref. 3) for $\theta=0(0.01°)90°$. In precision determinations, 2θ can be read to 0.01°, so that it would be desirable to double the table of $\sin^2\theta$, by taking θ in steps of 0.005°.

Other tables, however, exist which render the extension of the $\sin^2\theta$ table unnecessary, and which require multiplying the reciprocal-lattice lengths by $\lambda/\sqrt{2}$. The function to be used is the versine, for

$$(\lambda^2/2)Q(2\theta) = 1 - \cos 2\theta = \text{vers } 2\theta.$$

The existing tables (ref. 4) of sin x and cos x, for $x=0(0.01°)90°$, can be used simply as follows:

(1) For $2\theta\leq 90°$, let $x=2\theta$, so that vers $2\theta=1-\cos x$; look up cos x and write down its complement to 1.
(2) For $90°<2\theta<180°$, let $x=2\theta-90°$, so that vers $2\theta=1+\sin x$; look up sin x and add it to 1.

Example: if $2\theta=120°$, $x=30°$; you read sin 30°=0.50000 and write 1.50000.

The tables give too many decimal places, but the first five places are separated from the others, so that the tables can easily be used as five-place tables.

It may not be out of order at this point to suggest a mode of presentation for powder data. *All* the lines permitted by the space-group should be calculated from the cell dimensions and should be published. Their purpose is not only to index the lines actually observed on the pattern at hand, but also to help later workers, who, by using longer exposures or other wave lengths, may observe one or more additional lines. Having all *possible* lines on record will make it unnecessary for them to repeat the whole calculation in order to account for the few additional observed lines. In order to cope with the large number of possible lines, it might be advisable, so as to save journal space, to abandon the listing in columns and to print the data as continuous text, with observed values in bold-face type between parentheses after the corresponding calculated values.

Because the quantity that is actually obtained from measurement is

the angle 2θ, we would advocate the recording and comparing of $2\theta_{obs}$ and $2\theta_{calc}$, for the particular wave length used. The $2\theta_{calc}$ values can be read from the sine table once *vers* 2θ has been obtained by calculation. For comparison with the powder-data card catalogue, both d_{obs} (2θ) and d_{calc} (2θ) can then be read from the d-table for the appropriate wave length. Obtaining d_{calc} this way is simpler than deriving it from *vers* 2θ by either formula

$$d = \sqrt{\frac{1}{(2/\lambda^2) \text{ vers } 2\theta}} \quad \text{or} \quad d = \lambda/2 \sin \theta.$$

References

1*a*. Tables for Conversion of *X*-ray Diffraction Angles to Interplanar Spacing. U. S. Department of Commerce. Nat. Bureau of Standards, Applied Mathematics Series, 10. U. S. Govt. Printing Office, Washington, D. C. (1950). Price $1.75 (buckram).

1*b*. Tables for Abaques, par. A. J. Rose. C.N.R.S. 13, Quai Anatole-France, Paris 7e (1957). [Both tables 1*a* and 1*b* give $d=\lambda/2 \sin \theta$ for $\theta=0(0.01°)90°$; 5 sig. figs.; in Å; for $K\alpha_1$ of Cu, Ni, Co, Fe, Cr, Mo. The fifth figure is occasionally different, as table 1b uses the wavelengths of Cauchoy and Hulubei (transformed to Å). Note differences of *one* in the fifth place in the wave length of $CuK\alpha_1$ and $NiK\alpha_1$; of *two* in the fifth place for $CoK\alpha_1$.]

2. Tables for the Interpretation of *X*-ray Diffraction Data, giving the square of the reciprocal lattice vector to 5 decimals in terms of the deviation angle 2θ for every hundredth of a degree from 10.00° to 49.99° for $CuK\alpha$ and from 25.00° to 69.99° for $CuK\alpha_1$, by Gabrielle Donnay and J. D. H. Donnay. Publication of the Crystallographic Laboratory, The Johns Hopkins University, Baltimore 18, Maryland (1951). Limited Edition. (Reprinting, 1955) Price $5.00.

3a. Table of Sin θ and $\text{Sin}^2 \theta$ for Values of θ from 2° to 87°. Prepared by H. Anne Plettinger. Argonne Nat. Laboratory, Lemont, Illinois (1956). [to 5 dec. places for $\theta=2°(0.01°)87°$]

3b. Table of $\text{Sin}^2 \theta$, prepared by B. Rosenbaum and G. Pederzani. Nat. Bureau of Standards, Washington, D. C. (1957?). (Limited Mimeographed Edition)

4a. Table of Sines and Cosines to Fifteen Decimal Places at Hundredths of a Degree. U. S. Department of Commerce, Nat. Bur.au of Standards, Applied Mathematics Series, 5. U. S. Govt. Printing Office, Washington, D. C. (1949). Price 45 cents.

4b. Manual of Gear Design. Section One. Eight Place Tables of Angular Functions in Degrees and Hundredths of a Degree . . . etc. By Earle Buckingham. Machinery, 148 Lafayette St., New York (1944 printing).

4c. Natural Sines and Cosines to Eight Decimal Places, U. S. Coast and Geodetic Survey, Superintendent of Documents, Washington, D. C. (1942). Price $3.00. [Cp. M.T.A.C., **3**, 424, 1949.]

THE AMERICAN MINERALOGIST, VOL. 44, JANUARY–FEBRUARY, 1959

SYNTHESIS OF BASTNAESITE[1]

GEORGE J. JANSEN,[2] GEORGE B. MAGIN, JR., AND BETSY LEVIN,
U. S. Geological Survey, Washington 25, D. C.

In the course of a study of rare-earth fluocarbonate minerals, laboratory experiments were made in an attempt to synthesize bastnaesite. Seven of the runs were successful. Attempts to synthesize the rare-earth fluocarbonates directly from the rare-earth nitrates were unsuccessful. It was found, however, that the rare-earth carbonates could be converted to the fluocarbonate. For the successful runs the carbonate was first prepared by the reaction of the particular rare-earth nitrate with sodium carbonate. Analysis, in per cent, of the resultant basic carbonate, $Ce_2O(CO_3)_2 \cdot 4H_2O$, is as follows:

	Analysis	Theoretical
Ce_2O_3	66.9	67.3
CO_2	18.3	18.0
H_2O	15.1	14.7
Total	100.3	100.0

A 100-mg. sample of $Ce_2O(CO_3)_2 \cdot 4H_2O$ was dispersed in 500 ml. of hot distilled water in a CO_2 atmosphere and the stoichiometric amount (33 ml.) of very dilute HF (1/1000) was added slowly. The reaction product was kept in a CO_2 atmosphere and digested on the steam bath for 5 days. Subsequent experiments have shown that digestion on the steam bath over night is sufficient. Bastnaesite of the composition $CeFCO_3$ and (Ce, La)FCO_3 with Ce and La in a 1:1 ratio (in both the starting material and final product) were prepared in this manner.

Identification of the products was by *x*-ray powder diffraction patterns. A comparison between *d*-spacings and intensities of the lines of the natural and the synthetic bastnaesite is shown in Table 1.

Under the microscope the products from the runs appeared as very fine aggregates of grains with a high birefringence. The material is too fine grained for the optical sign to be determined, but it was found to have a low index (presumably ω) of $1.71\pm$ and a maximum index (ϵ) near 1.82. These indices agree with the optical properties of the natural material.

This work is part of a program being conducted by the U. S. Geological Survey on behalf of the Division of Research of the U. S. Atomic Energy Commission.

[1] Publication authorized by the Director, U. S. Geological Survey.

[2] Present address, Republic Steel Corporation, Cleveland, Ohio.

TABLE 1. *X*-RAY POWDER DATA FOR NATURAL AND SYNTHETIC BASTNAESITE

CuKα radiation, $\lambda = 1.5418$ Å, nickel filter; camera diameter 114.59 mm.; cutoff 12 Å

Synthetic bastnaesite, $CeFCO_3$ (Film no. 9502)[1] Hexagonal $P\bar{6}2c$, $a = 7.24$ Å, $c = 9.92$ Å[2]				Natural bastnaesite, $(Ce, La)FCO_3$ (Film no. 9943) Locality: Stove Mountain near Pikes Peak, Colorado Hexagonal $P\bar{6}2c$; $a = 7.12$ Å, $c = 9.80$ Å[2]			
I	*d*(meas.) Å	*d*(calc.) Å	*hkl*	I	*d*(meas.) Å	*d*(calc.) Å	*hkl*
71	4.96	4.94	002	35	4.90	4.88	002
100	3.62	3.63	110	71	3.56	3.56	110
100	2.92	2.92	112	100	2.88	2.87	112
9	2.46	2.48	004	6	2.44	2.45	004
2 b	2.29	2.31 2.28	104 203	2 2	2.28 2.23	2.28 2.24	104 203
50	2.09	2.09	300	50	2.06	2.05	300
50	2.03	2.05	301	35	2.01	2.01	301
35	1.92	1.925 1.925	302 123	50	1.892	1.897 1.897	302 123
6	1.81	1.813	220	13	1.778	1.779	220
18	1.70	1.700	222	24	1.675	1.674	222
2	1.64	1.653 1.642	006 132	1	1.629	1.614 1.633	006 132
13	1.59	1.597	304	13	1.573	1.575	304
9	1.49	1.504	116	6	1.482	1.484	116
9	1.46	1.462	224	13	1.437	1.440	224
4	1.37	1.356 1.368	126 140	9	1.344	1.338 1.346	126 140
18	1.32	1.319	142	24	1.296	1.298	142
4	1.29	1.296 1.291	306 207	4	1.277	1.278 1.275	306 207

b = broad

[1] All lines diffuse.

[2] Cell constants were obtained from the powder patterns which were then indexed on the basis of the space group given by Donnay, Gabrielle, and Donnay, J. D. H. (1953), The crystallography of bastnaesite, parisite, roentgenite, and synchisite: *Am. Mineral.*, **38**, 932–963.

THE AMERICAN MINERALOGIST, VOL. 44, JANUARY-FEBRUARY, 1959

POLARIZING ADAPTERS FOR THE WOLFE GONIOMETER

C. W. Wolfe, *Boston University, Boston, Massachusetts.*

The probable usefulness of polarized light, in conjunction with the mechanical framework of a two-circle goniometer has recently occurred to the author when faced with the problem of obtaining the crystallographic orientation of synthetic corundum boules. This note describes the method used to obtain the desired polarization of light and the procedures followed to obtain the optical orientation.

There is an plano-convex lens in the inner end of the collimator (23) and another in the inner end of the telescope (1) of the Wolfe 2-circle goniometer (Wolfe, 1948). These lenses are held in place by screw-on adapters. Discs with diameters equal to that of the lenses were cut from polaroid sheets. These discs were placed between the lenses and the outer noses of the adapters. The plane of polarization of each disc was determined and made to coincide with the vertical or horizontal axis of the adapters when these are screwed on completely. The result is the extinction of light from the light source when the telescope is directly in line with the collimator. Since the polarizing ability of polaroid is not perfect, some light comes through, of course; but the differential is so great that the polarization is completely adequate.

An optional accessory on the Wolfe goniometer is a flat circular tilting plate which is mounted on a central post. This post can be inserted in the central opening of the horizontal circle and locked, if desired, by a long set screw. If the lowest lock screw on the goniometer is released, the horizontal circle is then free to turn, and a one-circle goniometer is effectively obtained. With the long lock screw fastened, the center plate can be turned any amount, and the angles can be read on the horizontal circle. A non-opaque crystal or fragment can be mounted on the tilting table or on a goniometer head which can, in turn, be mounted on the tilting table or on the vertical circle unit. With the crystal unit set between the polarizer and analyzer certain optical properties of the substance can be readily determined. Foremost amongst these would be optical orientation.

It will be of interest to describe the procedure used to obtain the optical orientation of a corundum boule, by use of the above procedure. From a consideration of the uniaxial optical properties of Al_2O_3, it follows there is but one plane parallel to the axis, L, of the boule which is also parallel to an extinction direction (Fig. 1). This plane must include the c axis, which, it should be pointed out, is not parallel to the axis of elongation, L. If the boule is mounted on the tilting plate in such a way that L

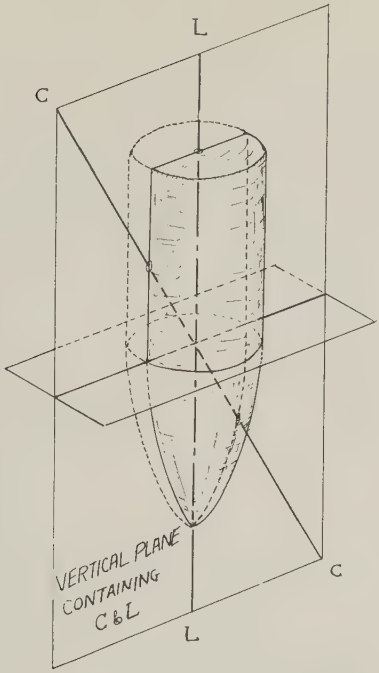

FIG. 1. Extinction positions on boule parallel or perpendicular to axis of elongation *L*. This position rigorously defines the *L*-*c* plane.

parallels the plane of polarization, and if the boule is observed through the telescope without the ocular, and if the boule be turned about the axis *L*, extinction will be noted in 2 positions 180° apart. The vertical plane through *L* and these two positions must then contain the *c* axis. The same result could be obtained if the boule or crystal were mounted on the vertical circle, in which case *L* would be horizontal and the plane which contains the *c* axis would be horizontal. The choice of procedure depends completely on the facility of mechanical operation in the two cases.

In most of the synthetic boules the *c* axis makes an angle of 52°–54° with *L*. If the plane containing the *c* axis and *L* has been carefully marked with pencil on the boule, it is a simple matter to turn the boule 90° on the horizontal tilting plate. At this position the boule is light. The boule can be inclined with the *c*-*L* plane perpendicular to the light source until extinction is obtained (Fig. 2). In this position the trace of a vertical line on the *c*-*L* plane must either be the *c* axis or a line at right angles thereto. By visual inspection it is possible to recognize whether the vertical line is closer to 54° than to its complement, 36°; and, thus, the

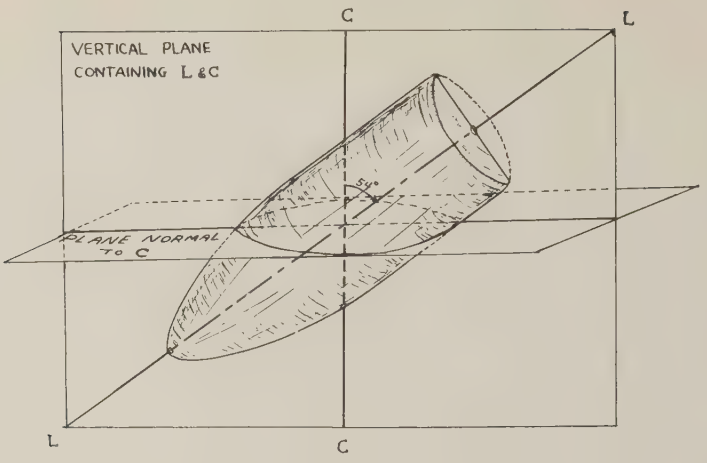

Fig. 2. Extinction positions in *c*-*L* plane, locating *c*.

c axis can be delineated. If the extinction angles to *L* do not approach 54°–36°, a thin slice must be cut from one edge of the boule parallel to the *c*-*L* plane. The slice can be checked for orientation and the extinction position corresponding to *c* can be determined with the quartz wedge or by the use of a flash figure. This can be most readily done with the petrographic microscope. Absorption is stronger parallel to *c*, also.

Any desired orientation of cut relative to the *c* axis can be made by the development of the proper type of jig. Of interest is the fact that the petrographic microscope can be used to solve boule orientation problems, but it is not so versatile, nor is the light penetration as satisfactory.

The use of the Wolfe 2-circle goniometer in the determination of the index of refraction of high index liquids by the hollow prism method has already been explained (Wolfe, 1949). The extension of applicability of the instrument to optical orientation problems with polarized light and to 1-circle goniometry increases the versatility of the instrument for laboratory purposes.

References

Wolfe, C. W. (1948), *Am. Mineral.*, **33**, 743.
——— (1949), *Am. Mineral.*, **34**, 893.

THE AMERICAN MINERALOGIST, VOL. 44, JANUARY–FEBRUARY, 1959

INFRA-RED ABSORPTION DATA FOR SERPENTINE MINERALS*

G. W. Brindley[1] and J. Zussman[2]

As a result of recent *x*-ray and electron diffraction studies of serpentine minerals (1) (2) (3) (4), samples were available of each of the known structural and morphological varieties of this group of minerals. It seemed worth while, therefore, to record their infra-red absorption spectra. Measurements were made with a Perkin-Elmer model 21 double-beam spectrometer using an NaCl prism. The finely powdered minerals were intimately mixed with powdered KBr using 0.75 mg. of mineral and 300 mg. of KBr, and were pressed into transparent discs under vacuum. A reference disc of pure KBr was prepared in a similar manner. The powdered materials were dried at 110° C. for 15 hr. and stored in a desiccator prior to weighing and efforts were made to reduce water-adsorption from the atmosphere to a minimum and to equalize the adsorptions on the two discs by using similar preparatory techniques. When measurements were made on different days, new KBr blanks were prepared.

The following minerals were studied:

1. Chrysotile, silky fibers, Transvaal, (ref. 3, p. 135)
2. Chrysotile, splintery fibers, Zermatt, (ref. 3, p. 135)
3. 1-layer ortho-serpentine (lizardite), massive, Snarum, Norway, (ref. 3, p. 135)
4. 1-layer ortho-serpentine (lizardite), platy, Cornwall, (ref. 3, p. 135)
5. 6-layer ortho-serpentine, massive, Unst, Shetland Isles, (ref. 3, p. 136; ref. 4)
6. 6-layer ortho-serpentine, fibrous, Unst, Shetland Isles, (ref. 3, p. 136; ref. 4)
7. Antigorite (picrolite), fibrous, Shipton, Quebec, (ref. 3, p. 136)
8. Antigorite, platy, Glen Urquhart, Scotland, (ref. 3, p. 136)

The absorption curves are shown in Fig. 1. In constructing this composite diagram, all essential features of the curves were carefully reproduced, but owing to small lateral displacements, the wavelengths cannot be read accurately from this diagram. The absorption maxima are listed separately in Table 1.

Discussion

Certain general results emerge from consideration of the data in Fig. 1 and Table 1. Since it is obviously difficult and unreliable to resolve the composite absorption bands in the 9–11 μ range into separate peaks, no

* The work described in this paper was undertaken at the Pennsylvania State University. Contribution No. 57–102.

[1] Head, Department of Ceramic Technology, The Pennsylvania State University University Park, Pa.

[2] Department of Geology, The University, Manchester, England.

FIG. 1. Infra-red absorption curves for serpentine minerals. (1) Silky chrysotile, (2) Splintery chrysotile, (3) 1-layer ortho-serpentine, massive, (4) 1-layer ortho-serpentine, platy, (5) 6-layer ortho-serpentine, massive, (6) 6-layer ortho-serpentine, fibrous, (7) antigorite, fibrous, (8) antigorite, platy.

attempt has been made to assign specific intensity values, such as strong, medium, weak, etc., to the data in Table 1. Tentative base lines are shown for some of the peaks in Fig. 1 by means of dashed lines.

Curves 7 and 8 for two antigorites, one a fibrous form and the other platy, are closely similar to one another but appreciably different from the curves for the other serpentines. The term "antigorite" is used for a mineral with the structural characteristics of the mineral from Antigorio, in particular, the long *a* parameter, usually in the range 33–45 Å (see ref. 3). It appears that the infra-red data may serve to distinguish an antigorite from other serpentine minerals. The antigorites show two

TABLE 1. INFRA-RED ABSORPTION MAXIMA FOR SERPENTINE MINERALS, IN MICRONS

(The more important absorption maxima are italicized)

1. Chrysotile silky fibers	*2.75*	—	*2.95*	6.20	—	—	*9.25*	9.85	—	*10.50*	—	—	—
2. Chrysotile splintery fibers	*2.75*	—	3.00	6.20	—	—	*9.35*	9.85	—	*10.55*	—	—	—
3. 1-Layer ortho (Lizardite) massive	*2.74*	—	2.95	6.20	—	—	*9.20*	—	—	*10.50*	11.45	—	—
4. 1-Layer ortho (Lizardite) platy	*2.75*		*2.95*	6.20	—	—	*9.15*	10.0	—	*10.70*	11.45	—	—
5. 6 Layer ortho massive	*2.76*	(2.85?)	3.05	6.25	—	—	*9.4*	(9.85?)	—	*10.55*	11.2	—	—
6. 6-Layer ortho fibrous	*2.76*	2.85	*2.95*	6.20	—	—	(9.3?)	9.70	10.05	*10.45*	11.35	12.6	—
7. Antigorite (picrolite) fibrous	*2.76*	—	3.00	6.25	8.35	8.95	*9.25*	—	*10.15*	10.50	11.45	12.9	14.2
8. Antigorite platy	*2.75*	—	*2.95*	6.15	8.35	8.90	*9.30*	—	*10.10*	10.45	—	12.9	14.1
	±0.01		±0.03	±0.04	±0.05	±0.05	±0.3	±0.1	±0.1	±0.05	±0.1	±0.1	±0.1

prominent peaks at about 9.25 and 10.15 μ as compared with three less well resolved peaks at about 9.30, 9.90 and 10.50 μ for other serpentines. The antigorites have only a weak absorption at about 10.5 μ, and no obvious absorption peak at 9.90 μ.

The similarity of the absorption curves for chrysotiles with tubular crystal lattices, and for the 1-layer and 6-layer ortho-serpentines with normal lattices is evident, but surprising in view of the different lattice types.

It was considered possible that water might be retained within or between the elementary tubular elements of chrysotile and thus give rise to characteristic differences in the "hydroxyl" range of the spectrum, 2.7–3.0 μ. The peak at about 2.75 μ is almost constant in shape, magnitude and position. The peak at about 2.95–3.00 μ is variable in magnitude but the variation has no obvious connection with lattice type. It is thought that this peak is related, in part at least, to adsorbed water and that the variability reflects changes in adsorption due to the precise way in which the specimens were prepared. When the mineral powder was purposely given additional opportunity to adsorb water vapor, the 3.0 μ peak was much enhanced. It would be necessary to regulate specimen preparation with extreme care before differences in the 3.0 μ peak from one sample to another could have any significance. On the other hand, the 2.75 μ peak seemed largely insensitive to precise specimen preparation and is probably related to hydroxyl units in the lattice structures.

Acknowledgment

These measurements constitute part of a broad study of serpentine minerals made possible by a grant by the National Science Foundation.

References

(1) Brindley, G. W., and Zussman, J. (1957), Structural study of the thermal transformation of serpentine minerals to forsterite, *Am. Mineral.*, **42,** 461–474.

(2) Whittaker, E. J. W., and Zussman, J. (1956), The characterization of serpentine minerals by x-ray diffraction, *Min. Mag.*, **31,** 107–126.

(3) Zussman, J., Brindley, G. W., and Comer, J. J. (1957), Electron diffraction studies of serpentine minerals, *Am. Mineral.*, **42,** 133–153.

(4) Zussman, J., and Brindley, G. W. (1957), Serpentines with 6-layer ortho-hexagonal cells, *Am. Mineral.*, **42,** 666–670.

THE AMERICAN MINERALOGIST, VOL. 44, JANUARY-FEBRUARY, 1959

MEASUREMENT OF DISORDER IN ZINC AND CADMIUM SULPHIDES

M. A. Short,* and E. G. Steward, *Research Laboratories of the General Electric Company Limited, Wembley, England.*

It is well known that the effect of mechanical work, such as grinding or the application of pressure, is progressively to convert zinc sulphide of initially hexagonal structure towards the cubic structure. In the course of an investigation (1) into the effect of grinding on the structure and luminescence of zinc and zinc-cadmium sulphides, it became necessary to measure the relative amounts of cubic and hexagonal stacking after various times of grinding.

Smith (2) and Wecker (3) have both suggested the use of relative intensities of certain *x*-ray powder reflections for evaluating the hexagonal:cubic stacking ratio. We have used the principle of the method suggested by Smith, but we have found it necessary to make two important modifications to the method as described by him.

Method

Smith's method is based upon consideration of the *x*-ray powder reflections that should be obtained from a number of different zinc sulphide polytypes. In the hexagonal-cubic transformation through the intermediate polytype structures, reflections from the (10.0) planes tend to extinguish, and a number of 10.*l* reflections appear between the 10.0 and 00.2 reflections (Fig. 1). Smith showed, by approximate calculation, that the value of the intensity of the 10.0 reflection plus the intensity of the polytype reflections *between* 10.0 and 00.2 decrease linearly from 2.04 at the hexagonal limit to zero at the cubic limit relative to the intensity of the combined 00.2 and overlapping polytype reflections, which increases nearly linearly from 1 at the hexagonal limit to 4 at the cubic limit (Fig. 1). Consequently Smith suggested using the ratio I(10.0+10.0 to 00.2) : I(00.2) as a measure of the hexagonal:cubic stacking ratio. Furthermore, he claimed that his procedure could be applied without modification to mixtures of cubic and hexagonal stacking whether on an atomic or a macroscopic scale, that is, for both random and "ordered" disorder. When the disorder is random, however, as in the case of hexagonal zinc sulphide that has been ground, diffraction patterns of the type Smith suggested to be typical of polytypes or mixtures of polytypes are not obtained. *X*-ray diffraction photographs of hexagonal zinc sulphide after grinding show the following features:

* Now at the Department of Fuel Technology, Pennsylvania State University, Pa.

(a) slight broadening of all reflections due to the introduction of lattice strain and reduced crystal size.

(b) diffuseness of reflections with $h+2k\neq 3n$, $(l=0)$, due to the introduction of random stacking disorder.

(c) appearance of reflections due to the specific formation of the cubic stacking sequence. These reflections are very diffuse because the stacking is of very short range, and the effective crystal size is therefore very small.

A microdensitometer trace of hexagonal zinc sulphide after grinding for two hours is shown in Fig. 1*d*. As expected, the 10.0 reflection shows only slight broadening due to grinding, and therefore any reflection between the 10.0 and 00.2 lines and between the 00.2 and 10.1 lines is due essentially to a broad cubic 111 reflection. It follows that in any ground

Fig. 1. (a) Positions and intensities for low-angle reflections from cubic ZnS.
(c) The same for hexagonal ZnS.
(c) Positions given by Smith for reflections from various ZnS polytypes.
(d) Microdensitometer trace for hexagonal ZnS after grinding for 2 hours.
(Originally published in *Z. phys. Chem.* (*Frankfurt*), **13**, 298 (1957).)

material the proportion of the hexagonal stacking present can be deduced from the ratio of the integrated intensity of the 10.0 reflection to the integrated intensity in the θ range $\theta_{10.0} < \theta < \theta_{10.1}$. Between $\theta_{00.2}$ and $\theta_{10.1}$ there will also be some disorder broadening of the 10.1 reflection, but this can be allowed for by measurement of the intensity distribution on the high θ side of the 10.1 reflection.

Intensity Values

The various relative intensities for the purely hexagonal and purely cubic structures can be denoted as follows:

	I(00.2+111)	I(10.0)
Hexagonal	1	α
Cubic	β	0

where α and β can be found.

If, in a given material, there is a fraction H of the hexagonal stacking sequence and, therefore, $(1-H)$ of the cubic stacking sequence, we can write:

$$\frac{I(10.0)}{I(00.2+111)} = \frac{H\alpha}{\beta - H(\beta - 1)}$$

The ratio I(10.0):I(00.2) for purely hexagonal zinc sulphide is also used by Smith in the method he has described. He obtained a ratio of 2.04 theoretically and for this he considered the crystals as "$\frac{2}{3}$ perfect." He preferred this theoretical figure owing to the wide variation in observed intensities reported by earlier workers. For *x*-ray *powder* work, however, the crystals constituting the powder should have been considered as "ideally imperfect," and calculation has shown (4) that the theoretical ratio of I(10.0):I(00.2) is, in fact, 1.56.

Our calculations confirmed Smith's statement that as the hexagonal stacking in zinc sulphide changes to cubic stacking, the value of the relative theoretical intensity of the 00.2 (111) reflection increases from 1 to 4. We also found that the 00.2 reflection intensity for cadmium sulphide increased from 1 to 4.

As it was proposed to apply the method of measuring the hexagonal:cubic stacking ratio to ground zinc-cadmium sulphides, it was important that the reference intensity ratios for both zinc and cadmium sulphides should be known accurately. For a solid solution of zinc-cadmium sulphide the appropriate values of α and β are determined from a linear combination of the values for the end-members.

It had previously been found (4) that the "highly reliable" intensity values obtained by the National Bureau of Standards for zinc sulphide (5) were in error due to the presence of disorder in their sample. A cursory

Table 1

hkl	ZnS			CdS		
	obs.	calc.	NBS (5)	obs.	calc.	NBS (6)
10.0	96	92	119	57	59	75
00.2	54	59	102	43	43	59
α	1.78	1.56		1.33	1.37	
10.1	100	100	100	100	100	100
11.0	64	67	88	50	49	57
10.3	64	67	62	50	50	42

examination of their figures for cadmium sulphide (6) suggested that here also their specimen may have contained some disorder. The whole question of the intensities of the x-ray reflections due to both cubic and to hexagonal zinc and cadmium sulphides has therefore been re-examined. With a refined microdensitometer technique, the observed intensities have been evaluated, using 19 cm. powder photographs as previously reported (4), for both zinc and cadmium sulphides. These intensity data and, for comparison, the N.B.S. data, are listed in Table 1.

The agreement obtained between our observed and calculated values confirms that our materials were essentially free from disorder.

Using the *experimental* values for α and putting $\beta = 4$, the fraction (H) of hexagonal stacking in a sample of disordered sulphide is given by the expression:

$$\frac{I(10.0)}{I(00.2 + 111)} = \left(\frac{1.78H}{4 - 3H}\right)_{ZnS} = \left(\frac{1.33H}{4 - 3H}\right)_{CdS}$$

In a similar way, H can also be determined by using the 11.0 and 10.3 reflections: The following expressions apply:

$$\frac{I(10.3)}{I(11.0 + 220)} = \left(\frac{H}{1.69 - 0.69H}\right)_{ZnS} = \left(\frac{H}{1.96 - 0.96H}\right)_{CdS}$$

It is found that these ratios are particularly sensitive to the presence of small amounts of cubic stacking.

References

(1) Short, M. A. and Steward, E. G. (1957), The effect of grinding on the structure and luminescence of zinc and zinc-cadmium sulphides: *Z. phys. Chem. (Frankfurt)*, **13**, 298.
(2) Smith, F. G. (1955), Structure of zinc sulphide minerals: *Am. Mineral.*, **40**, 658.
(3) Wecker, F. (1942/3), Röntgenographische Strukturuntersuchung an Zinksulfid-Kupfer-Phosphoren nach der Pulvermethode. *Ann. Physik.*, **42**, 561.

(4) Short, M. A. and Steward, E. G. (1955), *X*-ray powder diffraction data for hexagonal zinc sulphide: *Acta Cryst.*, **8**, 733.
(5) Swanson, H. E. and Fuyat, R. K. (1953), Standard *x*-ray diffraction powder patterns, *NBS Circular 539*, **2**, 14.
(6) Swanson, H. E., Fuyat, R. K. and Ugrinic, G. M. (1955), *ibid.*, **4**, 15.

Note added in proof: in a recent paper, V. G. Hill (*Can. Mineral.*, 1958, **6**, 234) has found α for ZnS to have the very high values of 2.17 (fine crystals) and 2.37 (ground crystals). This is probably due to his use of a diffractometric technique, which we have found to be unsatisfactory for the study of ZnS, and also, in the case of the ground crystals, to pulverisation.

THE AMERICAN MINERALOGIST, VOL. 44, JANUARY–FEBRUARY, 1959

THE DISPERSION AND THE TEMPERATURE COEFFICIENT OF THE BIREFRINGENCE OF SELENITE*

Myron A. Jeppesen and Richard E. Payne,
Bowdoin College, Brunswick, Maine.

Values of the indices of refraction of selenite ($CaSO_4 \cdot 2H_2O$) precise to five significant figures have been published by Tutton (1). For his measurements he used prisms with the crystal axes oriented so that the method of minimum deviation could be used. The birefringence obtained by taking differences between the indices of refraction so determined has a rather large uncertainty in the second significant figure and shows no consistent change with wavelength.

Using multiple-wave plates cleaved from natural crystals we have made direct measurements of the birefringence ($n_\gamma - n_\alpha$). A diagram of the experimental arrangement is shown in Fig. 1. The crystal is mounted

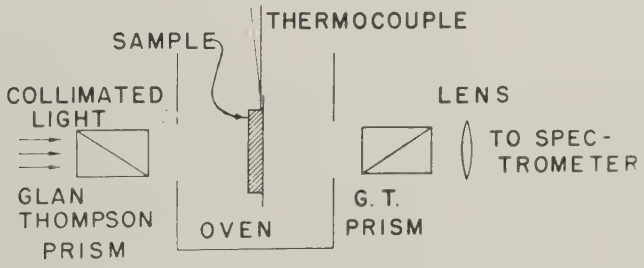

Fig. 1. Diagram of the apparatus for birefringence measurements.

normal to a collimated beam of light in a temperature controlled enclosure. The α and γ axes of the indicatrix are oriented at an angle of 45° to the transmission axes of a pair of Glan-Thompson prisms. An image of the crystal is formed on the slit of the spectrograph.

The crystal introduces a phase difference between the light vibration components parallel to the fast and to the slow axes. For those wave-

* From a project supported by the National Science Foundation.

lengths for which the phase difference is an integral multiple of 2π no light will pass the analyzer prism if the analyzer and the polarizer are crossed. Thus dark bands occur in the spectrum at those wavelengths for which

$$\frac{2\pi}{\lambda}(n_\gamma - n_\alpha)t = m2\pi \tag{1}$$

where m is an integer, t the crystal thickness, and λ the wavelength. If the polarizer and the analyzer are parallel m is replaced by $m+\frac{1}{2}$. Measurements of wavelength and thickness give a direct value of the birefringence $(n_\gamma - n_\alpha)$. The accuracy is dependent on the correct identification of the order number and on the thickness measurement.

The order number, m, in Eq. (1) is easily obtained for thin sections by observations with a visual spectrometer. A crystal 0.67 mm. thick gave seven dark bands in the visible region. It was known that the birefringence was approximately 0.009. By solving Eq. (1) for the m value of a band in the center of the spectrum using $(n_\gamma - n_\alpha) = 0.009$, an approximate value of m close to an integer was found. When this was rounded off to the nearest integer it appeared that it was the only possible value, as $m+1$ and $m-1$ gave birefringences of 0.01 and 0.008. A crystal 2.45 mm. thick was then examined and m was evaluated by the same method using the results from the thinner crystal. Finally, taking birefringence values from a graph representing results from several moderately thin crystals, Eq. (1) was used to obtain m for the crystal 9.58 mm. thick. The values obtained for bands in different parts of the visible spectrum

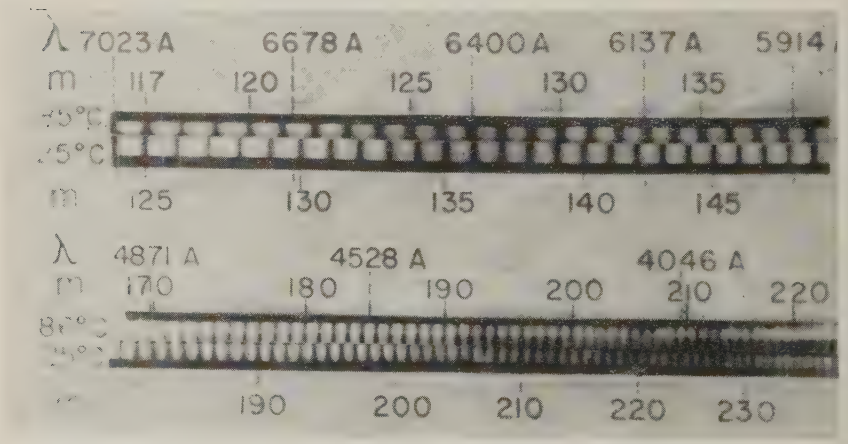

FIG. 2. Reproduction of spectrogram showing the multiple-wave plate bands. The comparison spectrum is from an iron arc. The selenite crystal was 9.58 mm. thick.

TABLE I. THE BIREFRINGENCE ($n_\gamma - n_\alpha$) OF SELENITE

25° C.			85° C.		
m	λ	$n_\gamma - n_\alpha$	m	λ	$n_\gamma - n_\alpha$
256	3597A	0.009612	240	3600A	0.009019
240	3808	9540	225	3803	8932
225	4034	9474	212	4004	8861
200	4490	9374	195	4318	8790
190	4706	9333	180	4644	8725
180	4945	9291	170	4894	8685
170	5209	9244	159	5205	8639
160	5506	9195	150	5490	8596
150	5840	9145	140	5853	8553
140	6220	9090	131	6223	8510
133	6519	9050	124	6546	8473
123	7000	8987	113	7135	8416

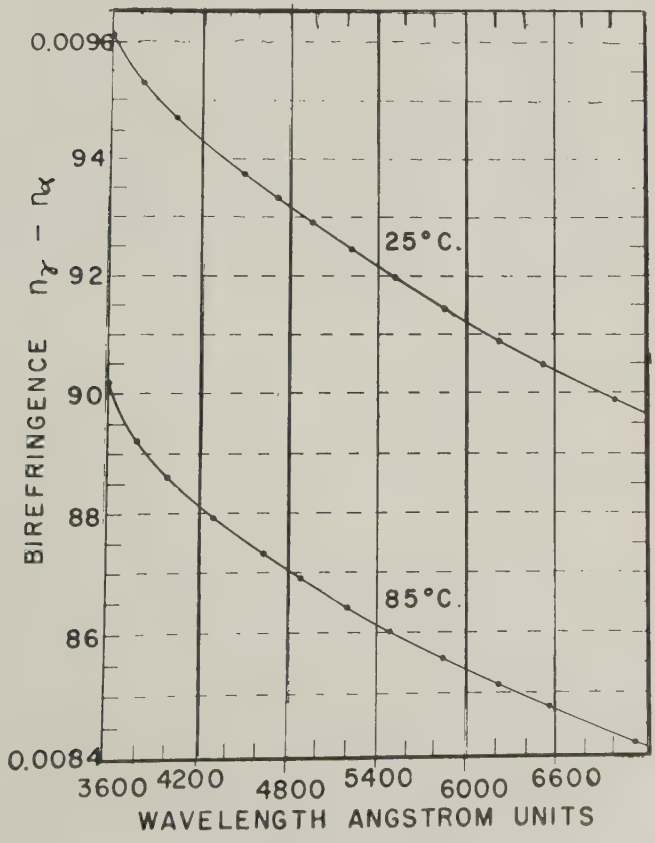

FIG. 3. $n_\gamma = n_\alpha$ as a function of wavelength at 25° C. and 85° C.

were consistent with each other when rounded off to the nearest integer. Having identified m for a given band at room temperature, the value of m at a different temperature was determined with a visual spectrometer by counting the bands that move by the cross hairs as the crystal is heated. The bands were then photographed with a ten foot diffraction grating spectrograph.

Figure 2 is a reproduction of spectrograms obtained with a crystal plate 9.58 mm. thick held at two different temperatures. An iron arc comparison spectrum was used for plate calibration.

The measurements on some of the bands are summarized in Table I. The values of $(n_\gamma - n_\alpha)$ recorded were checked by measurements on a crystal plate 12.27 mm. thick. The values obtained from a single spectrogram are self consistent to the fourth significant figure, but they differ slightly in the third figure from one determination to another. Probably one reason for this lack of adequate temperature control. Although the temperature indicated by the thermocouple did not fluctuate more than 0.5° C. during a run, the temperature error is probably greater than this because the thermocouple was not imbedded in the crystal.

Figure 3 shows $(n_\gamma - n_\alpha)$ plotted as a function of wavelength over the range 3600 Å to 7200 Å for temperatures of 25° C. and 85° C. The mean value of the temperature coefficient of birefringence over this range is -1.00×10^{-5}/° C. with an estimated uncertainty of 8 per cent.

Reference

(1) A. E. H. Tutton (1922), Crystallography and practical crystal measurement, Macmillan and Company, Ltd., London.

THE AMERICAN MINERALOGIST, VOL. 44, JANUARY–FEBRUARY, 1959

CALIBRATION SIGHTS FOR *X*-RAY POWDER CAMERA

Gabrielle Donnay, *Geophysical Laboratory, Carnegie Institution of Washington, Washington, D. C.*

AND

Joseph G. Smith, *Chemistry Department, The Johns Hopkins University, Baltimore, Maryland.*

The calibration sights have a twofold purpose. They permit determination of film shrinkage by direct measurement, provided the film has been developed with care so that film shrinkage will be uniform. They permit centering the film on the measuring device so that the midpoint of the *x*-ray diffraction rings comes at a convenient reading, say 100.00 mm. (Fig. 1). This procedure eliminates the need for finding the midpoint by reading ring positions on both sides of the punched hole. It simplifies the

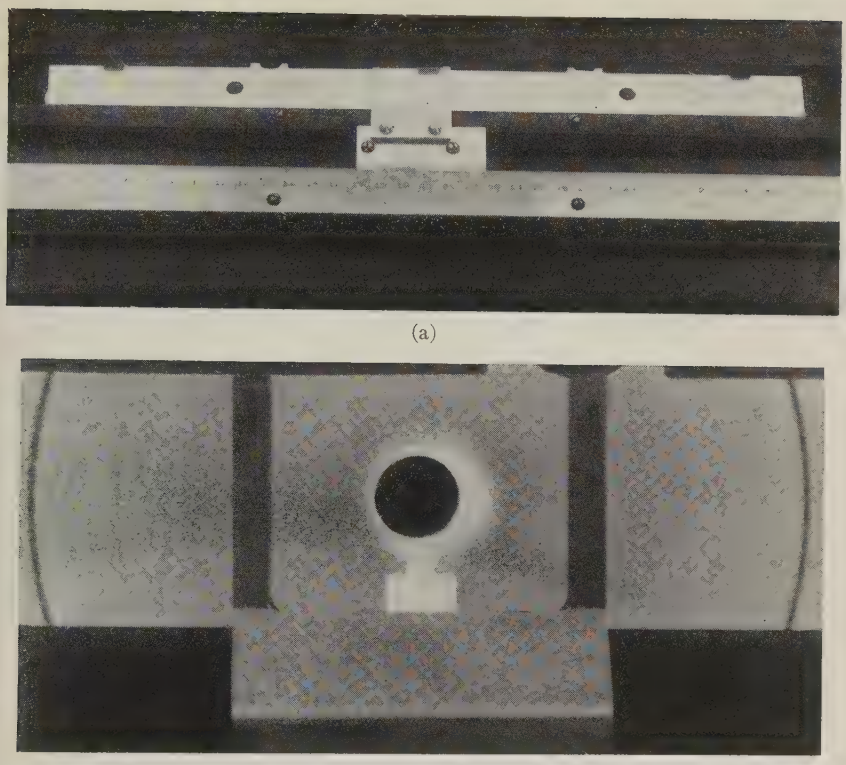

(a)

(b)

FIG. 1. (a) Calcite powder pattern (FeK α radiation), placed on viewing box so that reading is 100.00 mm. when hair line is centered (b) on M of forward reflections; reading at back-reflection M is 279.65 mm. Fiducial distance between M's in this camera: 180.12 mm.; shrinkage correction factor: 0.26%.

arithmetic of subtracting the midpoint reading from the reading of each ring.

The calibration sights are attached to a flat ring $\frac{1}{8}''$ thick (Fig. 2), made of aluminum alloy and of such size as to fit against the shoulder on the inside of the Buerger-type powder camera. A tight fit is assured by four fingers, 90° apart, which press against the shoulder with spring action. The two sights are M-shaped, made of brass, 8 mm. in height; they are mounted on the ring at the ends of a diameter. The M's are centered in the path of the x-ray beam by rotating the ring while sighting through the collimator. The ring is rotated by means of a punch placed into one of four blind holes drilled in the ring. Once the exact position is found, a hole previously drilled through the thickness of the ring is extended into the bottom of the camera and a pin is pushed into it.

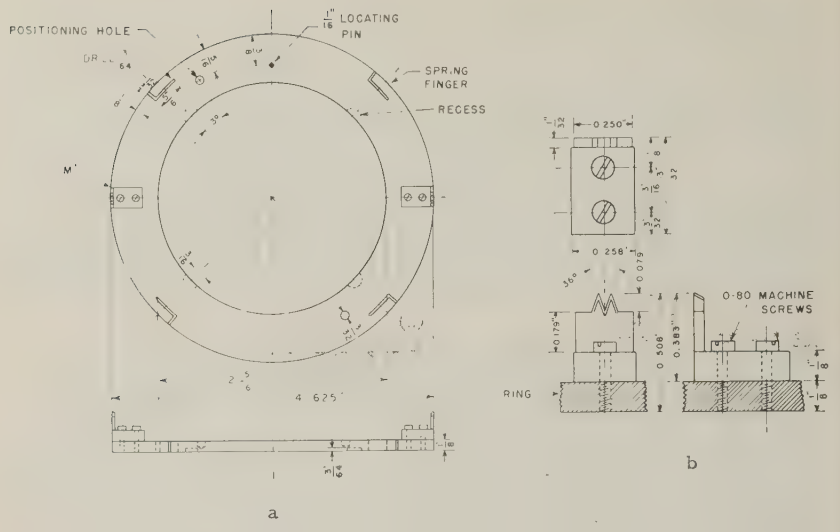

FIG. 2. (a) Top and front view of ring with "M's" mounted in position. Material used for ring: 24 ST aluminum alloy.

(b) Top, front, and side view of "M." Front and side view show "M" mounted on section of ring. Note chamfering of "M's" to give sharp shadow on film. Material used for "M": brass.

The ring can be lifted out of the camera by fitting a thin "L" shaped bar into a recess which is cut into the underside of the ring. The ring can be transferred to another camera of the same diameter. A slight difference in the size of the shoulder can be compensated for by appropriate bending of the spring fingers.

The fiducial distance between M's is obtained by exposing the loaded camera to a sun lamp. Both collimator and beam catcher are removed. The light is allowed to enter first from one side and then from the other side of the camera. After about an hour the shadows of the M's stand out on the undeveloped film with sufficient contrast. The positions of the M's can then be measured on a travelling microscope to ± 0.005 mm., which gives the fiducial distance to ± 0.01 mm.

Measurements on developed films were made on an electronic comparator (Dieke, Dimock, and Crosswhite, 1956) kindly placed at our disposal by Drs. Dieke and Crosswhite of The John Hopkins University. The instrument reads to 0.5 μ. This is more accuracy than we need for the readings of the calibration sights can be reproduced only to ± 0.002 mm.

The centering of the M's in the x-ray beam is checked with the help of a calcite pattern. The calcite lines can be measured with a reproducibility of ± 0.01 mm. in the forward-reflection region and ± 0.02 mm. in the

back-reflection region. The midpoints are of course known to the same accuracy. A comparison of the midpoints with the positions of the M's yields the permanent corrections Δ_1 and Δ_2 to be applied to the latter. It is convenient to set the M of the forward-reflection region at the reading $100.00-\Delta_1$ mm. on the film reader.

It might be argued that because the position of the M's is found with the help of a powder pattern, the accuracy with which it is known is no better than that with which the midpoints are measured for each film in turn using the customary procedure. This is not the case because for calibration we can choose a powder sample that gives sharp lines to high 2θ angles, whereas with the usual procedure one has to take the pattern as it comes. We have, for example, found the reproducibility of the readings to be no better than ± 0.03–0.05 mm. on several patterns of organic compounds.

If one does not wish to assume uniform film shrinkage, additional calibration sights can be mounted on the ring and fiducial distances determined as described above.

Reference

1. Dieke, G. H., Dimock, D. and Crosswhite, H. M. (1956), *J. Opt. Soc. Amer.*, **46**, 456

THE AMERICAN MINERALOGIST, VOL. 44, JANUARY–FEBRUARY, 1959

BRANDTITE AT THE STERLING HILL MINE, NEW JERSEY

Richard V. Gaines, *Grand Junction, Colorado*

Brandtite has been identified among specimens collected at the Sterling Hill mine, New Jersey, in 1940. So far as is known, this marks the first time that brandtite has been recognized from a United States locality, and adds one more mineral to the ever growing list of species that have been found at the Franklin and Sterling Hill mines.

The brandtite was found at Sterling between the 1400 and the 1500 foot levels. This portion of the orebody contained ore of two distinct types, which were mined and processed separately: the "black willemite" and the "brown willemite" ores. The former is a very fine-grained intergrowth of franklinite and willemite; the latter is coarse grained and consists essentially of brown willemite and calcite, with some franklinite. Sphalerite is also usually present up to several per cent, as an ore constituent. The brandtite-containing vug was found in the hanging wall of a black willemite stope, at a point where over-breakage had trespassed slightly into the adjacent brown willemite orebody. The cavity was a crack about two feet long lined with drusy and hairlike crystals of several

minerals. It was in the roof, which was very solid and hardly accessible, and only a few small specimens of matrix containing less than a gram of brandtite altogether could be collected.

The crystals are colorless, up to 8 mm. in their longest dimension, seldom as much as 1 mm. wide, and 0.2 mm. or less in thickness. Associated minerals are rhodochrosite as a fine grayish-pink drusy coating; chalcopyrite, as minute groups of crystals; an unidentified pink mineral as a thin powdery coating of crystals; and an unidentified transparent red mineral in rare crystals. These latter are square, tabular, apparently tetragonal, and have a luster and color similar to proustite. The groundmass consisted of a coarse intergrowth of calcite, franklinite, brown willemite, and sphalerite.

The brandtite crystals are simple and show the following forms in the unit and orientation of Dana (1951): *b*, *a*, *m*, *p*. Their habit is slender, prismatic, unlike the crystals from Harstig, Sweden, which are more nearly equant. Cleavage {010} perfect and {001} good. Colorless, transparent. Optically, the crystals are biaxial positive, with $\beta = 1.7070$ and $\gamma = 1.7215$. $r < v$, very strong. 2V small, $\cong 15°$.

X-ray powder photographs and single-crystal rotation and Weissenberg photographs confirmed that the material is identical with brandtite from Langban, Sweden. Insufficient material was recovered for chemical analysis, and the observed optics were close enough to those of brandtite from the type locality so that no major variation in the constituents would be expected.

THE AMERICAN MINERALOGIST, VOL. 44, JANUARY-FEBRUARY, 1959

CALIBRATION OF SINGLE-CRYSTAL WEISSENBERG FILMS

J. Fridrichsons, *Division of Chemical Physics, C.S.I.R.O. Chemical Research Laboratories, Melbourne, Australia.*

To supplement the calibration methods for Weissenberg films described in this *Journal* by Christ (1956) and Pabst (1957), it might be of interest to mention a simple method used in this laboratory for several years.

The crystal is mounted on a thin wire (*ca.* 0.1 mm.) of some pure metal with accurately known spacing values (Ag, Al, Pt). The drawn-out powder lines of the metal are superimposed on the Weissenburg pattern of the crystal over the whole width of the film, as shown in Fig. 1.

This method has the advantage that no alteration of the Weissenberg camera is necessary, the change of goniometer heads (with possible missetting errors) is obviated, no double or triple exposures are needed and

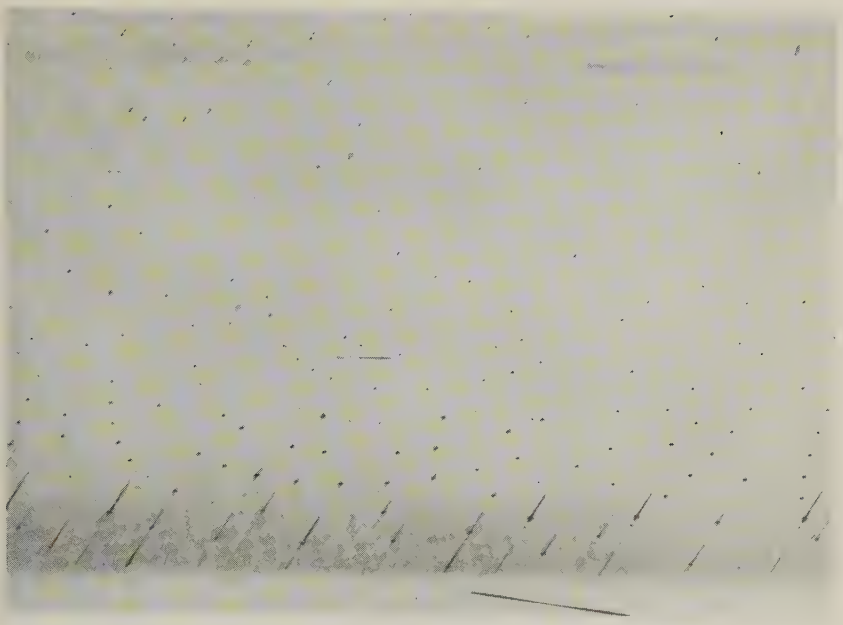

FIG. 1. Weissenberg photograph with continuous powder photograph lines from the wire mount.

the calibration is reliable in any region of the film, not merely in the region of the calibration strips, as in the methods mentioned above.

REFERENCES

CHRIST, C. L. (1956), *Am. Mineral.*, **41,** 569–580.
PABST, A. (1957), *Am. Mineral.*, **42,** 664–666.

NOTE ON LUZONITE

In the article "Luzonite, Famatinite and Some Related Minerals" which appeared in the November–December (1957) issue of this *Journal* reference was made on page 768 to the work of Professor Hideki Imai of the University of Tokyo. Imai's conclusion, as interpreted by the writer, was that "luzonite was a valid mineral species and that, although arsenic-rich, it did contain a little more antimony than enargite, yet considerably less than famatinite. Hence, in the series Cu_3AsS_4-Cu_3SbS_4, the mineral enargite corresponds to Cu_3AsS_4, while luzonite is an intermediate compound with a different structure."

In fairness to Prof. Imai, it must be said that this interpretation refers to only one of several possible alternatives discussed in his article. His over-all conclusion about this problem was the correct one, namely that

luzonite was in dimorphous relationship with enargite.

Imai's reference to Sawada's work on this subject was taken from the abstract of Sawada's paper, read before the semicentennial meeting of the Geological Society of Japan and the abstract published in the Journal of the Geological Society of Japan, Vol. 51 (1944), p. 21. Some of the figures given in this abstract differ from those communicated by Sawada to the writer, and hence Imai's reference to this work and the writer's were at variance.

RICHARD V. GAINES

Dr. Earl Ingerson, Treasurer of our Society since 1941, has recently become professor of geology at the University of Texas, and due to the pressure of professional work he found it necessary to resign from the office of Treasurer as of November 15, 1958. A glance at his reports during the past two decades shows a marked increase in the financial resources of our Society, thus testifying to his able management in this important area. In accepting his resignation at the recent annual meeting, the M.S.A. Council, on behalf of the members and fellows, expressed sincere gratitude to Earl Ingerson for his many years of able and loyal service to the Mineralogical Society of America.

The Council appointed Miss Marjorie Hooker, of the U. S. Geological Survey, to succeed Dr. Ingerson as Treasurer. Miss Hooker has ably assisted Dr. Ingerson for many years in the treasurer's office.

Dr. V. I. Mikheev, *x*-ray crystallographer of the Leningrad Mining Institute, died December 12, 1956, at the age of 45. His work was mainly on the *x*-ray powder method for the determination of minerals, especially in isomorphous series. The mineral mikheevite (=gorgeyite) was named for him.

Dr. Erwin Hellner of the Mineralogical Institute, University of Marburg, is currently serving as Visiting Associate Professor of Mineralogy in the Department of Geology, University of Chicago.

Dr. A. J. Frueh is spending the school year at the Mineralogical Museum in Oslo.

Dr. J. Laurence Kulp, head of the Geochemistry Laboratory of

Columbia University, has been appointed Professor of Geochemistry. He is spending the current academic year at Oxford University as a National Science Foundation Senior Postdoctoral Fellow.

American Crystallographic Association

The 1959 summer meeting of the American Crystallographic Association will be held at Cornell University, Ithaca, New York, July 19–24. The local chairman is Dr. J. L. Hoard, Department of Chemistry, Cornell University; the program chairman is Dr. David P. Shoemaker, Department of Chemistry, Massachusetts Institute of Technology, Cambridge 39, Massachusetts.

Officers of ACA for 1959

President—Dr. Robert E. Rundle (Iowa State College)
Vice-President—Dr. Jurg Waser (California Institute of Technology)
Treasurer—Dr. Thomas C. Furnas, Jr. (Picker X-Ray Corporation)
Secretary—Dr. Leroy E. Alexander (Mellon Institute, 4400 Fifth Ave., Pittsburgh 13, Pa.)

Russian Translation Journal "Crystallography"

The journal "Crystallography" of the Academy of Sciences of the USSR is being published in (complete) translation by the American Institute of Physics. The translation began with the 1957 issues.

This relatively new journal is quite broad in scope, offering both experimental and theoretical papers on crystal structure, lattice theory, diffraction studies and effects of external influences, including radiation damage on crystalline structure. It also publishes studies employing x-ray, electron and neutron diffraction of all materials of interest to the crystallographer, metallurgist, mineralogist, solid-state physicist, and chemist.

There are six issues per year, approximately 1,000 Russian pages. Annual subscriptions are $25.00 domestic, $27.00 foreign ($10.00 and $12.00 respectively for libraries of non-profit degree-granting institutions). Subscription orders and inquiries should be addressed to: Translation Journals—American Institute of Physics, 335 East 45 Street, New York 17, New York.

HANDBOOK OF CHEMICAL MICROSCOPY, Volume 1. Principles and Use of Microscopes and Accessories. Physical Methods for the Study of Chemical Problems. Third Edition, by Émile Monnin Chamot and Clyde Walter Mason. John Wiley and Sons, Inc., New York, N. Y., 1958. xii+502 pages, 1 fold-in color plate Michel-Levy scale of birefringence, 125 Figures, Price, $14.00.

Mineralogists, particularly those engaged in the study of chemicals, ceramic and similar products, will welcome the Third Edition of this well-known and most useful handbook. From a practical point of view, this book has two important and distinguishing features: (1) It contains many suggestions and remedies for the everyday as well as the unusual problems which face the practicing microscopist, and (2) It has several thousand literature references, many to special problems and applications, all arranged in convenient footnote form.

Several of the chapters of the Third Edition under review have been revised and modernized to a great extent from the previous edition (published in 1938); but, in some chapters, very few changes have been made. This edition contains a short chapter on the electron microscope. The discussion of the relation of optical properties to structure of crystals and aggregates has been enlarged and given chapter status; the added material is mostly basic crystallography. Newer techniques, such as phase contrast microscopy, are conveniently added to previously existing chapters.

In any attempt to completely modernize a textbook some of the older material might be expected to survive and we have no exception here. The reader will find several illustrations of somewhat antiquated equipment. In general, the illustrations are well chosen but this reviewer believes the petrographic microscope deserves more than a three-inch sketch (of an older model) especially when, for example, a photographic eyepiece and attached camera receive about one-half page. Some examples of past eras are still to be found within the text; for example, we might infer (p. 275) that the "cap" analyzer is still rather commonly used. These points are minor, especially when we consider that literature reference as late as 1958 are included.

The entire subject of optical crystallography is covered in about 50 pages, distributed among several chapters, in an order which would be unappealing to most mineralogists. Although all important subjects are covered, many are quite sketchy. The authors, however, do not intend their coverage to be adequate for all workers in the field and refer the reader to standard texts, many of them mineralogical. A new feature of the Third Edition is the Michel-Levy scale of birefringence provided by the Bausch and Lomb Optical Company and adapted from "Optical Mineralogy" by Rogers and Kerr. Unfortunately, the mineral names on the chart by Rogers and Kerr have been removed resulting in a chart with neither minerals nor chemical compounds illustrating the various birefringences. Under any condition, the usefulness of a Michel-Levy birefringence chart in this book is questionable.

There can be no doubt, however, that this book will be, quite deservedly, well received and continue to be one of the most widely used on the subject. In the opinion of the reviewer, this book illustrates the fact that mineralogists, with their superior training in petrographic methods, are far better equipped to tackle many problems in the general areas of chemical microscopy than are microscopists entering the field from other sciences. Teachers of optical mineralogy would do well to impress upon their students the value of the polarizing microscope in the ever increasingly important study of textiles, polymers, pigments, and other organic and inorganic materials of interest to industry.

A. A. Levinson
Dow Chemical Company
Freeport, Texas

MINERALOGY AND GEOLOGY OF RADIOACTIVE RAW MATERIALS, by E. Wm. Heinrich. 654 pp. McGraw-Hill Book Company, Inc., New York. $14.50.

In the past ten years an ever increasing volume of descriptions of new uranium deposits, new uranium minerals, analytical data, hypotheses of origin, and guides for the prospector has been published. In this bulk of material much sound information was waiting to be sorted out and put together as in a giant jigsaw puzzle. In undertaking the tremendous task of evaluating, classifying, and summarizing this information Professor Heinrich has been highly successful. His book is very timely because sufficient source material is now available for a worthwhile summary, but most people interested in the overall picture of uranium geology cannot possibly obtain and assimilate all the source material. The publication comes at a time when the first great uranium prospecting boom has found an unexpectedly large supply of uranium and, within a few years, the development of atomic power now getting underway will probably require much more uranium and thorium.

The book of 654 pages includes a good section of about 150 pages on the descriptive mineralogy of uranium and thorium and associated rare earths and other elements, and a section of about 400 pages summarizing a great deal of information on the geology of radioactive deposits which are grouped under 12 main types. The last 100 pages includes a selected bibliography of more than 1,000 references, an index of radioactive and rare-earth mineral species, an index of localities, and a subject index. Many foreign references and papers and abstracts in the AEC reports or in publications outside the well-known mineralogical and geological journals give a wide scope to the bibliography. Only a few preliminary or premature publications might profitably be culled from the list.

The organization is excellent, with a logical sequence of presentation of the geochemistry of the radioactive elements, the mineralogy of uranium and thorium, including minerals with minor amounts of U and Th, and the geology of the various types of deposits. The geologic discussion proceeds from the occurrence of uranium and thorium in igneous rocks to radioactive pegmatite deposits, carbonatite and related deposits, pyrometasomatic and hypothermal deposits, mesothermal and epithermal deposits, epigenetic stratiform deposits in sedimentary rocks, uraniferous phosphorites, uraniferous marine black shales, placer deposits of radioactive minerals, radioactive hydrocarbons, and deposits formed by weathering and ground water. In general the classification of individual deposits is sound, but each reader of the book probably will argue with the placing of some of the deposits. Additional knowledge obtained after more extensive mining of some deposits probably will require changes in classification. For example, the reviewer does not agree with the contrast made between deposits in the Todilto limestone and those in the Morrison formation in the Grants area of New Mexico, nor with the interpretation of the Woodrow and Jackpile mines.

Photographs of outcrops, photomicrographs, and line drawings are used to good advantage. Tables of mineral data and characteristics of various types of deposits help the reader "see the woods for the trees."

To do his duty a reviewer is supposed to find some typographical error in a new book. This book has very few, but the mineral names thucholite, montroseite, and paramontroseite are consistently misspelled (10 to 20 times).

A wealth of material is packed into this large volume. A significant omission, however, is discussion of the geochemical processes controlling the transportation and deposition of uranium. The sections headed "geochemistry" cover chiefly trace element association in various mineral deposits. Little attention is paid to the solution chemistry of uranium or thorium as it may affect their mode of transportation or migration in near-surface deposits.. Particularly, several references on uranyl-carbonate chemistry, which have contributed

to an understanding of uranium mobility, could have been added effectively.

This book is an excellent, useful, and readable summary of the present knowledge o the mineralogy and geologic occurrence of radioactive materials.

Alice D. Weeks
U. S. Geological Survey
Washington 25, D. C.

NEW MINERAL NAMES

Michenerite, Froodite

J. E. Hawley and L. G. Berry. Michenerite and froodite, palladium bismuthide minerals. *Canadian Mineralogist*, v. 6, 200–209 (1958).

These minerals were described by C. E. Michener (Ph.D. dissertation, Univ. of Toronto, 1940); to his work has been added comparison with recent x-ray work on synthetic compounds.

Michenerite is grayish-white, streak black, no visible cleavage, brittle, hardness B (2.5). Sp. gr. between those of sperrylite and galena, probably about 9.5. Optically isotropic. Etch reactions: HNO_3—effervesces slowly, blackens; $FeCl_3$—slowly stains dark, some negative; aqua regia—instantly stains black; HCl, KCN, KOH negative.

Chemical analyses (not given) by the dithizone method on 3 samples gave the ratio Pd:Bi = 2:3, but the indexed x-ray powder data are close to those for synthetic $PtBi_2$ and aurostibite ($AuSb_2$), so the composition is probably $PdBi_2$. a_0 6.68 Å. Strongest lines (in Å) are 2.99 (100), 2.01 (90), 2.73 (80), 1.79 (75), 0.870 (40). No compound corresponding to this was found by Burr and Peacock (Univ. Toronto Studies, Geol. Ser. 47, 19–20 (1942) in their study of alloys of Pd with Bi.

The name is for C. E. Michener, vice-president, Canadian Nickel Co., Ltd.

Froodite is gray, streak black, luster metallic, splendent on fresh cleavage, tarnishes quickly; fracture uneven; brittle, G. 12.6, 12.5. Optically anisotropic. Etch reactions: HNO_3 (1+1)—effervescence slow, turns brown and gives granular surface; KCN—slowly stains dark; $FeCl_3$—instantly stains black; HCl (1+1), KOH, and $HgCl_2$—negative. Synthetic material gives slightly different results.

Rotation and Weissenberg photographs by the late Harry Berman gave: monoclinic, a_0 5.71, b_0 4.29, c_0 6.37 Å, beta 102°27′ cleavages (001) very perfect, (100) less perfect. The mineral is identical with synthetic alpha-$PdBi_2$ prepared by Burr and Peacock which was monoclinic, $C2/m$, with a_0 12.75, b_0 4.29, c_0 5.67, β 102°52′, cleavages (100) and (102), G 11.5 (measured), 11.52 (calcd.). (Note that Berman's value for c must be doubled.)

The work on synthetic material indicates that the composition is close to $PdBi_2$. Michener's approximate analyses (not given) gave Pi:Bi near 1:3. Indexed x-ray powder data are given; the strongest lines are 2.77 (100), 1.556 (80), 2.97 (70), 2.48 (70), 2.21 (70), 1.637 (60), 1.419 (60).

The name is for the Frood Mine, Sudbury District, Ontario.

Michenerite and froodite were found in mill concentrates of arsenic- and lead-copper-rich ores of the Frood Mine. Michenerite is apparently the more abundant.

Michael Fleischer

Reinerite

B. H. Geier and K. Weber. Reinerit, $Zn_3(AsO_3)_2$, ein neues Mineral der Tsumeb Mine, Südwestafrika. *Neues Jahrb. Mineral., Monatsh.* **1958,** No. 7–8, 160–167.

The name was mentioned, without details, in an earlier paper. The mineral occurs rarely, associated with chalcocite and a little bornite in cavities in the "second oxidation zone" at a depth of about 900 meters (see under Stottite, *Am. Mineral.*, **43,** 1006 (1958)).

Analyses by W. Reiner gave: for a light-green variety ZnO 56.01, As_2O_3 48.83, sum 99.84%; for an ocean-blue variety ZnO 53.27, FeO 1.30, Cu 2.23, As_2O_3 42.51, S not detd., sum 99.76%, corresponding to $Zn_3(AsO_3)_2$. The Cu and probably part of the FeO are ascribed to inclusions of chalcocite and a little bornite. The mineral dissolves in cold (1+1) HCl.

Rotation, Guinier, and powder photographs show reinerite to be orthorhombic, space group D_{2h}^{5} ($Pmma$) with a_0 6.091±0.007, b_0 14.397±0.005, c_0 7.804±0.007 Å, $a:b:c$

$=0.4231:1:0.5421$, $Z=4$. Indexed x-ray powder data are given (81 lines); the strongest lines are 3.995 (vs)(121), 2.644 (s)(042), 1.440–1.436 (s)(−), 3.203 (s)(112), 3.432 (ms)(022), and 3.397 (ms)(131). The x-ray pattern is identical with that of synthetic $Zn_3(AsO_3)_2$, but is very different from that of armangite, $Mn_3(AsO_3)O_2$.

Reinerite occurs in rough crystals up to 4.7×2 cm. with the faces (010), 110), and (001) dominant, and (012) present. Cleavages (110) good, also (011) and (111). The color is ocean-blue to light yellow-green, luster vitreous to adamantine on fracture surfaces. Hardness 5–5½, G. (pycnometer) 4.27_0 (calcd. from x-ray) 4.27_8. Optically biaxial, neg., with ns (Na), $\alpha 1.74_9$, β 1.79_0, γ 1.82_1.

The name is for Willy Reiner, senior chemist of the Tsumeb Corp., Ltd. Not to be confused with the sulfosalt renierite, which also occurs at Tsumeb. To be grouped with the arsenites, Dana Class 45, but apparently not isostructural with any known arsenite.

M. F.

Arsenuranylite

L. N. Belova. Arsenuranylite, the arsenic analogue of phosphuranylite, *Zapiski Vses. Mineralog. Obshch.*, **87,** 589–602 (1958) (in Russian).

Analysis by L. E. Novorosova and V. L. Litenkova gave UO_3 68.64, CaO 3.48, As_2O_5 16.68, H_2O 9.12, sum 97.95%, corresponding to $CaO \cdot 3.89UO_3 \cdot 1.17As_2O_5 \cdot 8.1H_2O$ or $Ca(UO_2)_4(AsO_4)_2(OH)_4 \cdot 6H_2O$, analogous to the formula of phosphuranylite, but with more water.

The mineral occurs in lichen-like deposits, color more orange than that of phosphuranylite. Under the microscope appears as extremely fine yellow scales. Pleochroism not evident, ns α' 1.737, γ' 1.766. G not given.

An x-ray powder pattern by N. I. Organov is given, with partial indexing by analogy to phosphuranylite. The strongest lines are 7.72 (10)(200), 3.85 (10)(400), 8.41 (8)(−), 3.13 (8)(204), 3.42 (7)(004, 402), 1.778 (7)(−), 1.729 (7)(−), 1.612 (7)(−), 1.512 (7)(−), 2.57 (6)(−), 1.883 (6)(−). From these, the unit cell is calculated to be a_0 15.40, b_0 17.40, c_0 13.768 Å.

The mineral occurs in the oxidation zone of a deposit containing arsenic-bearing sulfides (no locality is given, as usual), associated with metazeunerite, uranospinite, and novacekite, which it replaces; it is replaced by schoepite and paraschoepite.

The name is for the composition and the relation to phosphuranylite.

M. F.

Zinalsite

F. V. Chukhrov. Zinc clays from the Akdzhal deposits in Kazakhstan. *Kora Vyvetrivaniya* (*The crust of weathering*), **2,** 107–123 (1956), from an abstract by E. M. Bonshtedt-Kupletskaya in *Zapiski Vses. Mineral. Obshch.*, **87,** 487–488 (1958).

Analysis by V. A. Moleva gave SiO_2 26.60, TiO_2 0.36, Al_2O_3 14.60, Fe_2O_3 1.34, ZnO 36.00, CuO 2.00, NiO 0.04, CoO 0.03, MgO 1.57, MnO 0.02, CaO 1.32, BaO 1.06, K_2O 0.20, P_2O_5 0.50, SO_3 1.02, H_2O^- 2.70, H_2O^+ 10.60, sum 99.96%, corresponding to $Zn_7Al_4(SiO_4)_6 \cdot (OH)_2 \cdot 9N_2O$. Dissolves in 10% HCl or 30% NaOH. The absorption curve with methylene blue is not affected by the addition of KCl (difference from montmorillonite).

The mineral occurs in cryptocrystalline dense aggregates, resembling halloysite, in the zone of oxidation of the Akdzhal and Achisai deposits, Kazakhstan, associated with hydromicas and with other Zn clays; also noted from Sterling Hill, N. J. Color white, rose, to reddish-brown. Does not give a plastic mass with water. G 3.007, hardness 2½–3. Under the microscope appears as very fine anisotropic grains, biaxial, negative, mean n 1.56–1.58. Electron microscope photographs show irregular forms.

The x-ray pattern has strong lines at 10.46 and 7.30, other lines at 4.55, 3.58, 2.71 2.425, and 1.559.

The name is for the composition: Zn, Al, Si.

M. F.

Polynite

E. A. Yarilova and E. I. Parfenova. New formation of clay minerals in soils. *Pochvoved.* **1957,** No. 9, 37–48; from an abstract by E. M. Bonshtedt-Kupletskaya in *Zapiski Vses. Mineral. Obshch.*, **87,** 488–489 (1958).

The name is given to a clay mineral of variable composition; 11 samples, separated from the illuvial horizons of different soils, contained: SiO_2 54.83–50.90, P_2O_5 0.17–0.01, Al_2O_3 31.51–24.14, Fe_2O_3 15.74–9.24, CaO 2.52–0.98, MgO 3.74–2.29, K_2O 3.99–1.40, Na_2O 0.33–0.15; the ratio $SiO_2:Al_2O_3$ 2.51–3.81. The DTA curve shows endothermal breaks at 95–120°, at 250–350°, a very weak one at 835°, and an exothermal break at 915–930°. The adsorptive capacity ranges from 45 to 65 meq./100 g.

The mineral has collomorphic texture. Color yellowish. Variable ns; alpha 1.555–1.562 (and up to 1.5 with higher Fe), gamma 1.570–1.585. Pleochroism distinct, X straw-yellow, Z greenish-brown. Under the electron microscope consists of flake-like aggregates; the particles have irregular outlines. Distinguished from kaolinite and montmorillonite by the x-ray lines at 7 and 14 kX. The innermost lines are characteristically broad and very intense, varying in the range 13.47–12.51 kX in inner diameter, and 10.67–9.85 kX in outer; the variation is not the result of the treatment of the mineral.

The name is for B. B. Polynov, "investigator of the process of clay formation in soils."

Discussion.—As the abstractor points out, this may be a mixture and the name is not warranted.

M. F.

Kremenchugite

M. M. Dobrokhotov. A new variety of chlorite from iron-bearing quartzites of the Galeshchin deposits of the Kremenchug region. *Mineralog. Sbornik, Lvov Geol. Obshch.* No. **11,** 295–302 (1957), from an abstract by E. M. Bonshtedt-Kupletskaya in *Zapiski Vses. Mineral. Obshch.*, **87,** 488 (1958).

Analysis, after deducting quartz and siderite, gave SiO_2 27.47, TiO_2 0.34, Al_2O_3 6.19, Fe_2O_3 16.44, FeO 30.43, MnO 0.28, MgO 6.32, CaO 1.76, K_2O+Na_2O 1.15, H_2O^+ 9.62, total 100.00%. Easily decomposed by dilute HCl with separation of gelatinous silica. Color dark green, G. 3.27, b_0 9.41, $c_0 \sin \beta$ 14.2 kX. The x-ray diagram and DTA curve are stated to correspond to those of the iron-rich chlorites (thuringite, chamosite, cronstedtite, etc.), the mineral is distinguished from these by its high refraction. ns, alpha 1.697, gamma 1.703, strongly pleochroic, X clear reddish-brown, Z dense dark green, absorption $Z=Y>X$. Occurs in fine scales, associated with quartz, magnetite, and siderite in quartzites of the Kremenchug region, Ukraine.

The name is for the locality.

Discussion.—An unnecessary name.

M. F.

Dzhulukulite

N. N. Shishkin. Dzhulukulite—a new cobalt mineral. *Doklady Akad Nauk S.S.S.R.*, **121,** 724–726 (1958) (in Russian).

The mineral occurs in cobalt ore in quartz-ankerite veins associated with tennantite, chalcopyrite, glaucodot, pyrite, and bornite, 10 km. N.E. of Lake Dzhulu-Kul, Tuva Autonomous Region. Analysis by H. M. Mikhailova gave Co 26.00, Ni 7.72, Fe 0.55, Cu

1.05, As 45.52, S 18.81, SiO_2 0.40, sum 100.05%. Spectrographic analysis also showed Sb, Ag, Bi, Al, Mg, and Ca, and traces of Pb, Zn, and Mn. A partial analysis of another sample by K. S. Yurina gave Co 18.20, Ni 13.80, Fe 1.20%. The formula is (Co,Ni)AsS.

Color gray, luster metallic, streak gray, hardness 6, sp. gr. 6.36, a_0 5.575±0.01 Å. Unindexed x-ray powder data on two samples are given. In polished section grayish-white, relief less than for pyrite, strongly etched by (1+1 HNO_3.

Discussion.—An unnecessary name for nickeloan cobaltite, in the series cobaltite-gersdorffite.

M. F.

Arshinovite

E. G. Razumnaya, G. A. Smelyanskaya, K. G. Korolev, and G. V. Pokul'nis. On arshinovite, a new metacolloidal variety of zircon. Methods of study of raw materials, *Gosgeoltekhizdat*, **1957,** 45–50; from an abstract by E. M. Bonshtedt-Kupletskaya in *Zapiski Vses. Mineral. Obshch.*, **87,** 486 (1958).

The name is given to a metacolloidal variety of zircon, occurring in phosphorites, in phosphate-containing tuffs, and in the cement of phosphate-containing sandstones and conglomerates. Rarely forms visible fine veinlets of dense, jasper-like texture with a network of fissures. Color greenish light-gray, hardness low, G. about 3.3, also 3.0–2.8. Isotropic or weakly anisotropic, n (nearly colorless) 1.650–1.660, (yellowish, brownish) n 1.664–1.70. Recalculation of analyses of mixtures indicates the composition to be close to that of zircon with SiO_2:ZrO_2 about 1:1, Hf:Zr 0.5:0.8, contains tenths of a per cent U. Soluble in HNO_3 and HCl. The x-ray pattern is that of zircon but with diffuse lines.

The name is in memory of Professor V. V. Arshinov.

Discussion.—An unnecessary name.

M. F.

DISCREDITED MINERALS

Condurrite (=Tenorite+Cuprite)

P. G. Embrey. Condurrite: a mixture and not domeykite. *Mineralog. Mag.*, **31,** 979–980 (1958).

Condurrite (Phillips, 1827) has been listed as a synonym of domeykite. It does occur with domeykite and β-domeykite, but the original description specifically restricted the name to the black mineral present, now found by x-ray study of type material to be a mixture with cuprite and tenorite predominant, and chalcocite and domeykite present.

M. F.

AMERICAN MINERALOGIST

Price Information

Back issues of the AMERICAN MINERALOGIST can be purchased at the prices given below, but certain issues as listed are available only in microtext edition. The microtext edition is on 3 x 5 inch cards, each card containing 48 pages of text material, with a heading in regular type to indicate the volume, number, pages and date. Microtext will be furnished on all orders where necessary, unless specific instructions are received to the contrary. Prices apply to both the regular and microtext editions, and postage is charged except on indexes. Agents and dealers are allowed the usual 10% discount on orders. Subscriptions for the current volume (calendar year) are available to libraries, colleges, and other organizations at $6.00, postpaid. Individuals can receive the current volume by becoming members of the Mineralogical Society of America.

Volume	Year	Price per volume	Price per issue (except special issues)
1-9	1916-1924	$3.00	$ .50
10-19	1925-1934	4.00	.50
20-28	1935-1943	6.00	.80 (monthly issue)
29-42	1944-1957	6.00	1.60 (bimonthly issue)

Microtext Edition

Vol.	No.	Year	Vol.	No.	Year
1-5	Complete	1916-1920	27	1-12	1942
7	2	1922	28	1-8	1943
9	3	1924	29	1-8	1944
10	3	1925	30	1-4, 7-8	1945
11	3	1926	31	1-4	1946
25	5	1940	32	1-4	1947
26	1-3, 6-9, 12	1941			

Special Issues

Year	Issue	Vol.	No.	Price	Year	Issue	Vol.	No.	Price
1925	Michigan	10	9	$1.00	1945	Quartz Symposium	30	5-6	$3.00
1925	Harvard	10	11	1.00	1950	Larsen	35	9-10	2.50
1927	Harvard	12	4	1.00	1953	Hunt	38	1-2	2.00
1928	Harvard	13	7	1.00	1953	Ross-Schaller	38	11-12	3.00
1930	Harvard	15	8	1.00	1955	Kraus	40	11-12	2.00
1932	Harvard	17	7	1.00	1957	Harvard	42	11-12	2.00
1937	Palache	22	7	3.00					
1938	Harvard	23	11	1.50					

Indexes

Vols. 1-20 (1916-1935) $2.00; $1.00 to members; postpaid
21-30 (1936-1945) 3.00; 2.00 to members; postpaid
31-40 (1946-1955) 5.00; 3.00 to members; postpaid

Send all orders to

MINERALOGICAL SOCIETY OF AMERICA

Marjorie Hooker, Treasurer

c/o U. S. Geological Survey, Washington 25, D.C.

RECENT ACQUISITIONS

ANAPAITE. Spain. Greenish white xls in concretion 2 x 2", $3.50; 3 x 3", $7.50

BETAFITE. Ontario. Large brown cubo-octahedral crystals ¾", $2.50; 1", $5.00; 1½", $15.00; 2 x 2½", $25.00

CANCRINITE. Maine. Yellow massive in syenite. 4½ x 7", $7.50; 5½ x 7", $7.50

CYLINDRITE. Bolivia. Curious cylindrical masses in rock. 3 x 4", $15.00

DANBURITE. Japan. Terminated white crystals, some partly clear. 1" to 2", $1.50, $2.50, $3.50

FERGUSONITE. Ontario. Large prismatic crystal sections with feldspar, mica 1 x 2", $1.50; 2 x 2", $3.50; 2 x 3", $6.00; 3 x 4", $12.50

GRATONITE. Peru. A rare lead arsenic sulfide. Groups of small prismatic crystals ½" to 1", $2.50; $5.00; 1 x 3", $7.50, $10.00

LEAD. Sweden. A nearly pure mass 2 x 3", $35.00

METAHEWETTITE. Utah. Brown xline with rauvite, carnotite in sandstone 3½ x 5½", $25.00

MILLERITE. Ontario. Cleavable masses (rare) with chalcopyrite, etc. 2 x 2", $3.00; 2 x 3", $5.00; 3 x 4", $15.00

NAVAJOITE. Arizona. Fibrous with hewettite, carnotite, rauvite, 3½ x 4", $17.50

PASCOITE. Utah. Orange brown with cobaltomenite on sandstone 2 x 3½", $10.00

SILVER. Ontario. Splendid nearly pure sheet 5½ x 7", $35.00

SPHALERITE. England. Xled with xled galena and dolomite, very showy 9 x 11½", $35.00

TRIDYMITE. Pure artificial. $15.00 per gram.

VOLBORTHITE. Utah. Yellow green scales on sandstone 2 x 3", $7.50; 2½ x 3½", $10.00; 3½ x 5", $17.50

ZIRCON. Ontario. Dark brown crystals, good terminations, average ¼ inch, 10 for $1.50

Prices are list at Rochester, N.Y.

Ward's Geology Catalog. The most comprehensive catalog ever published by Ward's for the geological field. It contains a listing of mineral, rock and fossil collections, minerals, rocks and reference clay minerals in bulk or student specimens; color slides for geology (a very popular series). The section on equipment for field and laboratory includes expanded listings on storage and display equipment and an especially fine section on thin section equipment. There is an illustrated section on crystallographic aids.

Ward's Specimen Catalog. This contains listings of "one of a kind" minerals suitable for display, study or research work. Free.

Ward's Geology Newsletter. Published periodically to list new acquisitions. Free.
If you are not on our mailing list to receive these publications, write for them today.

WARD'S *NATURAL SCIENCE ESTABLISHMENT, INC.*
P.O. BOX 1712 ROCHESTER 3, N.Y.

GEORGE BANTA COMPANY, INC., MENASHA, WISCONSIN, U.S.A.